UNCLASSIFIED

AD NUMBER
AD869906
LIMITATION CHANGES
TO: **Approved for public release; distribution is unlimited.**
FROM: **Distribution: Further dissemination only as directed by Aeronautical Systems Division, Attn: ASZTH, Wright-Patterson AFB, OH 45433, MAY 1970, or higher DoD authority. This document contains export-controlled technical data.**
AUTHORITY
ASD, USAF ltr, 8 Feb 1974

THIS PAGE IS UNCLASSIFIED

FTC-SD-70-9

FTC-SD-70-9

AD869906

AFFTC

CATEGORY II PERFORMANCE AND FLYING QUALITIES TESTS OF THE HH-53C HELICOPTER

WAYNE J. BARBINI
Project Engineer

PAUL J. BALFE
Major, USAF
Project Pilot

CLARK E. LOVRIEN Jr.
Major, USAF
Project Pilot

SUBSTANTIATING DOCUMENT No. 70-9

MAY 1970

AIR FORCE FLIGHT TEST CENTER
EDWARDS AIR FORCE BASE, CALIFORNIA
AIR FORCE SYSTEMS COMMAND
UNITED STATES AIR FORCE

FTC-SD-70-8

CATEGORY II PERFORMANCE AND FLYING QUALITIES TESTS OF THE HH-53C HELICOPTER

WAYNE J. BARBINI
Project Engineer

PAUL J. BALFE
Major, USAF
Project Pilot

CLARK E. LOVRIEN, Jr.
Major, USAF
Project Pilot

FOREWORD

The Category II Performance and Flying Qualities Tests of the HH-53C Helicopter USAF S/N 67-14993, were conducted at Sikorsky Aircraft Division of United Aircraft Corporation in Stratford, Connecticut, from 26 August 1969 to 27 February 1970. This substantiating document contains the quantitative data obtained during this evaluation along with the test techniques and the data analysis methods. The technical report, FTC-TR-70-8, (reference 1), was published in April 1970 and contained the results, conclusions, and recommendations. This test program was requested by the Aeronautical Systems Division and was conducted under the authority of AFFTC Project Directive 69-2 (Program Structure 482A).

Engineering assistance from Lieutenant Rodney L. Ritter is acknowledged.

Foreign announcement and dissemination by the Defense Documentation Center are not authorized because of technology restrictions of the U.S. Export Control Acts as implemented by AFR 400-10.

Prepared by:

Wayne J. Barbini
WAYNE J. BARBINI
Project Engineer

Reviewed and approved by:

7 May 1970

Thomas J. Cecil
THOMAS J. CECIL
Colonel, USAF
Commander, 6512th Test Group

Alton D. Slay
ALTON D. SLAY
Brigadier General, USAF
Commander

ABSTRACT

This substantiating document contains the test techniques, data analysis methods, and test data for the Category II Performance and Flying Qualities Tests of the HH-53C Helicopter. The results, conclusions, and recommendations were presented in FTC-TR-70-8, Category II Performance and Flying Qualities Tests of the HH-53C Helicopter, April 1970.

Table of Contents

List of Illustrations

List of Abbreviations and Symbols

Item	Definition	Units
A	rotor disc area	ft^2
ac	alternating current	- - -
C_P	power coefficient	dimensionless
C_T	thrust coefficient	dimensionless
EAPS	engine air particle separators	- - -
IGE	in ground effect	- - -
KCAS	knots calibrated airspeed	- - -
KTAS	knots true airspeed	- - -
M_{TIP}	advancing blade tip Mach number	dimensionless
N_1	gas producer speed	pct
N_r	rotor speed	rpm
P_a	ambient pressure	in. Hg
P_{t_2}	compressor inlet total pressure	in. Hg
Q	torque	ft-lb
R	rotor radius	ft
SHP	shaft horsepower	$550 \frac{\text{ft-lb}}{\text{sec}}$
T	temperature	deg K
V_t	true airspeed	kt
W_f	fuel flow	lb per hr
θ	temperature ratio (T_{t_2}/T_a)	dimensionless
μ	rotor advance ratio	dimensionless
ρ	air density	slugs per ft^3
Ω	rotor angular velocity	rad per sec
σ	rotor solidity ratio	dimensionless
δ	pressure ratio (P_{t_2}/P_a)	dimensionless

Subscript		
c	indicates parameter affected by compressibility	- - -

INTRODUCTION

The test helicopter was a production HH-53C which was instrumented by the contractor for performance and flying qualities. A test pitot-static head for measurement of airspeed and altitude was mounted on the refueling probe for the test program.

The objective of the Category II Performance and Flying Qualities Tests was to obtain data for inclusion in the Flight Manual (reference 2) and determine if selected requirements of MIL-H-8501A (reference 3) were met.

Tests not conducted during this test program which are normally completed during Category II were hover, takeoff, and height-velocity tests at a high altitude test site and level flight performance in extreme temperature conditions necessary to completely define the effects of compressibility.

A flight log of the tests flown during this program is presented in appendix I.

TEST AND EVALUATION

GENERAL

Dimensional analysis of the major items affecting helicopter performance yields several sets of dimensionless variables which may be used to present performance data in nondimensional form. The C_P, C_T, μ method is useful only when compressibility effects are not significant. These variables are defined as follows:

$$C_P = \frac{SHP \times 550}{\rho A(\Omega R)^3}$$

$$C_T = \frac{W}{\rho A(\Omega R)^2}$$

$$\mu = \frac{V_t}{\Omega R}$$

Since compressibility was a major item affecting the performance of the HH-53C, an additional dimensionless variable was required to make the C_P, C_T, μ method valid. The additional variable, the advancing blade tip Mach number was defined as:

$$M_{TIP} = \frac{V_t + \Omega R}{38.967\sqrt{T_a}}$$

HOVERING PERFORMANCE

In-ground-effect (IGE) and out-of-ground-effect (OGE) hovering performance data were obtained by tethered and free flight techniques to update the Flight Manual's estimated data. All hovering was done with the 450-gallon external fuel tanks installed and the landing gear down. Hovering performance data were obtained at wheel heights of 5, 10, 22, 47, 80 and 100 feet at a pressure altitude of sea level and referred rotor speed ($N_r/\sqrt{\theta}$) of 175 to 195 rpm. All hover tests were conducted in less than 3 knots of wind. During the tests a constant rotor tip Mach number was maintained by changing the rpm as ambient temperature changed to maintain a constant $N_r/\sqrt{\theta}$.

During the tethered hovering tests the helicopter was tethered to the ground by a cable and load cell. The load cell measured cable tension. Thrust produced by the helicopter was assumed equal to the gross weight of the helicopter, cable, load cell and cable tension. Power was determined by using the engine torquemeters and rotor speed.

Significant rotor blade compressibility was encountered during the hover tests as evidenced by an increase in power required at a constant thrust coefficient C_T as M_{TIP} was varied from minimum to the maximum obtainable. This effect became more evident as M_{TIP} and C_T were increased. Since tethered hovering was conducted at only one pressure altitude and a limited temperature range, this effect could not be completely determined for the entire range of operational conditions the HH-53C can encounter.

Figures 1 through 6, appendix I, show the power coefficient C_P plotted versus the thrust coefficients for each wheel height and at constant tip Mach numbers. These fairings were used to construct the nondimensional cross plots which define the power coefficient at a constant wheel height for various thrust coefficients and tip Mach numbers.

SAWTOOTH CLIMBS

Two-engine sawtooth climbs were flown during the test program to determine the climb performance and to make a comparison with the climb performance presented in the Flight Manual.

The tests were flown at military power when not limited by up collective at pressure altitudes of 4,500, 7,000, and 14,000 feet with the landing gear up and at a mid cg (340). Each climb was repeated on a reciprocal heading to average out the effects of wind. The observed rate of climb was corrected to test day tapeline rate of climb using the following equation:

$$R/C_t = \frac{dh}{dt} \times \frac{T_{a_t}}{T_{a_s}}$$

when R/C_t was the tapeline rate of climb in feet per minute, dh/dt being the slope of the pressure altitude versus time curve in feet per minute. T_{a_t}/T_{a_s} was the ratio of test day ambient temperature to the standard day temperature for the test altitude.

The results in table I indicate a considerable discrepancy between the Flight Manual and test results in both the test climb airspeed and the rate of climb. Test results are shown in figure 7, appendix I.

Table I

SAWTOOTH CLIMB PERFORMANCE					
		Test Results		Flight Manual	
Gross Weight (lb)	Altitude (ft)	Best Climb Speed (KCAS)	Rate of Climb (fpm)	Best Climb Speed (KCAS)	Rate of Climb (fpm)
35,000	4,500	88	2,700	75	2,250
35,000	7,000	79	2,300	73	1,950
35,000	14,000	61	1,960	66	950

LEVEL FLIGHT PERFORMANCE

Th level flight tests were conducted to determine the power required as a function of airspeed, gross weight, and tip Mach number, and to define range and endurance characteristics. Data were not obtained with the personnel door or cargo ramp open, at forward or aft cg's, with the engine anti-ice on, or with only one engine operating.

The level flight performance tests were flown at a constant C_t/σ (σ being the rotor solidity ratio) and $N_r/\sqrt{\theta}$. This required varying rotor rpm to maintain $N_r/\sqrt{\theta}$ constant as ambient temperature changed. By using $N_r/\sqrt{\theta}$ the equation for computing C_T becomes a function of the gross weight to ambient pressure ratio (GW/δ). This technique required increasing pressure altitude as fuel was consumed to maintain a constant C_T. The test data were corrected for adiabatic temperature rise. Power required was determined from the installed engine torquemeters and rotor rpm. Plots of Cp versus μ are presented in figures 8 through 24, appendix I. The fairings were obtained from cross plots of Cp versus C_T at a constant μ.

An analysis of these level flight performance data was conducted to determine if there were any changes in power required when fuselage Reynolds number (R_e) was varied and all other independent variables were held constant. With the flight conditions and configurations flown during this program the R_e effects were not significant, reference figures 11 and 12, appendix I.

One speed-power was flown at a C_T/σ of 0.0785 to determine the drag penalty of extended landing gear. There was a 9.5-percent increase in power required at 144 KCAS, and this value gradually decreased until, at approximately 75 KCAS, there was no significant increase in power required. A comparison of the results is presented in figure 25, appendix I.

A level flight test to determine the effects on aircraft performance when both engines were equipped with engine air particle separators (EAPS) was conducted at a C_T/σ of 0.0595. At 155 KCAS there was a 5.5-percent increase in power required which decreased to less than 1 percent at 120 KCAS. The results of this test are presented in figure 26, appendix I.

AUTOROTATIONAL CHARACTERISTICS

Sawtooth autorotation descents were conducted in conjunction with the sawtooth climbs to determine the speed for minimum rate of descent and speed for maximum range in autorotation. The test conditions were the same as in the sawtooth climbs. The observed rate of descent was corrected to test day tapeline rate of descent by the following equation:

$$R/D_t = \frac{dh}{dt} \times \frac{Ta_t}{Ta_s}$$

when R/D_t was the tapeline rate of descent in feet per minute, dh/dt being the slope of the pressure altitude versus time curve in feet per minute. Ta_t/Ta_s was the ratio of test day ambient temperature to the standard day temperature for the test altitude. Figure 27, appendix I, shows R/D_t versus calibrated airspeed for the condition investigated.

The speed for minimum rate of descent was established as the minimum point on the curve. The tangent to this curve from the 0-0 point of the axis established the speed for maximum range in autorotation. Although the major portion of the autorotation testing was conducted at 185 rpm (100 percent) sufficient qualitative data were obtained at the lower rotor rpm of 176 (95 percent) to determine that the rate of descent was lowered by approximately 150 feet per minute. When operating at this lower rotor speed there was no noticeable difference in handling qualities of the helicopter.

AIRSPEED CALIBRATION

The standard airspeed system and the test airspeed system were calibrated throughout the airspeed range during level flight. A ground speed course was used and the test was conducted at 185 rotor rpm, 30,000-pound gross weight, mid cg, and a density altitude of sea level. The test was flown in nearly calm air (less than 3 knots).

The test system used a boom with a swivel pitot-static head. The standard airspeed system calibration was obtained for climb, level flights, and autorotation using the level flight ground speed course calibration for the test system. This assumed that the swivel pitot-static head used on the test system was unaffected by pitch and yaw angles of less than 20 degrees. The test and standard airspeed system calibration is presented in figure 28, appendix I.

POWER DETERMINATION AND ENGINE CHARACTERISTICS

The HH-53C employed an electronic torque monitoring system to measure the percent of torque being applied by each engine to the main transmission. A torque reading of 100 percent was equivalent to 3,200 shaft horsepower. The torque sensing system was located at the engine input section to the nose gearbox and was made up of the torque shaft, torque pickup, the phase detector, and the torque indicator. The torque sensor shaft consisted of an inner and outer shaft arranged so that the inner shaft was subjected to the power turbine load. The major diameter on each shaft was machined to contain 72 teeth. This portion of the shaft was the exciter. The torque pickup was a coil installed in the torque tube opposite the exciter.

The system measured torque by measuring the twist in the shaft connecting the engine to the load. To measure this twist a pickup was installed in the torque tube opposite a pair of gear teeth on the rotating shaft. As the shaft rotated, two ac signals were induced in the pickup coils. As the torque in the shaft increased, the two sets of teeth were displaced from each other as the shaft twisted and the phase angle difference between the two ac voltages changed. The output of the pickup coils was fed into a phase detector that electronically measured the phase angle change. This phase angle was then converted to an output voltage proportional to torque. Test shaft horsepower was determined from inflight torquemeter readings and rotor rpm using the following equation:

$$\frac{\text{SHP}}{\text{engine}} = \frac{(13{,}600)\ (\%\ \text{rpm})\ (\%\ Q)\ (1{,}235)}{5{,}250}$$

Shaft horsepower, fuel flow, gas producer speed, and turbine inlet temperature were corrected to standard atmospheric conditions. The engine characteristics were defined by the plots of the following parameters:

$$\frac{SHP}{\delta\sqrt{\theta}} \quad \text{vs} \quad \frac{N_1}{\sqrt{\theta}}$$

$$\frac{N_1}{\sqrt{\theta}} \quad \text{vs} \quad \frac{W_f}{\delta\sqrt{\theta}}$$

$$\frac{T_5}{\theta} \quad \text{vs} \quad \frac{N_1}{\sqrt{\theta}}$$

where

$$SHP = SHP_t \left(\frac{H_P}{CTP}\right)\sqrt{\frac{Ta_{SL}}{Tt_2}}$$

$$N_1 = N_{1_t}\sqrt{\frac{Ta_{SL}}{Tt_2}}$$

$$T_5 = T_{5_t}\left(\frac{Tt_2}{Ta_{SL}}\right)$$

and are presented in figures 168 through 175, appendix I.

STATIC LONGITUDINAL SPEED STABILITY

Static longitudinal speed stability tests were conducted at a fixed collective pitch setting. Specifically, longitudinal stick position versus airspeed and longitudinal stick movement required throughout the speed range were to be determined for most allowable cg locations. The test gross weights were varied from 31,000 to 41,000 pounds and pressure altitudes from 4,000 to 13,000 feet. Trim conditions were level flight at 35 KCAS, 0.6 V_{MAX}, 0.8 V_{MAX}, and V_{MAX}, climb at best climb airspeed, autorotation at the airspeed for minimum rate of descent, and partial power descent at 35 KCAS. Hover trim points were not obtained since the weather was not favorable at the time the speed stability testing was conducted.

The static longitudinal stability was generally positive for the conditions tested except for some neutral or slightly negative speed stability around the 35 KCAS trim point for level flight and partial power descent. The amount of negative stability encountered was not objectionable. Figure 1 shows control position as a function of airspeed for forward and aft center of gravity locations. As shown in figure 1, the slope of the curve was generally the same for both conditions and the cyclic control was displaced forward approximately 2 inches for the aft center of gravity loading, but did not change the stability characteristics of the helicopter. Tests were conducted per MIL-H-8501A.

NOTES:
LEVEL FLIGHT
AVG GROSS WEIGHT - 31,000 pounds
AVG PRESSURE ALTITUDE - 4,000 feet
ROTOR SPEED - 185 rpm

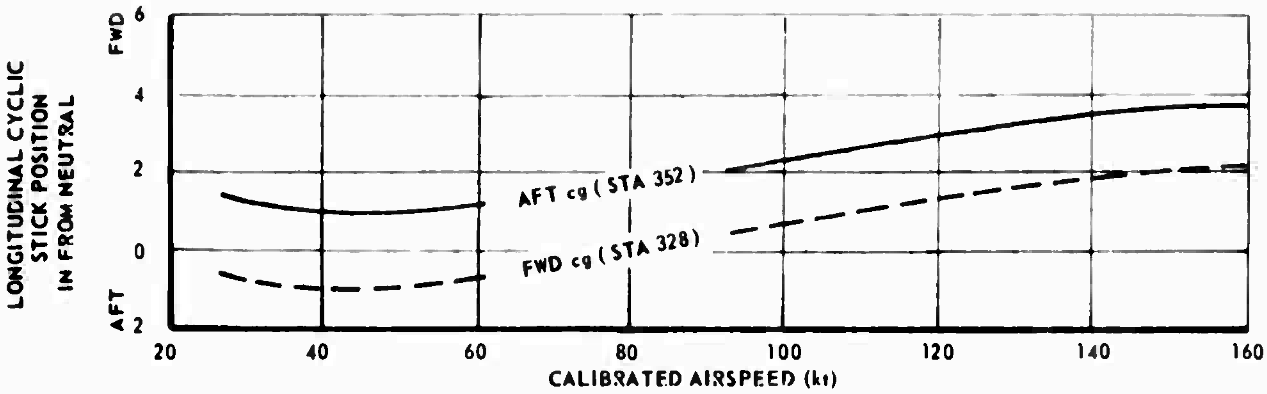

Figure 1 CENTER OF GRAVITY EFFECTS ON LONGITUDINAL CONTROL POSITION

The HH-53C did not meet the requirements of MIL-H-8501A in that the maximum airspeed trim points were usually limited by full up collective pitch. At the maximum airspeed trim point with an aft center of gravity, there was approximately 10-percent of the longitudinal cyclic control remaining. All the static longitudinal speed stability testing was conducted at 100-percent rotor speed (185 rpm) and therefore speed stability characteristics at a different rotor speed were not determined. Results of the static longitudinal speed stability tests are presented in figures 29 through 50, appendix I.

STATIC DIRECTIONAL STABILITY

Static directional stability of the HH-53C was investigated for similar flight conditions as the static longitudinal speed stability to determine compliance with MIL-H-8501A requirements. All static directional stability tests were conducted at the full aft cg location (352) with the AFCS operative and inoperative.

In conducting this test, the aircraft was trimmed in stabilized flight at a zero sideslip angle, and then the sideslip angle was introduced in both directions by opposite use of lateral stick and directional pedals while maintaining a constant airspeed.

In level flight the dihedral effects increased with increasing airspeed and altitude. Inoperative AFCS had no effect on the static directional stability characteristics of the aircraft. The data in figures 51 through 65, appendix I, show positive dihedral effect and static directional stability for the flight conditions and aircraft configurations investigated.

SIDEWARD AND AND REARWARD FLIGHT

Sideward and rearward flight tests were conducted on the HH-53C to determine the static stability characteristics of the helicopter in these flight regimes and determine compliance with MIL-H-8501A.

The HH-53C had acceptable sideward flight characteristics. Below translational lift (15 knots), smooth and steady flight was possible with a minimum of control inputs and no difficulty was encountered in holding the desired heading. During translational lift (15 to 25 knots) directional control was difficult and numerous control inputs were required to hold the desired heading. Above 25 knots, sideward flight was again smooth and steady. Examination of this data showed that there was adequate lateral cyclic control and directional control for sideward flight to the left and right up to 35 KTAS. The result of the sideward flight test is presented in figure 66, appendix I. At 35 KTAS to the right, there was less than 1 inch of pedal control remaining, which is less than 10 percent of the total control travel available. Adequate lateral control to hold attitude was available and from figure 66, appendix I, it can be observed that a linear gradient of lateral stick required versus airspeed existed from hover to 35 KTAS right. From translational lift sideward to the left, the lateral stick gradient was essentially flat and required approximately 1/2-inch left lateral stick out to 35 KTAS. This flat gradient presented no problems for sideward flight out to 35 KTAS.

Sideward flight tests with an asymmetric loading were not conducted during this test program. From the data obtained at the symmetrical loading condition investigated, it would seem likely that with an asymmetric loading (a full left external fuel tank and a jettisoned right external fuel tank) that the maximum airspeed obtainable in right sideward flight may be limited by directional pedal control. Therefore, with an asymmetric loading it would appear that the maximum crosswind component will be reduced when hovering over a spot, resulting in a degradation of the mission capability.

Rearward flight was tested from 0 to 32 KTAS. From a hover the helicopter accelerated easily into rearward flight. As translational lift was reached the HH-53C had a nose down tendency which required a 1-inch aft cyclic input to prevent nose down pitching. Above translational lift speed, the longitudinal cyclic stick gradient becomes nearly flat out to 32 KTAS when approximately 2 inches or 20 percent of aft longitudinal stick control remained. The graphic results of the rearward flight test are presented in figure 67, appendix I. To recover from rearward flight, the nose was lowered slightly to slow down, and at about 15 KTAS a turn to the right was started with the directional pedals. This resulted in a roll to the left. Full right cyclic control was just sufficient to stop this, but not enough to initiate a roll back to the right. An attempt to use the above maneuver to recover from rearward flight with an asymmetric loading, as described in sideward flight, would result in very marginal handling qualities and would be hazardous.

The sideward and rearward flight tests were conducted at 41,000 pounds gross weight with a cg location at the forward limit of 328 inches. The sideward and rearward flight operations were conducted in ground effect at a wheel height of approximately 20 feet at 185 rpm rotor speed.

DYNAMIC STABILITY

Dynamic stability characteristics were determined by analysis of the aircraft reaction to pulse type control inputs. The duration of the pulses were approximately 1 second with a magnitude of approximately 1 inch for longitudinal and lateral control and 2 inches for the directional control. A mechanical jig was used in making precise pulse inputs.

Hover

Dynamic stability in a hover (IGE) at sea level was investigated at forward and aft cg locations at 31,000 and 41,000 pounds gross weight with the AFCS both operative and inoperative. Aircraft reactions to all control inputs were comparable regardless of the gross weight or cg location.

The HH-53C was dynamically stable about all axes with the AFCS on and its rates were damped out within 2 seconds after the pulse inputs.

A pitch-roll-yaw coupling with the AFCS inoperative was slightly evident during longitudinal pulse disturbances. This coupling characteristic became more evident as gross weight was increased.

A pitch-roll-yaw coupling was produced during a lateral disturbance with the AFCS inoperative. Following the lateral pulse the helicopter's initial motion was in the proper direction, and approximately 1 second after pulse input the aircraft began to roll in the opposite direction at a slower rate accompanied by an oscillating pitch attitude and an increasing yaw rate in the direction of control input; this continued until recovery was made.

A directional pedal pulse produced a pitch-roll-yaw coupling of which the lateral-directional coupling was the most significant. Following a directional input the helicopter motion was an immediate yaw in the proper direction and this was accompanied by a roll oscillation in a direction opposite to the control input.

The results of the hover dynamic stability testing are presented in the form of time histories in figures 68 through 73, appendix I.

Climb

Dynamic stability characteristics during climb were investigated at a climb speed of 62 KCAS. Test conditions were 31,000 pounds gross weight, 15,000 feet density altitude, and an aft cg location with the AFCS on and off. A rotor speed of 185 rpm was used during the climb dynamic stability investigation.

The helicopter was stable about all axes following an artificial disturbance with the AFCS on. With the AFCS off, recovery was necessary in approximately 1-1/2 seconds following a longitudinal control pulse because of the high pitching attitudes.

The aircraft reaction to a lateral pulse with the AFCS off produced a pitch-roll-yaw coupling with the lateral-directional coupling predominating. The rolling motion was in the proper direction, followed by a divergent rolling motion in the opposite direction, requiring corrective action approximately 2-1/2 seconds after the pulse input.

Helicopter motion following a directional pedal pulse with the AFCS off produced an evident roll-yaw coupling. This significant yaw oscillation was accompanied by a roll in the direction of control pulse input, requiring a recovery maneuver approximately 3 seconds after control input. The results of the climb dynamic stability testing are presented in figures 74 through 79, appendix I.

Level Flight

Dynamic stability characteristics in level flight were determined at 31,000 and 41,000 pounds gross weight, 5,000 and 15,000 feet density altitude, and at the full forward and aft cg locations with the AFCS on and off. Airspeeds investigated were 50 KCAS, 0.6 V_{MAX}, and 0.8 V_{MAX}.

With the AFCS operative, the helicopter exhibited good dynamic stability about all axes after pulse inputs. Damping was high about the longitudinal and lateral axes and only slightly positive following a directional disturbance. With the AFCS inoperative, a longitudinal pulse input produced a divergent pitching moment in the proper direction requiring a recovery maneuver within 1 second at 0.8 V_{MAX}. This value increased to 2 seconds at 50 KCAS. In both cases, recovery was started after about 15 degrees of attitude change.

Following a lateral disturbance with the AFCS inoperative, an immediate pitch-roll-yaw coupling was present. Lateral-directional coupling was the most significant. A rolling motion was produced in the direction of control input followed by a divergent rolling oscillation in the other direction requiring a recovery maneuver. This divergence in roll was accompanied by a diverging pitch attitude. This coupling was more noticeable at the higher airspeeds.

Pitch-roll-yaw coupling was present for disturbances about the directional axis with the AFCS inoperative. Again the lateral-directional coupling was the most significant. Directional pulses resulted in attitude changes in the direction of input. The attitudes, rates, and accelerations generated required aircraft recovery when divergence in one or more axes became evident.

Representative time histories of the helicopter motion following pulse control displacement during level flight are presented in figures 80 through 85, appendix I.

CONTROLLABILITY

Time histories resulting from approximately 1 inch step control inputs were used in evaluating the controllability. Control power, control response, and control sensitivity were determined for various magnitudes of control displacement. As in dynamic stability, a jig was used to insure a constant control displacement. Flight conditions investigated were similar to those evaluated during the dynamic stability portion of the test program.

Hover

The controllability in hover IGE was determined by analysis of the time histories resulting from the step control displacement. The helicopter's control power, control response, and control sensitivity obtained from various magnitudes of control inputs are plotted in figures 110 through 115, appendix I. Table II presents a general summary of these results obtained from a 1-inch control step input. As indicated by this table, the longitudinal and lateral requirements of MIL-H-8501A were met for both VFR and IFR flight with the AFCS both operative and inoperative, but these requirements were not met in the directional axis. Time histories resulting from 1-inch step inputs are presented in figures 86 through 109, appendix I.

Climb and Autorotation

The climb and autorotational longitudinal and lateral controllability characteristics were similar. The directional angular acceleration and velocity were slightly greater during autorotation than climb. In any case there was always adequate control power to correct for gust disturbances and for maneuvering during climbs and autorotations. These

Table II

AIRCRAFT RESPONSE TO STEP INPUT IN HOVER

Gross Weight = 31,000 Pounds   Pressure Altitude = Sea Level

Axis	Attitude Displacement (deg/in.)	Time Lapse (sec)*	Maximum Angular Velocity (deg/sec/in.)	Time Lapse (sec)**	Maximum Angular Acceleration ($deg/sec^2/in.$)	Time Lapse (sec)**
AFCS ON, AFT CG (352 INCHES)						
Pitch	2.6 UP /3.0 DOWN	1.0	4.0 UP /3.5 DOWN	0.87	9.0 UP /7.5 DOWN	0.33
Roll	2.0 LEFT/2.2 RIGHT	0.5	6.0 LEFT/6.0 RIGHT	0.56	10.7 LEFT/12.5 RIGHT	0.19
Yaw	2.7 LEFT/2.3 RIGHT	1.0	4.0 LEFT/3.7 RIGHT	0.89	6.0 LEFT/5.0 RIGHT	0.14
AFCS OFF, AFT CG (352 INCHES)						
Pitch	3.5 UP /3.7 DOWN	1.0	6.5 UP /8.3 DOWN	1.50	9.0 UP /7.5 DOWN	0.32
Roll	2.8 LEFT/3.5 RIGHT	0.5	10.5 LEFT/11.8 RIGHT	1.09	13.0 LEFT/11.2 RIGHT	0.19
Yaw	3.7 LEFT/3.5 RIGHT	1.0	5.3 LEFT/5.0 RIGHT	0.83	6.0 LEFT/5.0 RIGHT	0.21
AFCS ON, FWD CG (328 INCHES)						
Pitch	2.4 UP /2.2 DOWN	1.0	3.5 UP /4.0 DOWN	1.0	6.7 UP /6.8 DOWN	0.4
Roll	2.2 LEFT/2.0 RIGHT	0.5	7.0 LEFT/6.5 RIGHT	0.5	16.0 LEFT/19.0 RIGHT	0.19
Yaw	2.0 LEFT/1.6 RIGHT	1.0	10.0 LEFT/10.0 RIGHT		7.0 LEFT/6.5 RIGHT	0.15
AFCS OFF, FWD CG (328 INCHES)						
Pitch	3.1 UP /3.2 DOWN	1.0	7.5 UP /7.7 DOWN	1.5	6.7 UP /6.8 DOWN	0.4
Roll	4.4 LEFT/4.1 RIGHT	0.5	12.0 LEFT/14.0 RIGHT	1.2	16.0 LEFT/19.0 RIGHT	0.24
Yaw	2.5 LEFT/2.5 RIGHT	1.0	18.5 LEFT/16.0 RIGHT		8.5 LEFT/8.3 RIGHT	0.25

*MIL-H-8501A specified these time delays before measuring attitude change following a 1-inch control step input.

**Time required to reach maximum angular velocity or angular acceleration.

conditions and results of the 1-inch control step inputs are tabulated in table III. Time histores resulting from 1-inch step control inputs are presented in figures 116 through 127, appendix I. The aircraft's sensitivity and response for various control inputs are presented in figures 128 through 130, appendix I.

Level Flight

Time histories resulting from approximately 1-inch step inputs were obtained during level flight and are presented in figures 131 through 142, appendix I. AFCS had very little effect, under the conditions tested, on the longitudinal and lateral response and sensitivity to the above control inputs. These results are summarized in table IV, and were obtained from the various controllability plots presented in figures 143 through 145, appendix I. Overall, the control effectiveness was lower during level flight than while hovering or during climb and autorotation.

AFCS HARDOVERS

The AFCS incorporated in the HH-53C was composed of two systems which gave redundancy in pitch and roll but not in yaw. Hardover failures were electrically induced in one axis of one AFCS while the remaining axis of that AFCS and the remaining axes of the second AFCS were operating normally. The gross weight and cg location for these tests were 31,000 pounds and 328 inches.

Table III

AIRCRAFT RESPONSE TO STEP INPUT DURING CLIMB AND AUTOROTATION

Gross Weight = 31,000 Pounds   Pressure Altitude = 15,000 Feet

AFCS ON, MID CG (340 INCHES)

Maximum Angular Velocity (deg/sec/in.)	Time Lapse (sec)*	Maximum Angular Acceleration (deg/sec^2/in.)	Time Lapse (sec)*
CLIMB AT 62 KCAS			
3.0 UP /3.7 DOWN	1.09	4.5 UP /4.7 DOWN	0.37
5.7 LEFT/6.0 RIGHT	0.56	9.0 LEFT/10.3 RIGHT	0.19
1.5 LEFT/1.8 RIGHT	1.45	2.5 LEFT/3.5 RIGHT	0.14
AUTOROTATION AT 72 KCAS			
3.0 UP /3.7 DOWN	0.92	4.5 UP /4.7 DOWN	0.32
5.7 LEFT/6.0 RIGHT	0.53	9.0 LEFT/10.3 RIGHT	0.26
2.5 LEFT/2.2 RIGHT	1.75	3.7 LEFT/3.5 RIGHT	0.13

*Time required to reach maximum angular velocity or angular acceleration.

Table IV

AIRCRAFT RESPONSE TO STEP INPUT DURING LEVEL FLIGHT Gross Weight = 41,000 Pounds Pressure Altitude = 7,000 Feet 113 KCAS			
Maximum Angular Velocity (deg/sec/in.)	Time Lapse (sec)*	Maximum Angular Acceleration ($deg/sec^2/in.$)	Time Lapse (sec)*
AFCS ON, FWD CG (328 INCHES)			
2.5 UP /2.0 DOWN	0.67	3.0 UP /3.5 DOWN	0.45
3.0 LEFT/3.5 RIGHT	0.54	5.5 LEFT/5.2 RIGHT	0.33
1.0 LEFT/1.0 RIGHT	0.63	1.3 LEFT/1.1 RIGHT	0.20
AFCS OFF, FWD CG (328 INCHES)			
2.8 UP /2.0 DOWN	0.75	4.5 UP /4.5 DOWN	0.58
5.5 LEFT/5.2 RIGHT	0.53	8.0 LEFT/8.0 RIGHT	0.48
1.0 LEFT/1.0 RIGHT	0.75	1.3 LEFT/1.1 RIGHT	0.20

*Time required to reach maximum angular velocity or angular acceleration.

While hovering, a hardover about the pitch axis resulted in a mild pitch up or pitch down in the appropriate direction. After the failure of the pitch channel, about 2 seconds were required before the redundant AFCS system damped this pitching moment and the aircraft then assumed a new pitch altitude up to 10 degrees different than before hardover. A hardover about the yaw axis resulted in a pure divergent yaw in the correct direction. After a hardover in yaw, corrective action was initiated after an attitude change of 15 degrees. This was reached 2 seconds after the hardover was induced. A 10 degree per second rate was the maximum encountered during a yaw hardover in either direction. In all cases investigated the aircraft had a mild reaction to all AFCS hardovers during hover.

AFCS hardovers were conducted for climb and autorotation at airspeeds for best rate of climb and minimum rate of descent. Maximum pitch rates of 5 degrees per second were encountered 1 second after the hardover was induced, and this same rate was obtained from a roll hardover in 1/2 second. Response to hardover inputs in yaw during climb and autorotation were divergent with rates of 6 degrees per second occurring 2 seconds after hardover.

During level flight, hardovers were induced in each axis at 50 and 130 KCAS. Maximum pitch and roll rates of 5 degrees per second were reached 1 second and 1/2 second, respectively, after the AFCS hardover was induced. AFCS yaw hardover at 50 KCAS resulted in divergent yawing with a maximum yaw rate of 6 degrees per second obtained in 1-1/2 seconds. The same results were obtained at 130 KCAS, and in addition the aircraft had a 5 degree per second roll rate in the direction of yaw.

Time histories of the hardovers conducted during this test program are presented in figures 146 through 167, appendix I.

APPENDIX I

data plots and flight log

5 - Foot Wheel Height
450 - gallon tiptanks installed
engines not equipped with EAPS

NOTE: Solid symbols denote free flight hover.

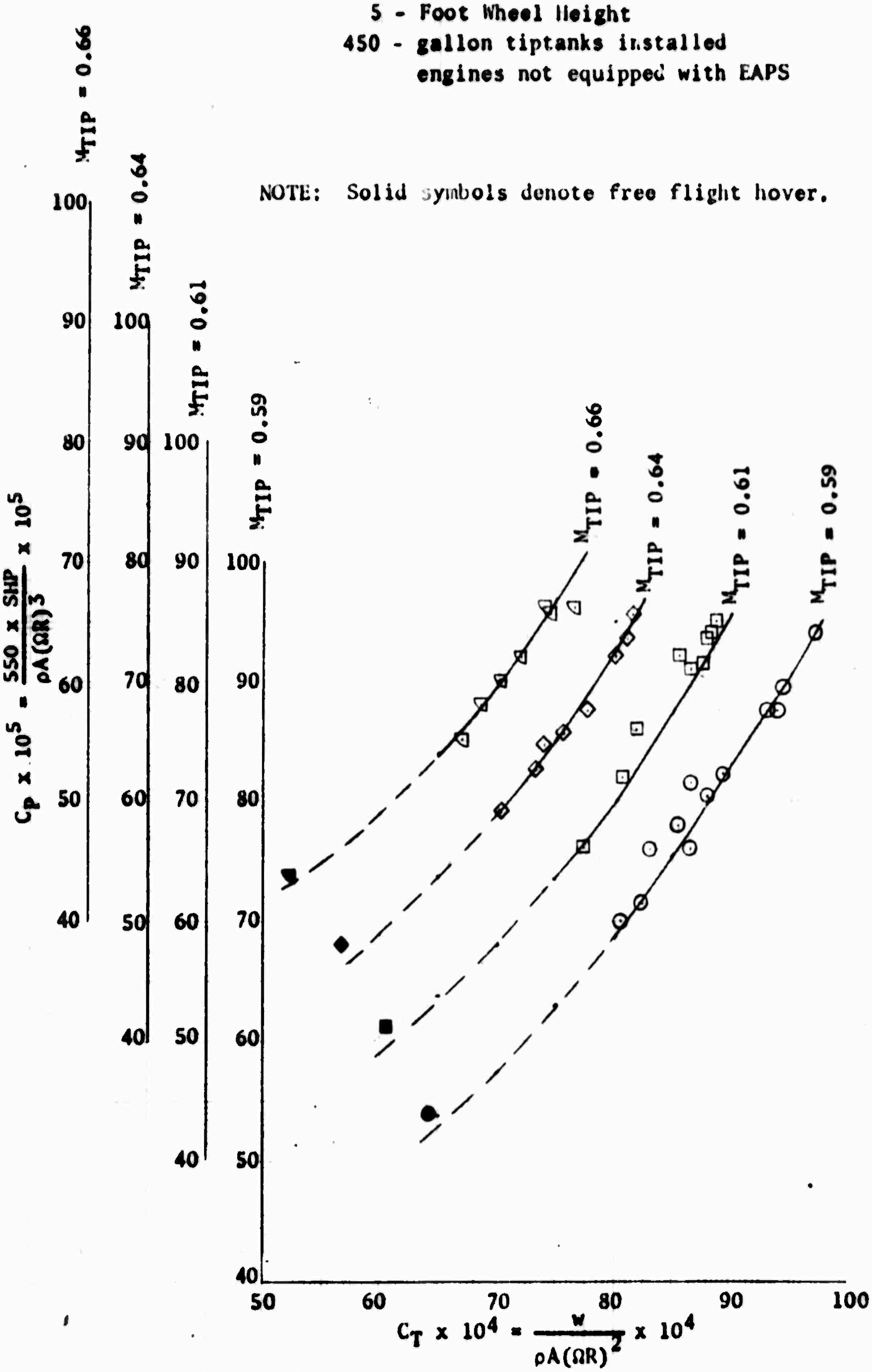

Figure 1. Nondimensional Hovering Performance

HH-53C USAF S/N 62-12577
T64-GE-7 Engines

10 - Foot Wheel Height
450 - gallon tiptanks installed
engines not equipped with EAPS

NOTE: Solid symbols denote free flight hover.

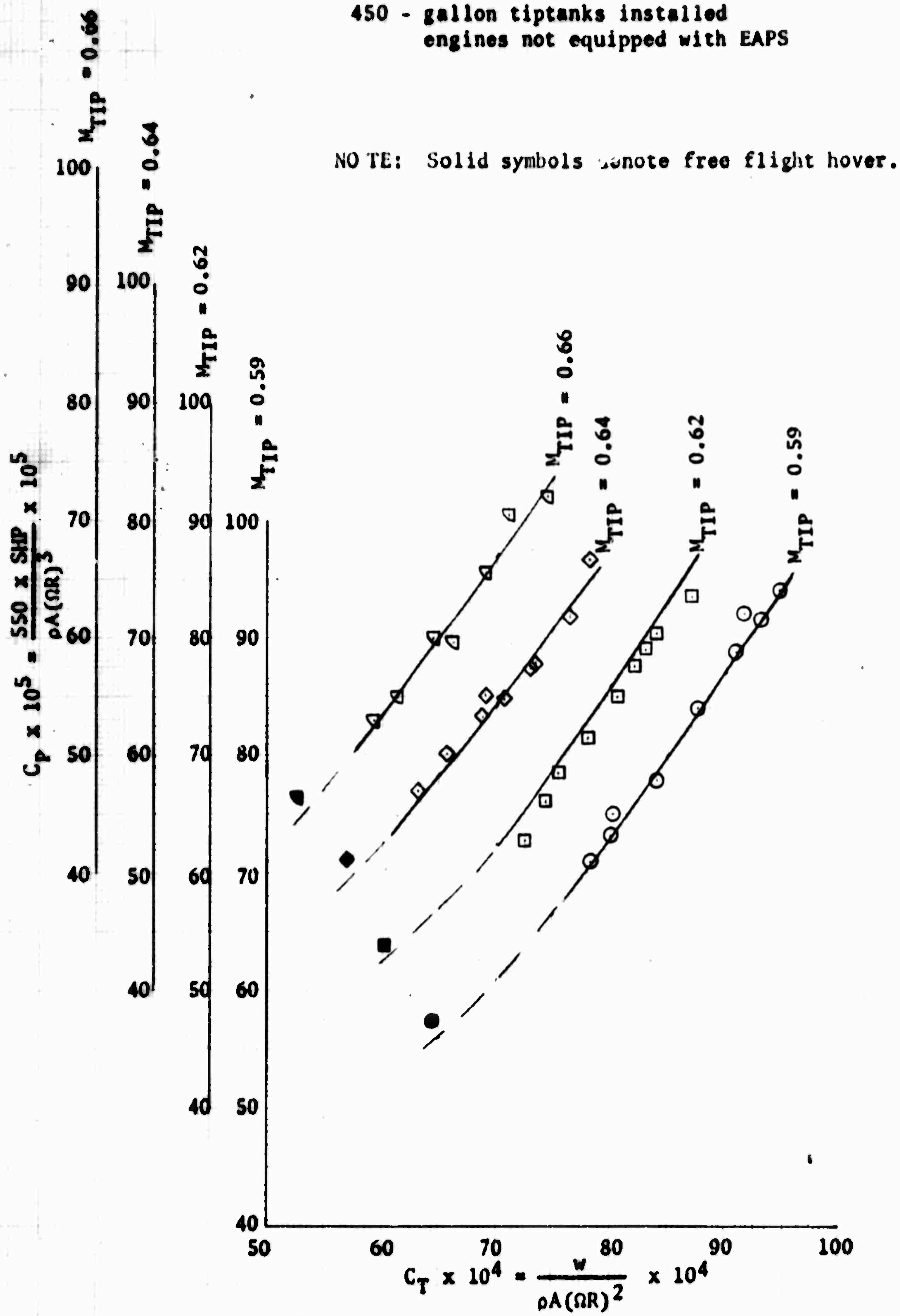

Figure 2. Nondimensional Hovering Performance

HH-53C USAF S/N 62-12577
T64-GE-7 Engines

22 - Foot Wheel Height
450 - gallon tiptanks installed
engines not equipped with EAPS

NOTE: Solid symbols denote free flight hover.

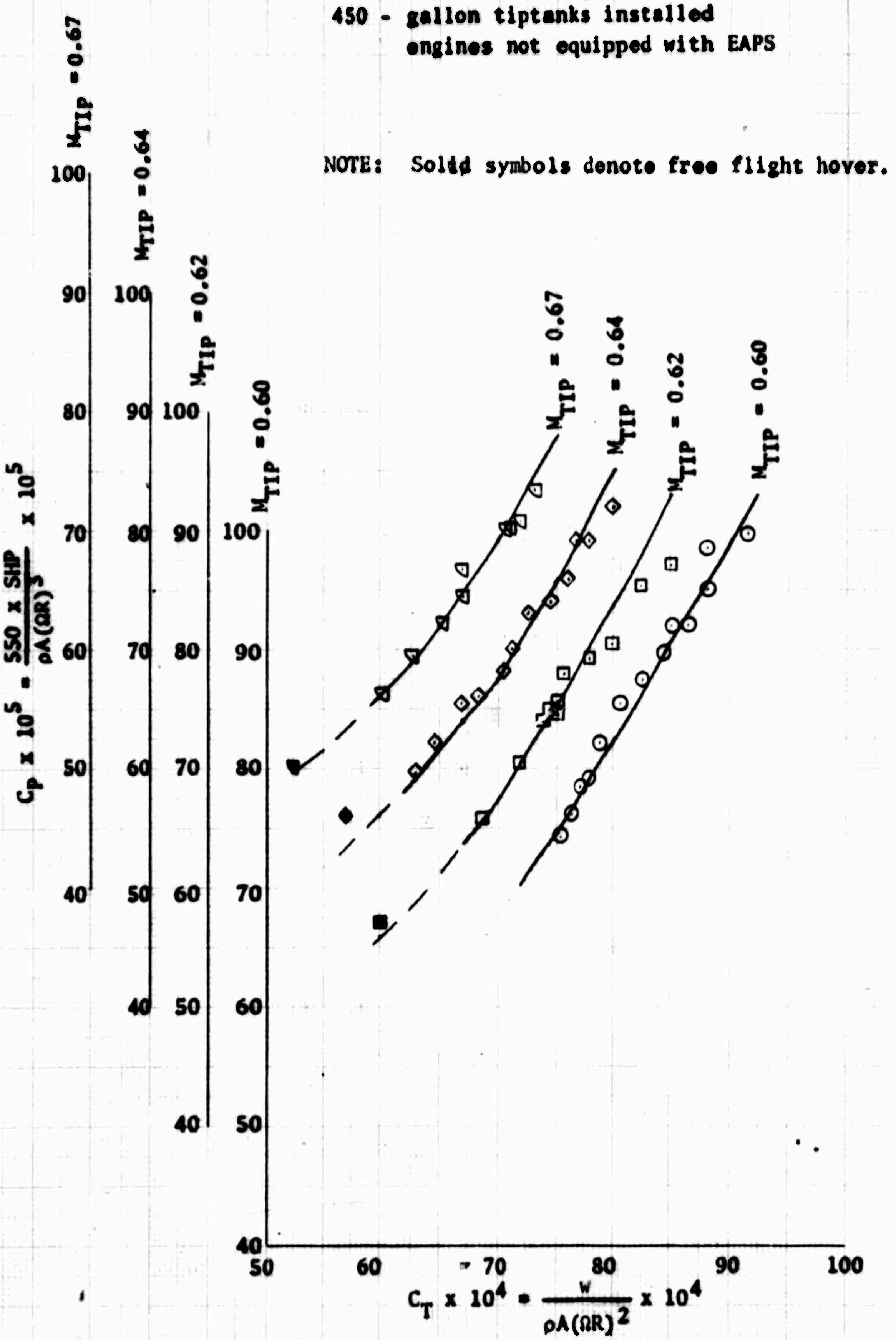

Figure 3. Nondimensional Hovering Performance

HH-53C USAF S/N 62-12577
T64-GE-7 Engines

47 - Foot Wheel Height
450 - gallon tiptanks installed
engines not equipped with EAPS

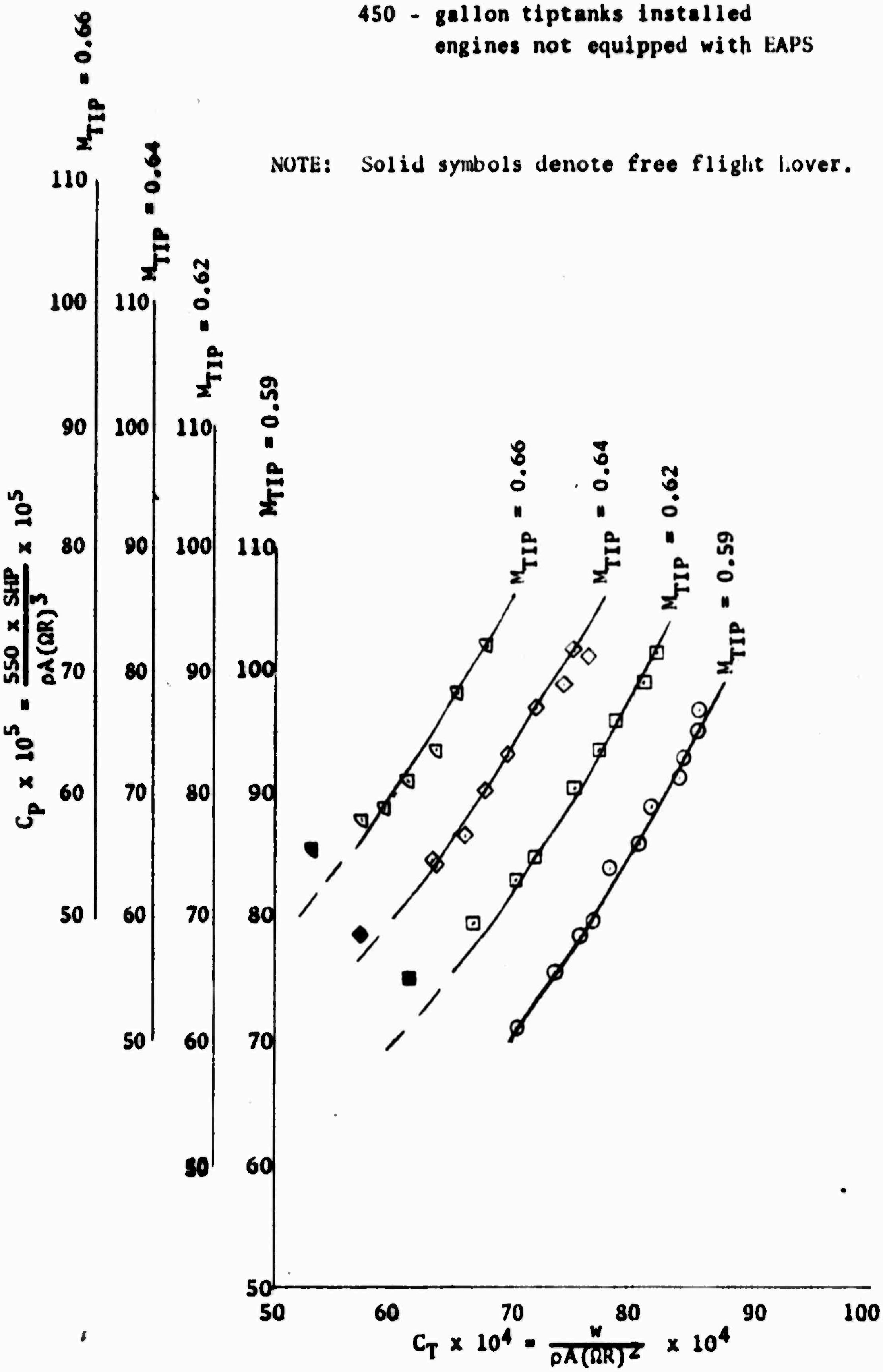

Figure 4. Nondimensional Hovering Performance

HH-53C USAF S/N 62-12577
T64-GE-7 Engines

80 - Foot Wheel Height
450 - gallon tiptanks installed
engines not equipped with EAPS

NOTE: Solid symbols denote free flight hover.

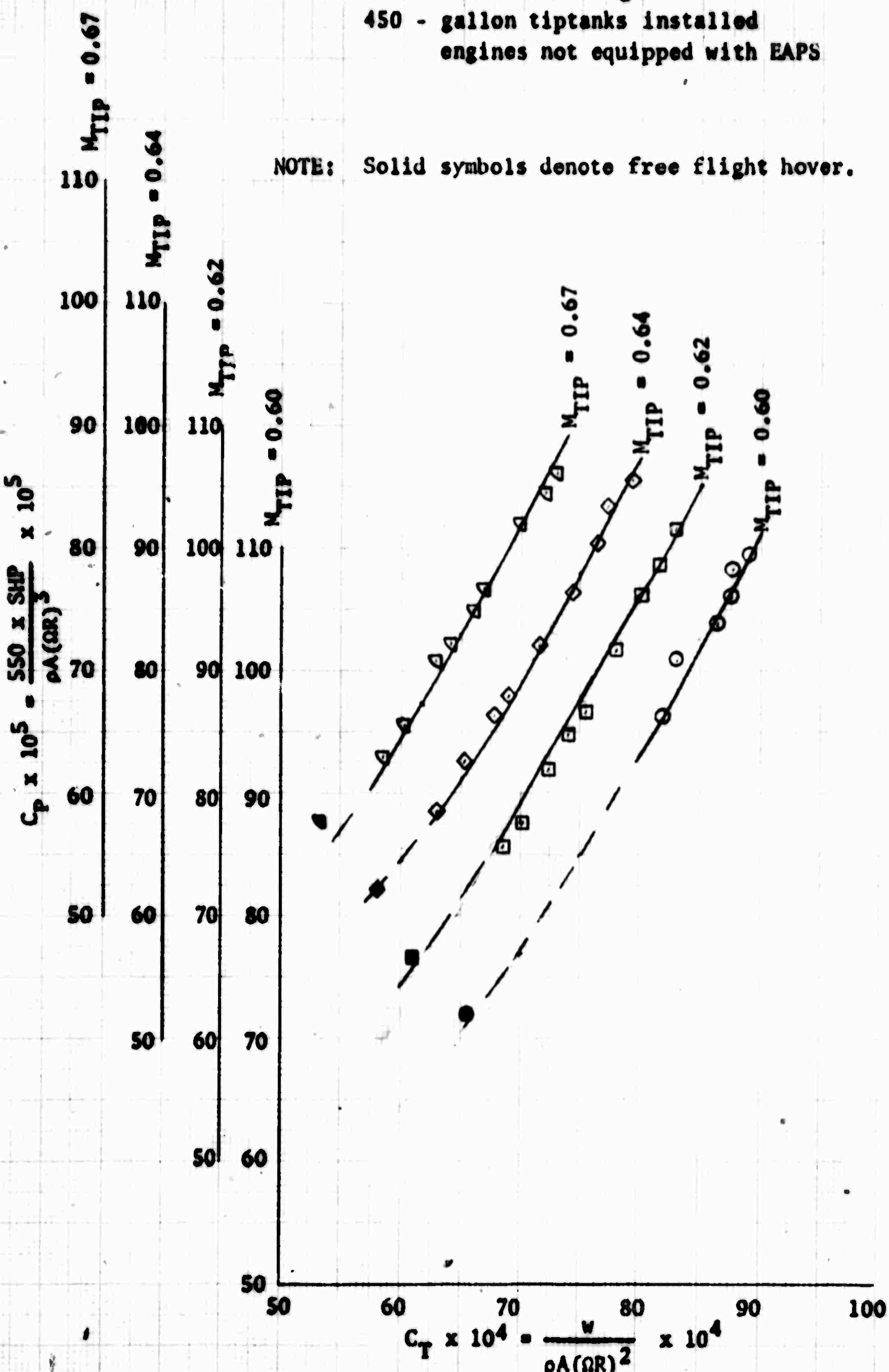

Figure 5. Nondimensional Hovering Performance

HH-53C USAF S/N 62-12577
T64-GE-7 Engines

100 - Foot Wheel Height
450 - gallon tiptanks installed
engines not equipped with EAPS

NOTE: Solid symbols denote free flight hover.

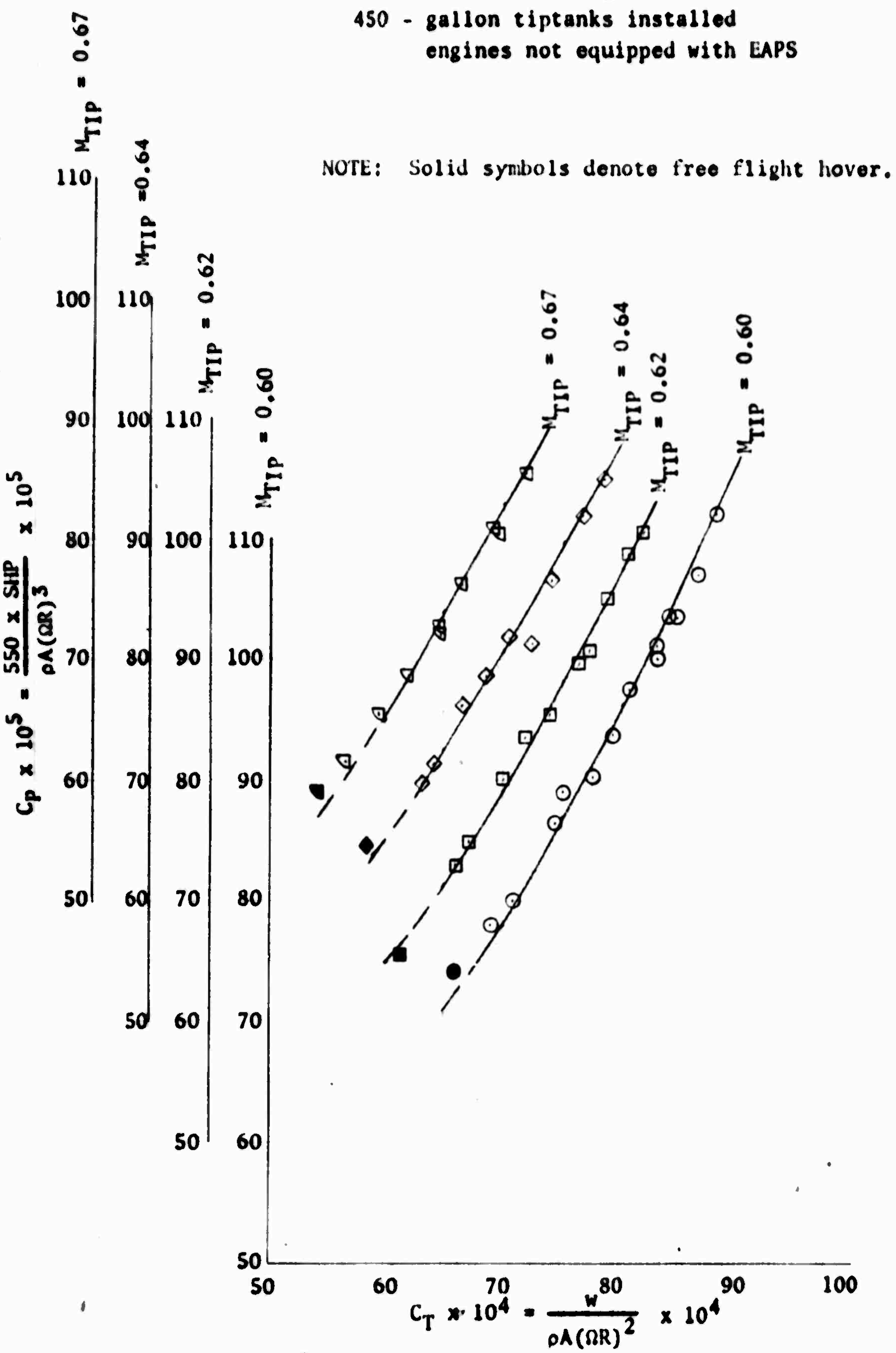

Figure 6. Nondimensional Hovering Performance

HH-53C USAF S/N 67-14993
T64-GE-7 Engines

Symbol	Avg GW (lb)	Avg Press Alt (ft)	Avg FAT (°C)	Avg cg (in)	Rotor Speed (rpm)
◇	35,000	4,500	6	340	185
□	35,000	7,000	17	340	185
○	35,000	14,000	2	340	185

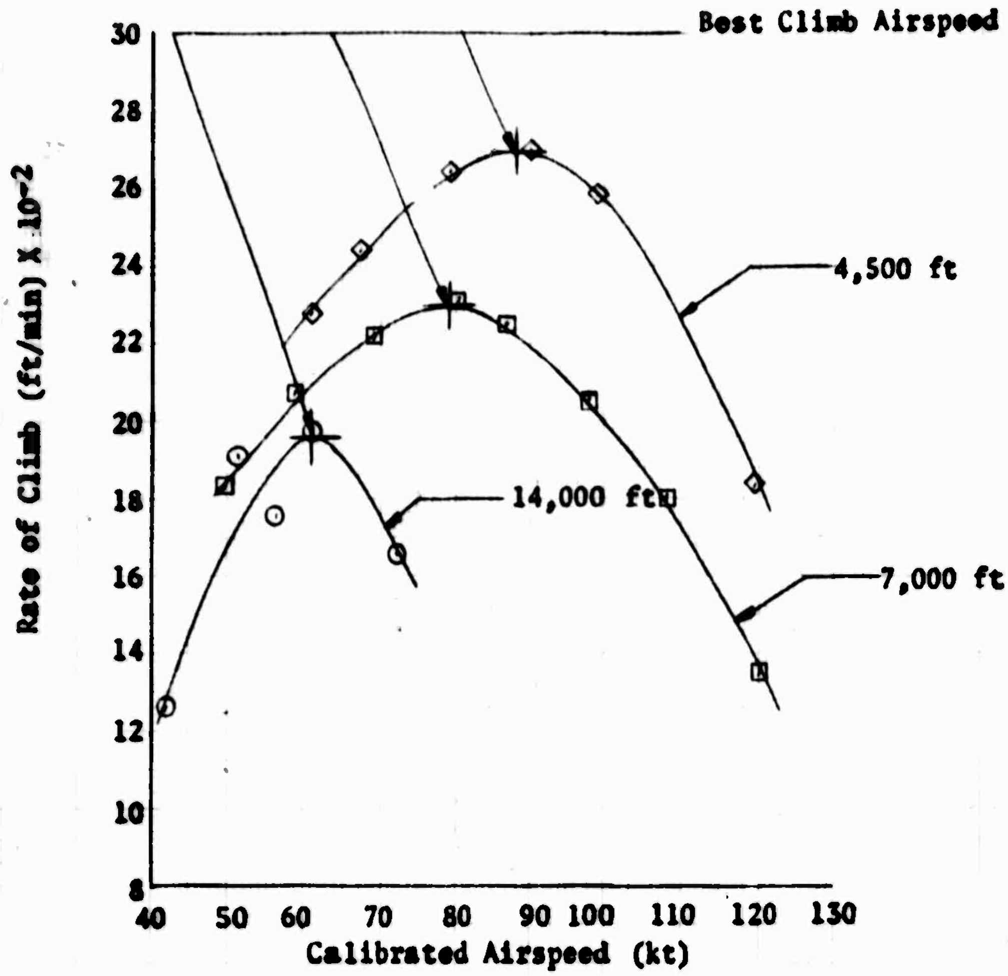

Figure 7 Sawtooth Climb Performance

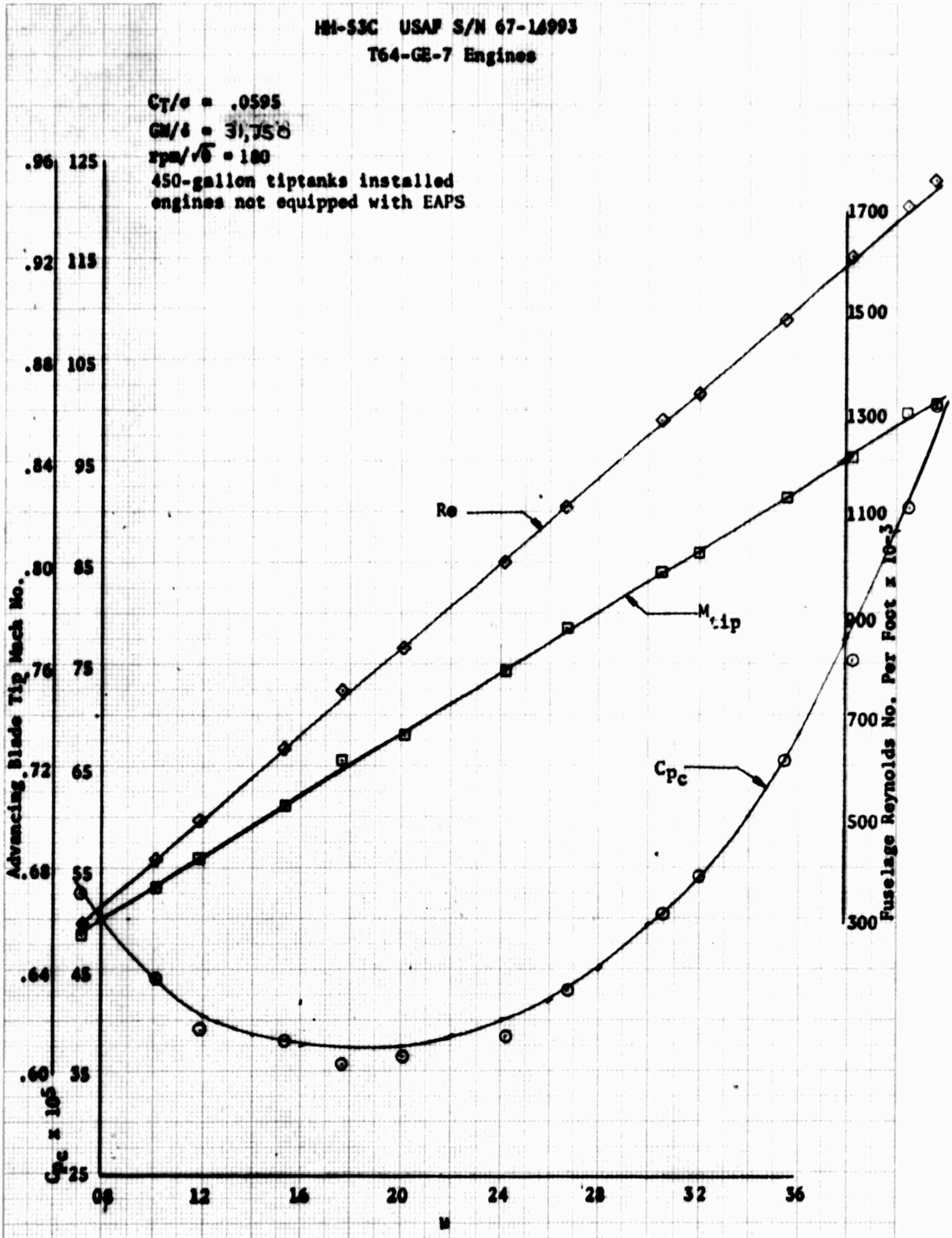

Figure 8. Level Flight Performance

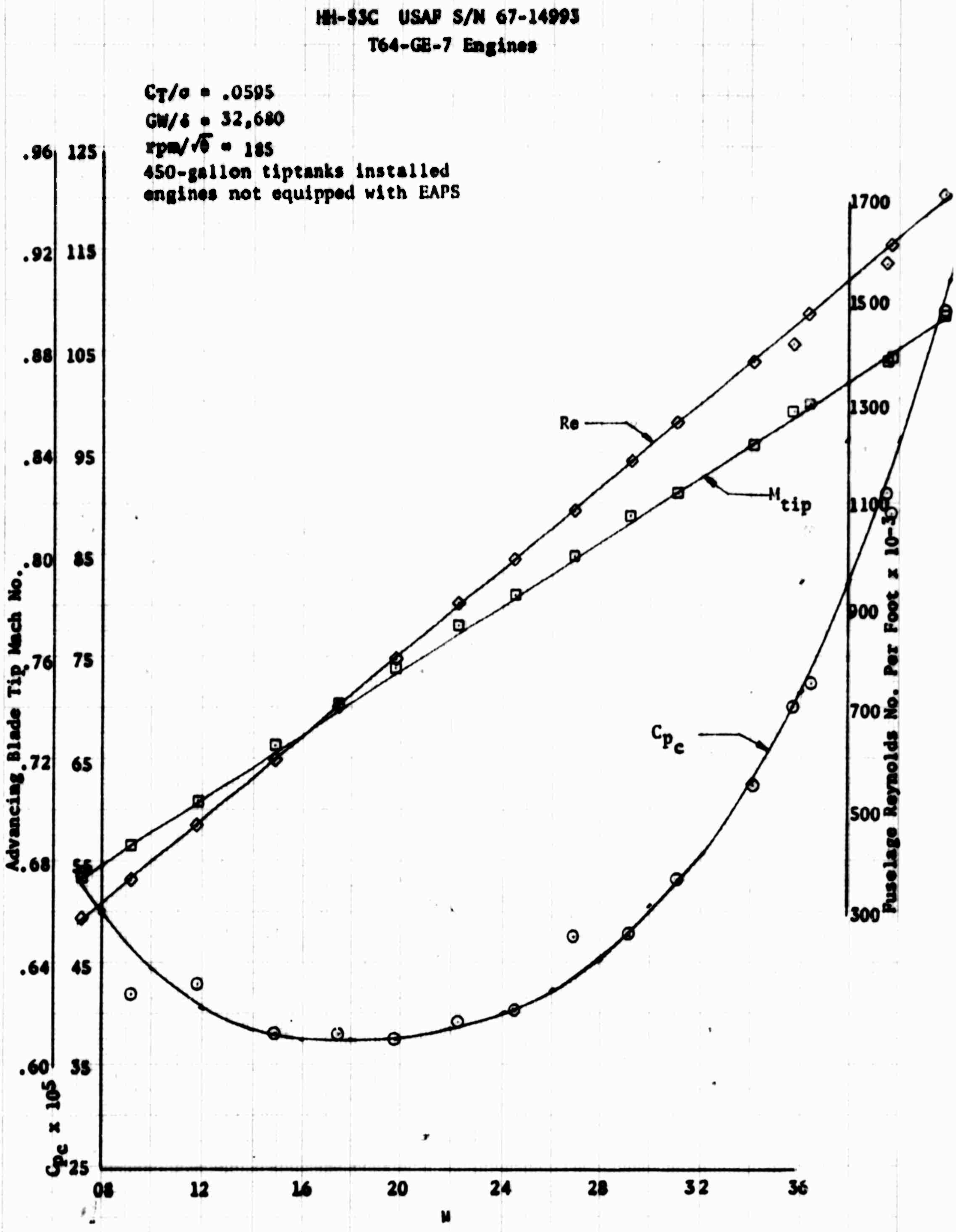

Figure 9. Level Flight Performance

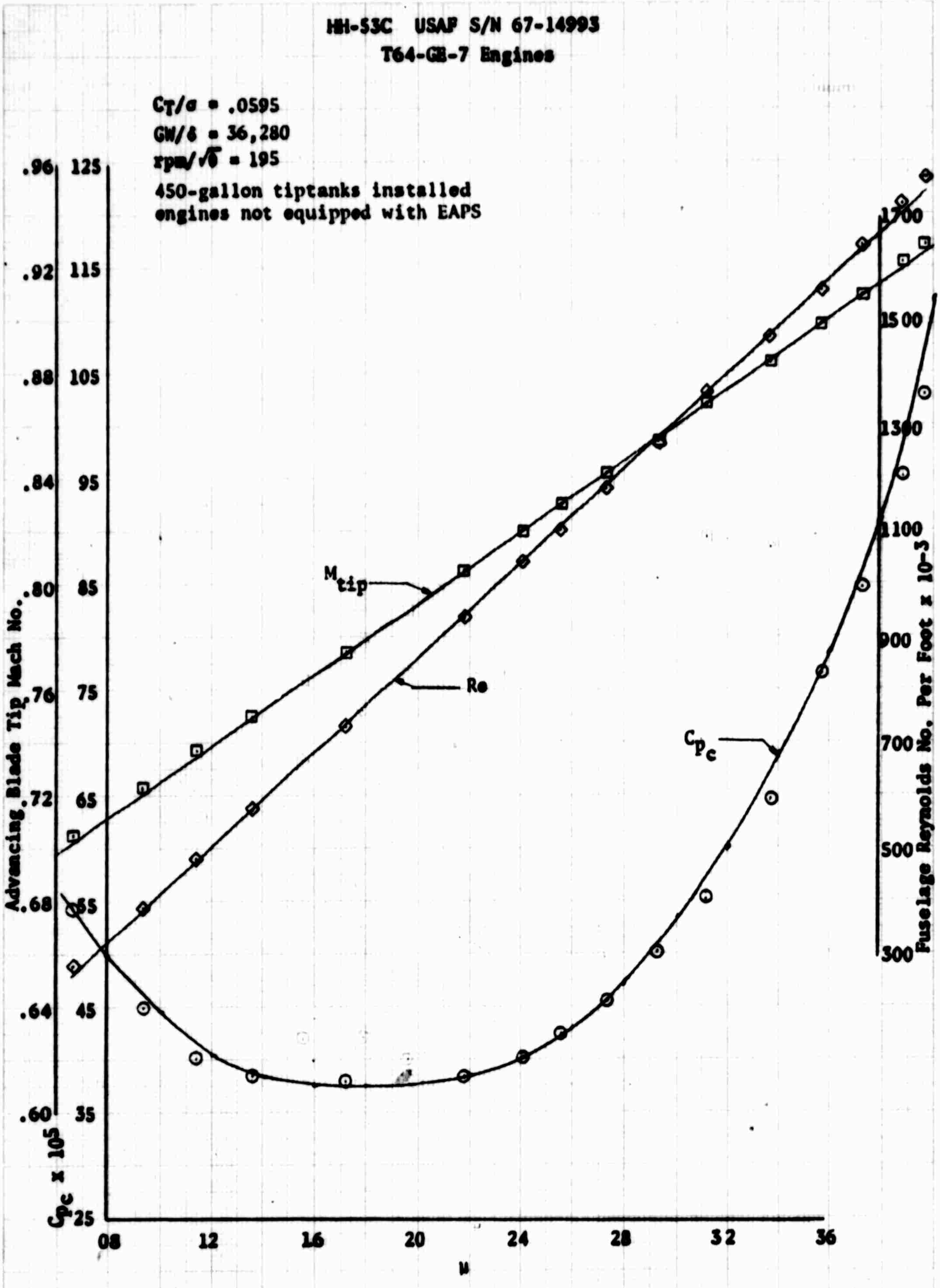

Figure 10. Level Flight Performance

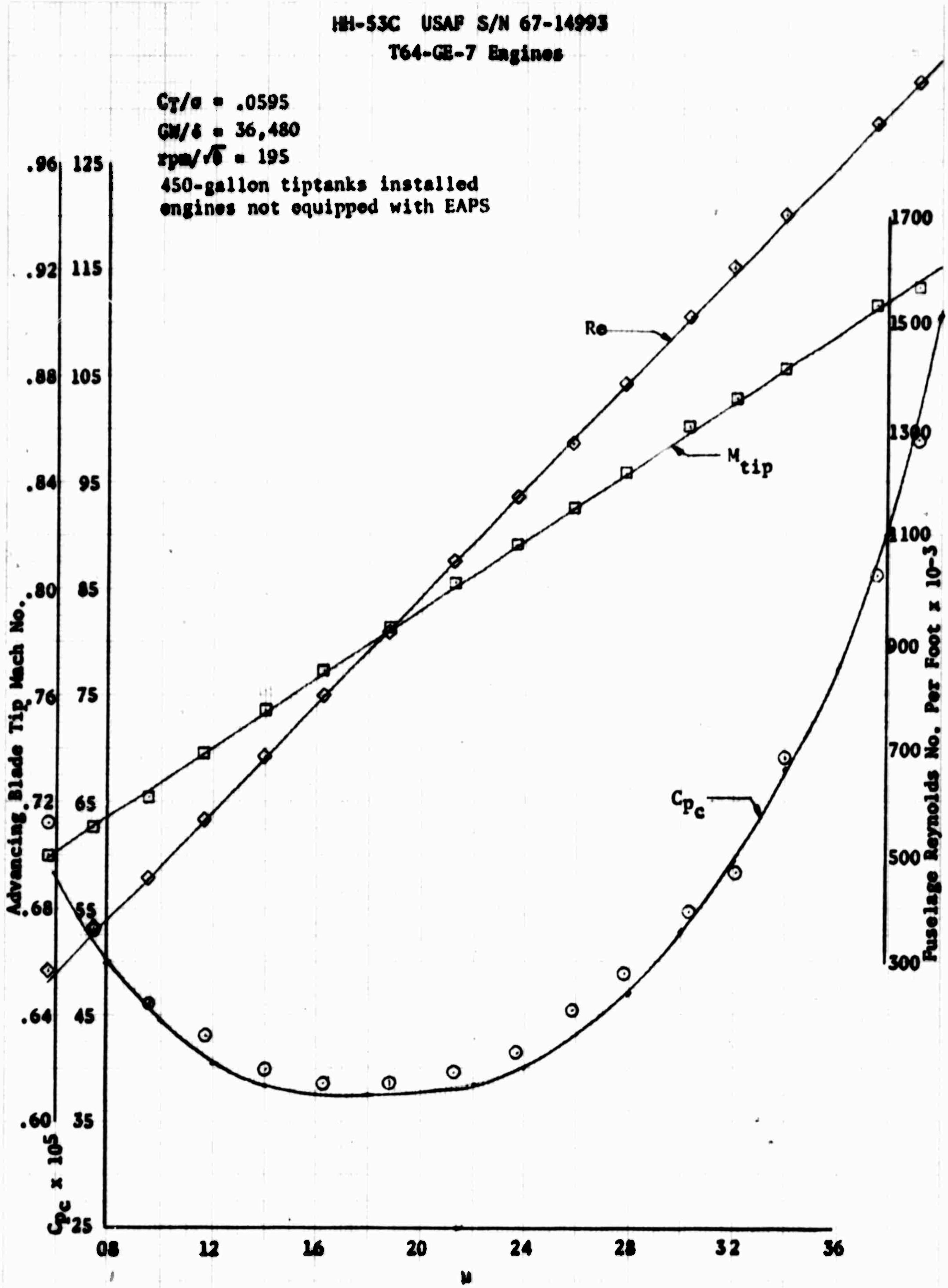

Figure 11. Level Flight Performance

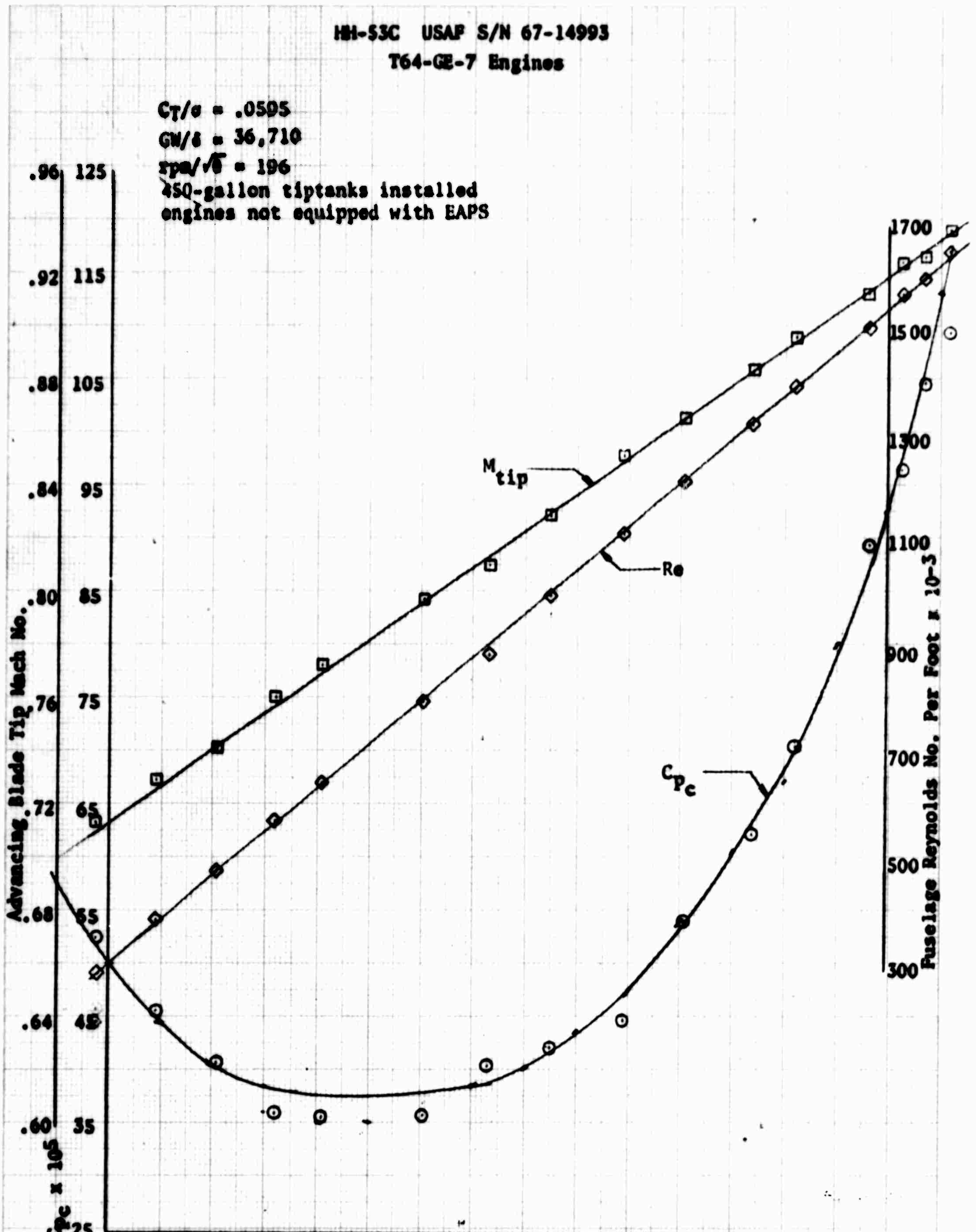

Figure 12. Level Flight Performance

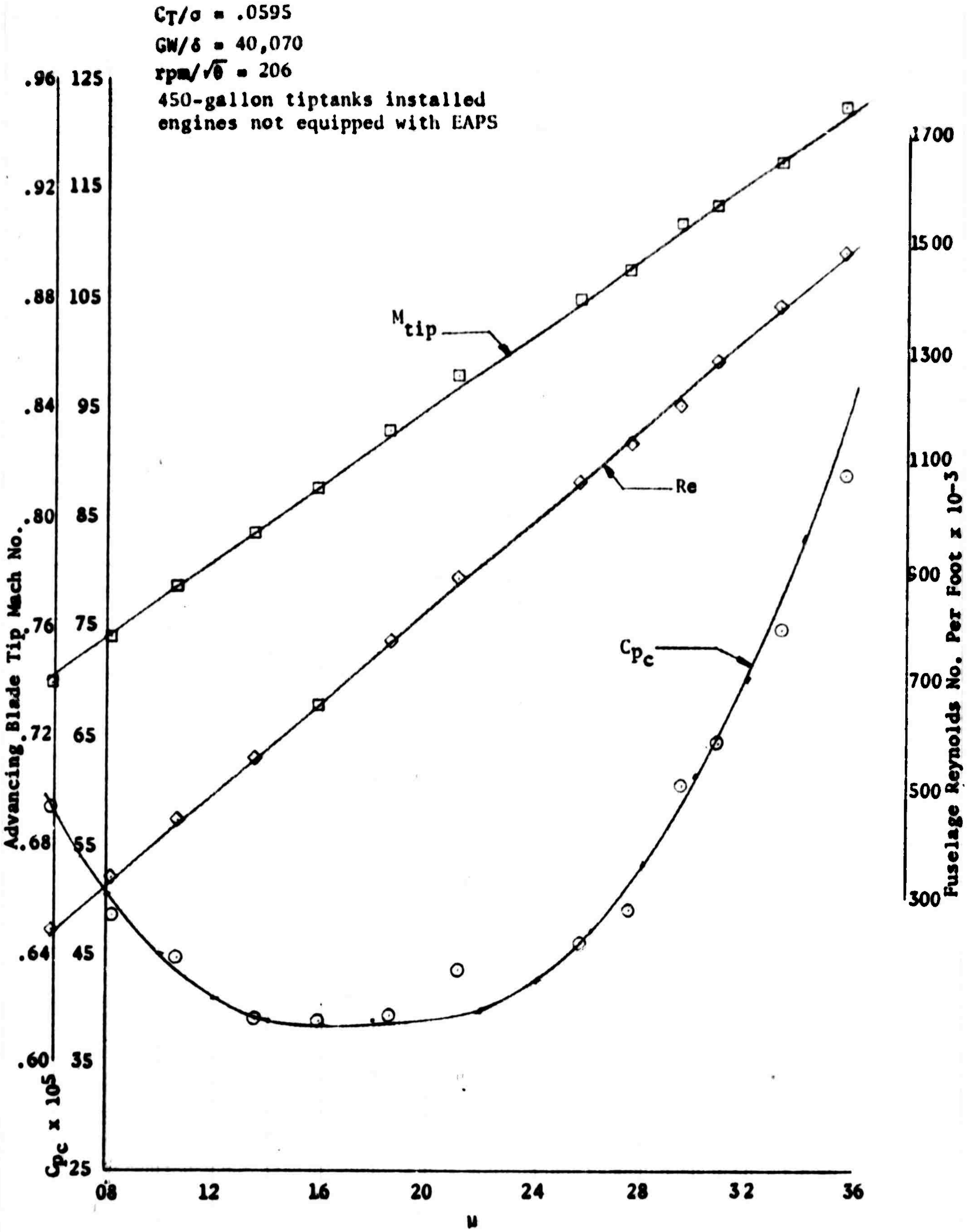

Figure 13. Level Flight Performance

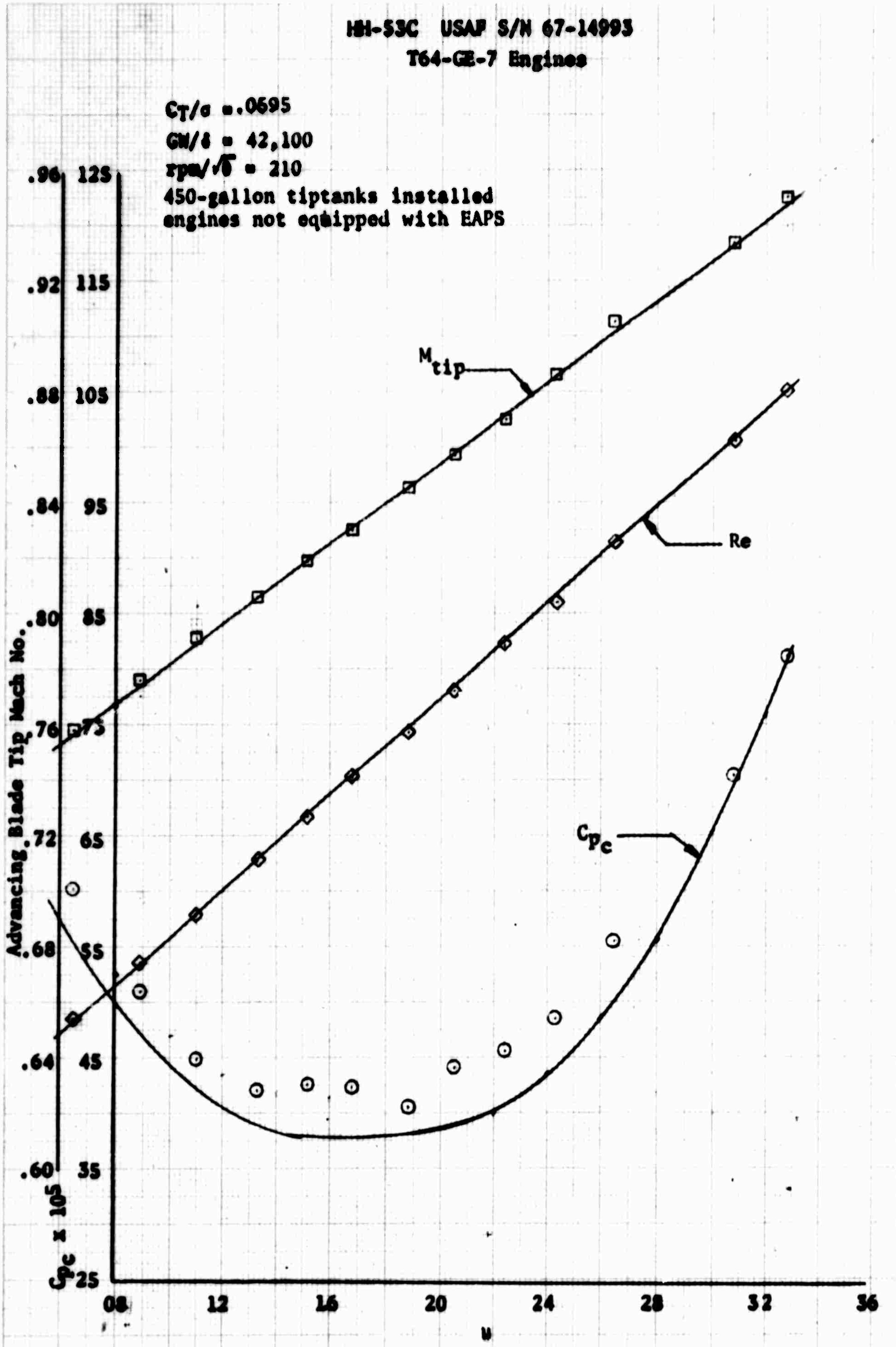

Figure 14. Level Flight Performance

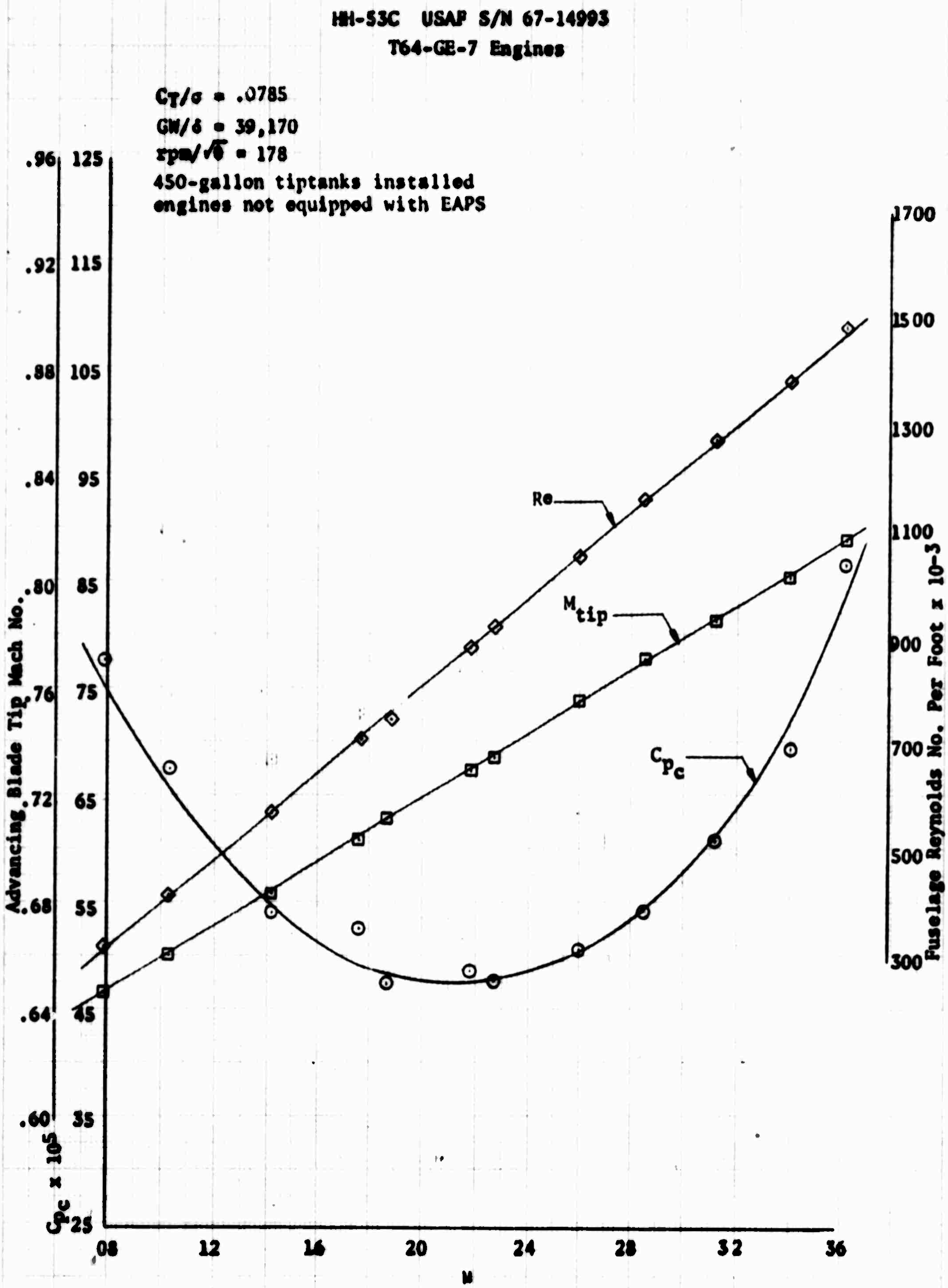

Figure 15. Level Flight Performance

HH-53C USAF S/N 67-14993
T64-GE-7 Engines

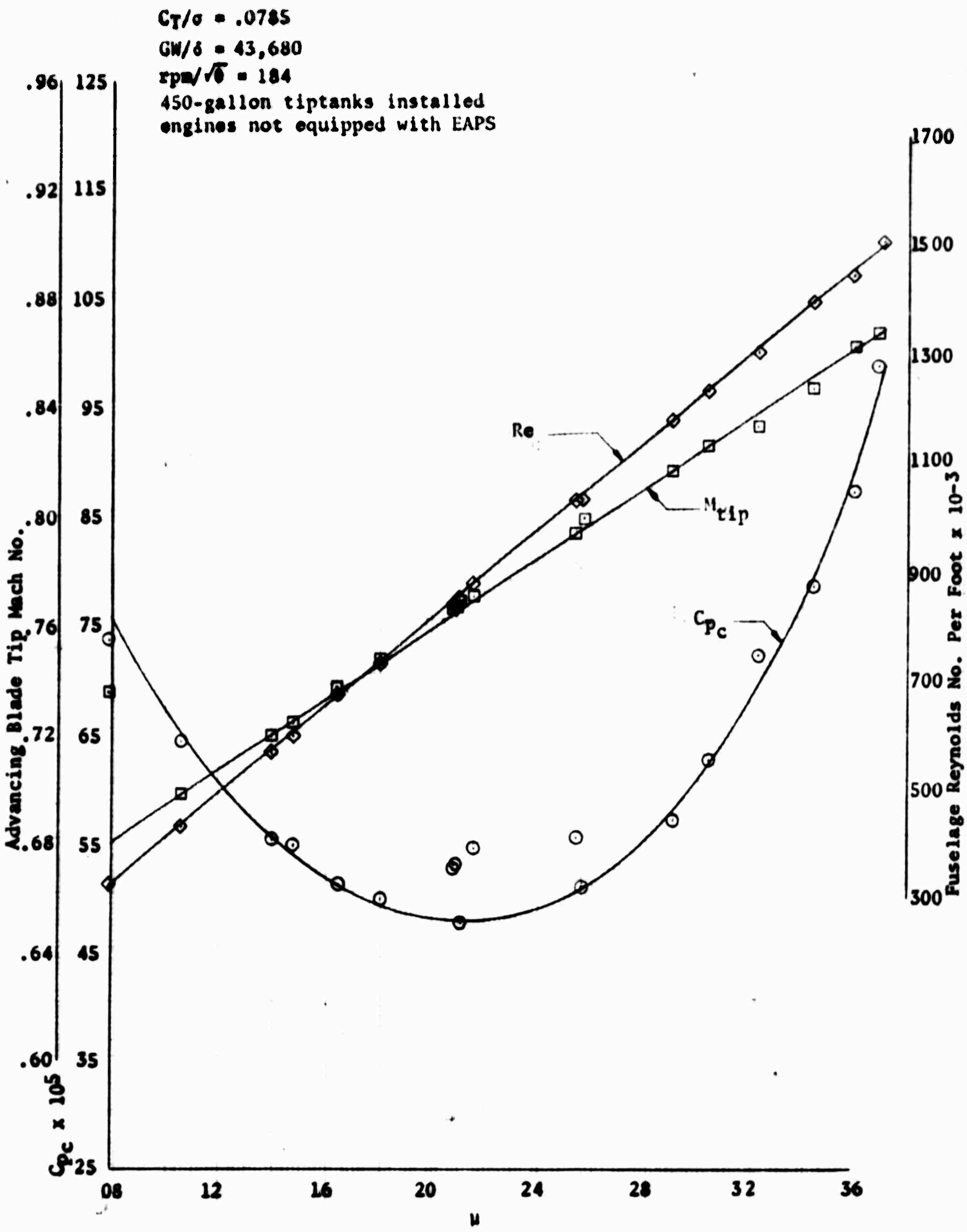

Figure 16. Level Flight Performance

HH-53C USAF S/N 67-14993

T64-GE-7 Engines

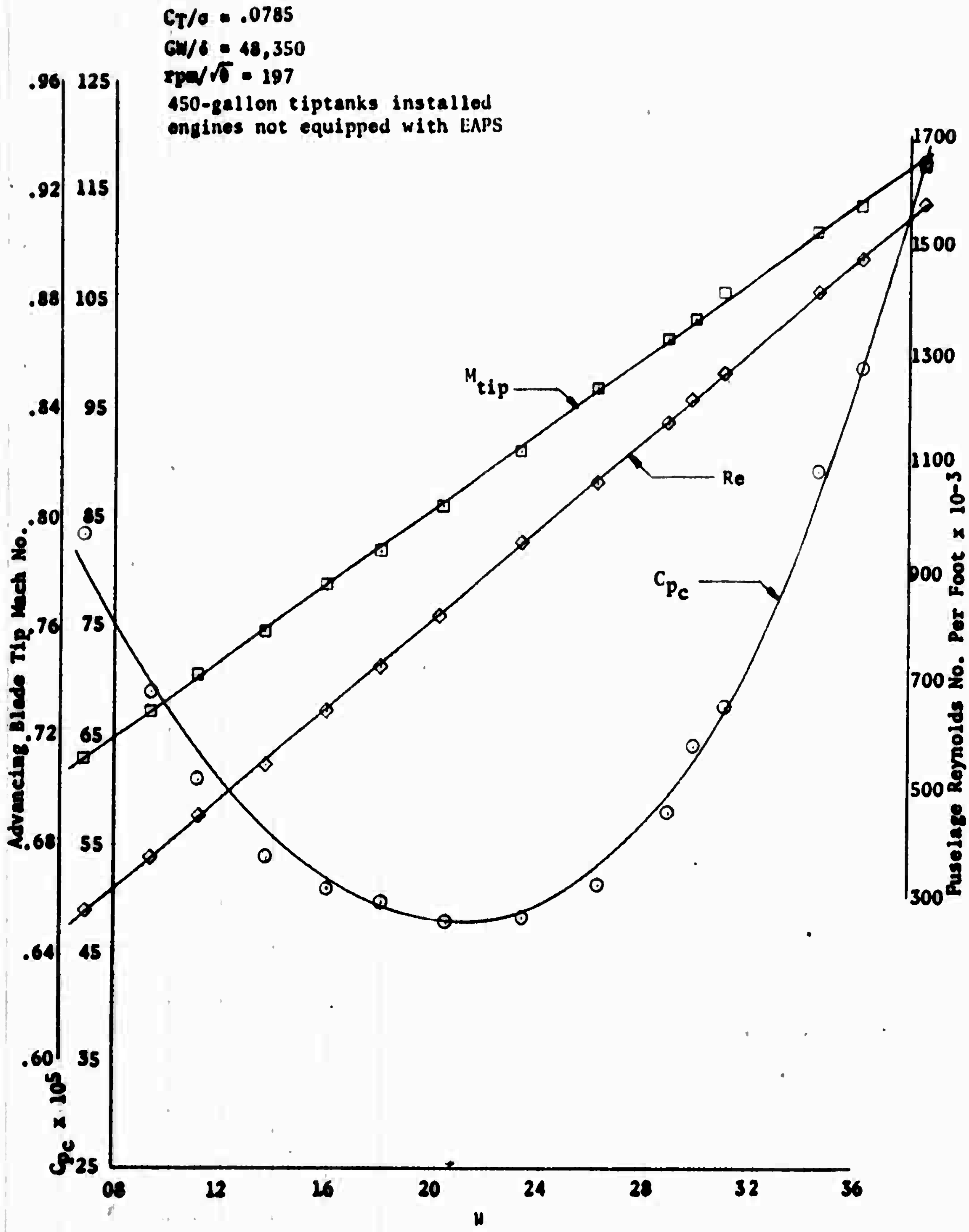

Figure 17. Level Flight Performance

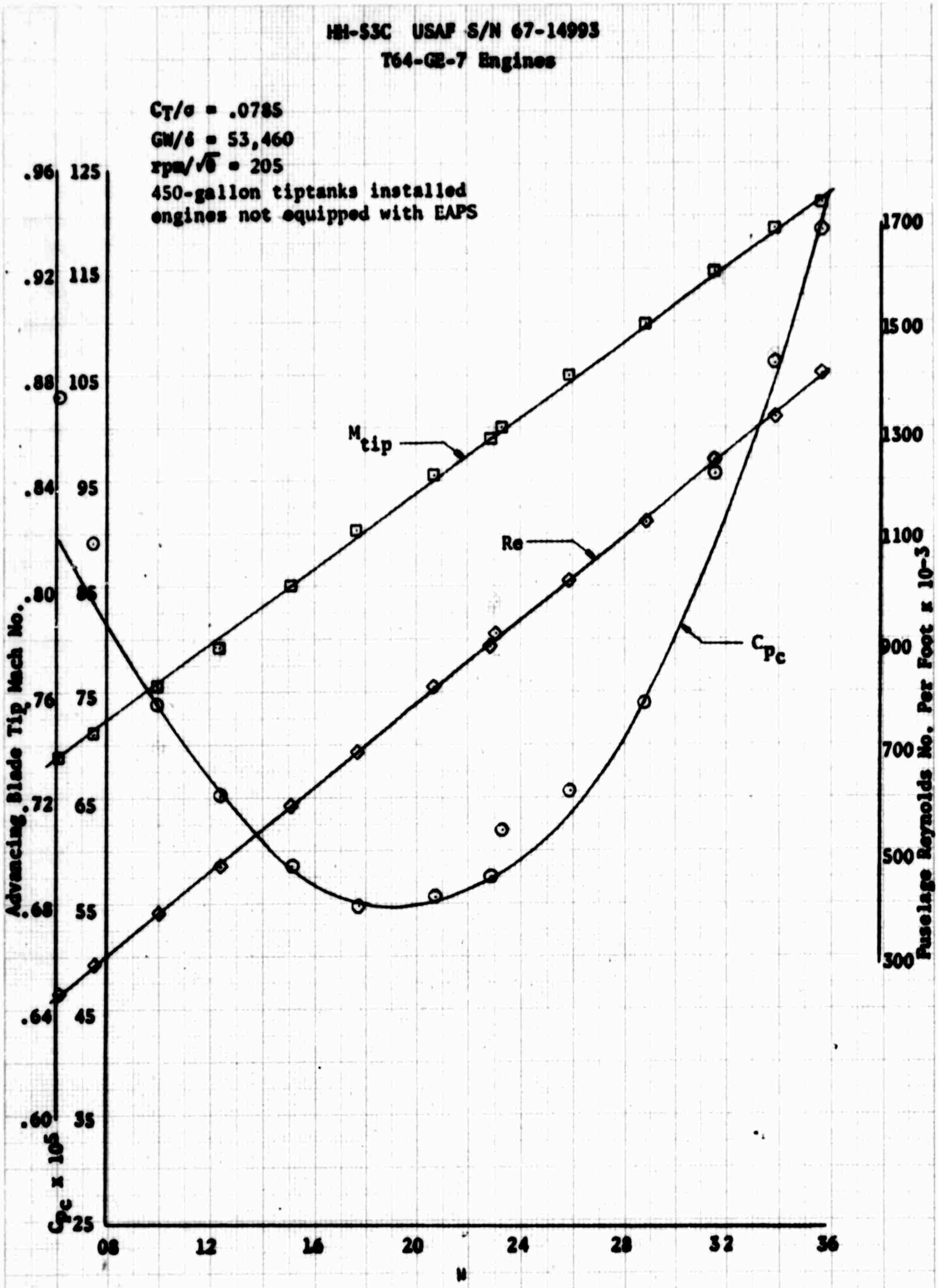

Figure 15. Level Flight Performance

HH-53C USAF S/N 67-14993
T64-GE-7 Engines

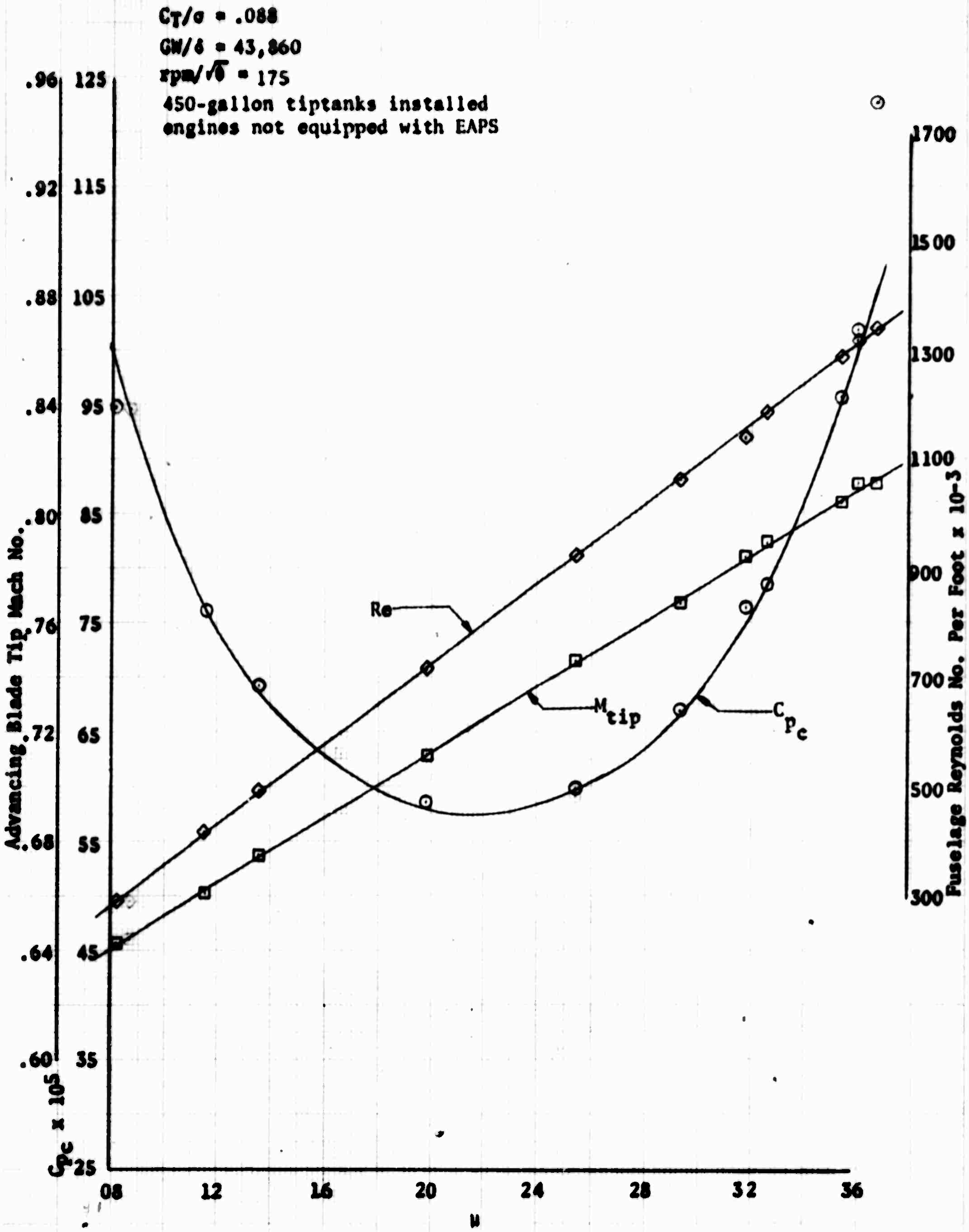

Figure 17. Level Flight Performance

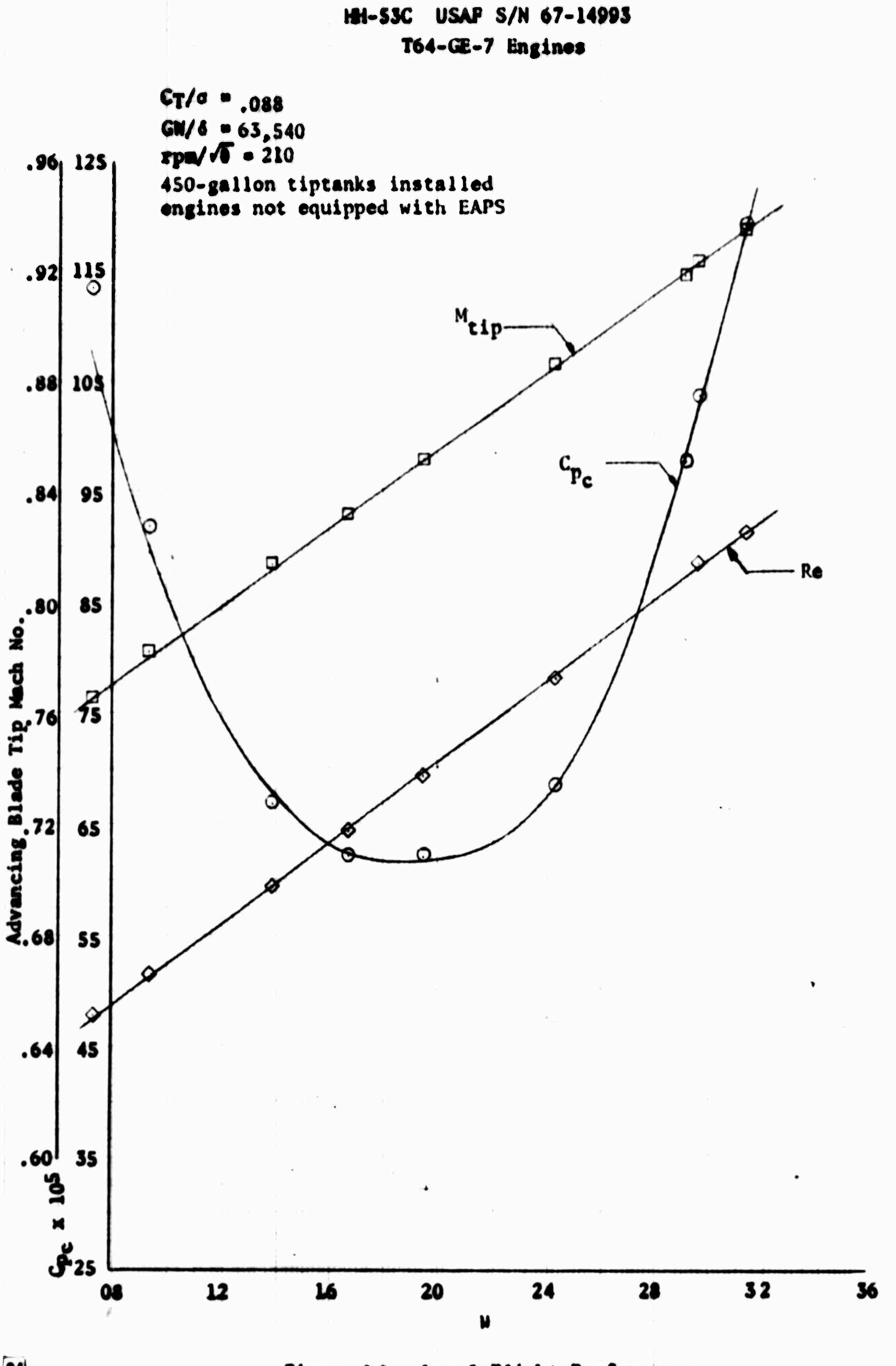

Figure 20 Level Flight Performance

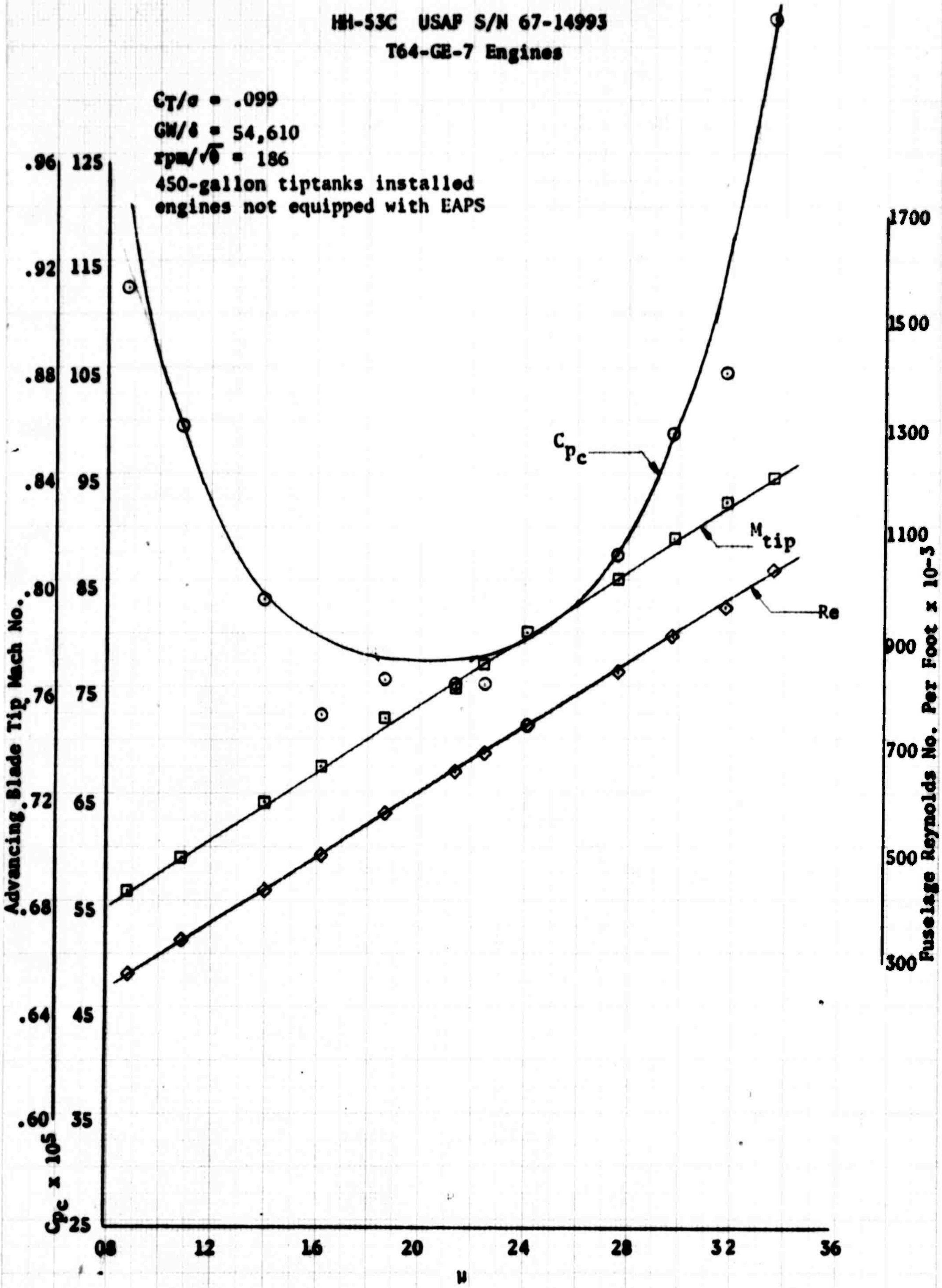

Figure 21. Level Flight Performance

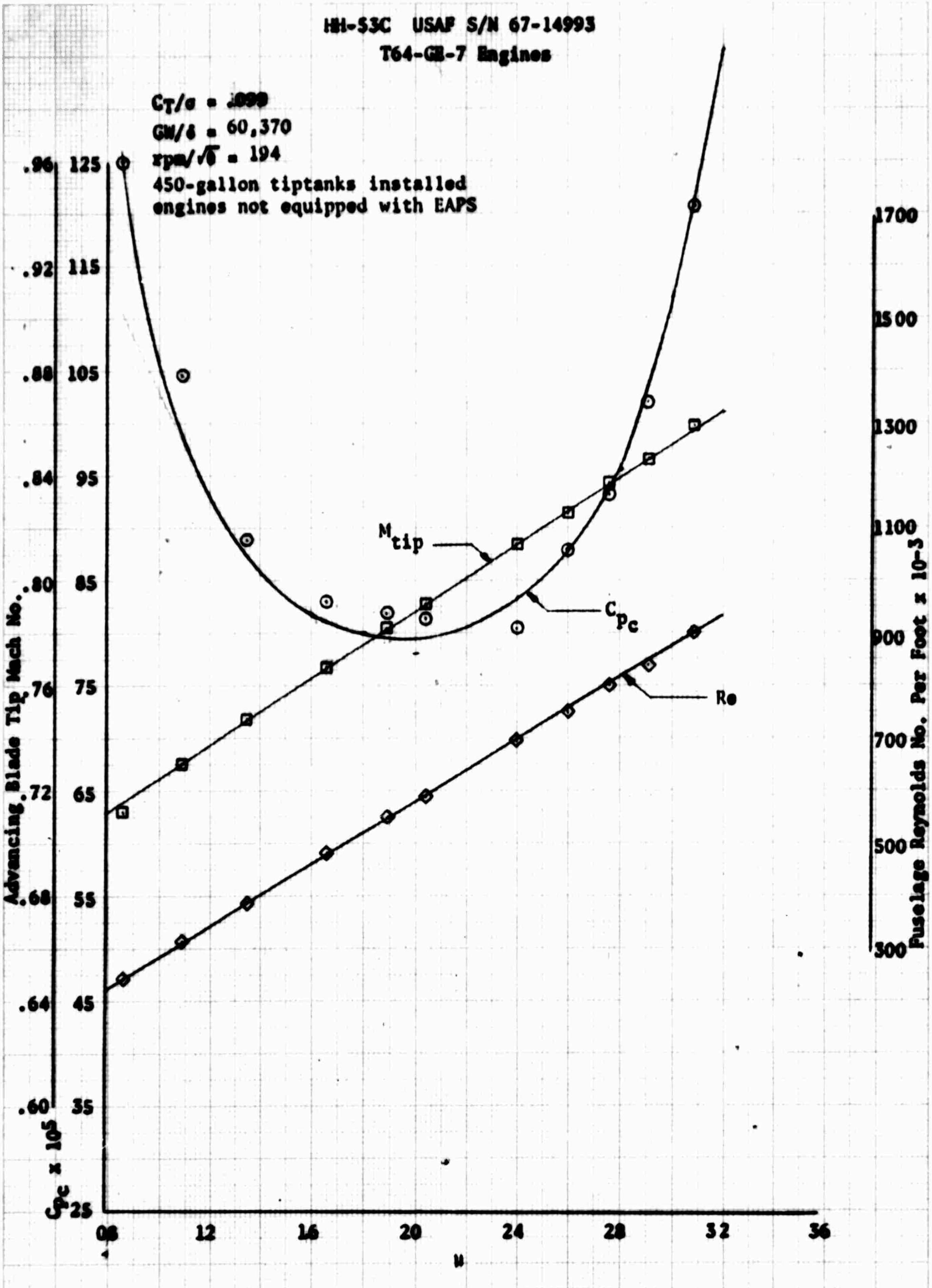

Figure 22. Level Flight Performance

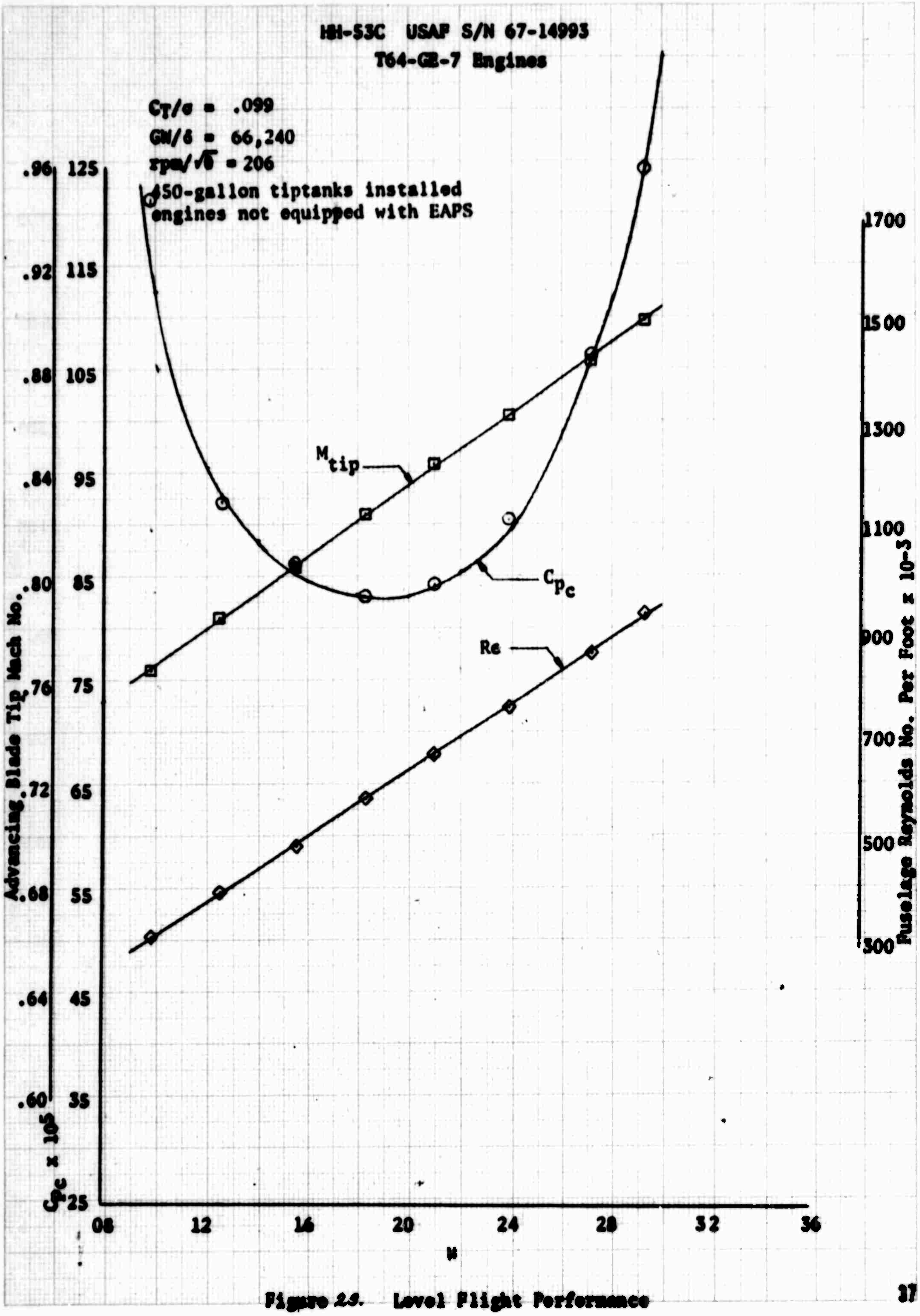

Figure 29. Level Flight Performance

HH-53C USAF S/N 67-14993

T64-GE-7 Engines

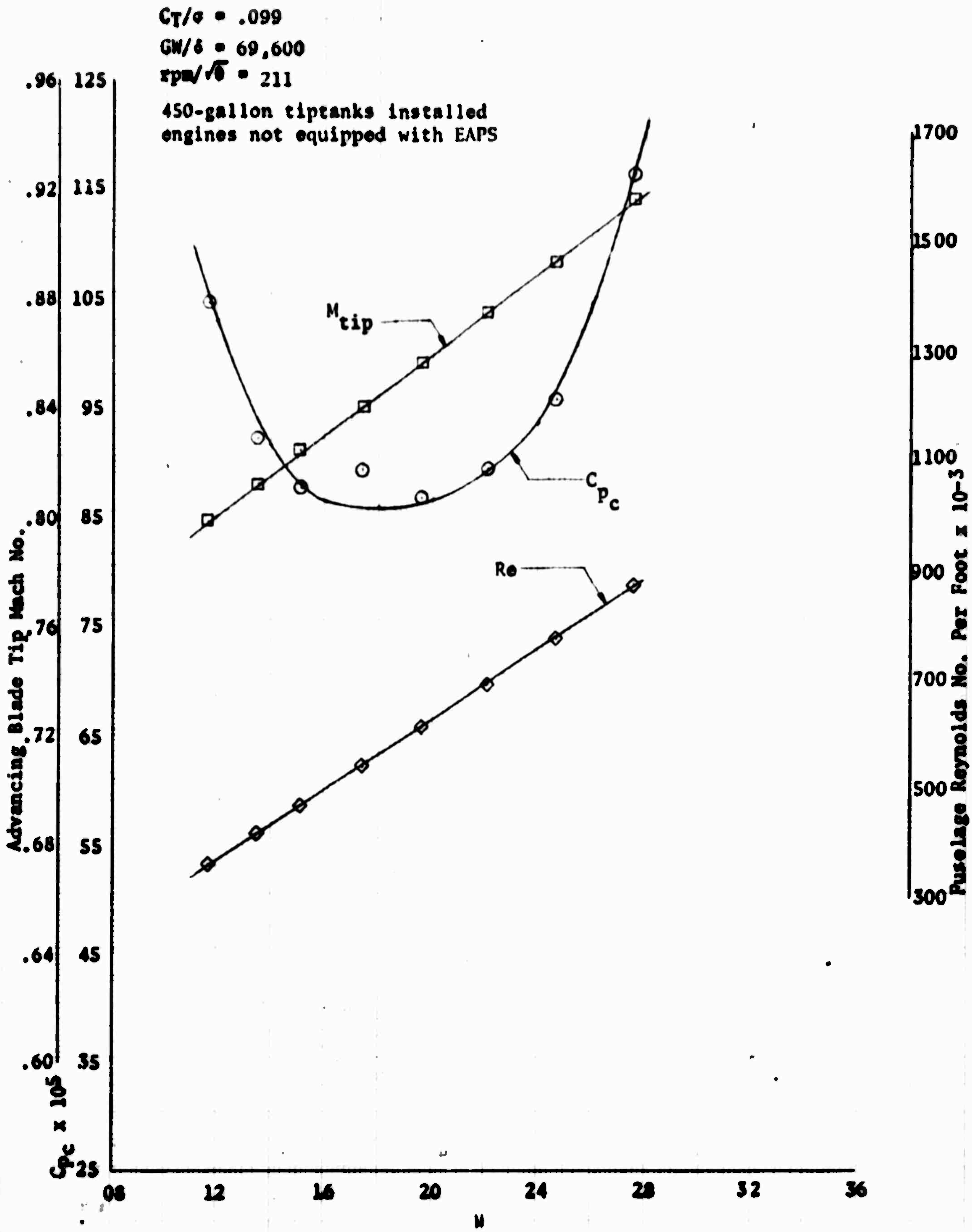

Figure 24. Level Flight Performance

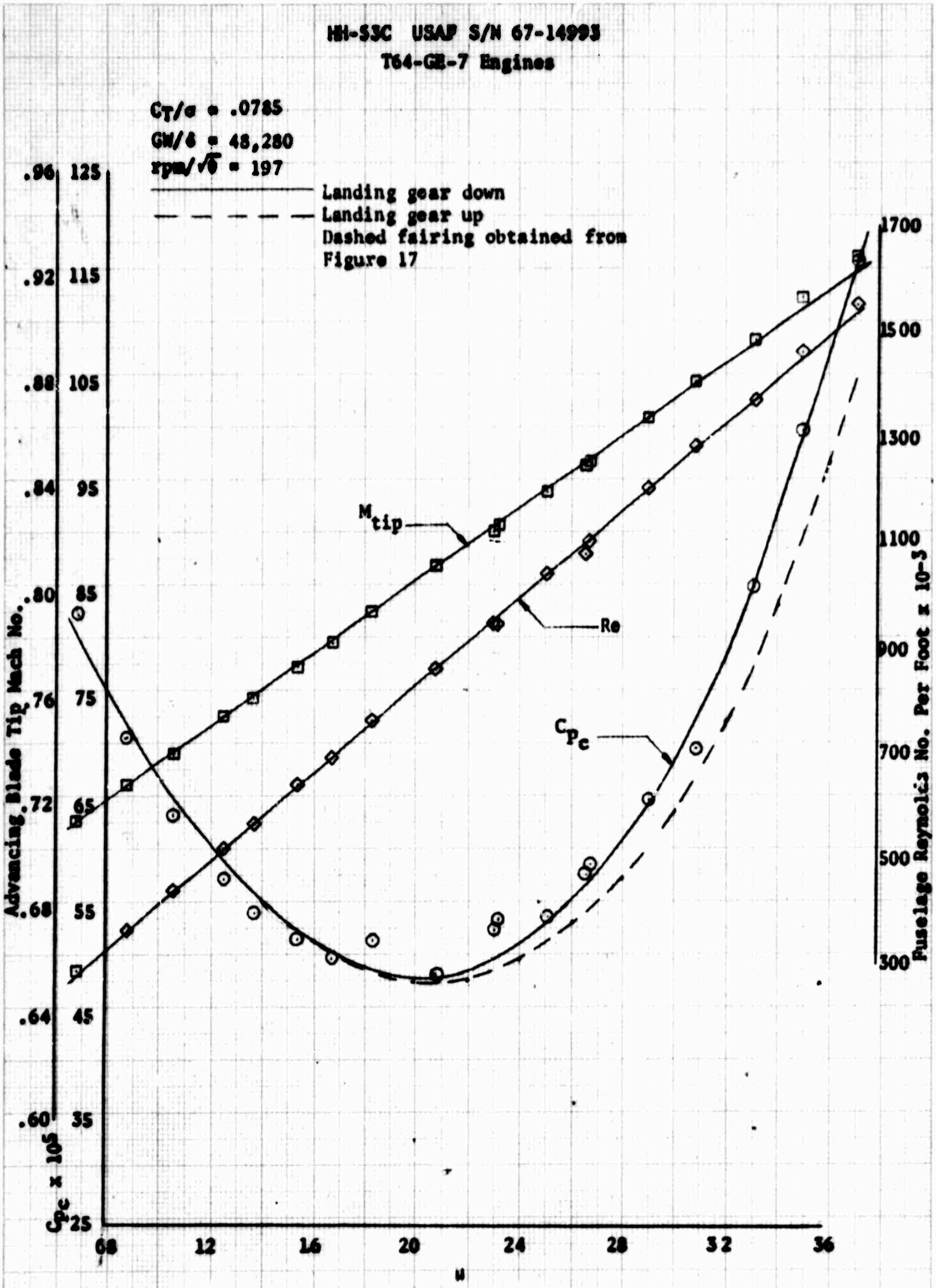

Figure 26. Level Flight Performance

HH-53C USAF S/N 67-14993
T64-GE-7 Engines

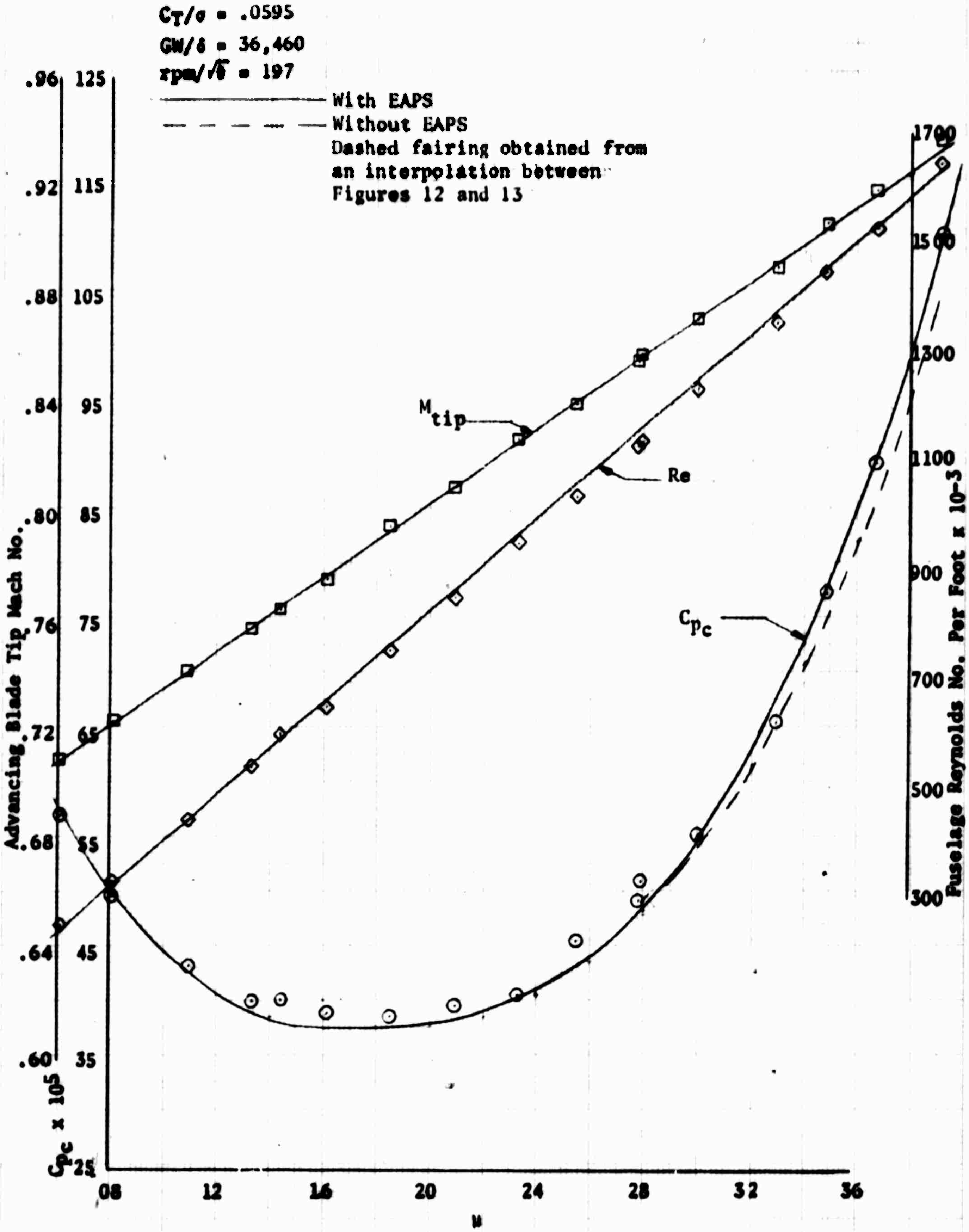

Figure 26. Level Flight Performance

HH-53C USAF S/N 67-14993

T64-GE-7 Engines

Symbol	Avg GW (lb)	Avg Press Alt (ft)	Avg FAT (°C)	Avg cg (in)	Rotor Speed (rpm)
○	35,000	4,500	6	340	185
□	35,000	7,000	17	340	185
◇	35,000	14,000	2	340	185

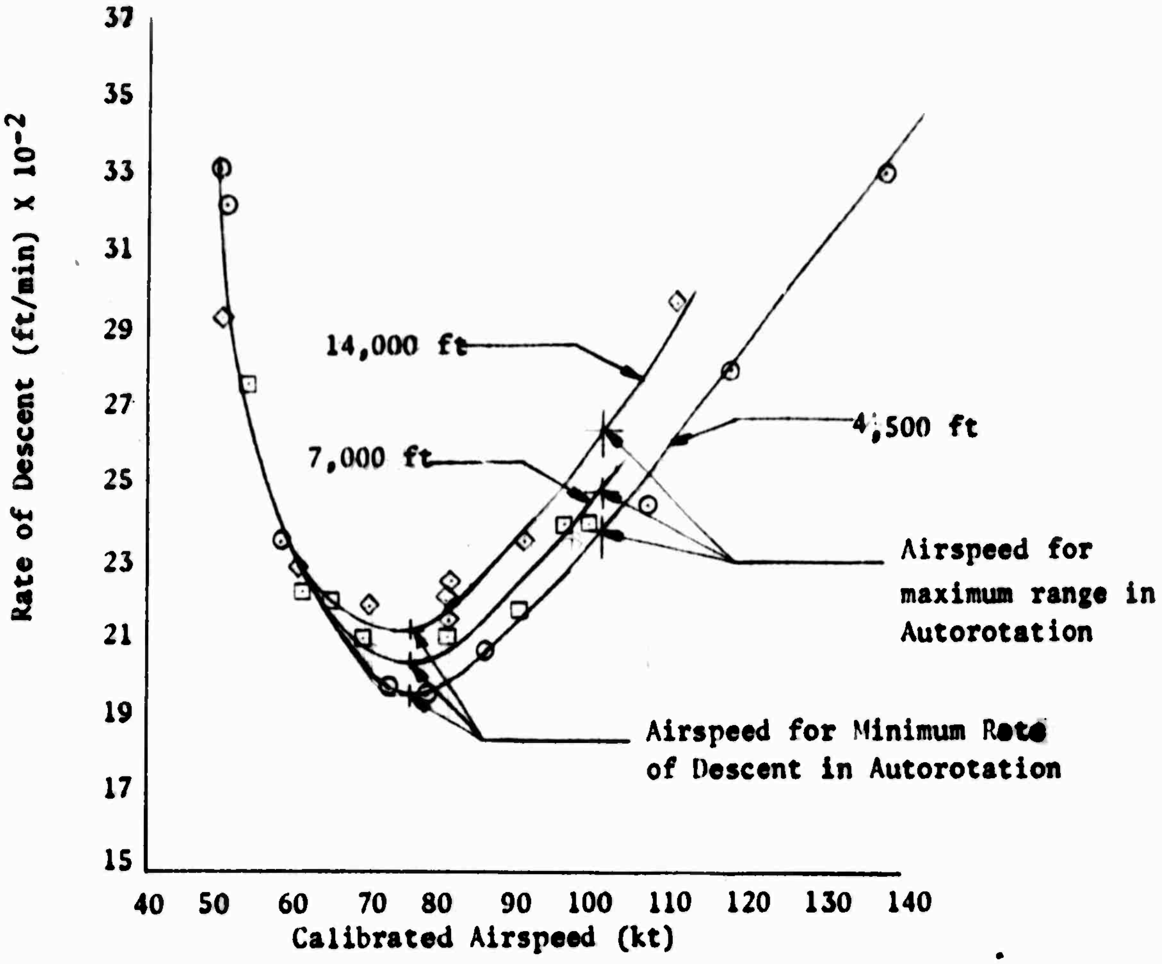

Figure 27. Performance in Autorotation

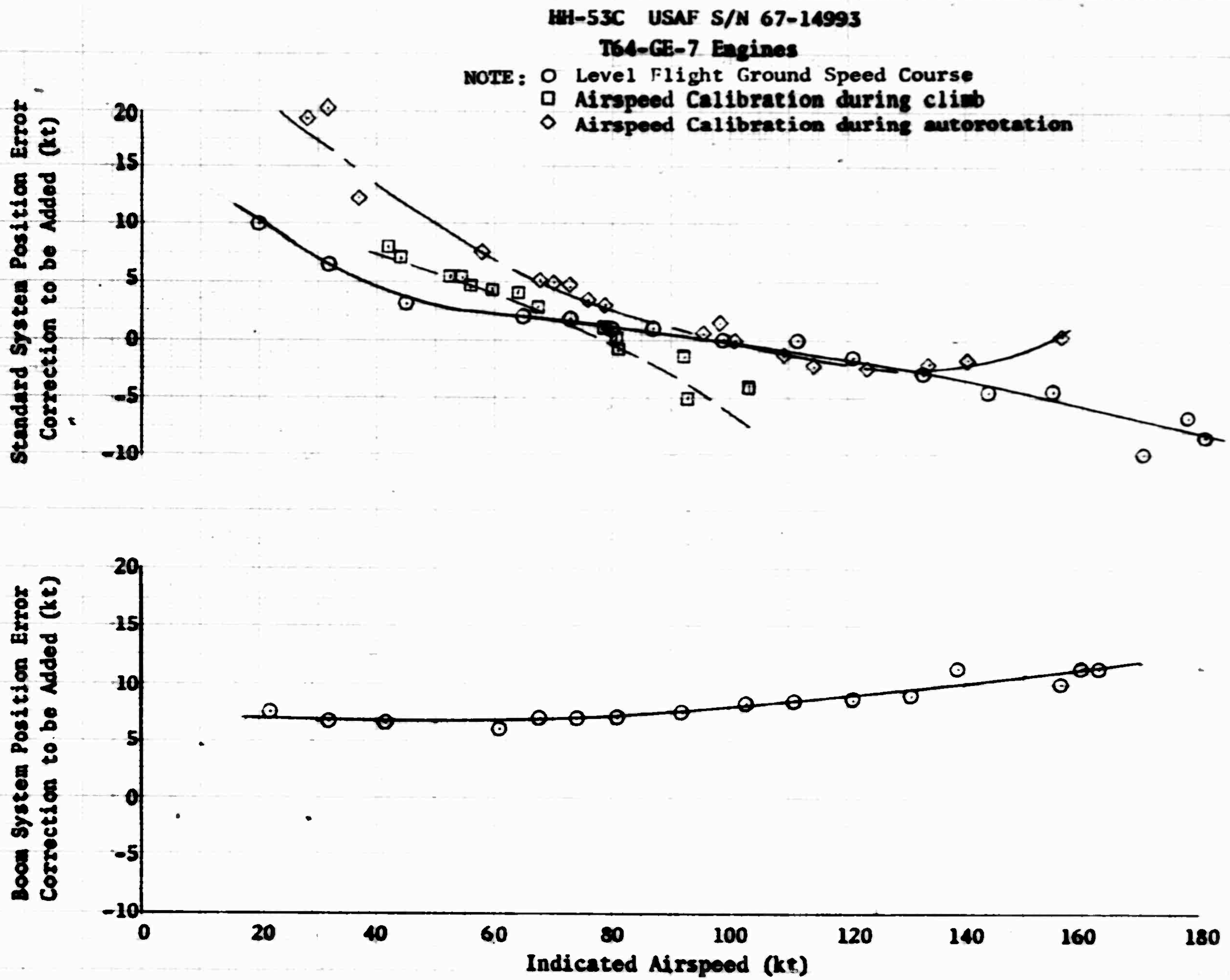

Figure 28. Airspeed Calibration

HH-53C USAF S/N 67-14993

Sym	Flight Condition	Avg GW (lb)	Avg cg (in.)	Avg Press. Alt (ft)	Avg FAT (°C)	Rotor Speed (rpm)	AFCS
⊙	Level Flight	31,000	352	4,000	15	185	ON

NOTE: Solid Symbols Denote Trim Conditions

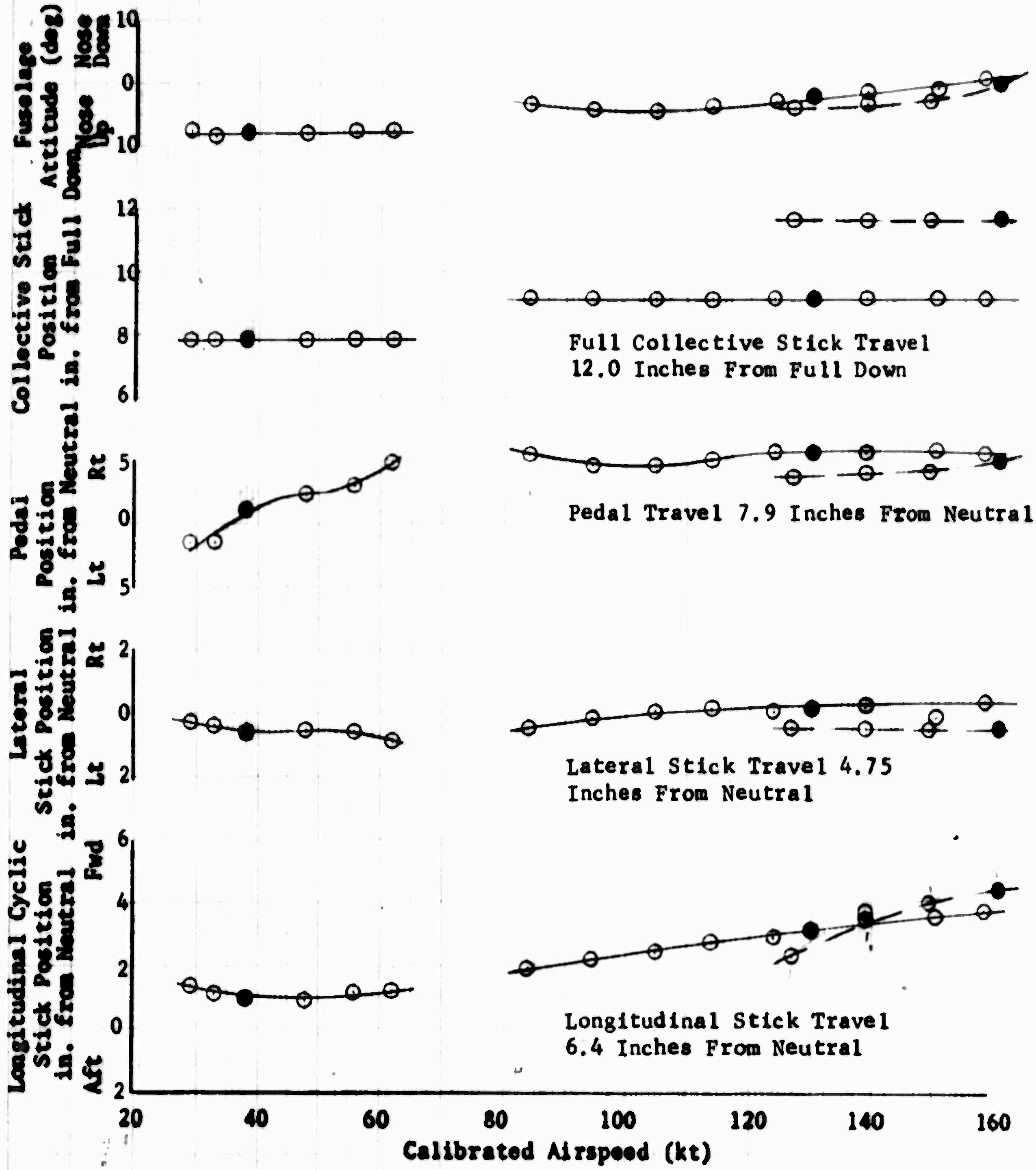

Figure 29. Static Longitudinal Speed Stability

HH-53C USAF S/N 67-14993

Sym	Flight Condition	Avg GW (lb)	Avg cg (in.)	Avg Press. Alt (ft)	Avg FAT (°C)	Rotor Speed (rpm)	AFCS
○	Climb	31,000	352	4,000	15	185	ON
◇	Auto.	31,000	352	4,000	15	185	ON
□	Partial Power Descent	31,000	352	4,000	15	185	ON

NOTE: Solid Symbols Denote Trim Conditions

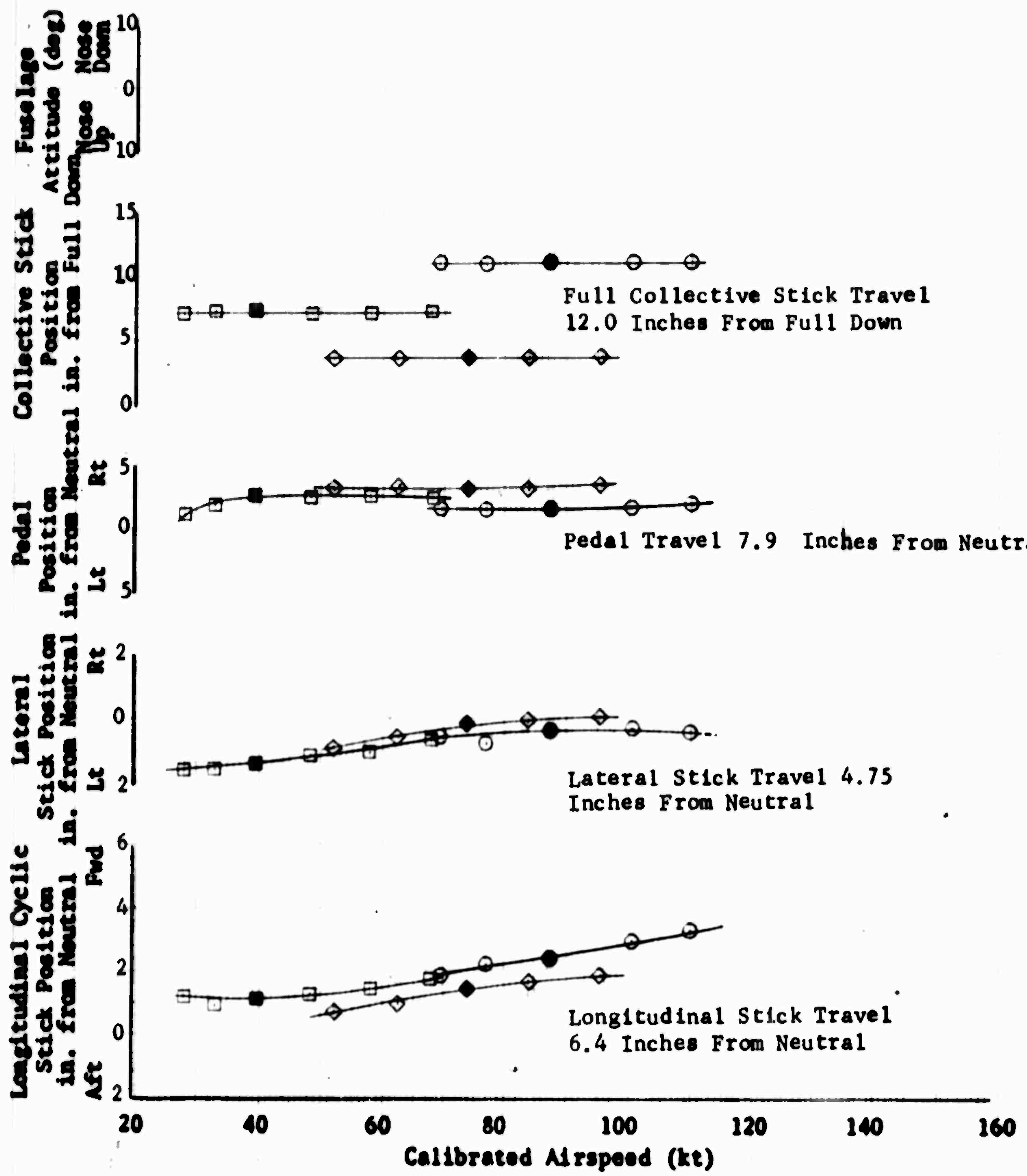

Figure 90. Static Longitudinal Speed Stability

Sym	Flight Condition	Avg GW (lb)	Avg cg (in.)	Avg Press. Alt (ft)	Avg FAT (°C)	Rotor Speed (rpm)	AFCS
○	Level Flight	31,000	328	4,000	16	185	ON

NOTE: Solid Symbols Denote Trim Conditions

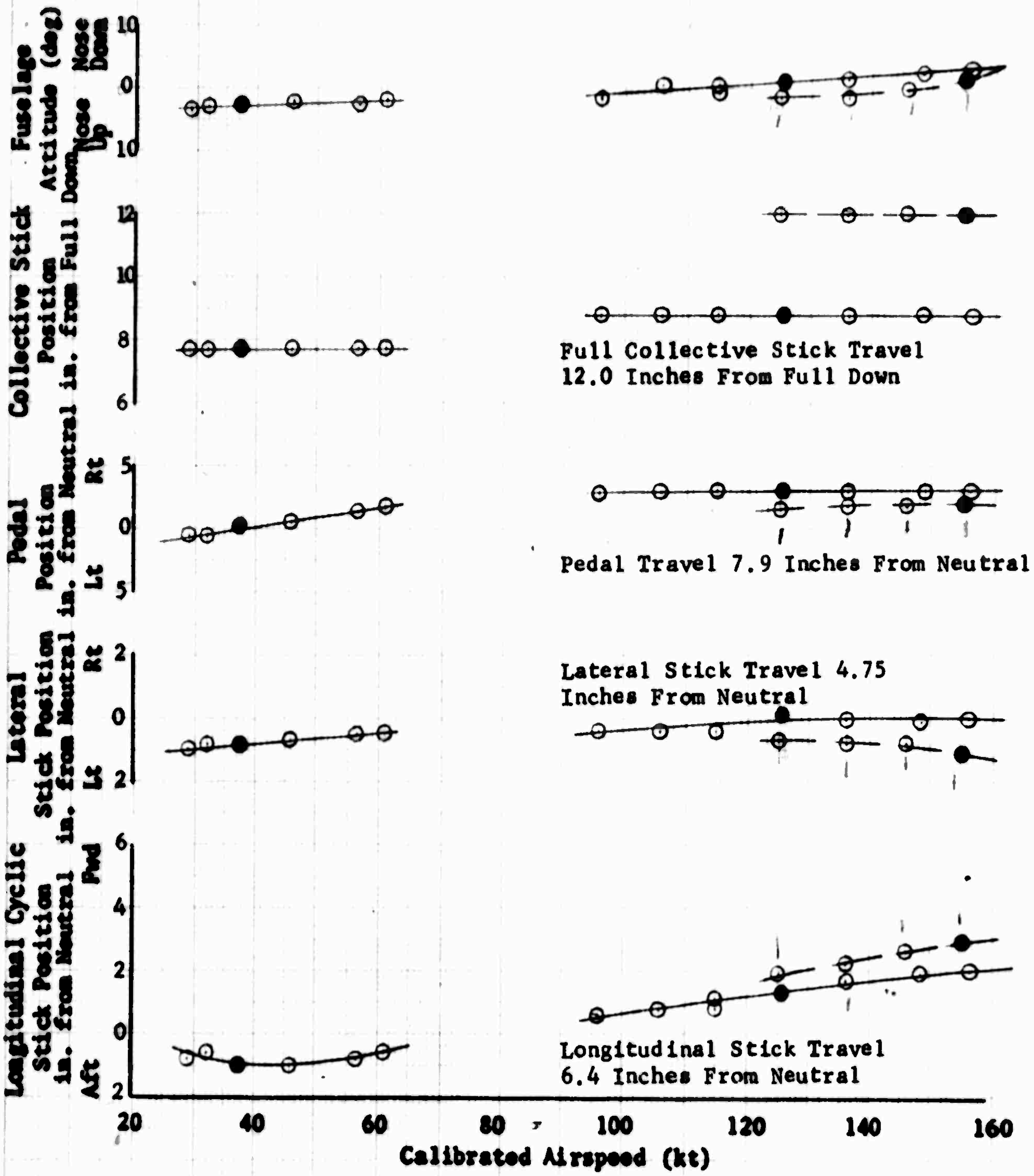

Figure 31. Static Longitudinal Speed Stability

HH-53C USAF S/N 67-14993

Sym	Flight Condition	Avg GW (lb)	Avg cg (in.)	Avg Press. Alt (ft)	Avg FAT (°C)	Rotor Speed (rpm)	AFCS
□	Climb	31,000	328	4,000	16	185	ON
◇	Auto.	31,000	328	4,000	16	185	ON
○	Partial Power Descent	31,000	328	4,000	16	185	ON

NOTE: Solid Symbols Denote Trim Conditions

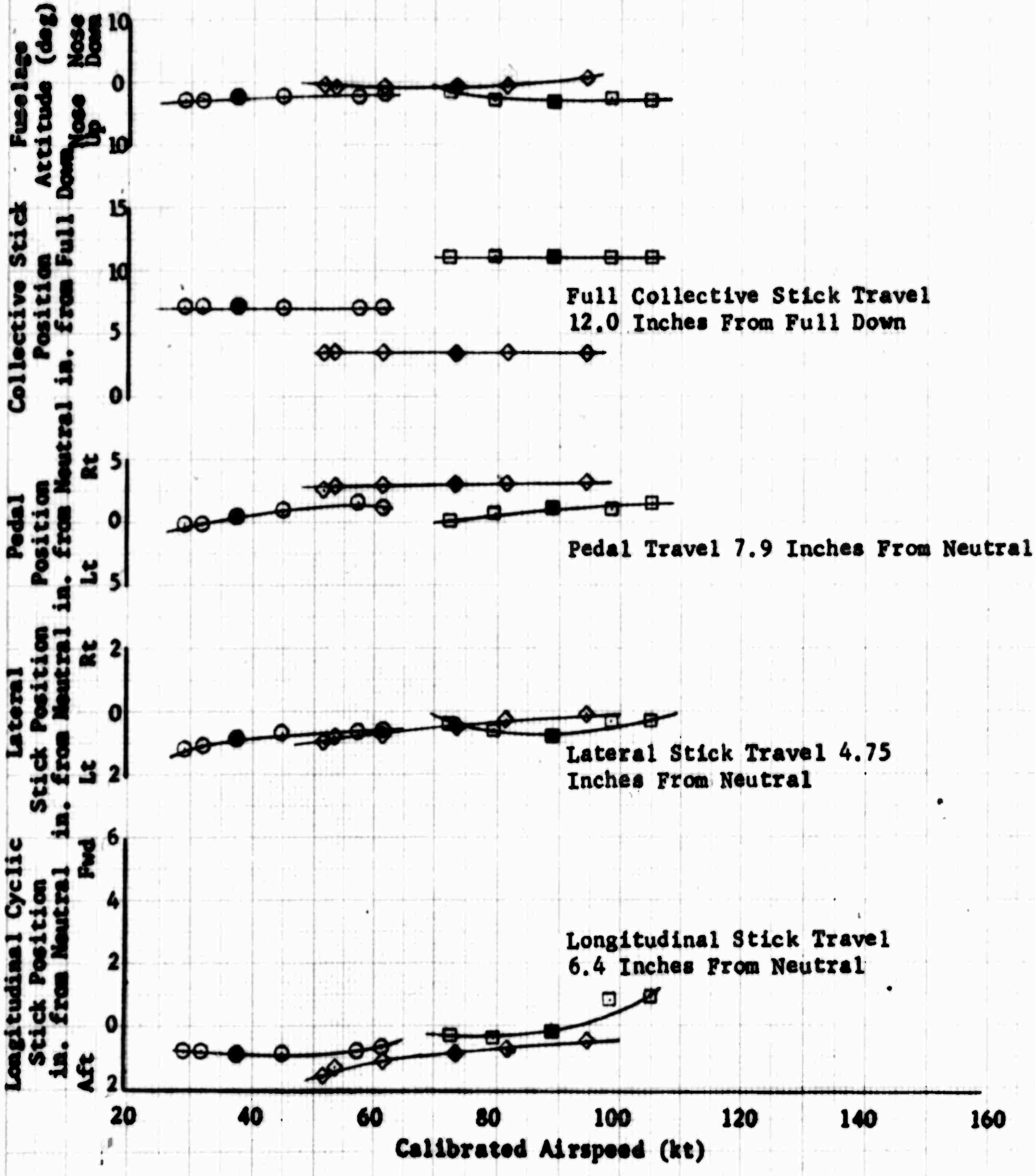

Figure 32. Static Longitudinal Speed Stability

HH-53C USAF S/N 67-14993

Sym	Flight Condition	Avg GW (lb)	Avg cg (in.)	Avg Press. Alt (ft)	Avg FAT (°C)	Rotor Speed (rpm)	AFCS
○	Climb	31,000	352	9,500	5	185	ON
◇	Auto.	31,000	352	9,500	5	185	ON
□	Partial Power Descent	31,000	352	9,500	5	185	ON

NOTE: Solid Symbols Denote Trim Conditions

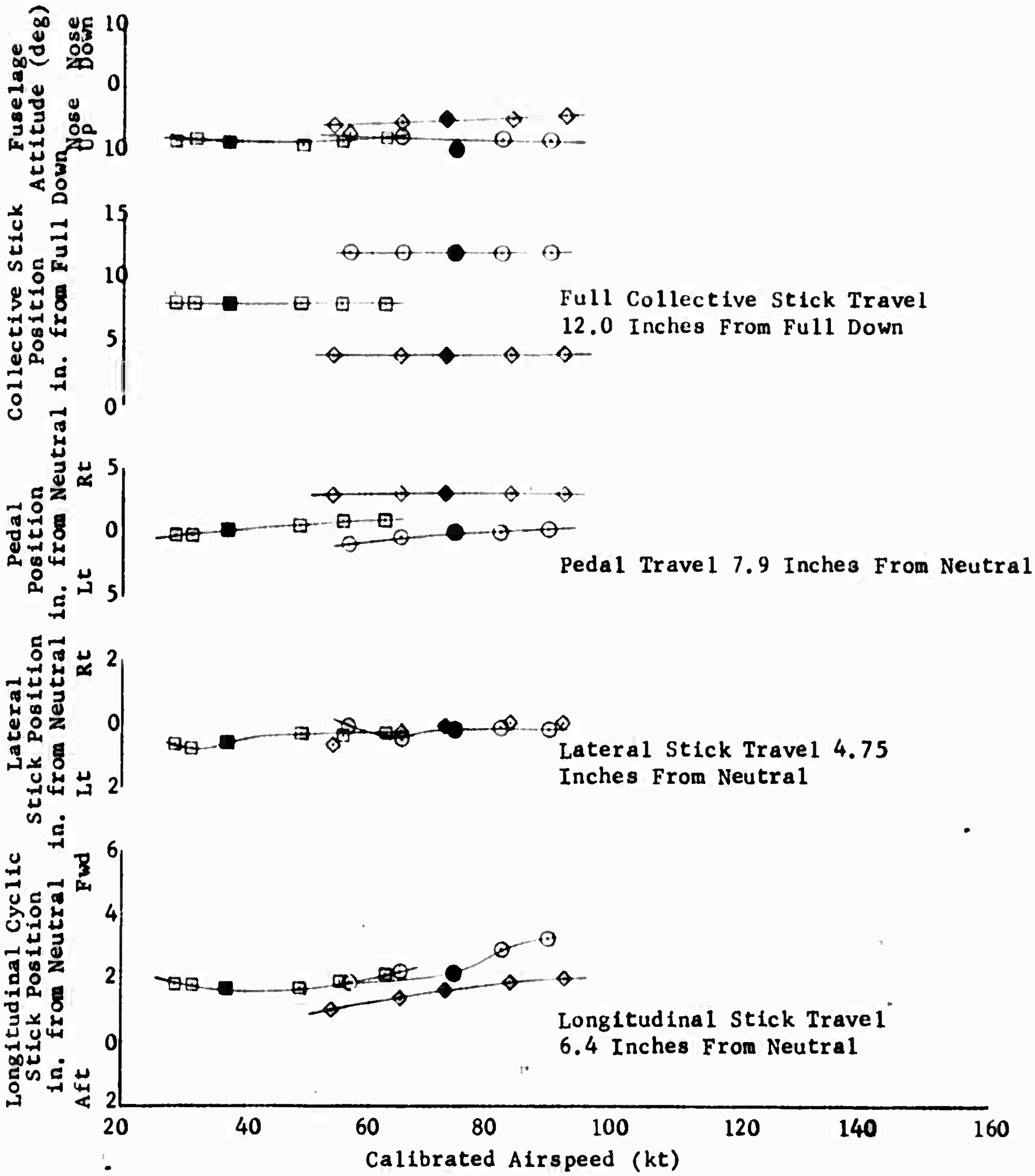

Figure 33. Static Longitudinal Speed Stability

HH-53C USAF S/N 67-14993

Sym	Flight Condition	Avg GW (lb)	Avg cg (in.)	Avg Press. Alt (ft)	Avg FAT (°C)	Rotor Speed (rpm)	AFCS
○	Level Flight	31,000	352	9,500	5	185	ON

NOTE: Solid Symbols Denote Trim Conditions

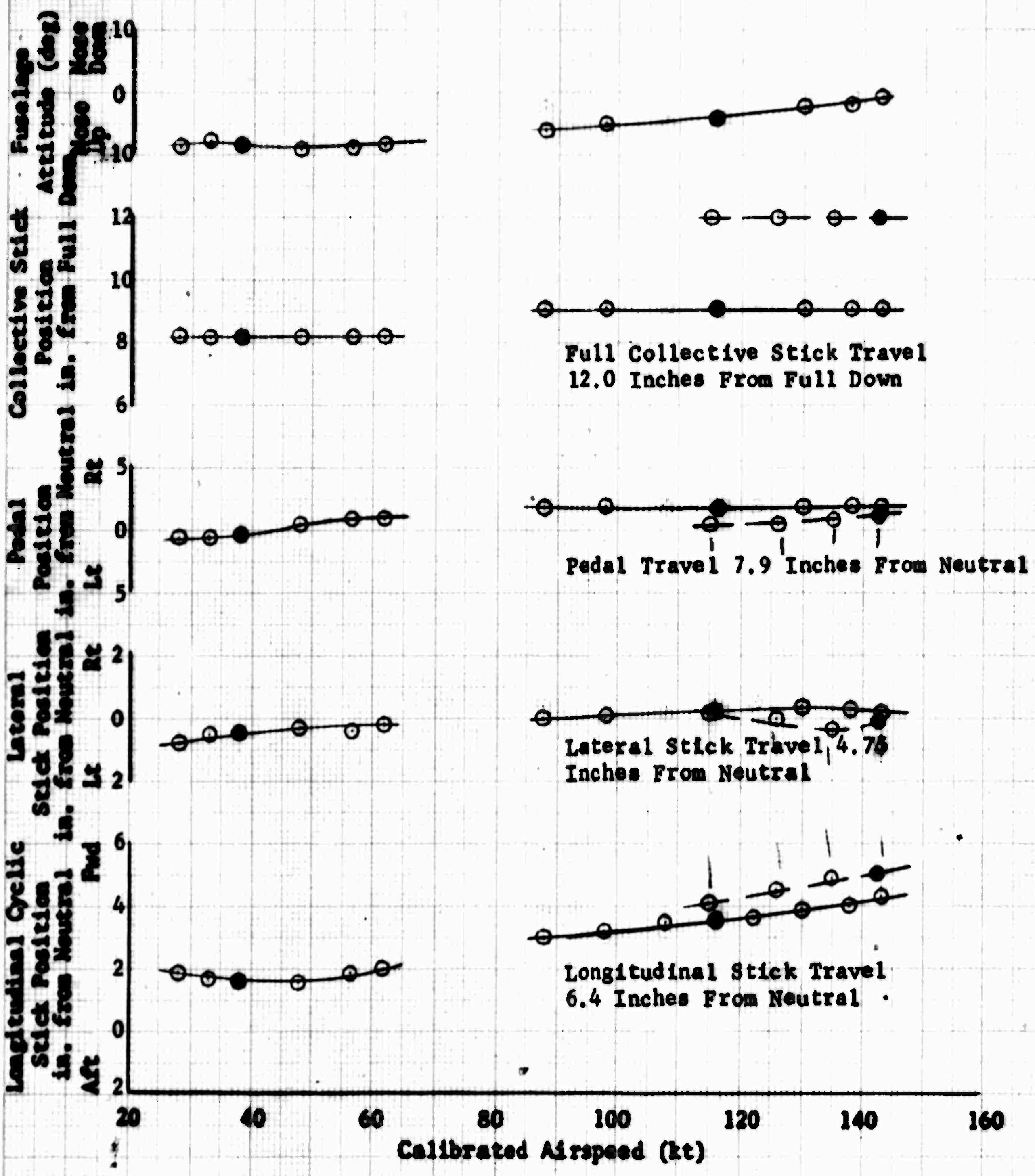

Figure 34 Static Longitudinal Speed Stability

Sym	Flight Condition	Avg GW (lb)	Avg cg (in.)	Avg Press. Alt (ft)	Avg FAT (°C)	Rotor Speed (rpm)	AFCS
○	Level Flight	31,000	352	13,000		185	ON

NOTE: Solid Symbols Denote Trim Conditions

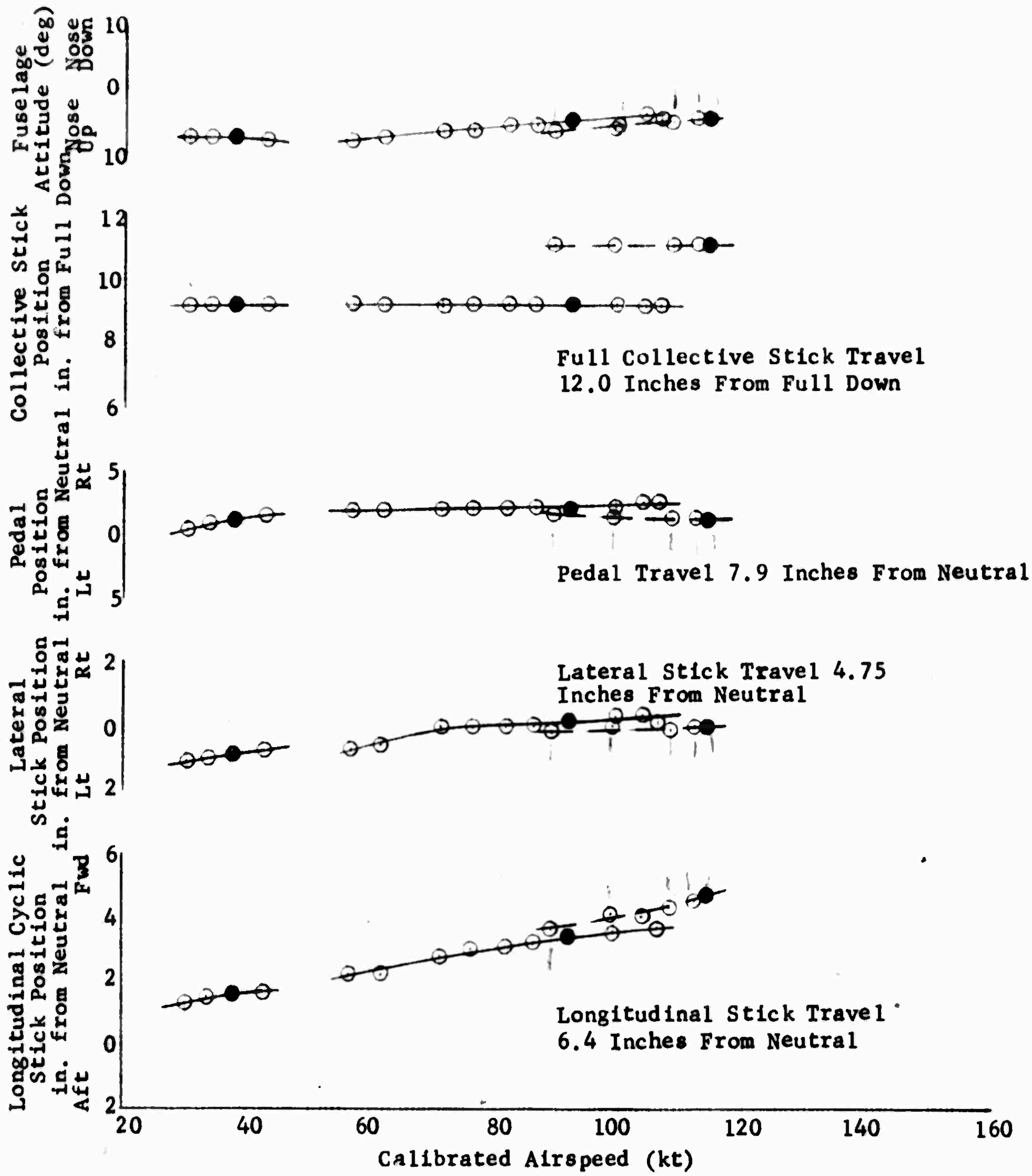

Figure 35. Static Longitudinal Speed Stability

HH-53C USAF S/N 67-14993

Sym	Flight Condition	Avg GW (lb)	Avg cg (in.)	Avg Press. Alt (ft)	Avg FAT (°C)	Rotor Speed (rpm)	AFCS
○	Climb	31,000	352	13,000	6	185	ON
◇	Auto.	31,000	352	13,000	6	185	ON
□	Partial Power Descent	31,000	352	13,000	6	185	ON

NOTE: Solid Symbols Denote Trim Conditions

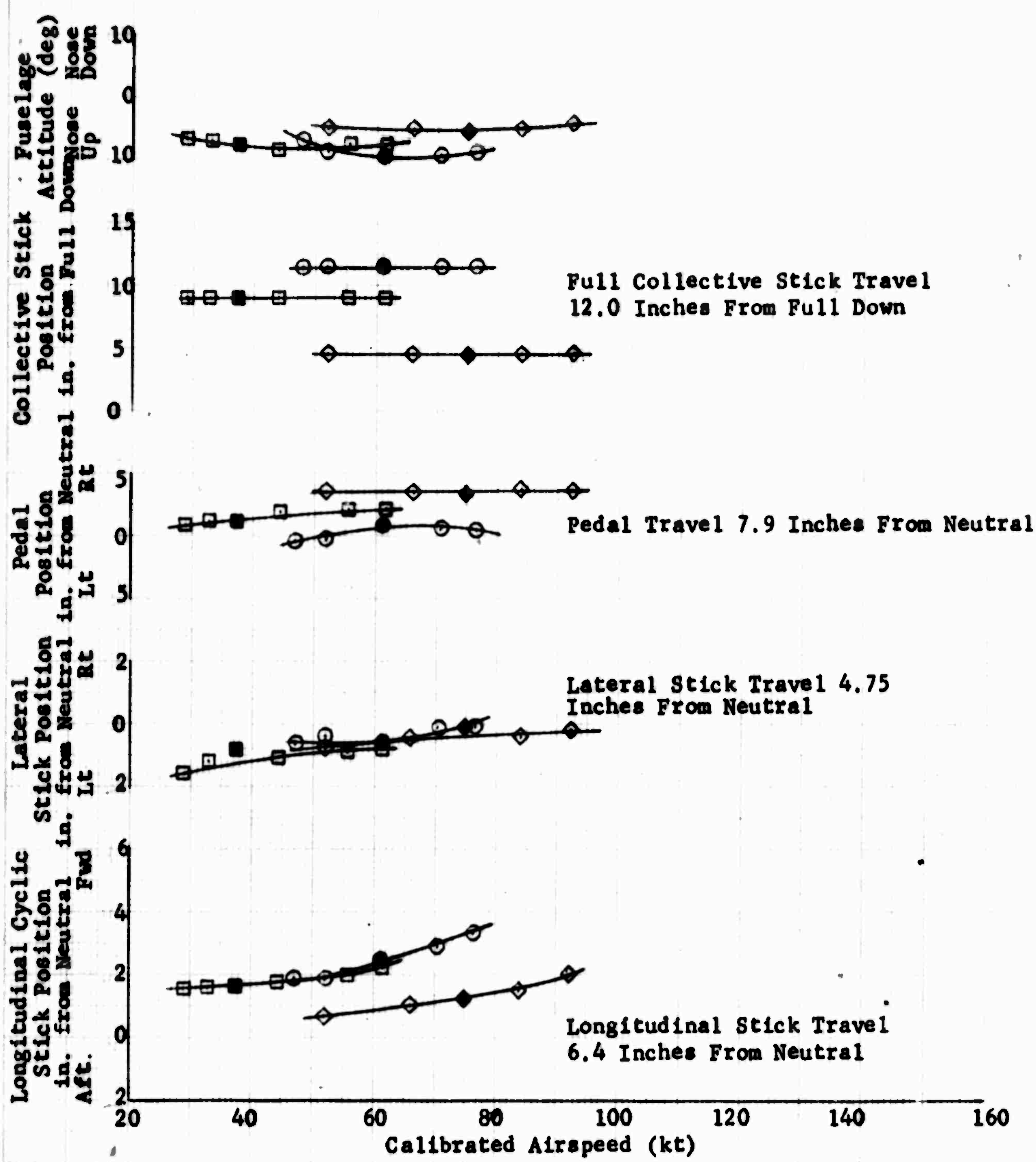

Figure 36. Static Longitudinal Speed Stability

HH-53C USAF S/N 67-14993

Sym	Flight Condition	Avg GW (lb)	Avg cg (in.)	Avg Press. Alt (ft)	Avg FAT (°C)	Rotor Speed (rpm)	AFCS
○	Level Flight	37,000	352	4,500	10	185	ON

NOTE: Solid Symbols Denote Trim Conditions

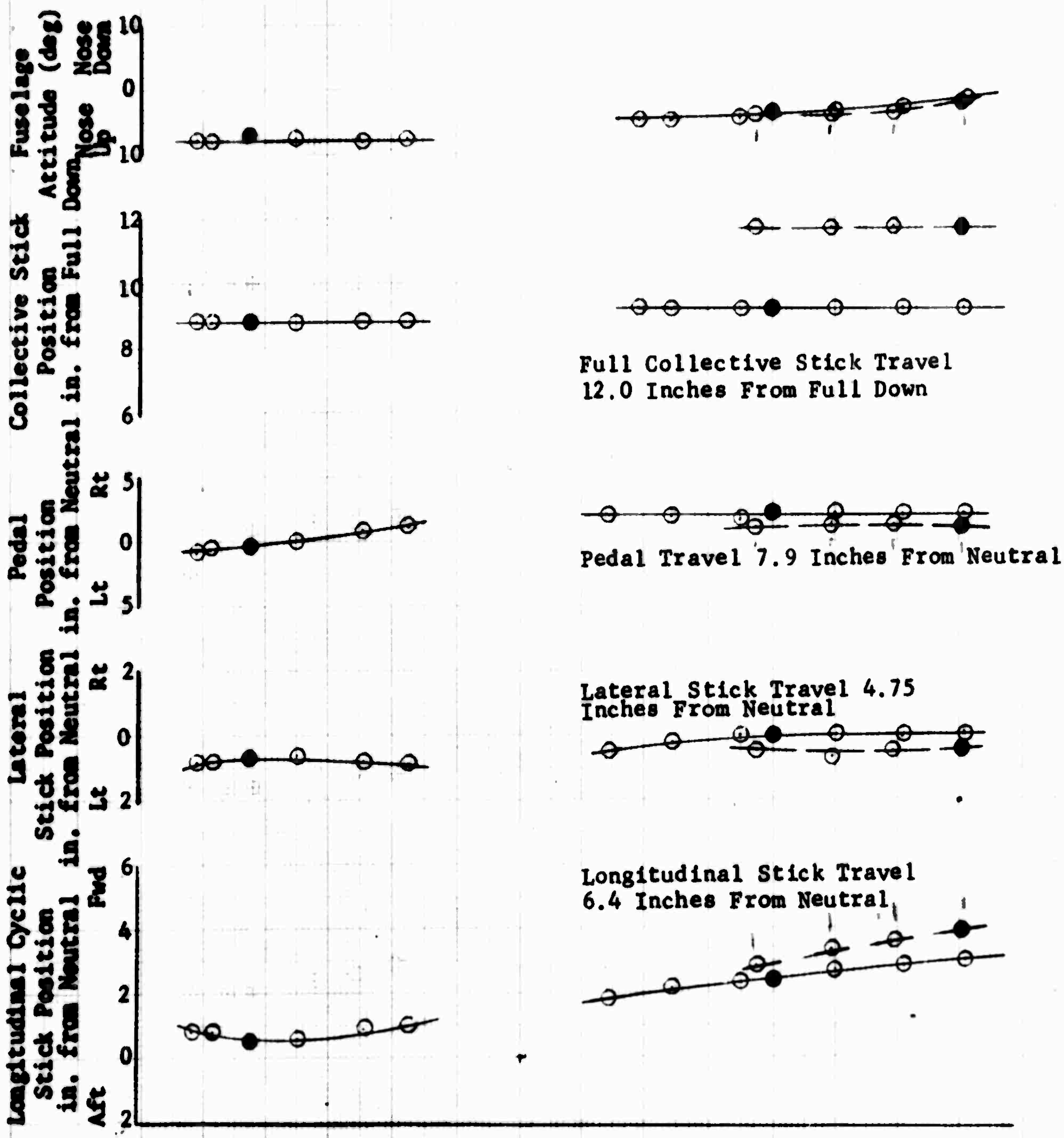

Figure 97. Static Longitudinal Speed Stability

HH-53C USAF S/N 67-14993

Sym	Flight Condition	Avg GW (lb)	Avg cg (in.)	Avg Press. Alt (ft)	Avg FAT (°C)	Rotor Speed (rpm)	AFCS
○	Climb	37,000	352	4,500	10	185	ON
◇	Auto.	37,000	352	4,500	10	185	ON
□	Partial Power Descent	37,000	352	4,500	10	185	ON

NOTE: Solid Symbols Denote Trim Conditions

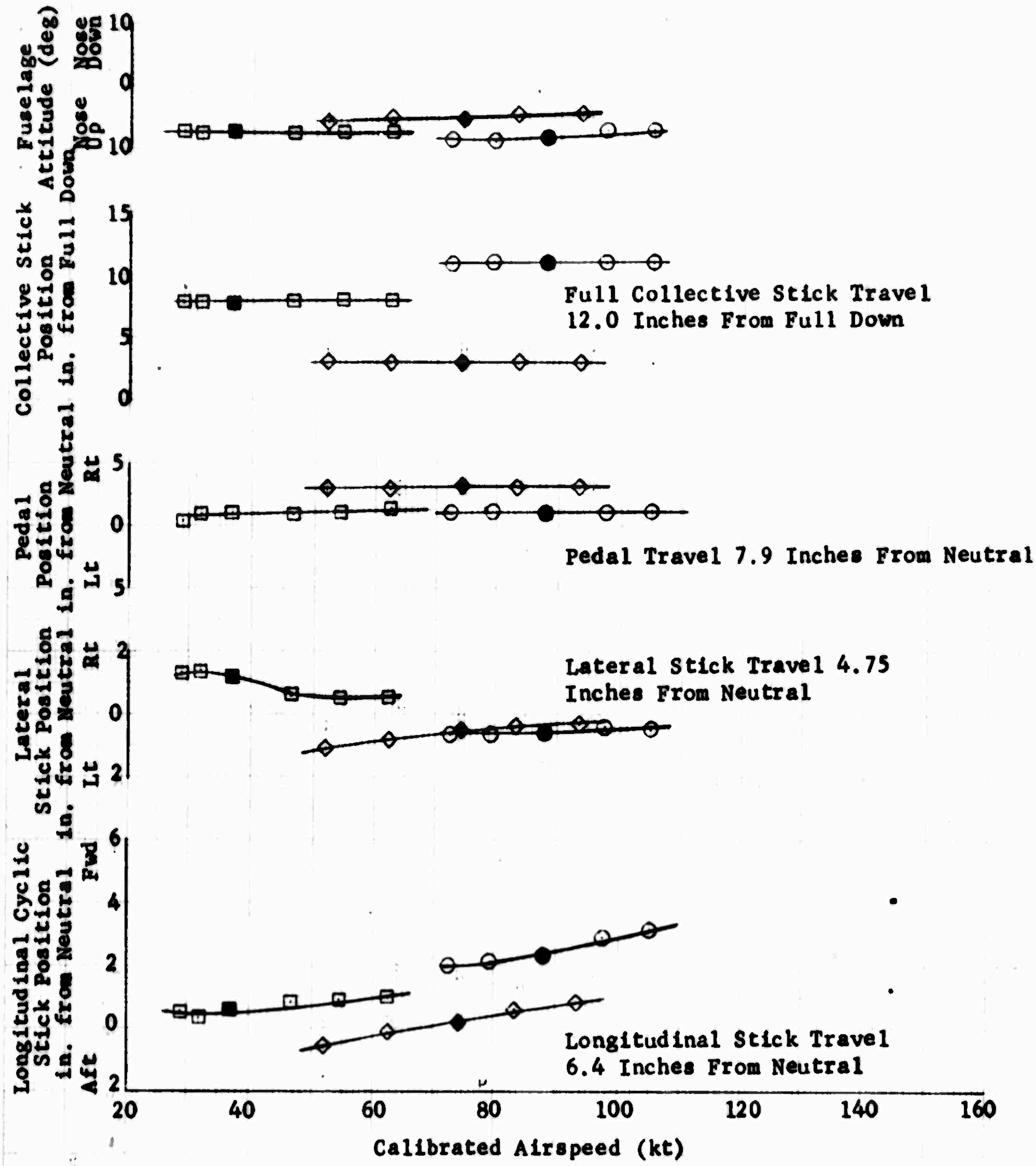

Figure 38. Static Longitudinal Speed Stability

HH-53C USAF S/N 67-14993

Sym	Flight Condition	Avg GW (lb)	Avg cg (in.)	Avg Press. Alt (ft)	Avg FAT (°C)	Rotor Speed (rpm)	AFCS
O	Level Flight	37,000	328	4,000	16	185	ON

NOTE: Solid Symbols Denote Trim Conditions

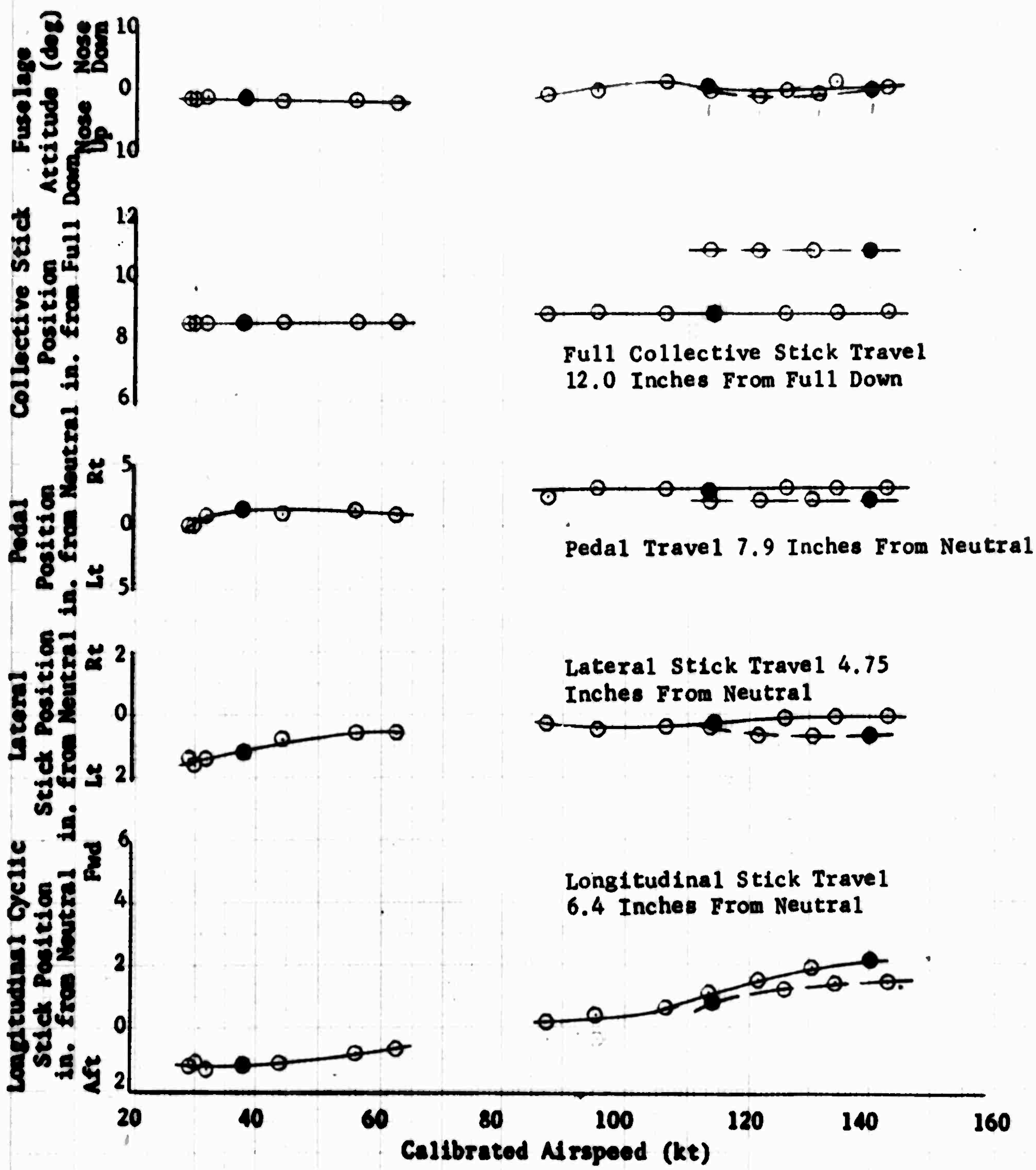

Figure 37. Static Longitudinal Speed Stability

HH-53C USAF S/N 67-14993

Sym	Flight Condition	Avg GW (lb)	Avg cg (in.)	Avg Press. Alt (ft)	Avg FAT (°C)	Rotor Speed (rpm)	AFCS
○	Climb	37,000	328	4,000	16	185	ON
◇	Auto.	37,000	328	4,000	16	185	ON
□	Partial Power Descent	37,000	328	4,000	16	185	ON

NOTE: Solid Symbols Denote Trim Conditions

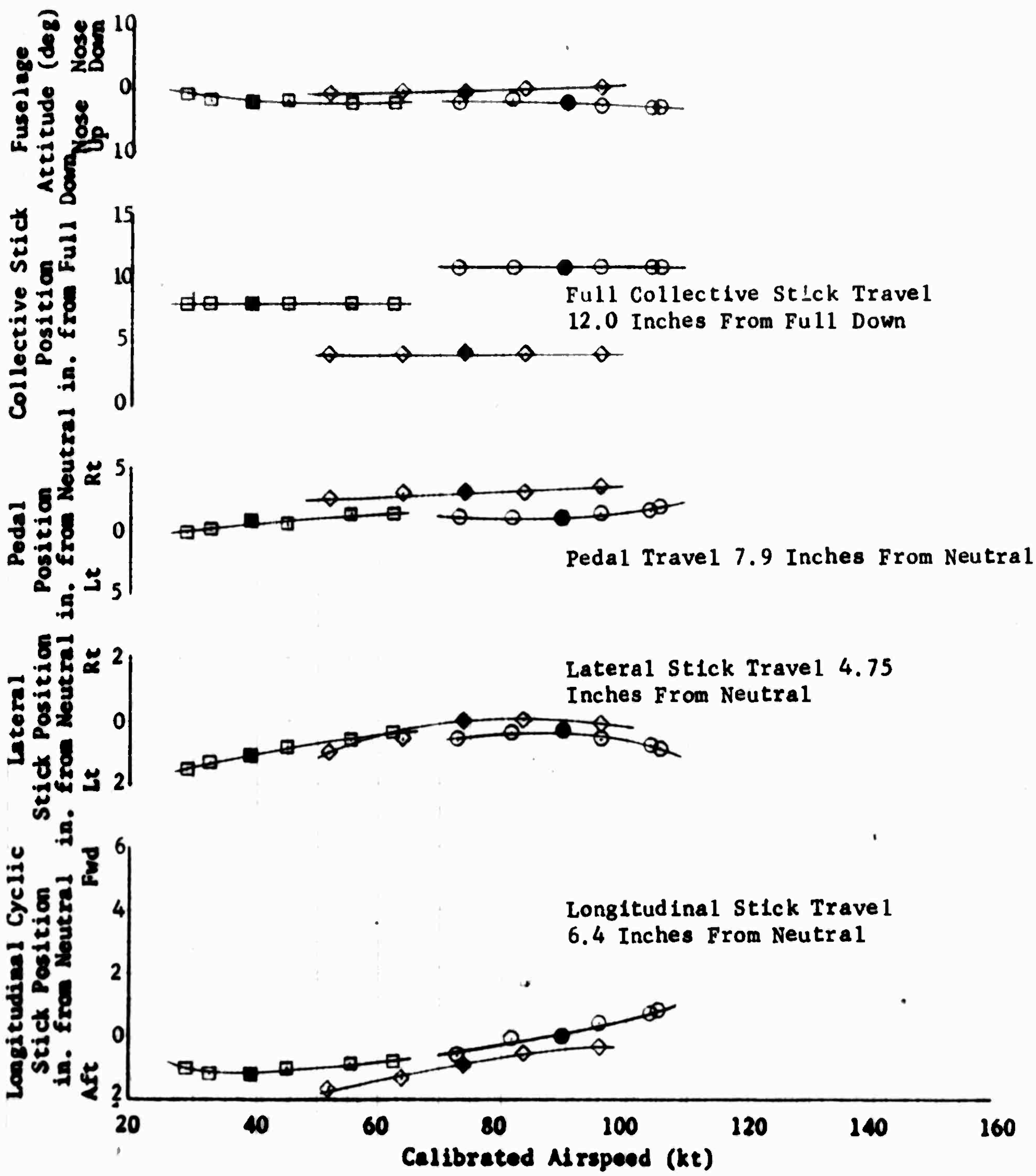

Figure 40. Static Longitudinal Speed Stability

HH-53C USAF S/N 67-14993

Sym	Flight Conditon	Avg GW (lb)	Avg cg (in.)	Avg Press. Alt (ft)	Avg FAT (°C)	Rotor Speed (rpm)	AFCS
○	Level Flight	37,000	352	13,300	2	185	ON

NOTE: Solid Symbols Denote Trim Conditions

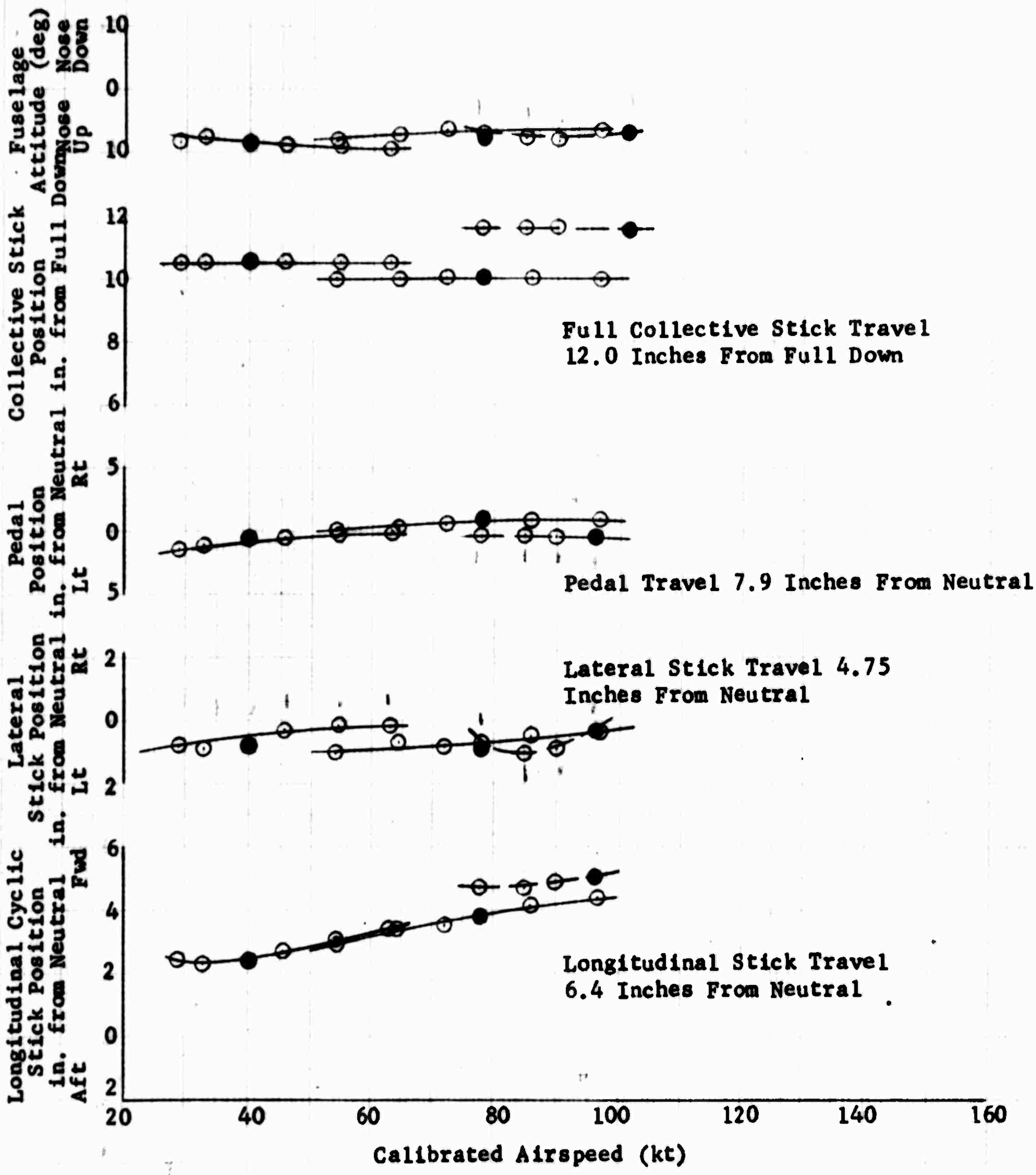

Figure 41. Static Longitudinal Speed Stability

HH-53C USAF S/N 67-14993

Sym	Flight Condition	Avg GW (lb)	Avg cg (in.)	Avg Press. Alt (ft)	Avg FAT (°C)	Rotor Speed (rpm)	AFCS
○	Climb	37,000	352	13,300	2	185	ON
◇	Auto.	37,000	352	13,300	2	185	ON
□	Partial Power Descent	37,000	352	13,300	2	185	ON

NOTE: Solid Symbols Denote Trim Conditions

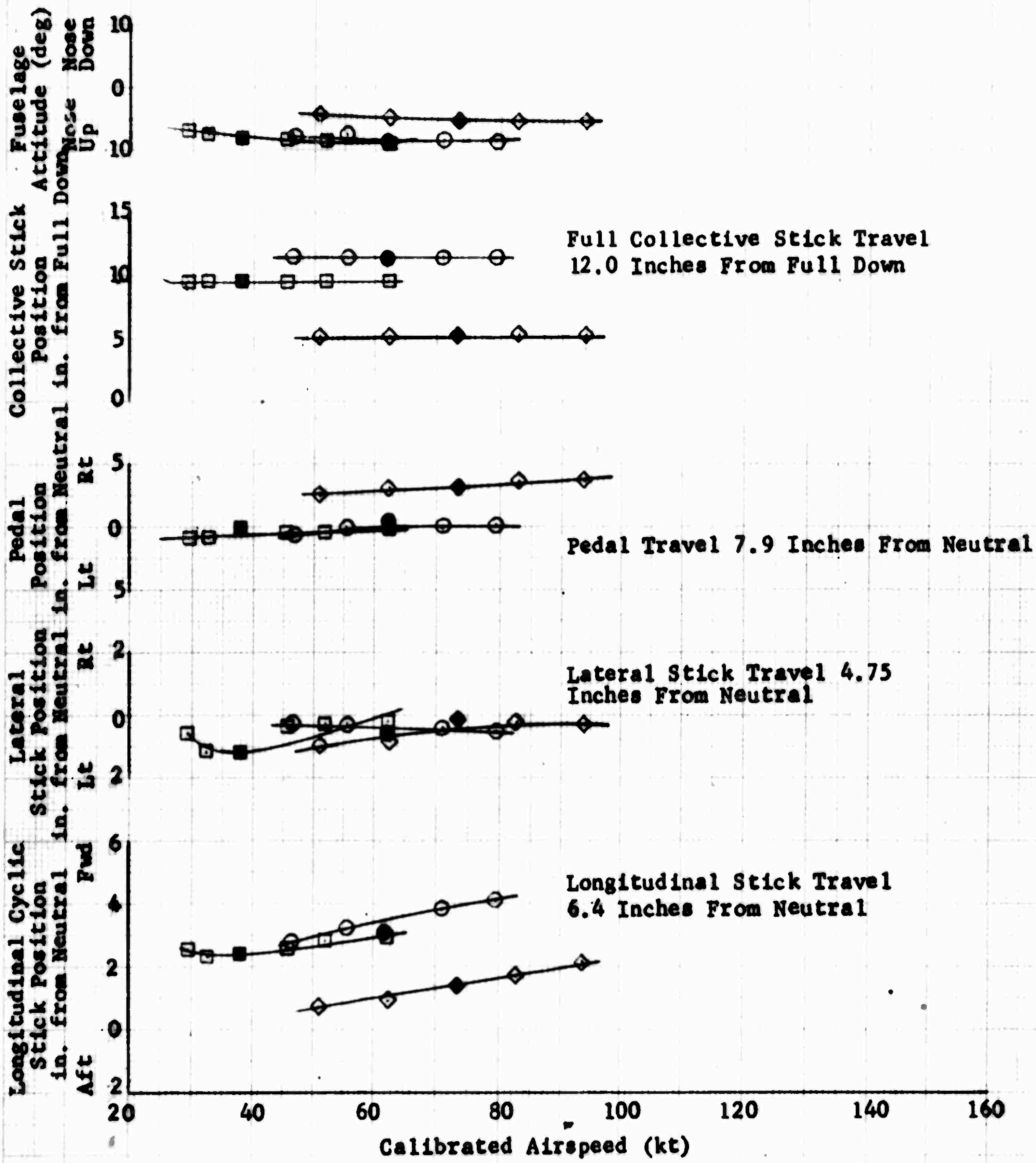

Figure 42. Static Longitudinal Speed Stability

HH-53C USAF S/N 67-14993

Sym	Flight Condition	Avg GW (lb)	Avg cg (in.)	Avg Press. Alt (ft)	Avg FAT (°C)	Rotor Speed (rpm)	AFCS
○	Level Flight	41,000	352	4,000	16	185	ON

NOTE: Solid Symbols Denote Trim Conditions

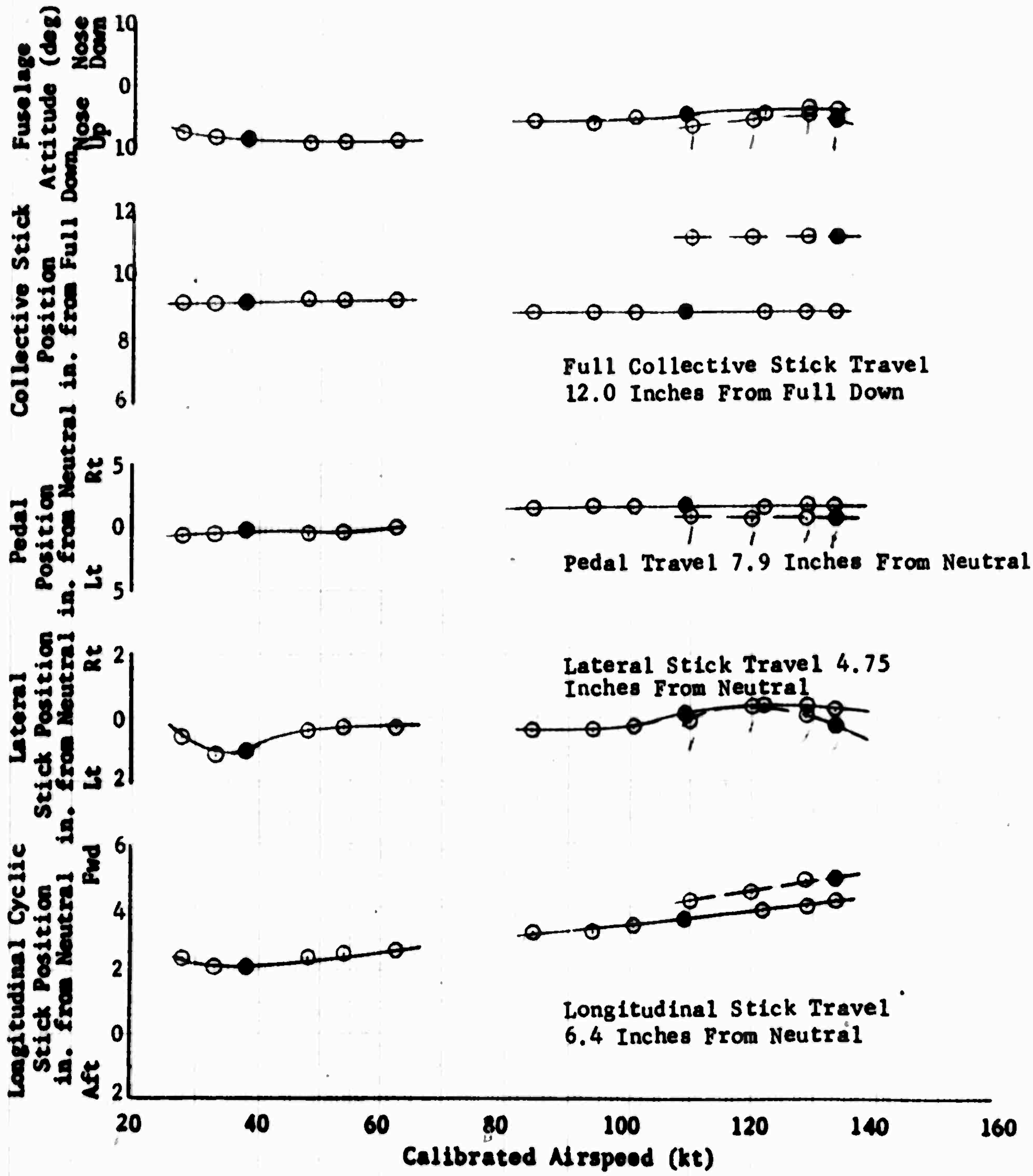

Figure 43. Static Longitudinal Speed Stability

HH-53C USAF S/N 67-14993

Sym	Flight Condition	Avg GW (lb)	Avg cg (in.)	Avg Press. Alt (ft)	Avg FAT (°C)	Rotor Speed (rpm)	AFCS
○	Climb	41,000	352	4,000	16	185	ON
◇	Auto.	41,000	352	4,000	16	185	ON
□	Partial Power Descent	41,000	352	4,000	16	185	ON

NOTE: Solid Symbols Denote Trim Conditions

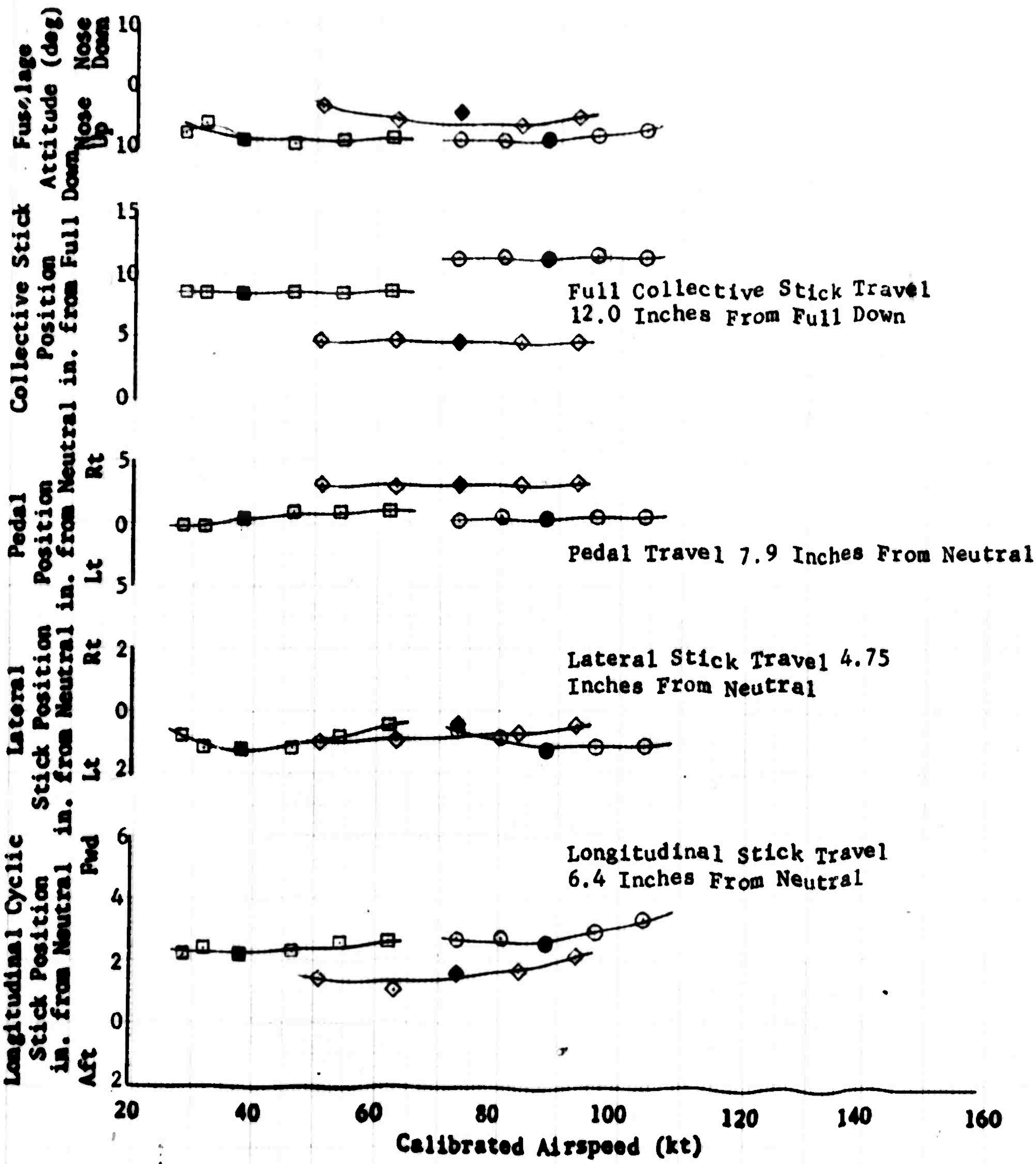

Figure 44. Static Longitudinal Speed Stability

HH-53C USAF S/N 67-14993

Sym	Flight Condition	Avg GW (lb)	Avg cg (in.)	Avg Press. Alt (ft)	Avg FAT (°C)	Rotor Speed (rpm)	AFCS
O	Level Flight	41,000	328	4,700	10	185	ON

NOTE: Solid Symbols Denote Trim Conditions

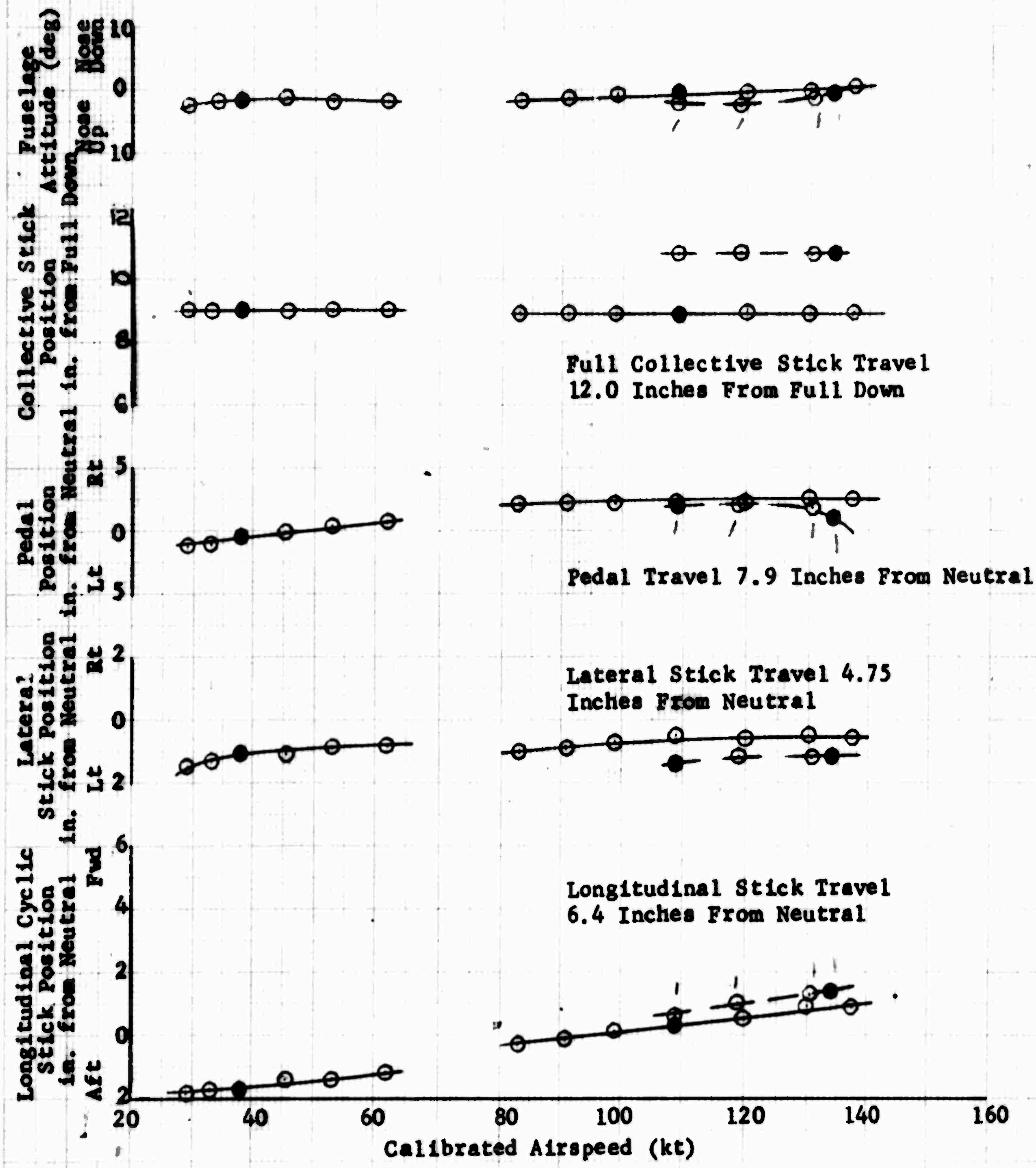

Figure 45. Static Longitudinal Speed Stability

Sym	Flight Condition	Avg GW (lb)	Avg cg (in.)	Avg Press. Alt (ft)	Avg FAT (°C)	Rotor Speed (rpm)	AFCS
○	Climb	41,000	328	4,700	10	185	ON
◇	Auto.	41,000	328	4,700	10	185	ON
□	Partial Power Descent	41,000	328	4,700	10	185	ON

NOTE: Solid Symbols Denote Trim Conditions

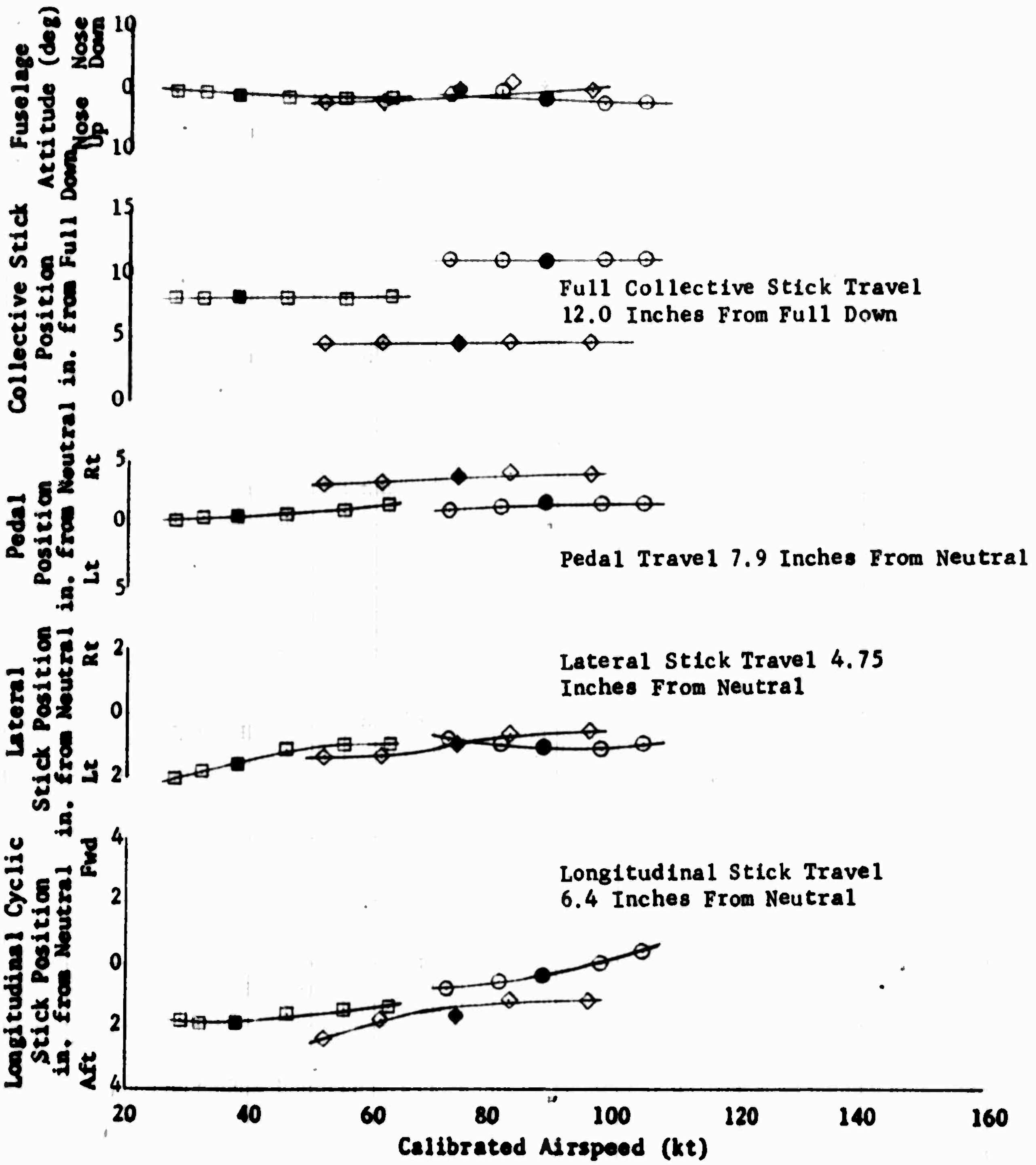

Figure 46. Static Longitudinal Speed Stability

HH-53C USAF S/N 67-14993

Sym	Flight Condition	Avg GW (lb)	Avg cg (in.)	Avg Press. Alt (ft)	Avg FAT (°C)	Rotor Speed (rpm)	AFCS
○	Level Flight	41,000	352	8,000	16	185	ON

NOTE: Solid Symbols Denote Trim Conditions

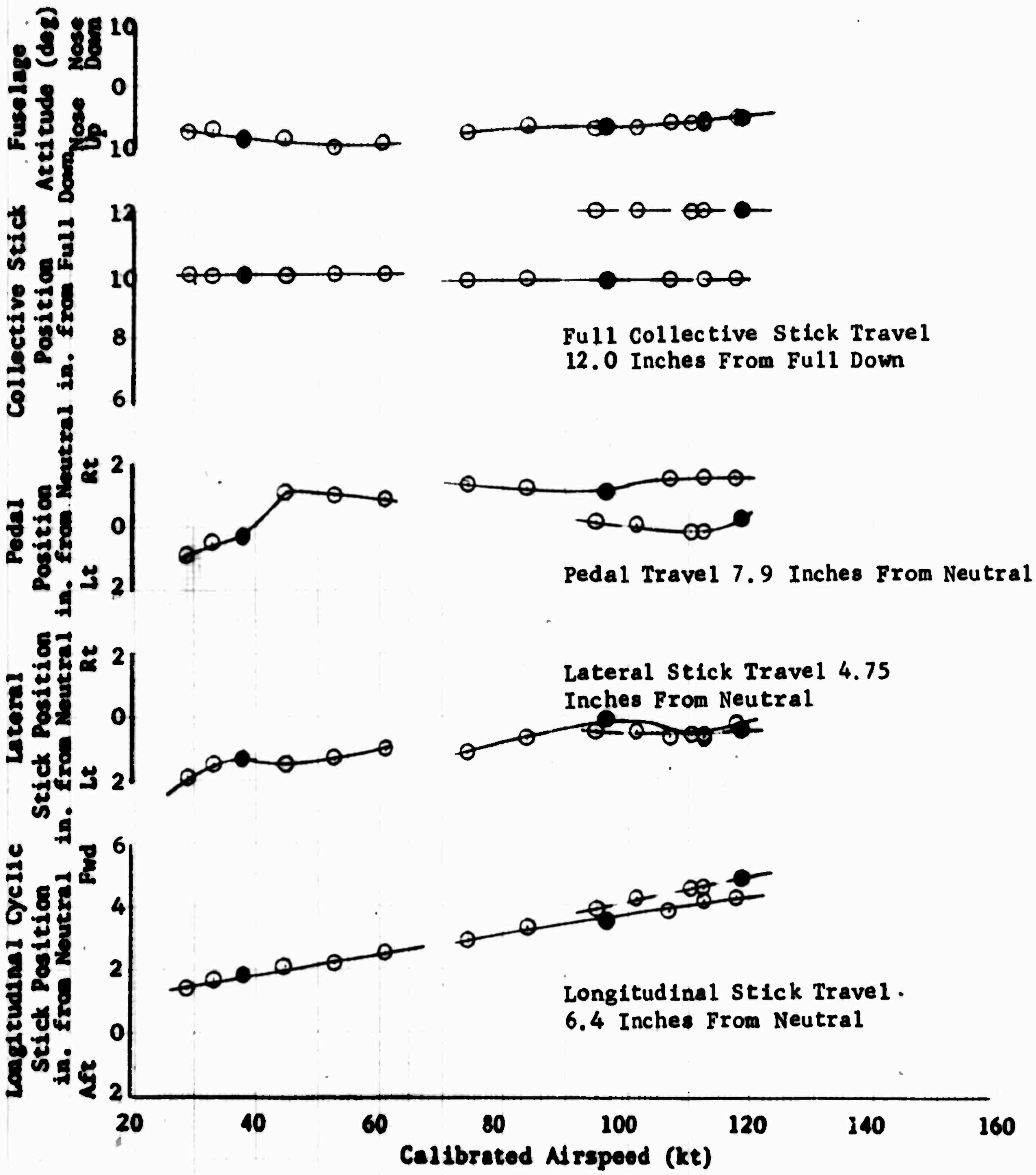

Figure 47. Static Longitudinal Speed Stability

HH-53C USAF S/N 67-14993

Sym	Flight Condition	Avg GW (lb)	Avg cg (in.)	Avg Press. Alt (ft)	Avg FAT (°C)	Rotor Speed (rpm)	AFCS
○	Climb	41,000	352	8,000	16	185	ON
◇	Auto.	41,000	352	8,000	16	185	ON
□	Partial Power Descent	41,000	352	8,000	16	185	ON

NOTE: Solid Symbols Denote Trim Conditions

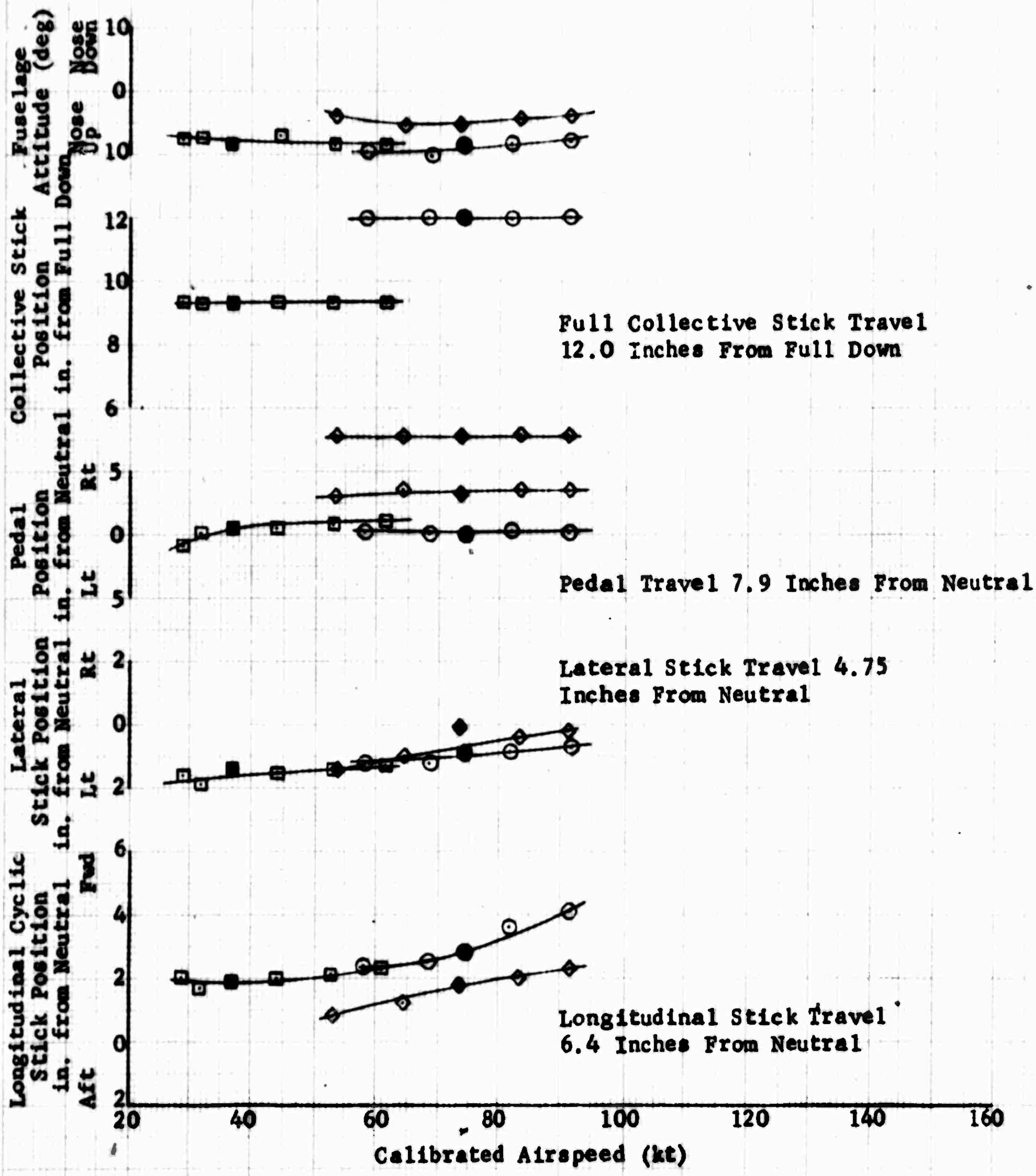

Figure 48. Static Longitudinal Speed Stability

Sym	Flight Condition	Avg GW (lb)	Avg cg (in.)	Avg Press. Alt (ft)	Avg FAT (°C)	Rotor Speed (rpm)	AFCS
O	Level Flight	41,000	352	9,000	7	185	ON

NOTE: Solid Symbols Denote Trim Conditions

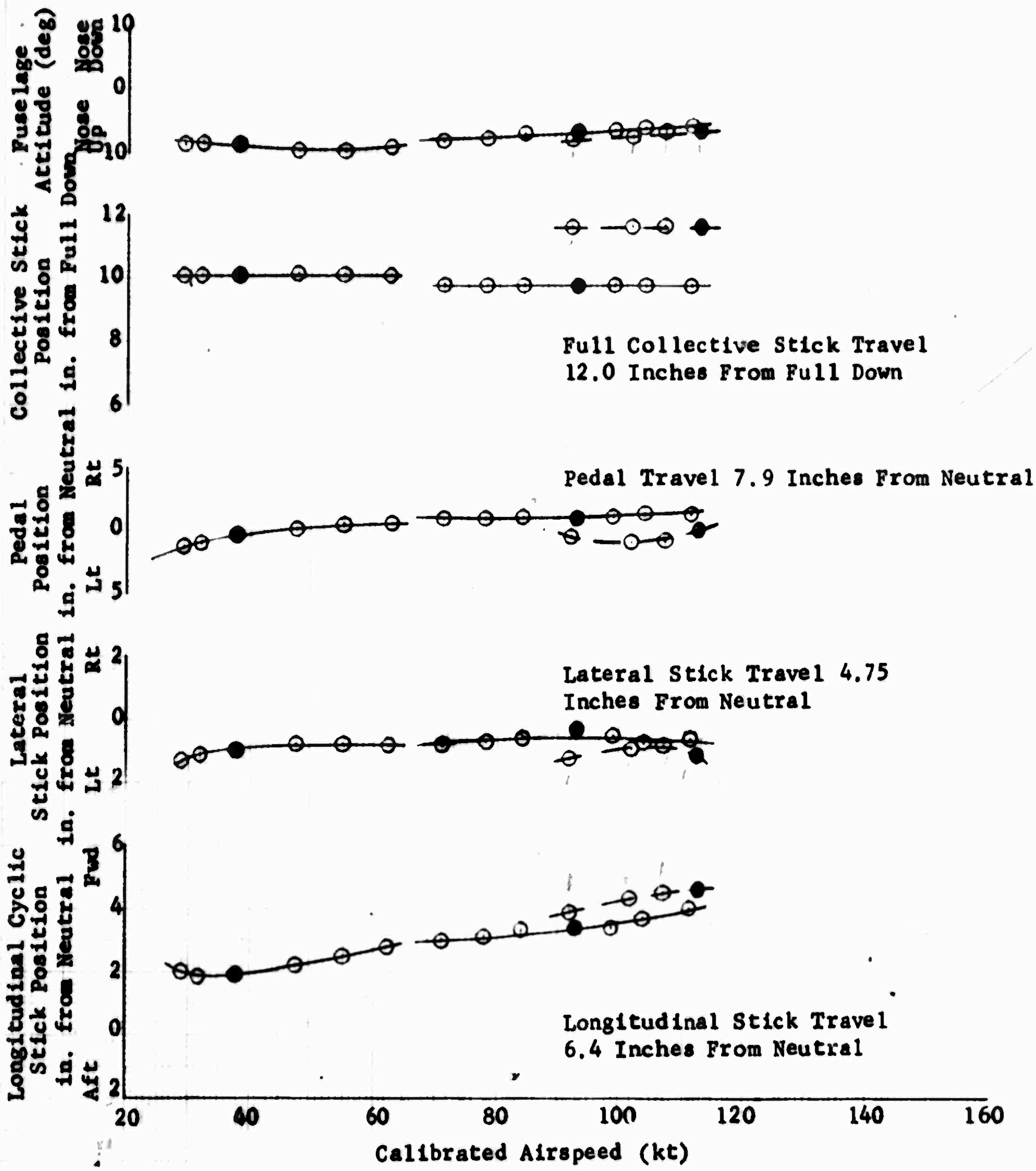

Figure 47. Static Longitudinal Speed Stability

HH-53C USAF S/N 67-14993

Sym	Flight Condition	Avg GW (lb)	Avg cg (in.)	Avg Press. Alt (ft)	Avg FAT (°C)	Rotor Speed (rpm)	AFCS
○	Climb	41,000	352	9,000	7	185	ON
◇	Auto.	41,000	352	9,000	7	185	ON
□	Partial Power Descent	41,000	352	9,000	7	185	ON

NOTE: Solid Symbols Denote Trim Conditions

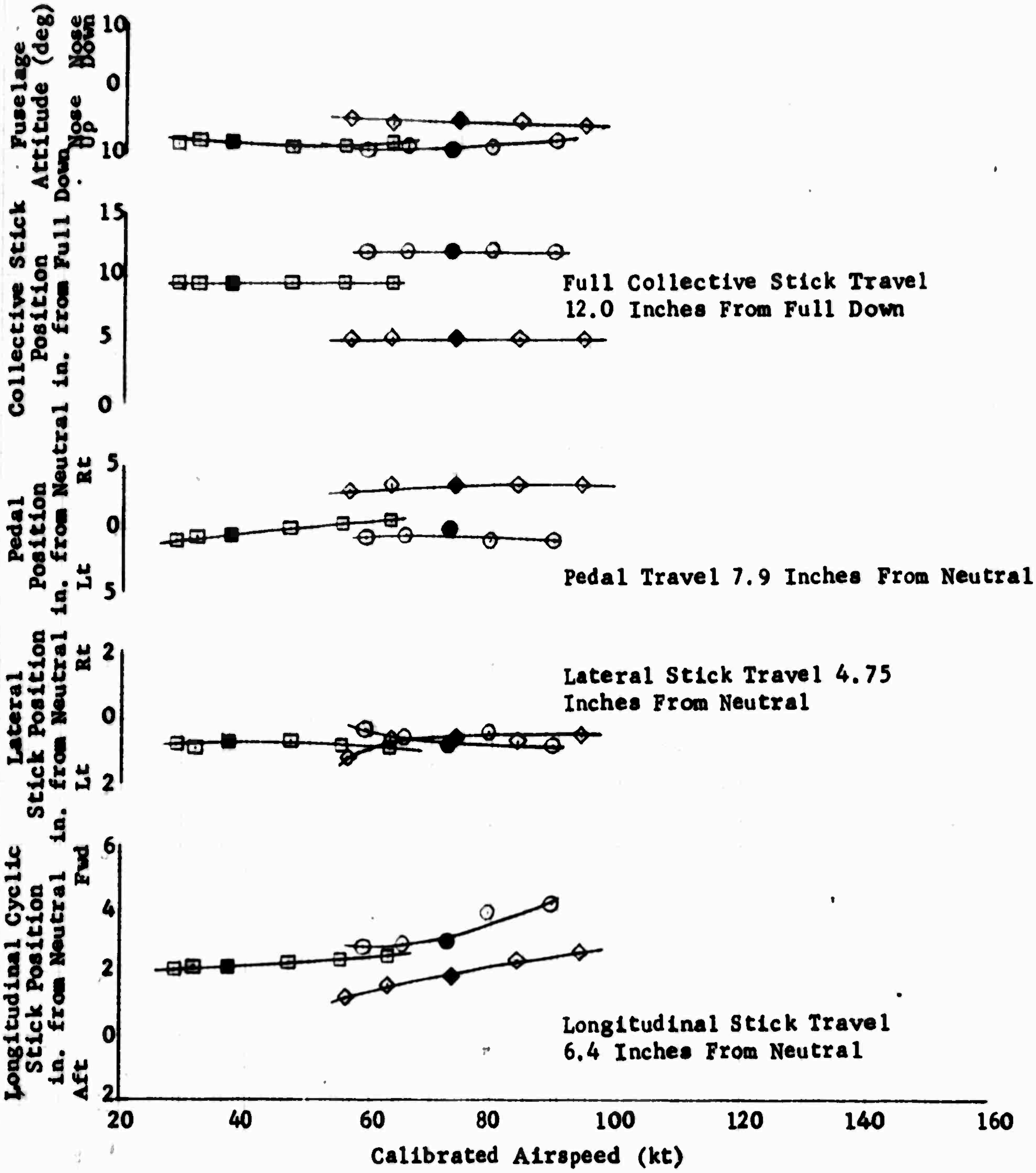

Figure 50. Static Longitudinal Speed Stability

HH-53C USAF S/N 67-14993

Flight Condition	Avg GW (lb)	Avg cg (in.)	Avg Press. Alt (ft)	Avg FAT (°C)	Rotor Speed (rpm)	AFCS	KCAS
Level Flight	31,000	352	5,100	5	185	ON	160

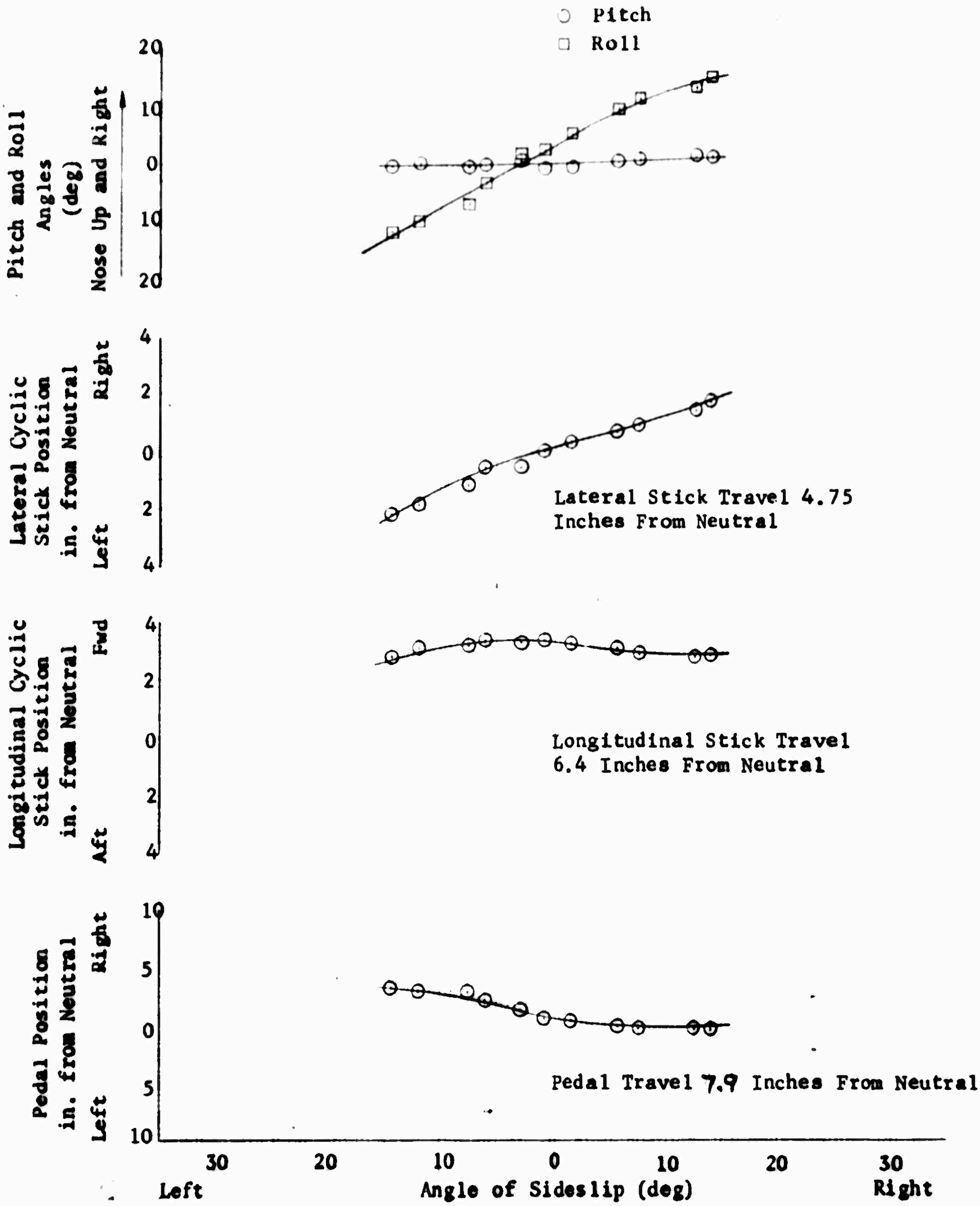

Figure 51 Static Directional Stability

HH-53C USAF S/N 67-14993

Flight Condition	Avg GW (lb)	Avg cg (in.)	Avg Press. Alt (ft)	Avg FAT (°C)	Rotor Speed (rpm)	AFCS	KCAS
Level Flight	31,000	352	5,100	5	185	ON	100

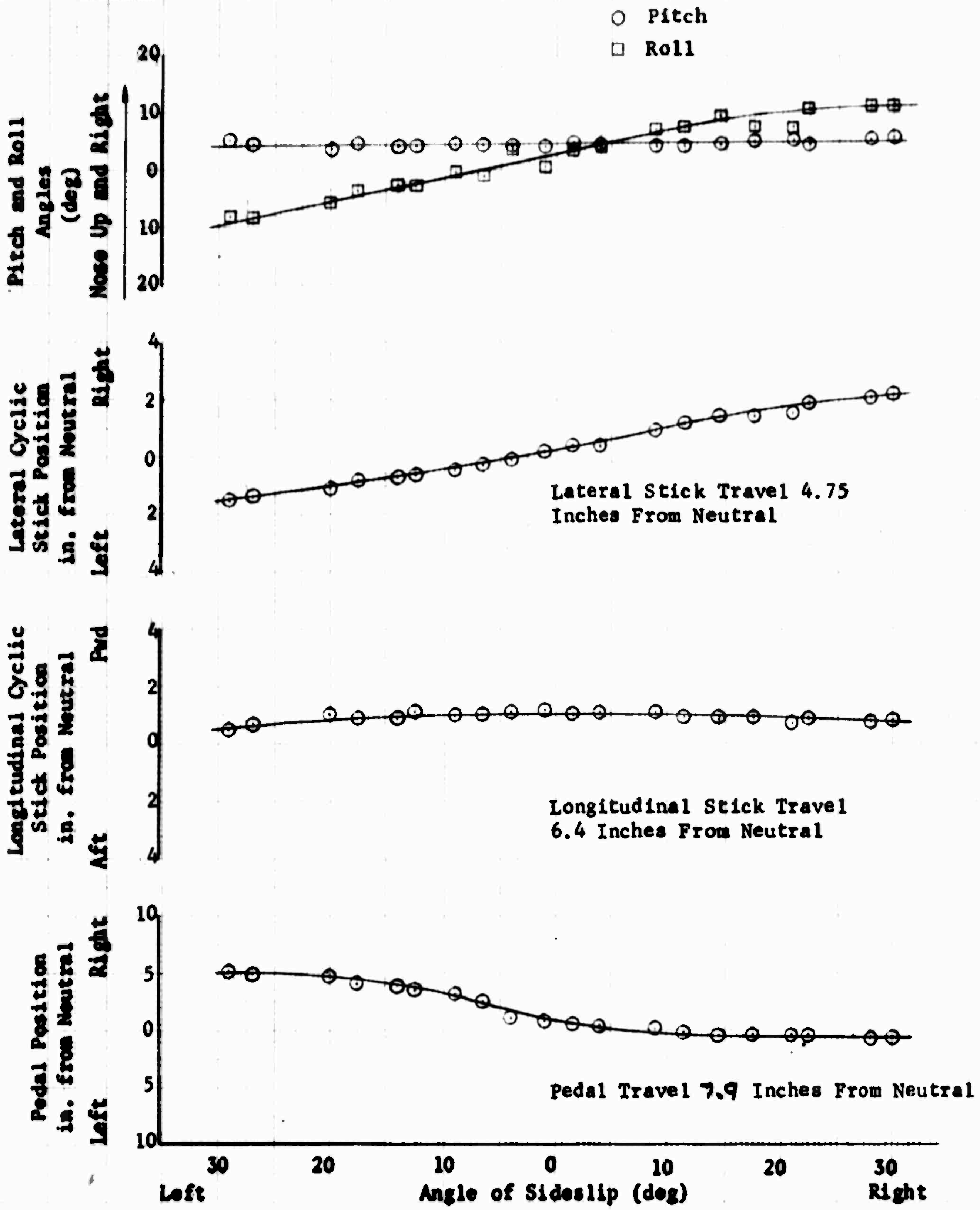

Figure 62. Static Directional Stability

Flight Condition	Avg GW (lb)	Avg cg (in.)	Avg Press. Alt (ft)	Avg FAT (°C)	Rotor Speed (rpm)	AFCS	KCAS
Level Flight	31,000	352	5,100	5	185	ON	60

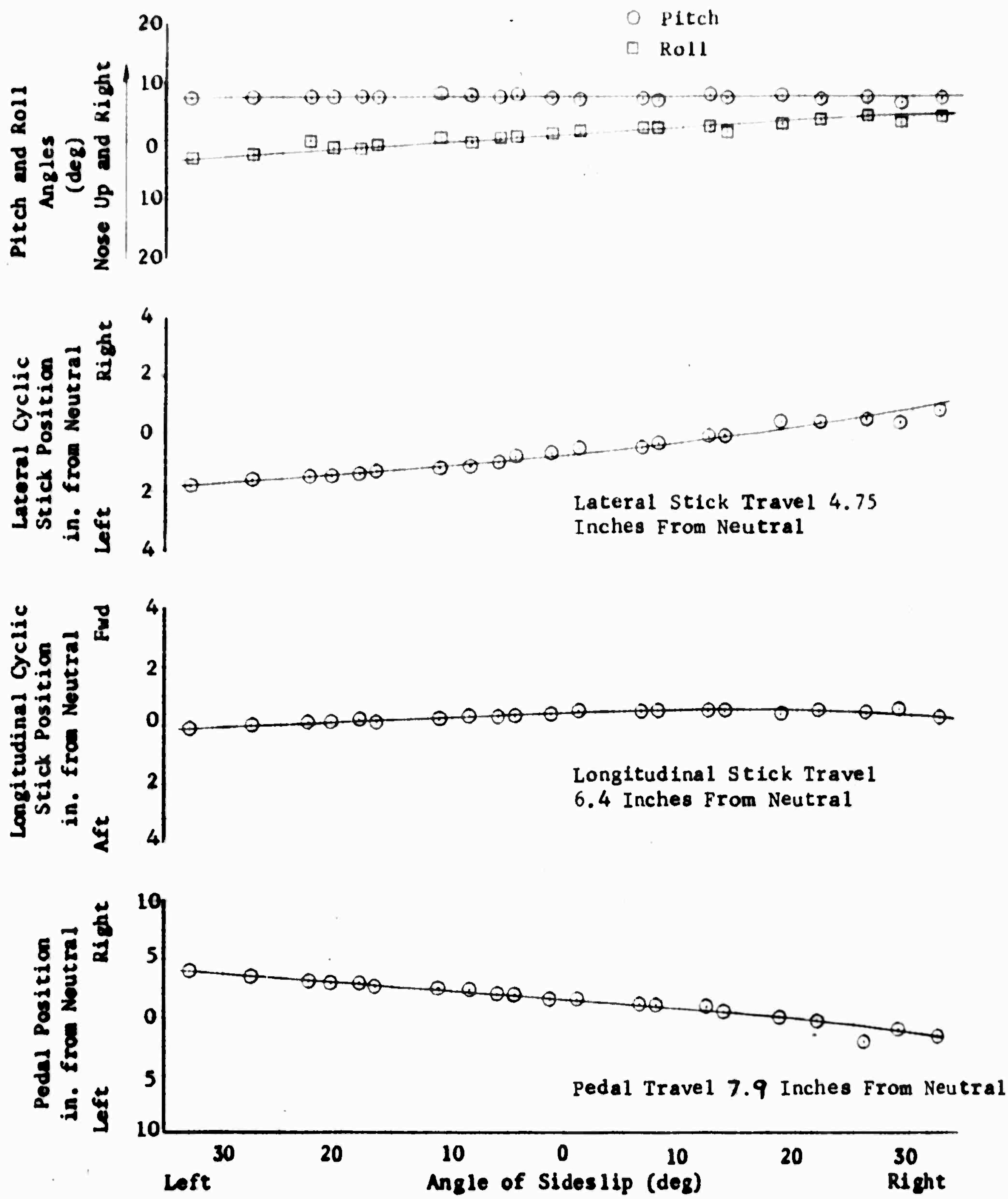

Figure 53. Static Directional Stability

HH-53C USAF S/N 67-14993

Flight Condition	Avg GW (lb)	Avg cg (in.)	Avg Press. Alt (ft)	Avg FAT (°C)	Rotor Speed (rpm)	AFCS	KCAS
Level Flight	31,000	352	14,800	-10	185	ON	53

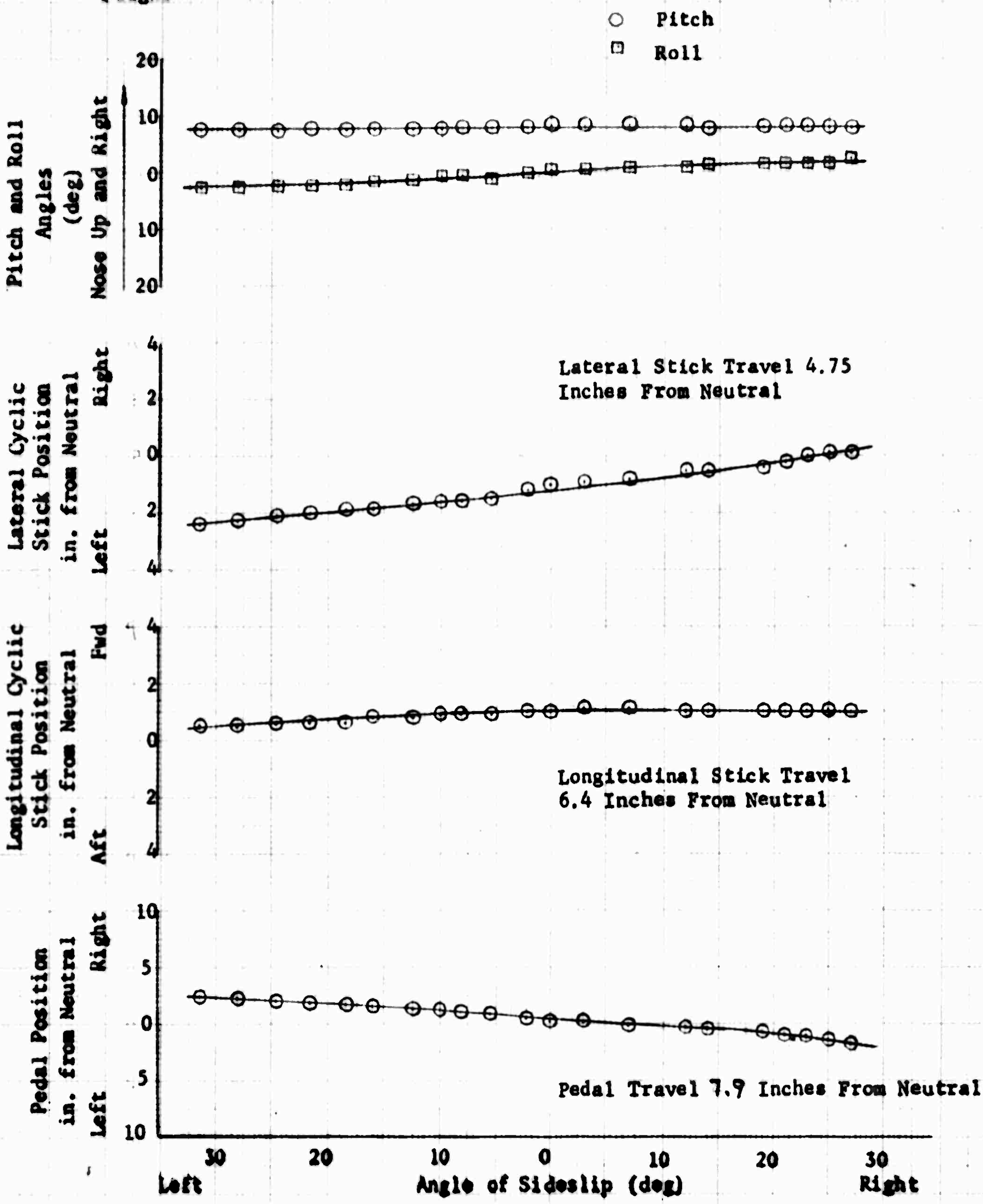

Figure 54 Static Directional Stability

Flight Condition	Avg GW (lb)	Avg cg (in.)	Avg Press. Alt (ft)	Avg FAT (°C)	Rotor Speed (rpm)	AFCS	KCAS
Level Flight	31,000	352	14,800	-10	185	ON	96

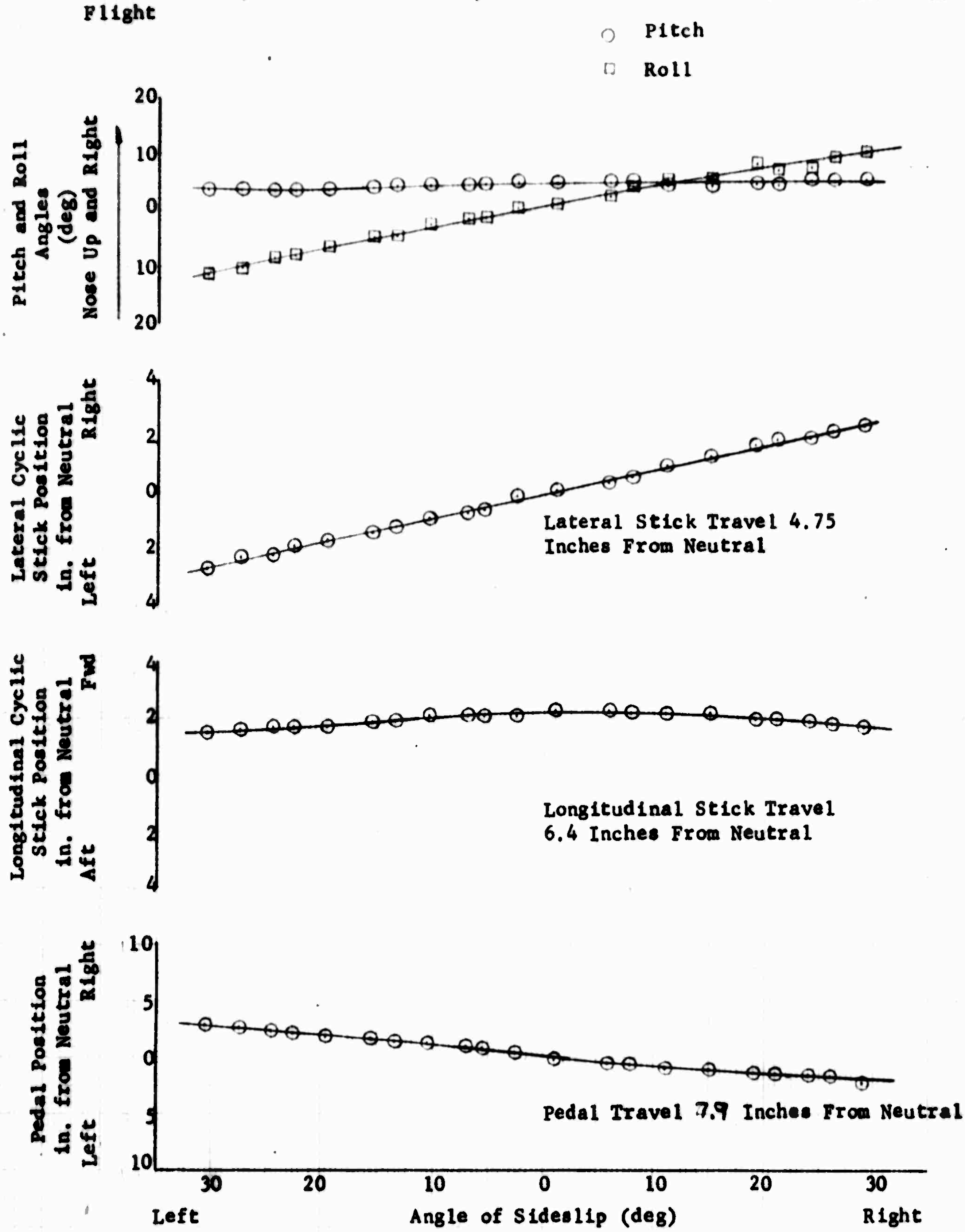

Figure 66. Static Directional Stability

HH-53C USAF S/N 67-14993

Flight Condition	Avg GW (lb)	Avg cg (in.)	Avg Press. Alt (ft)	Avg FAT (°C)	Rotor Speed (rpm)	AFCS	KCAS
Climb	31,000	352	14,500	-11	185	ON	63

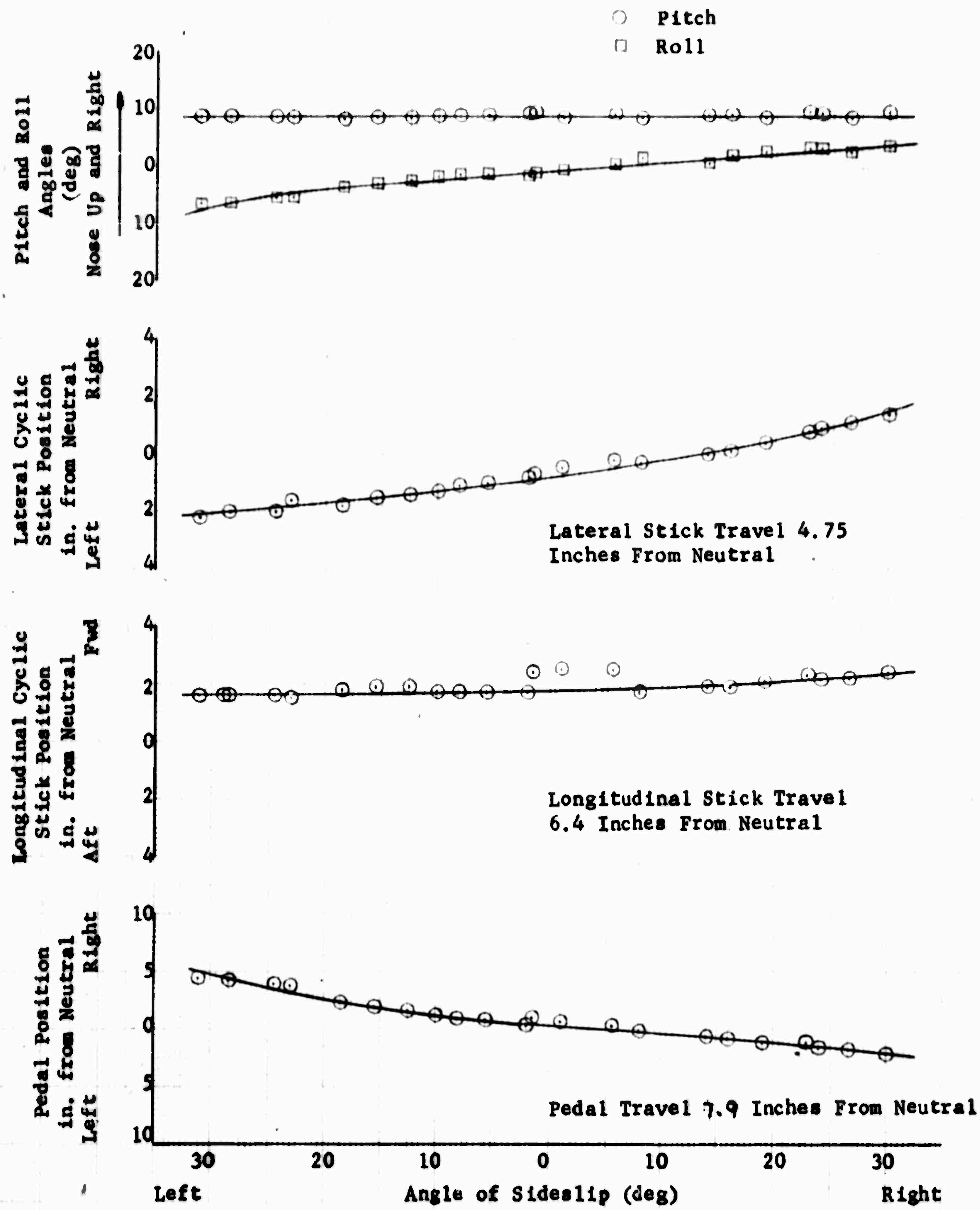

Figure 56. Static Directional Stability

Flight Condition	Avg GW (lb)	Avg cg (in.)	Avg Press. Alt (ft)	Avg FAT (°C)	Rotor Speed (rpm)	AFCS	KCAS
Partial Power Descent	31,000	352	14,800	-10	185	ON	53

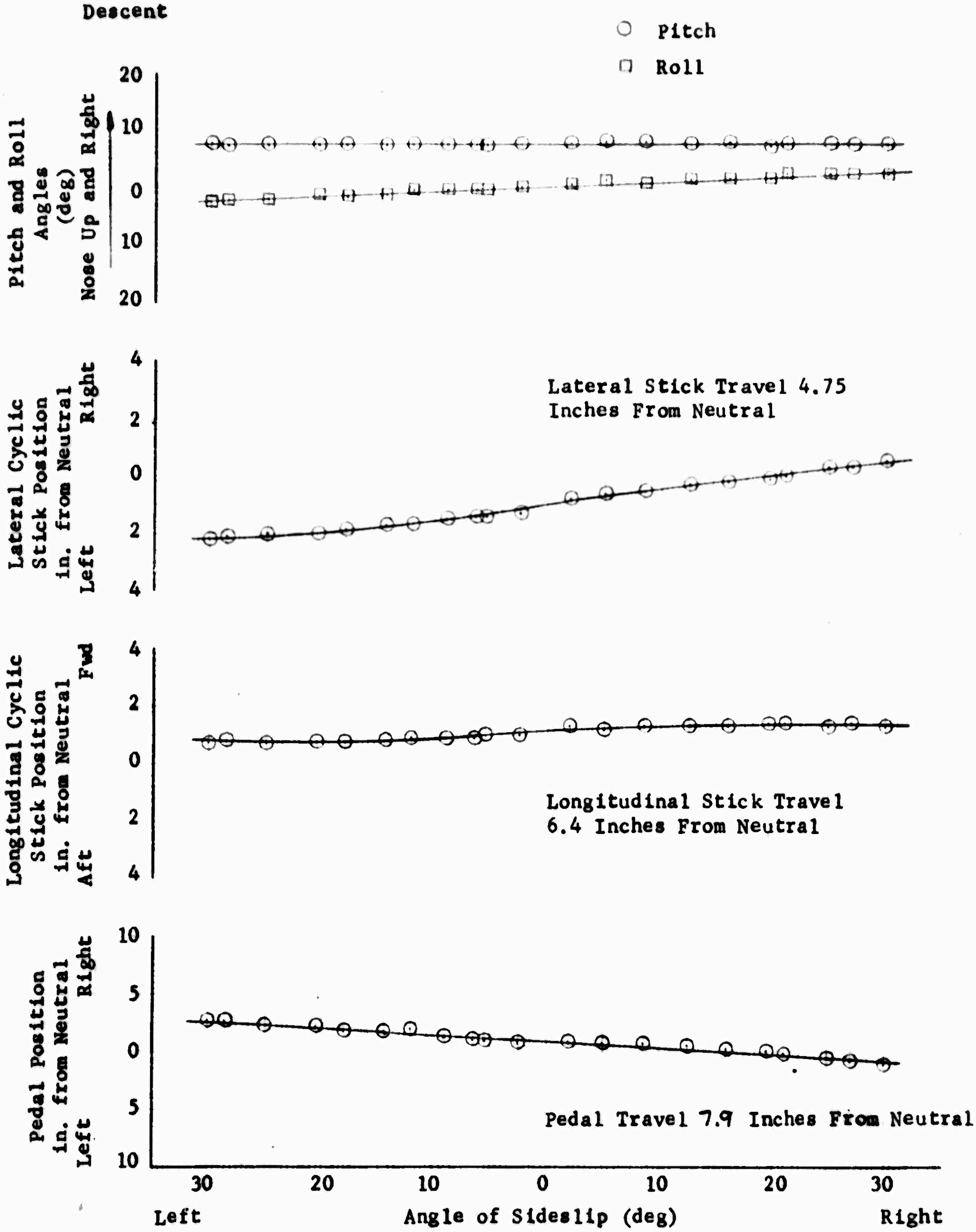

Figure 57. Static Directional Stability

HH-53C USAF S/N 67-14993

Flight Condition	Avg GW (lb)	Avg cg (in.)	Avg Press. Alt (ft)	Avg FAT (°C)	Rotor Speed (rpm)	AFCS	KCAS
Level Flight	41,000	352	5,500	6	185	ON	134

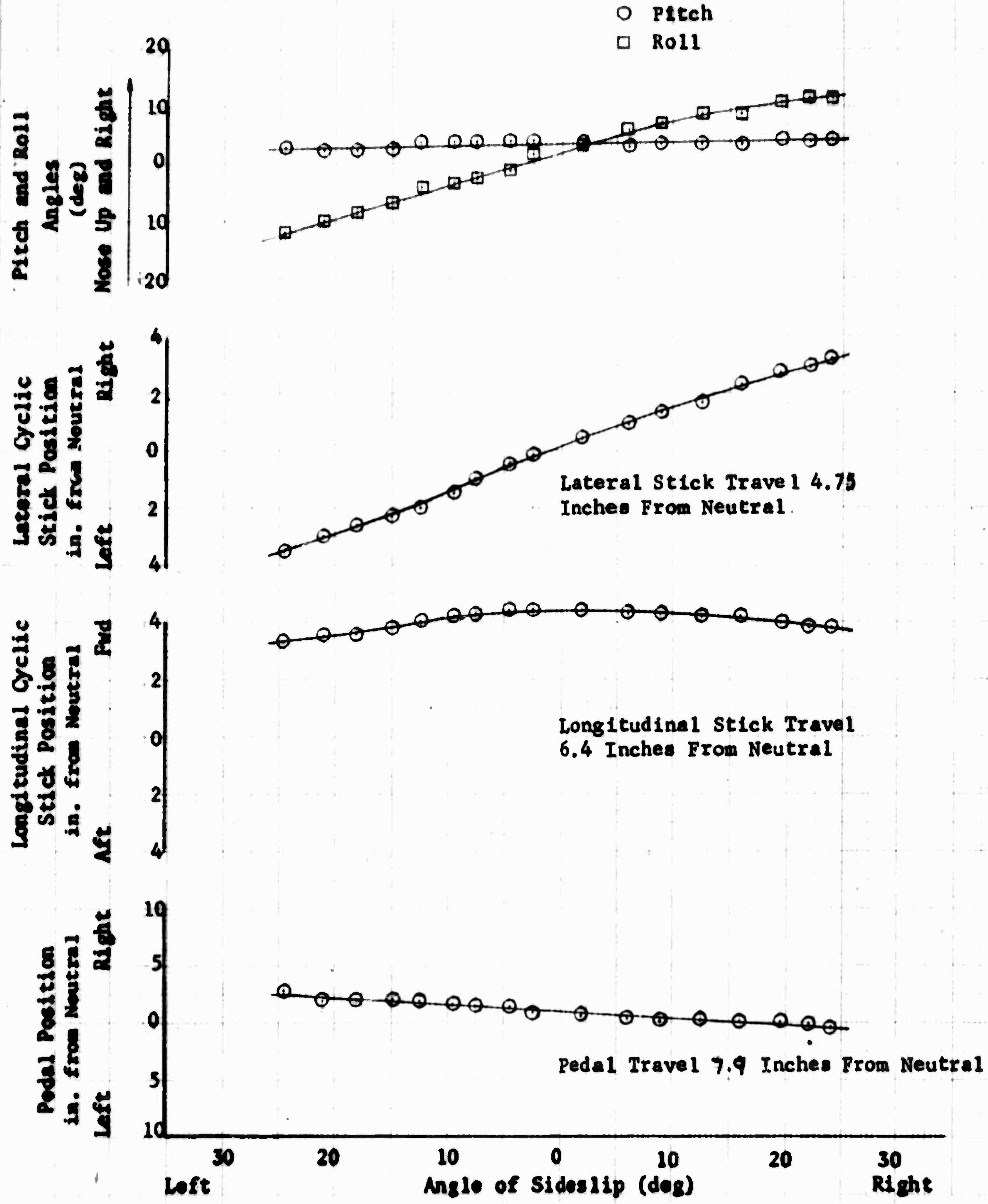

Figure 58. Static Directional Stability

HH-53C USAF S/N 67-14993

Flight Condition	Avg GW (lb)	Avg cg (in.)	Avg Press. Alt (ft)	Avg FAT (°C)	Rotor Speed (rpm)	AFCS	KCAS
Level Flight	41,000	352	5,500	6	185	ON	87

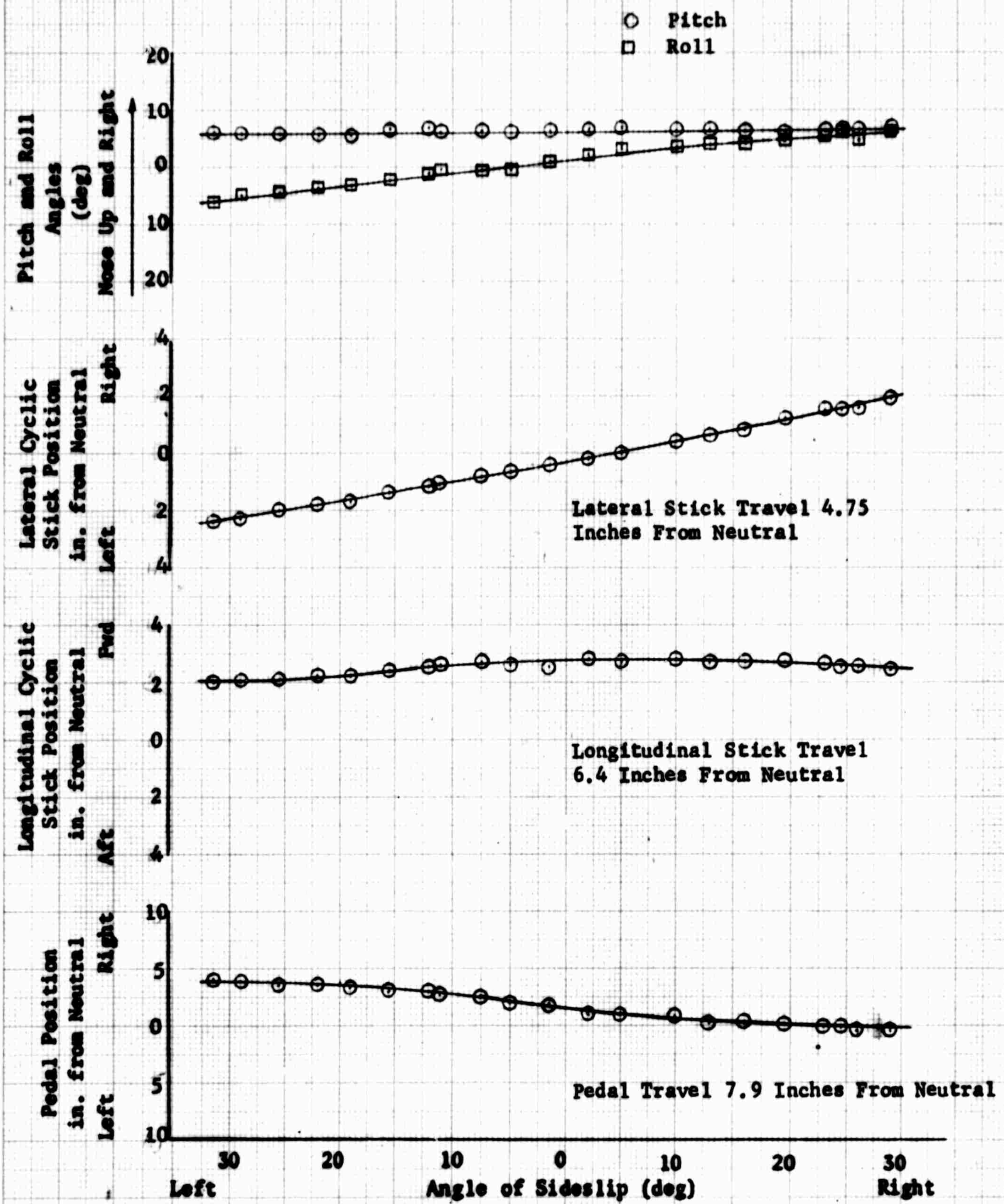

Figure 57. Static Directional Stability

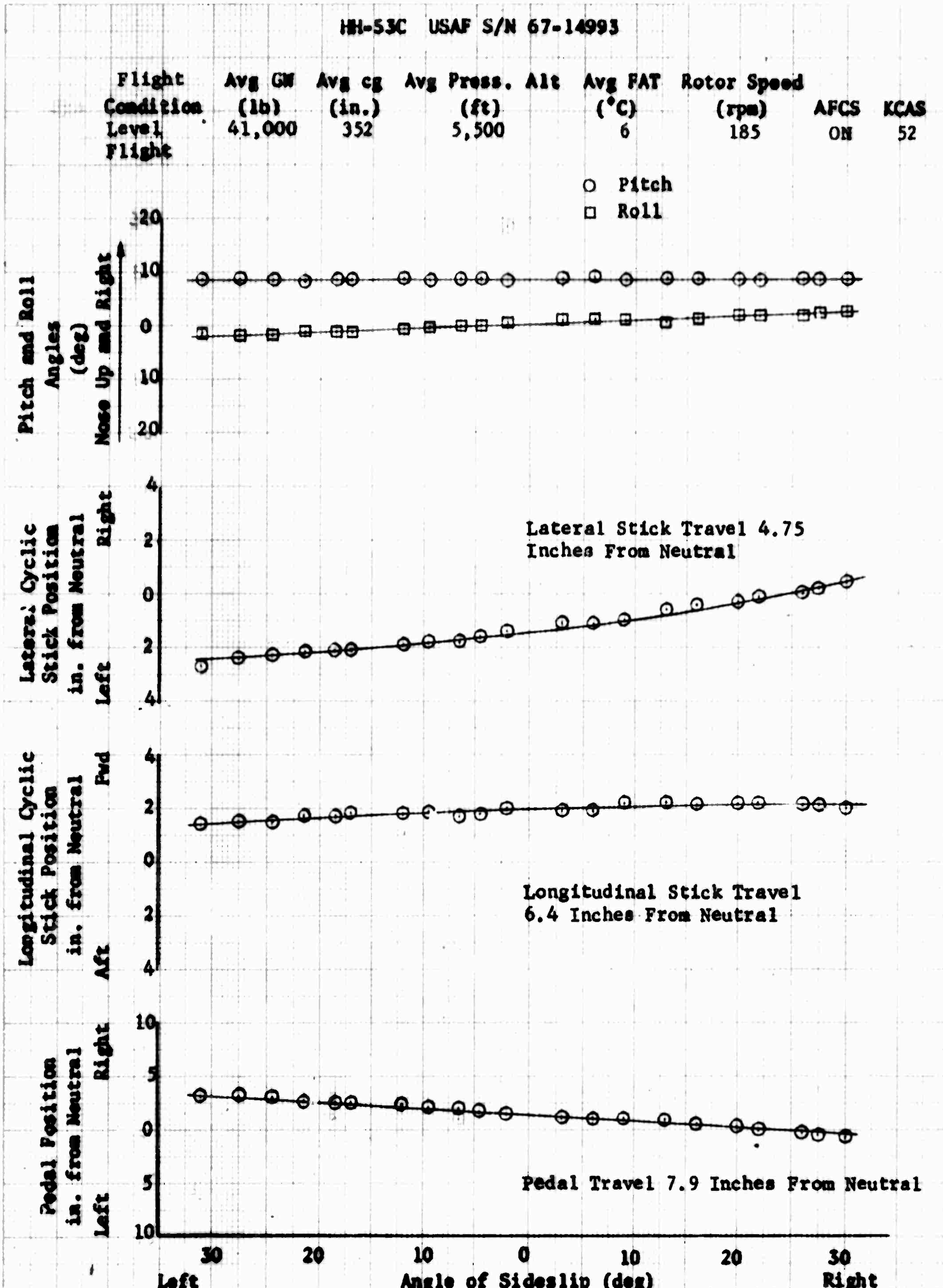

Figure 60. Static Directional Stability

HH-53C USAF S/N 67-14993

Flight Condition	Avg GW (lb)	Avg cg (in.)	Avg Press. Alt (ft)	Avg FAT (°C)	Rotor Speed (rpm)	AFCS	KCAS
Level Flight	41,000	352	13,000	-6	185	ON	74

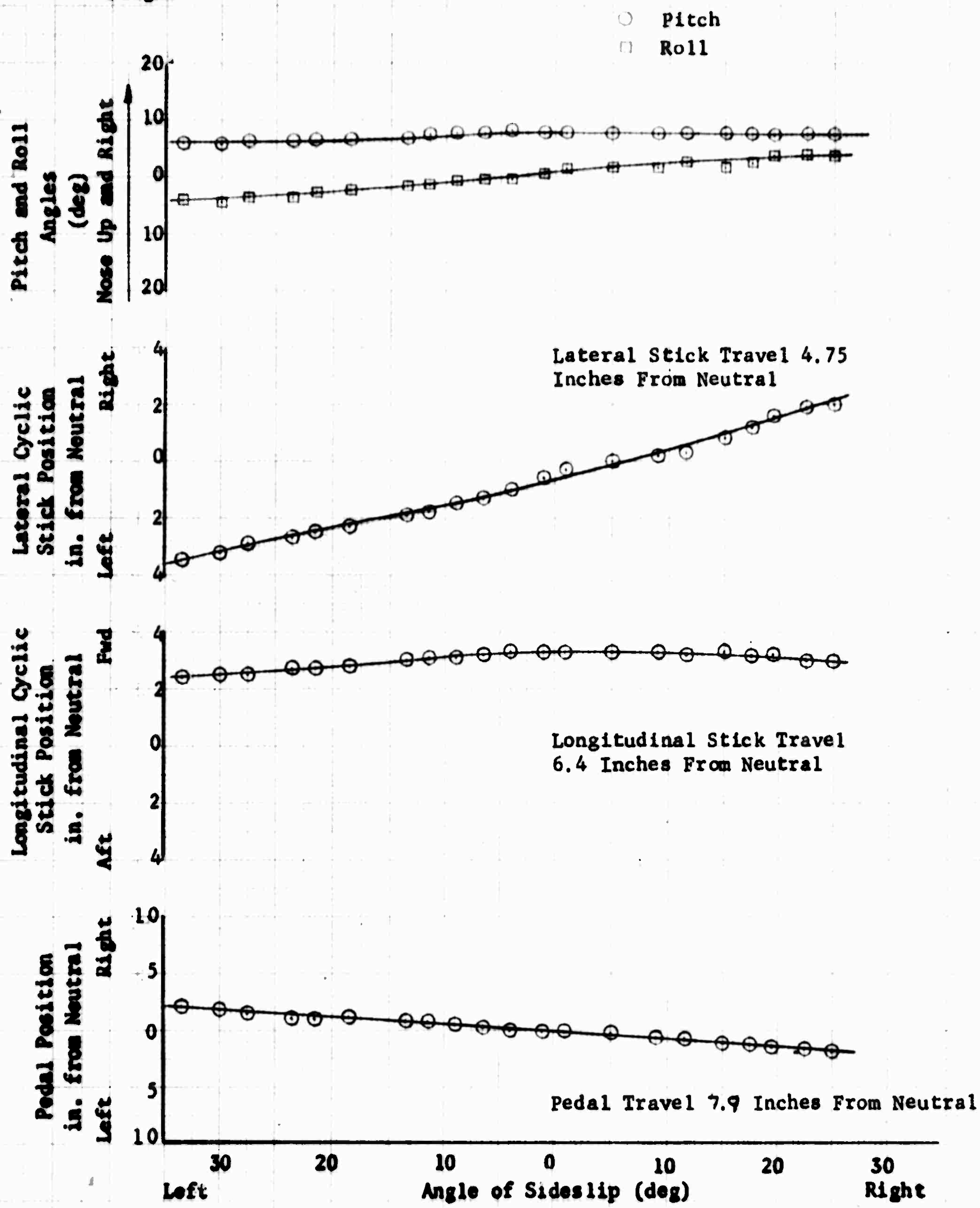

Figure 61. Static Directional Stability

HH-53C USAF S/N 67-14993

Flight Condition	Avg GW (lb)	Avg cg (in.)	Avg Press. Alt (ft)	Avg FAT (°C)	Rotor Speed (rpm)	AFCS	KCAS
Level Flight	41,000	352	13,000	-6	185	ON	53

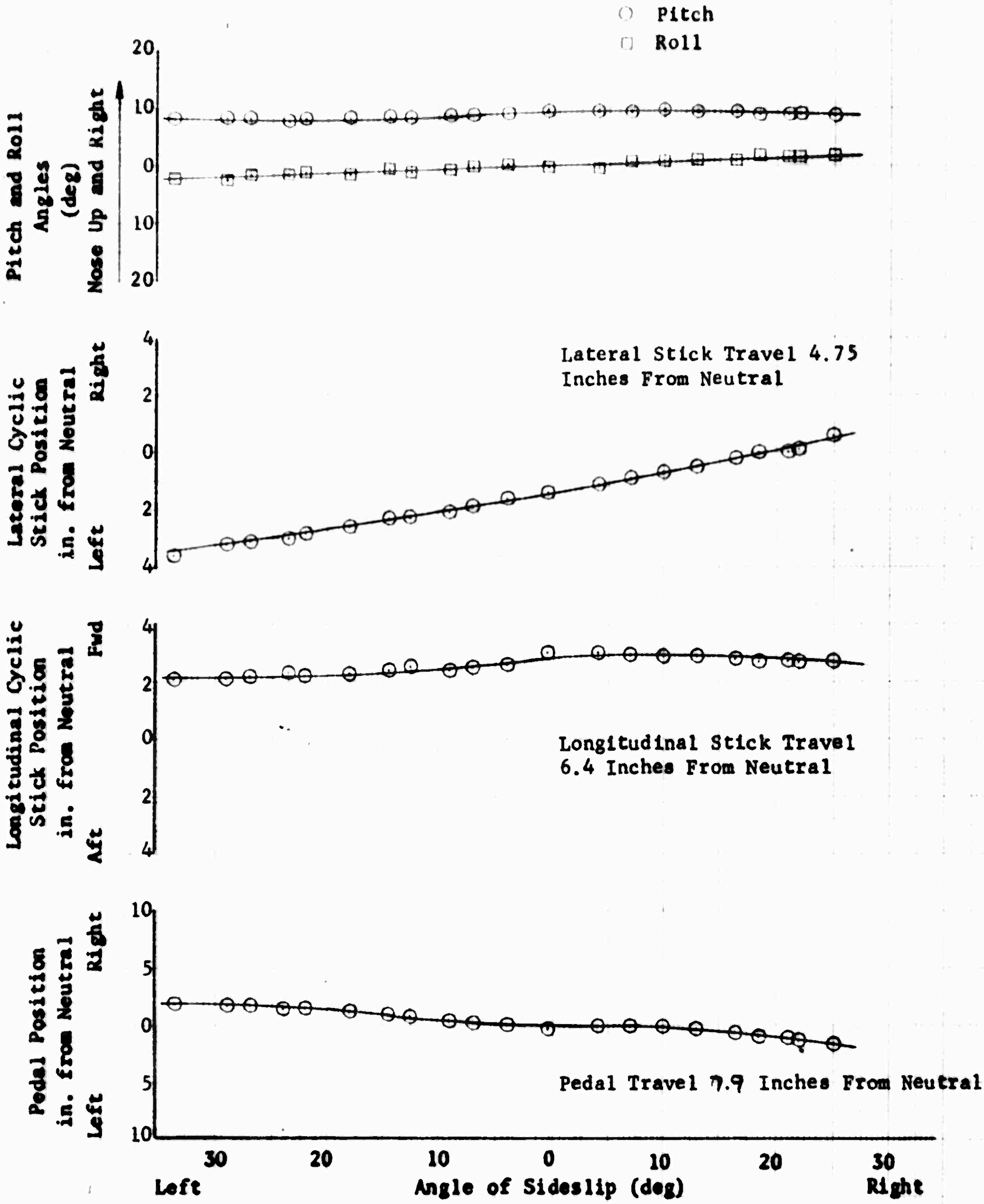

Figure 62. Static Directional Stability

HH-53C USAF S/N 67-14993

Flight Condition	Avg GW (lb)	Avg cg (in.)	Avg Press. Alt (ft)	Avg FAT (°C)	Rotor Speed (rpm)	AFCS	KCAS
Climb	41,000	352	6,000	-5	185	ON	87

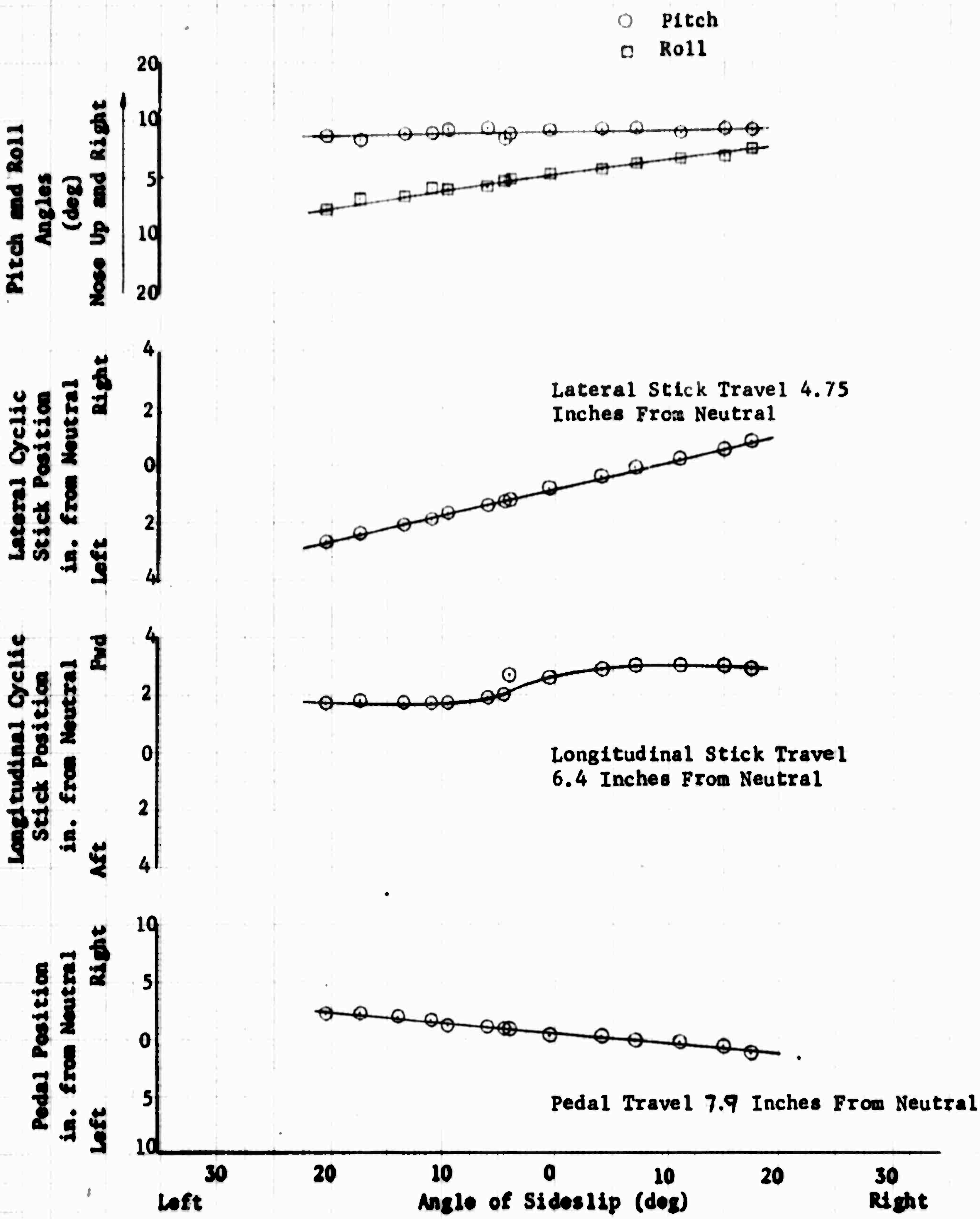

Figure 63. Static Directional Stability

HH-53C USAF S/N 67-14993

Flight Condition	Avg GW (lb)	Avg cg (in.)	Avg Press. Alt (ft)	Avg FAT (°C)	Rotor Speed (rpm)	AFCS	KCAS
Partial Power Descent	41,000	352	5,000	5	185	ON	130

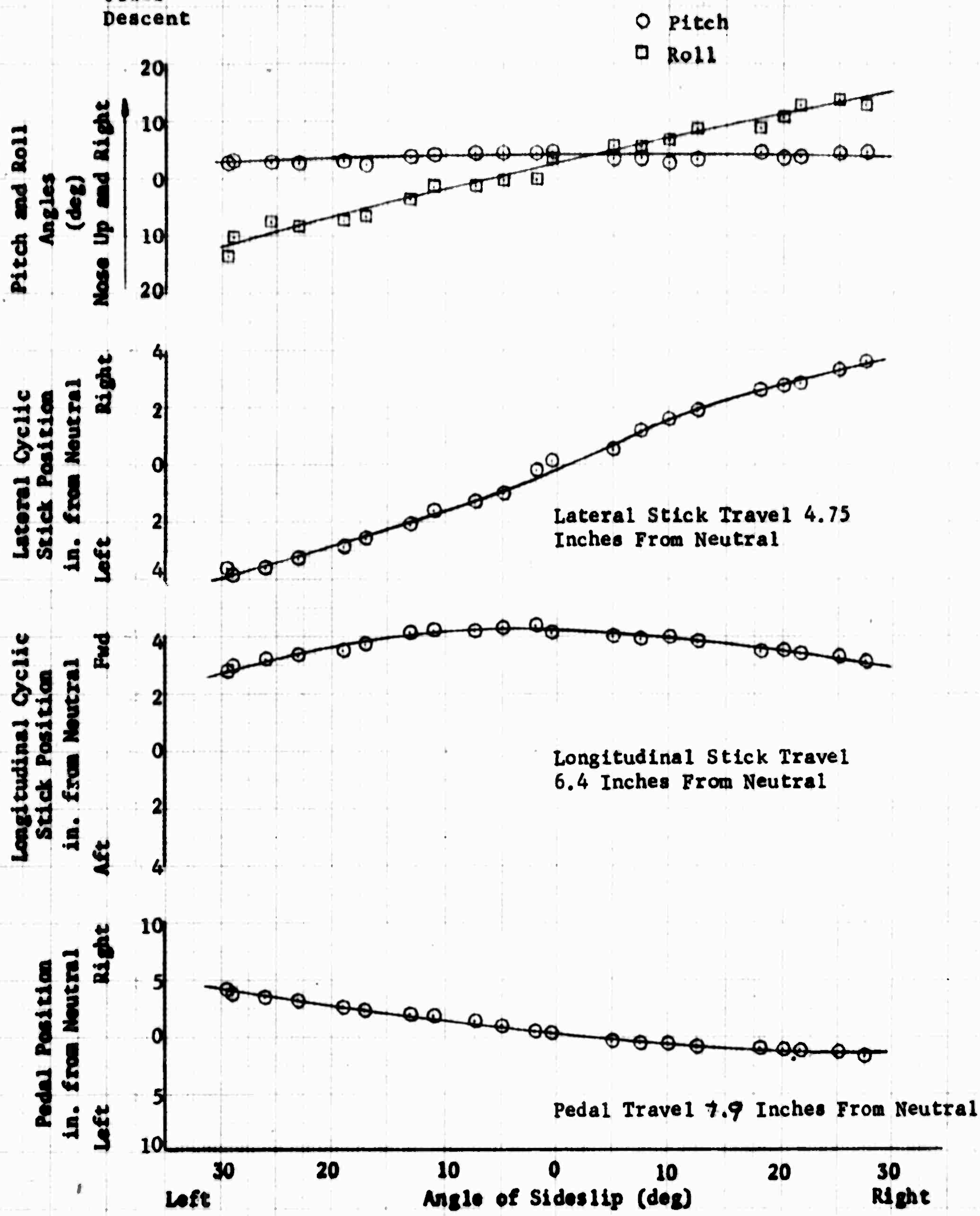

Figure 64 Static Directional Stability

HH-53C USAF S/N 67-14993

Flight Condition	Avg GW (lb)	Avg cg (in.)	Avg Press. Alt (ft)	Avg FAT (°C)	Rotor Speed (rpm)	AFCS	KCAS
Auto-Rotation	41,000	352	5,500	6	185	ON	74

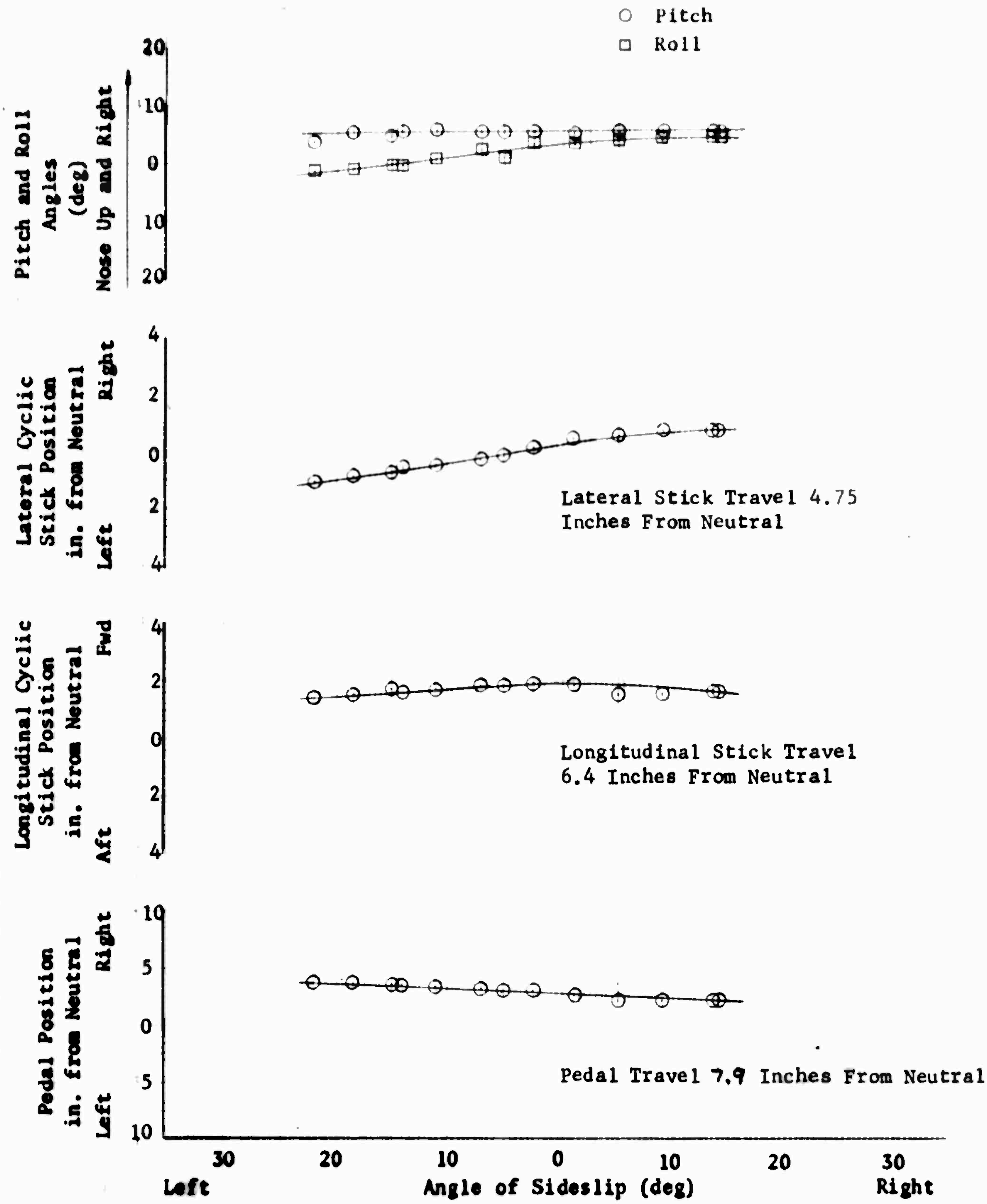

Figure 65. Static Directional Stability

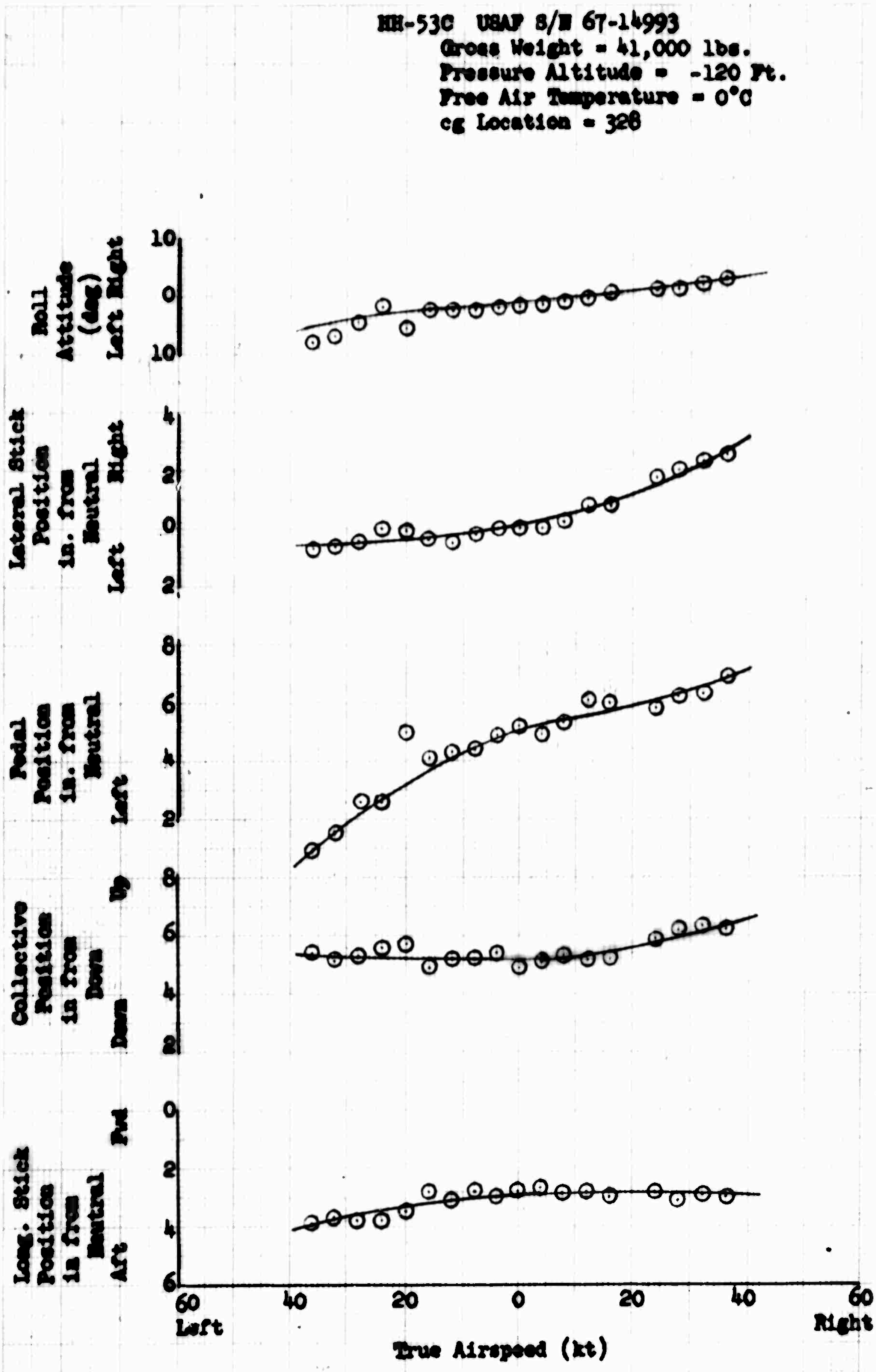

Figure 66. Control Position in Sideward Flight

HH-53C USAF S/N 67-14993
Gross Weight = 41,000 lbs.
Pressure Altitude = 120 Ft.
Free Air Temperature = 0°C
cg Location = 328

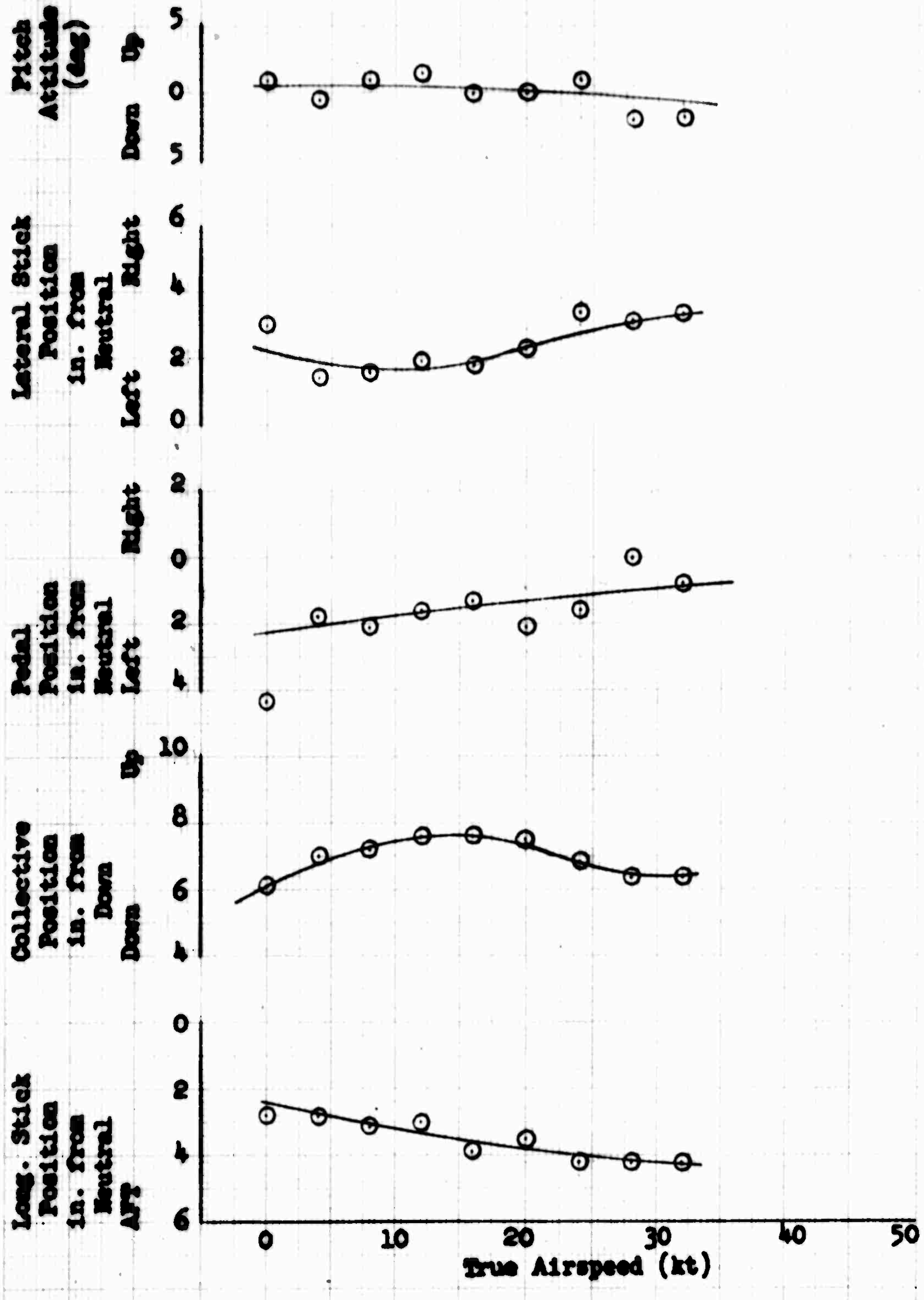

Figure 67 Control Position in Rearward Flight

HH-53C USAF 67-14993

FLIGHT COND	AVG GW (LBS)	AVG CG (IN)	AVG ALT (FT)	AVG FAT (DEG C)	ROTOR SPEED (RPM)	AFCS COND
HOV IGE	31000	328	300	10	185	ON

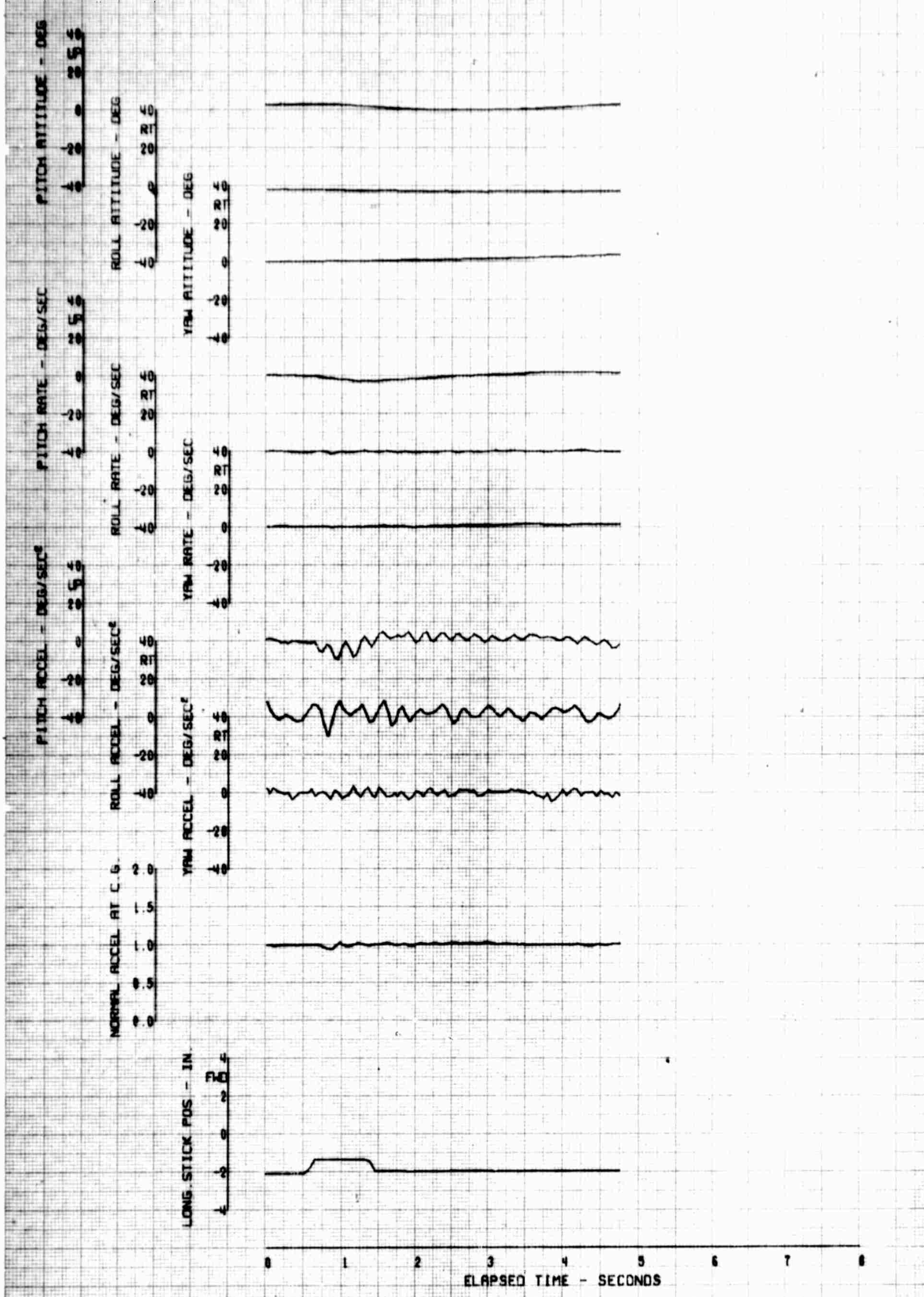

FIGURE 6a REACTION TO A FORWARD LONGITUDINAL PULSE

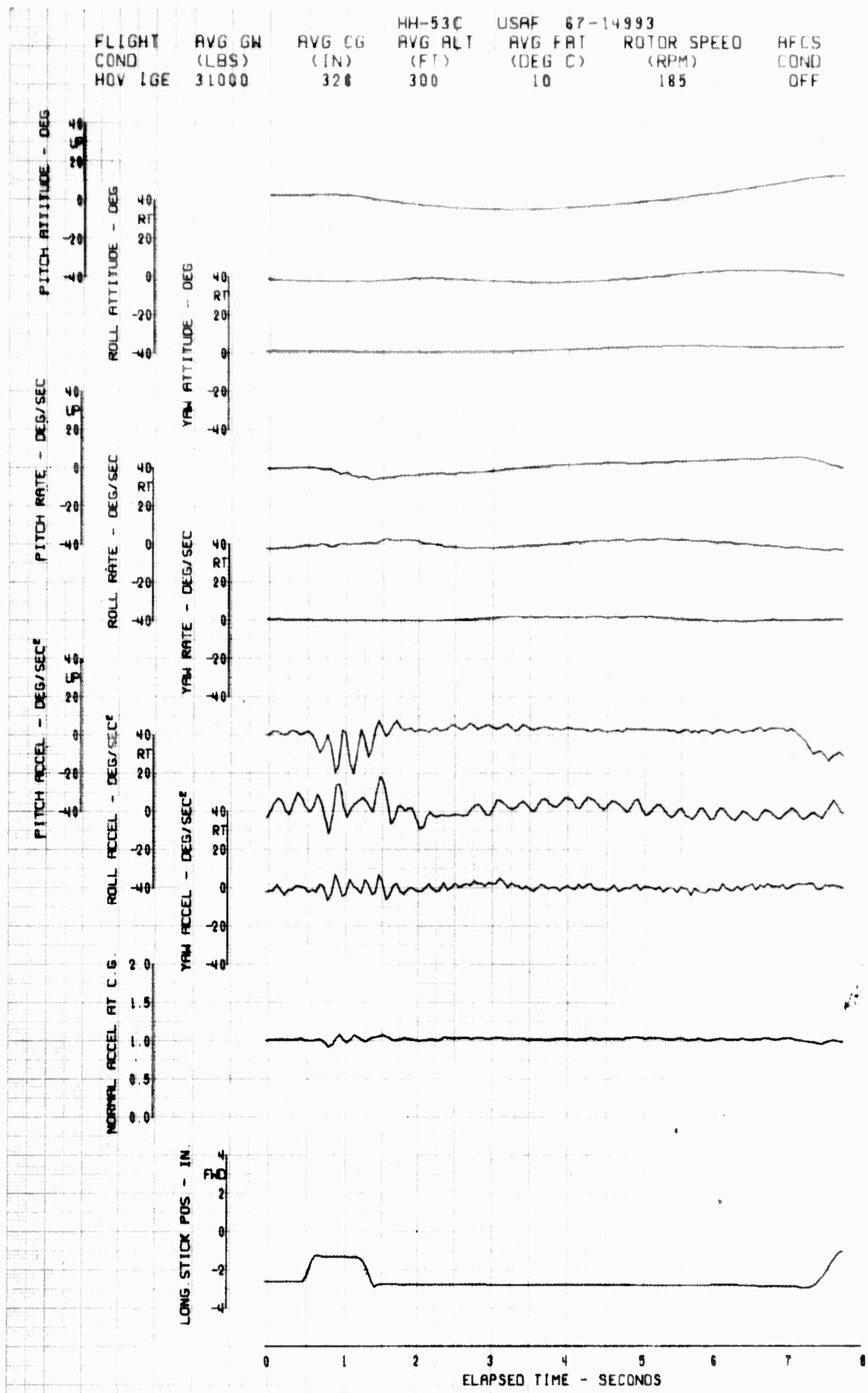

FIGURE 67 REACTION TO A FORWARD LONGITUDINAL PULSE

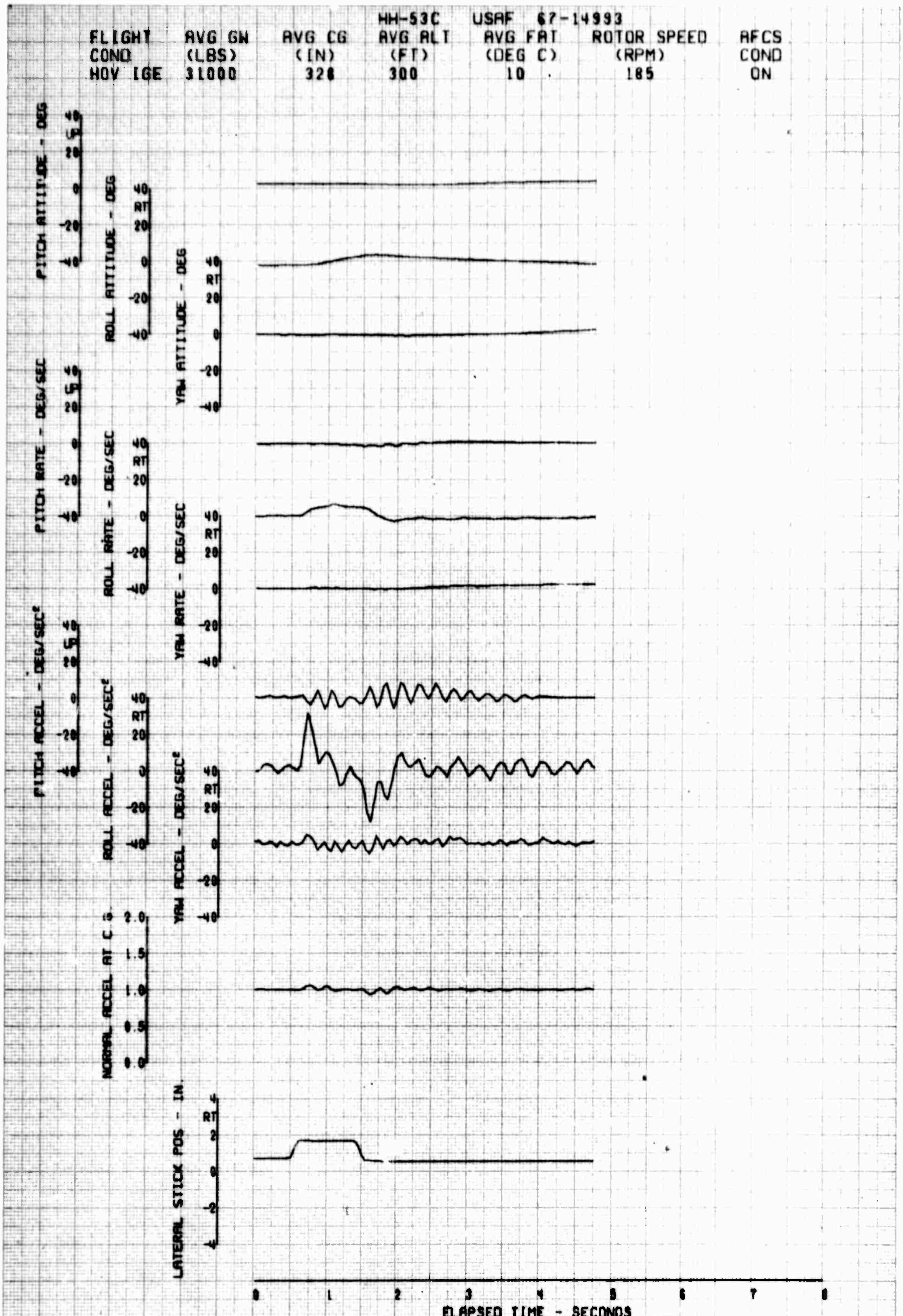

FIGURE 70. REACTION TO A RIGHT LATERAL PULSE

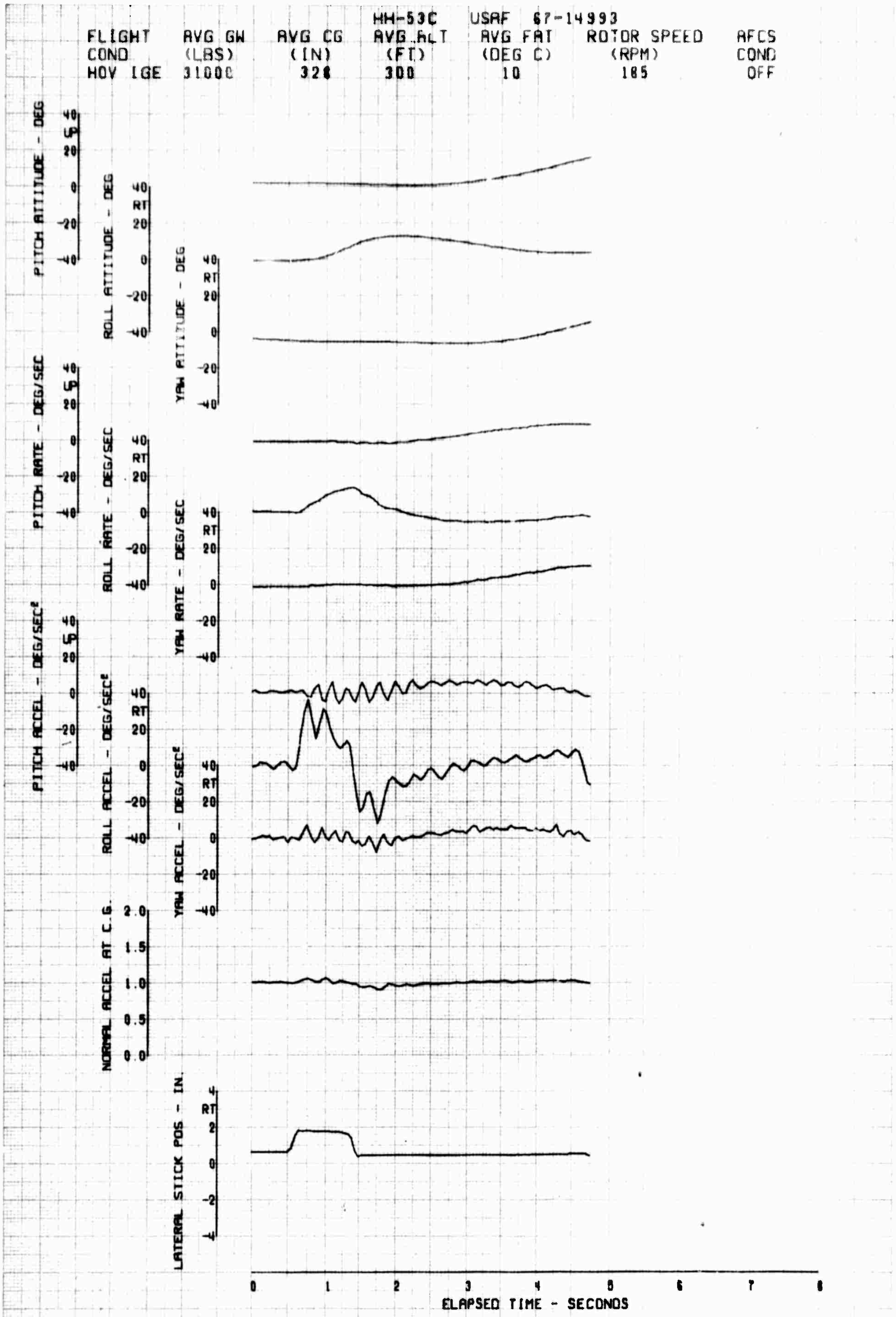

FIGURE 71. REACTION TO A RIGHT LATERAL PULSE

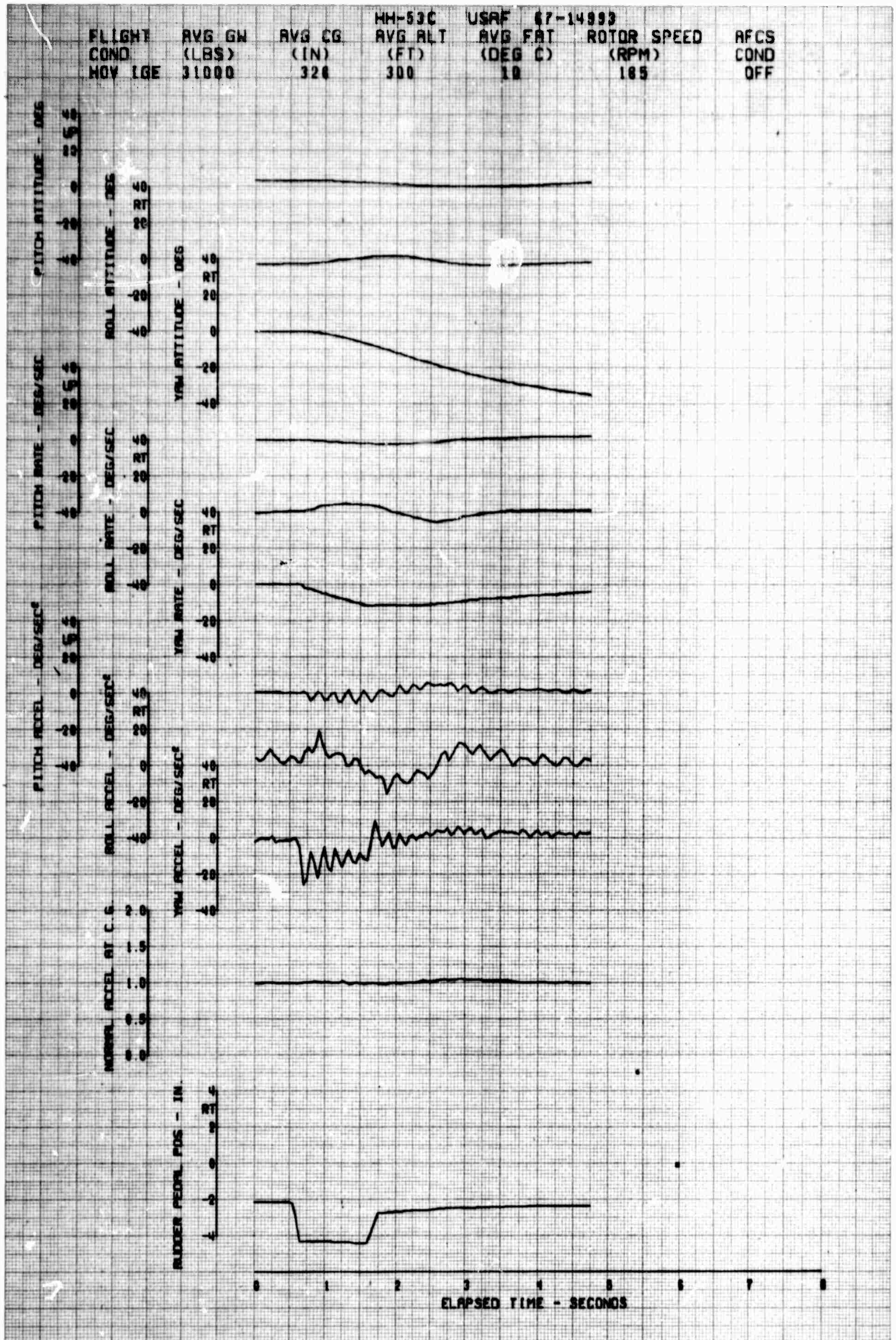

FIGURE 76. REACTION TO A LEFT DIRECTIONAL PULSE

HH-53C USAF 67-14993

FLIGHT COND	AVG GW (LBS)	AVG CG (IN)	AVG ALT (FT)	AVG FAT (DEG C)	ROTOR SPEED (RPM)	AFCS COND
HOV IGE	31000	328	300	10	185	ON

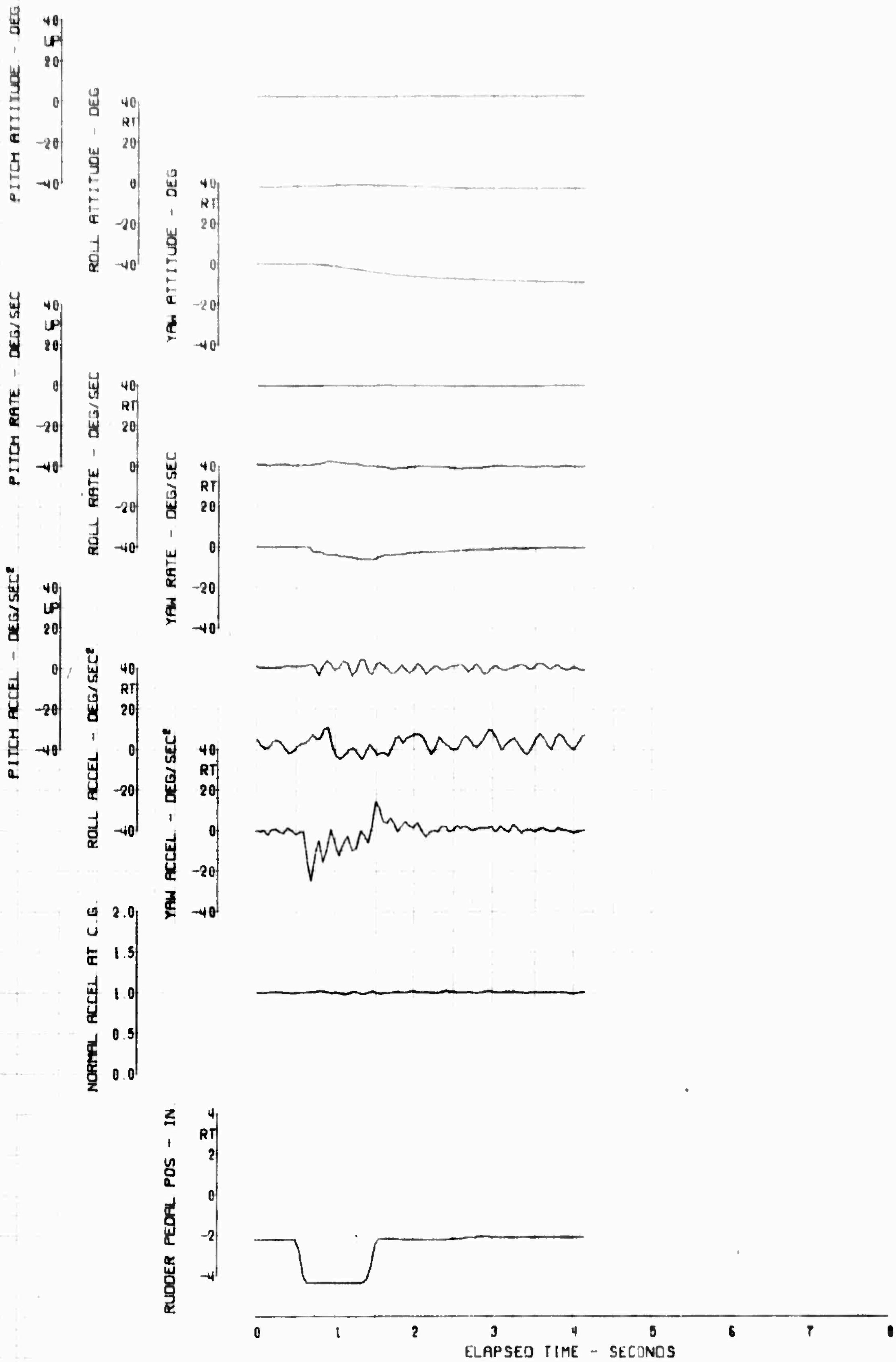

FIGURE 73. REACTION TO A LEFT DIRECTIONAL PULSE

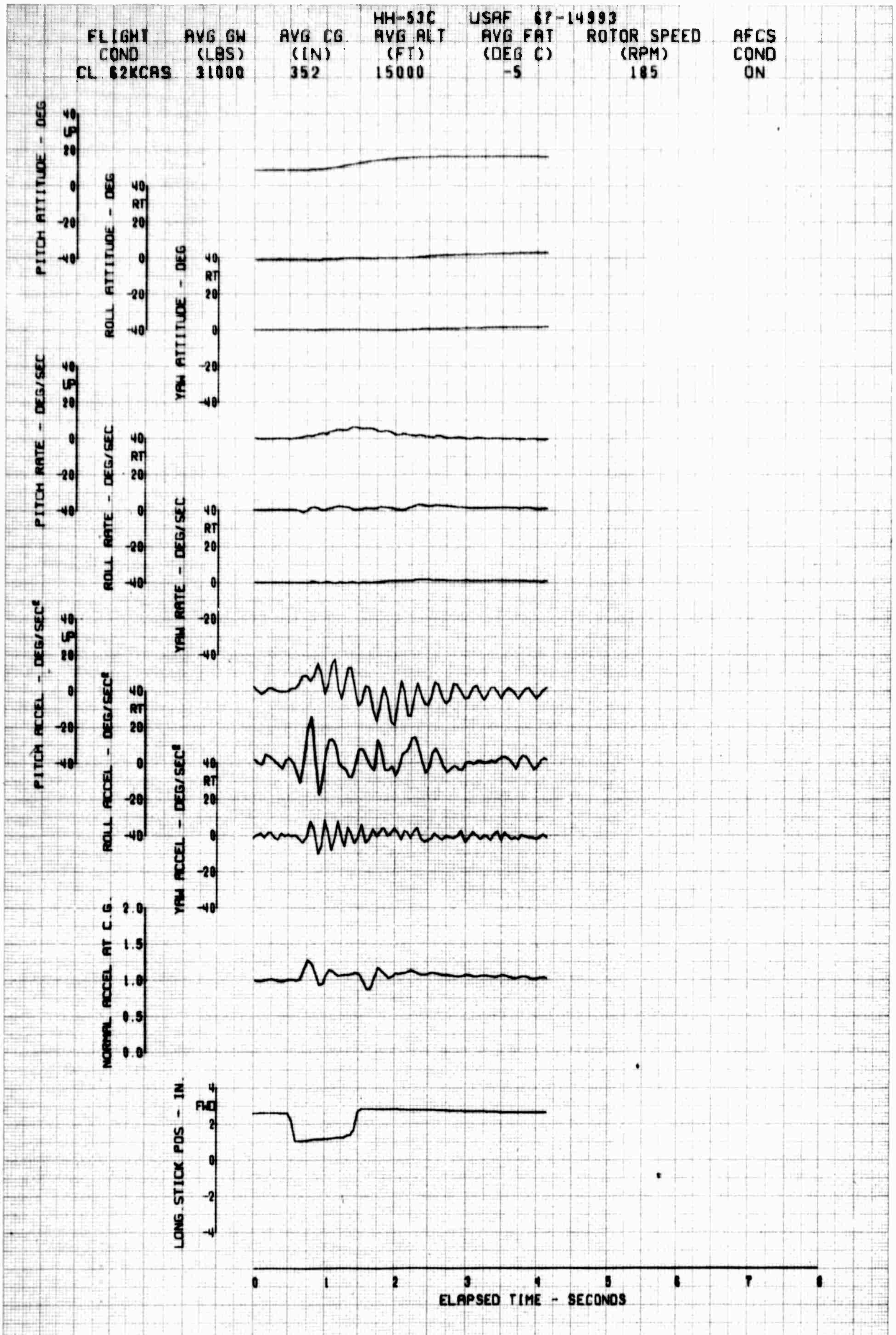

FIGURE 74 REACTION TO AN AFT LONGITUDINAL PULSE

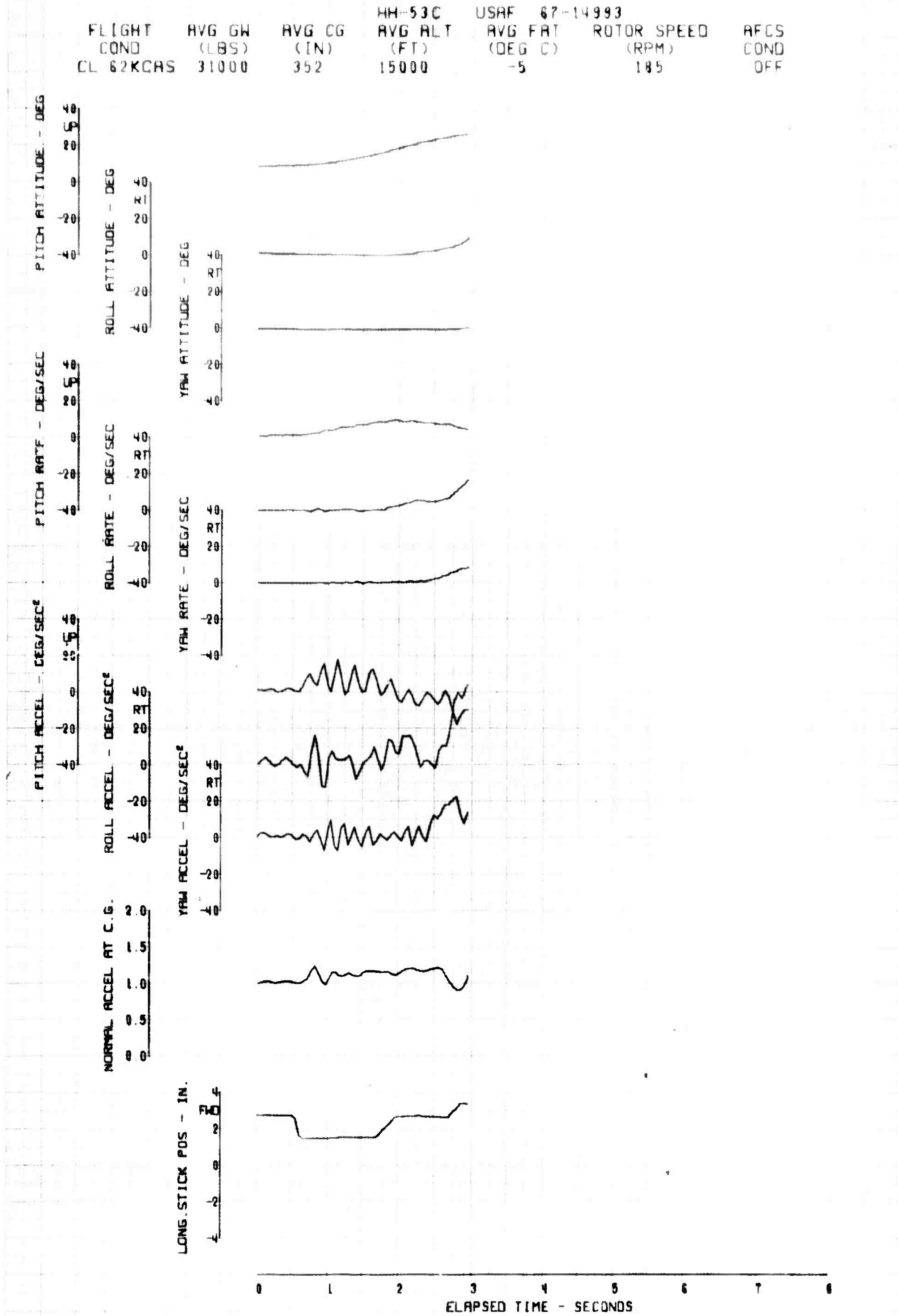

FIGURE 75 REACTION TO AN AFT LONGITUDINAL PULSE

HH-53C USAF 67-14993

FLIGHT COND	AVG GW (LBS)	AVG CG (IN)	AVG ALT (FT)	AVG FAT (DEG C)	ROTOR SPEED (RPM)	AFCS COND
CL 62KCAS	31000	352	15000	-5	185	ON

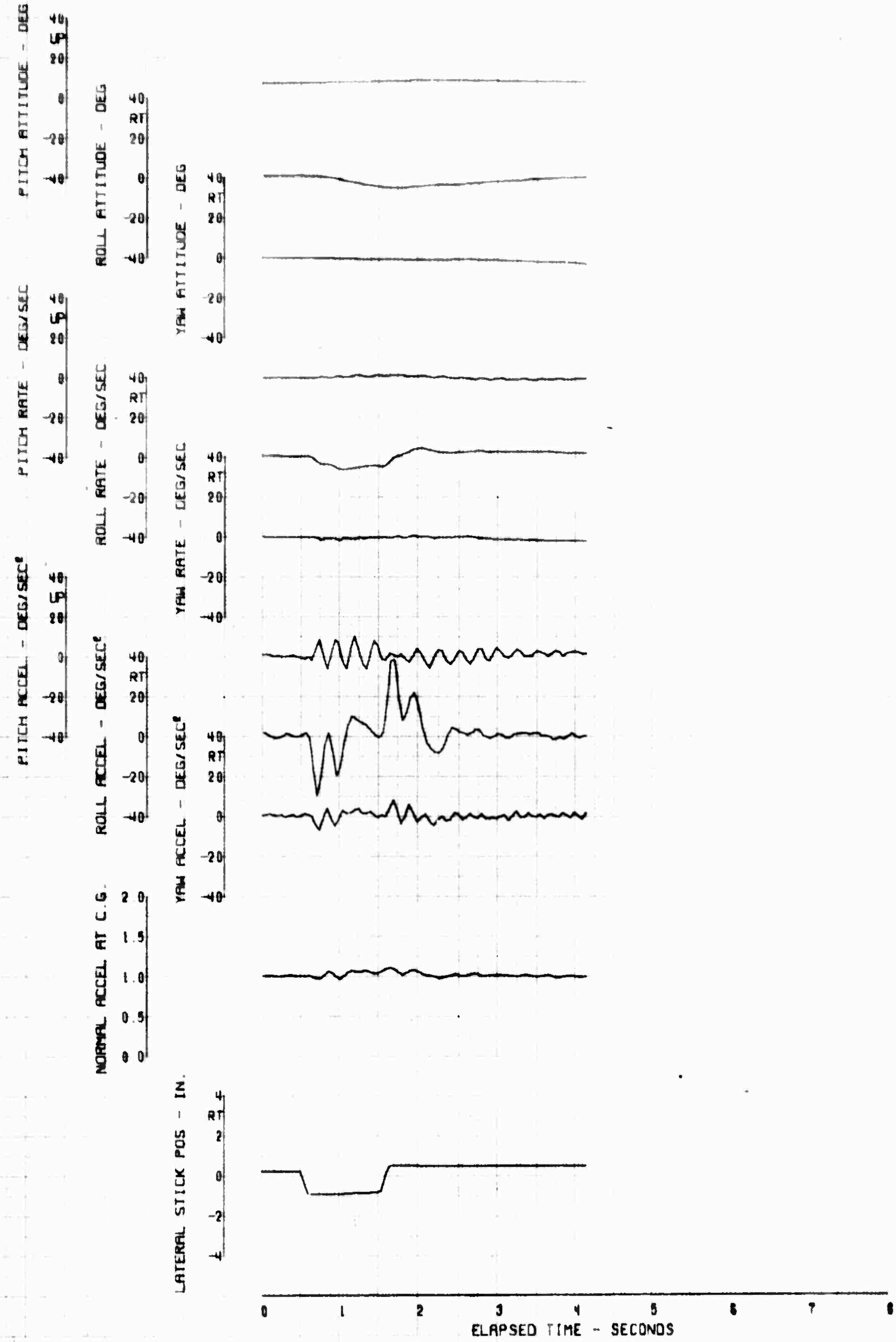

FIGURE 76. REACTION TO A LEFT LATERAL PULSE

HH-53C USAF 67-14993

FLIGHT COND	AVG GW (LBS)	AVG CG (IN)	AVG ALT (FT)	AVG FAT (DEG C)	ROTOR SPEED (RPM)	AFCS COND
CL 62KCAS	31000	352	15000	-5	185	OFF

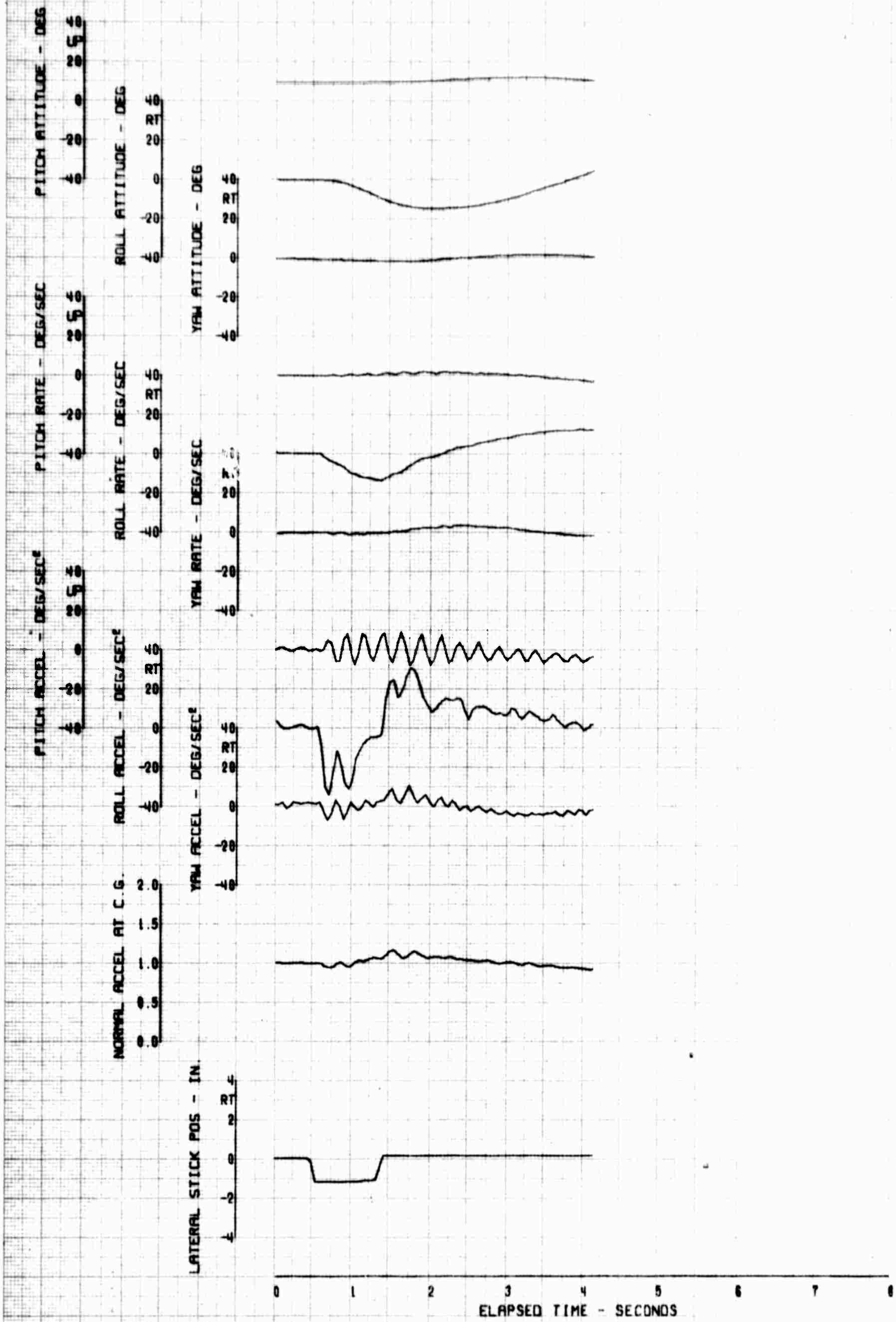

FIGURE 77 REACTION TO A LEFT LATERAL PULSE

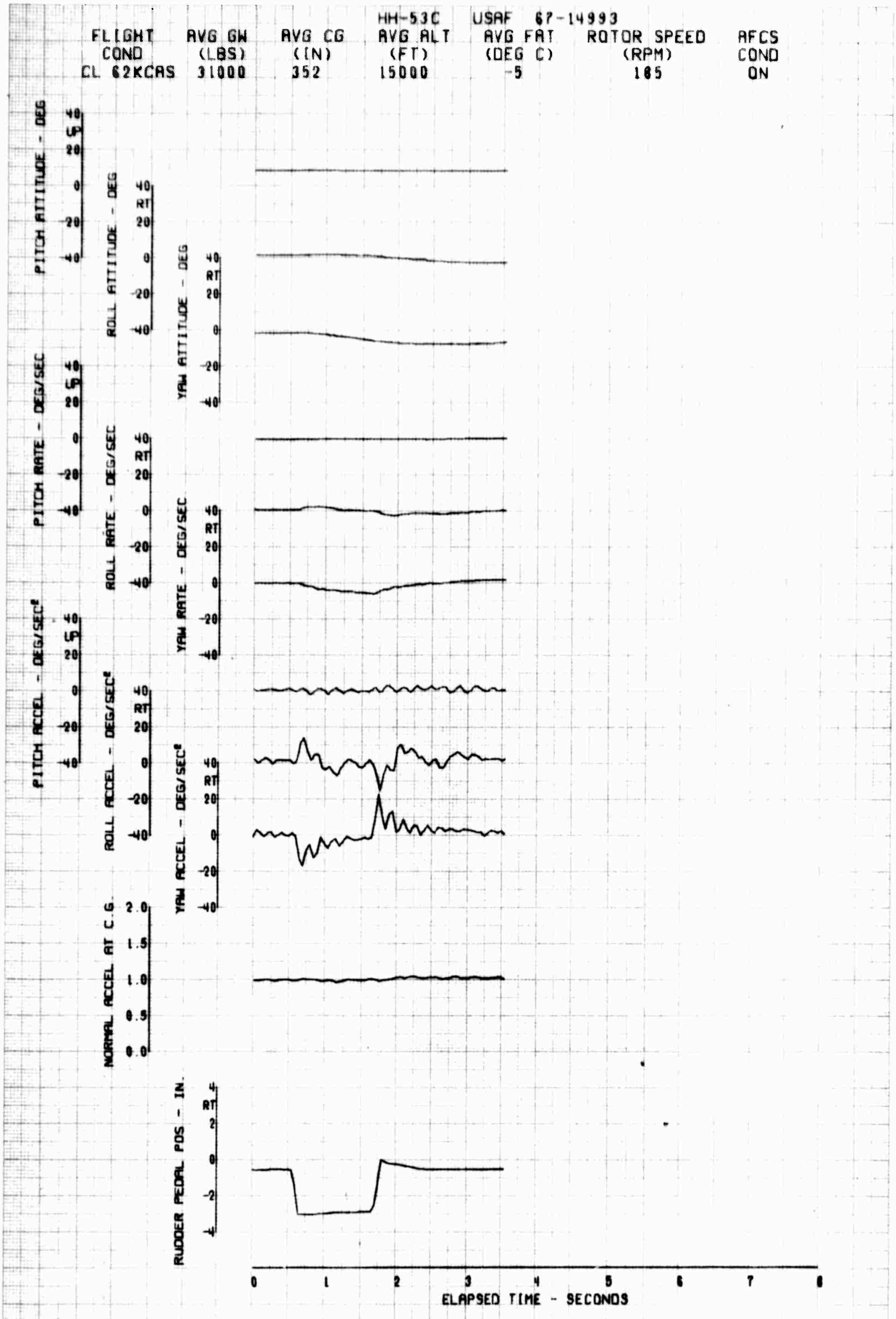

FIGURE 78. REACTION TO A LEFT DIRECTIONAL PULSE

HH-53C USAF 67-14993

FLIGHT COND	AVG GW (LBS)	AVG CG (IN)	AVG ALT (FT)	AVG FAT (DEG C)	ROTOR SPEED (RPM)	AFCS COND
CL 62KCAS	31000	352	15000	-5	185	OFF

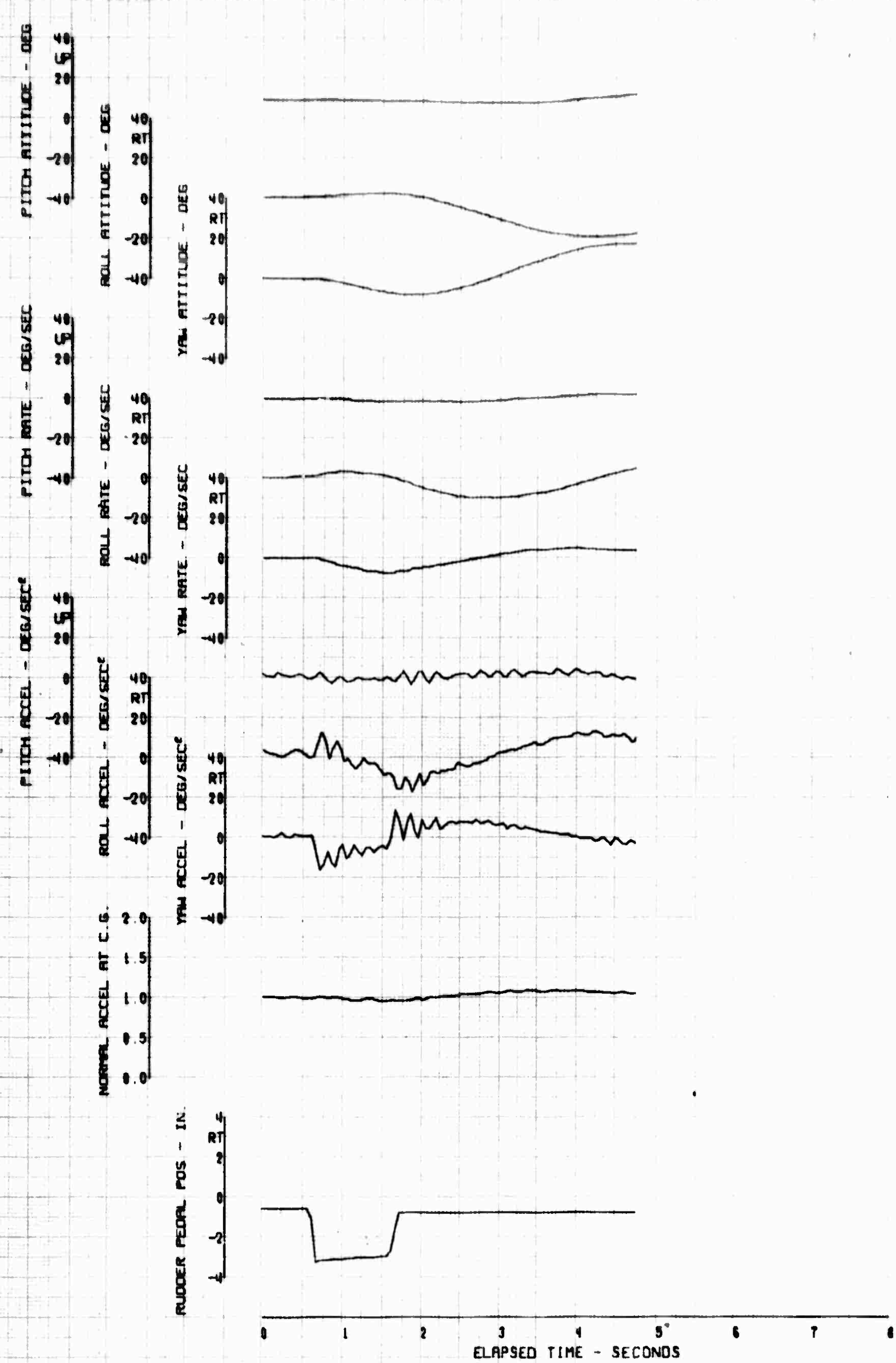

FIGURE 79. REACTION TO A LEFT DIRECTIONAL PULSE

HH-53C USAF 67-14993

FLIGHT COND	AVG GW (LBS)	AVG CG (IN)	AVG ALT (FT)	AVG FAT (DEG C)	ROTOR SPEED (RPM)	AFCS COND
LF 113KCAS	41000	328	7000	-18 0	185	ON

EXTERNAL TANKS FULL

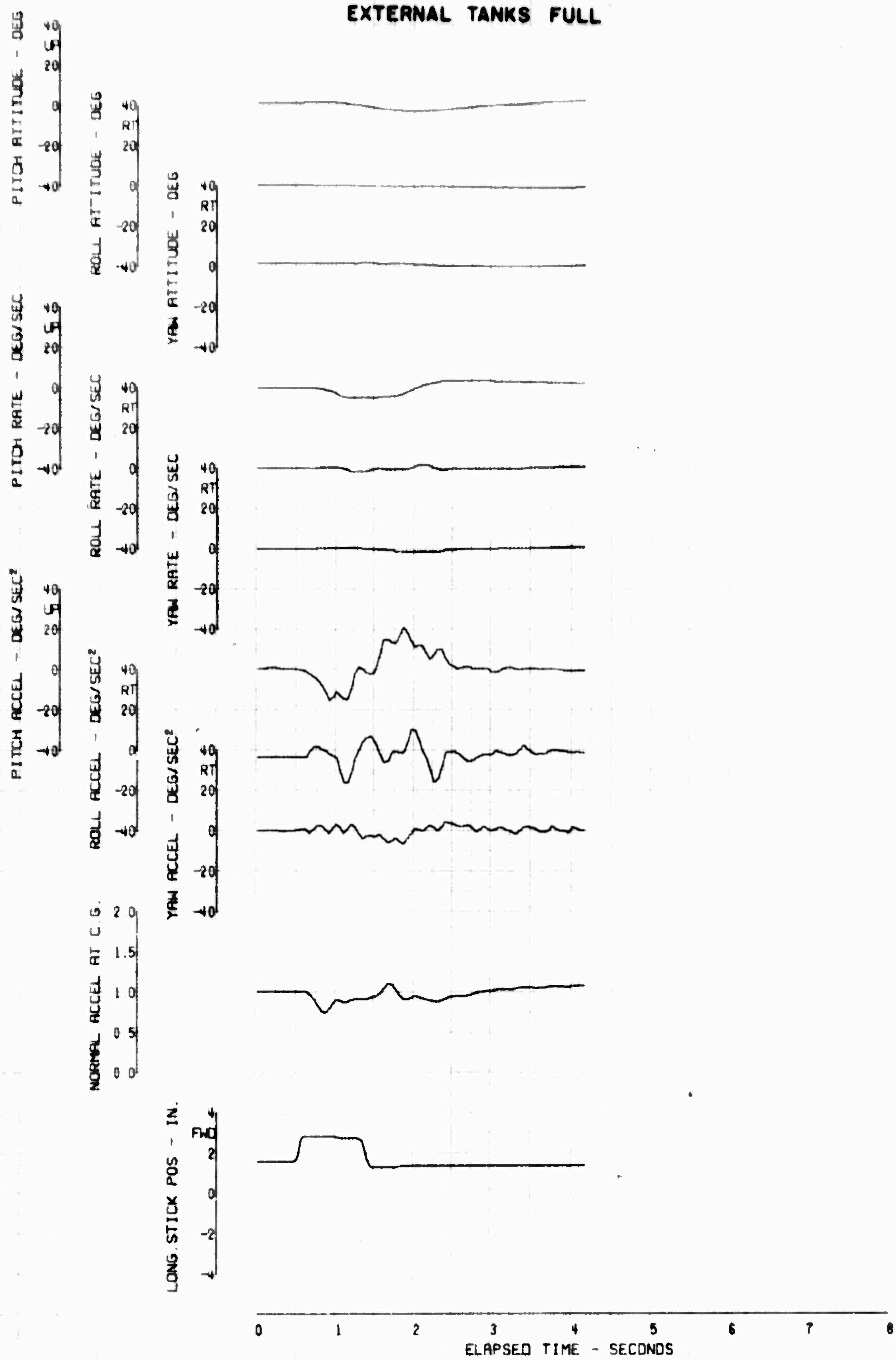

FIGURE 80 REACTION TO A FORWARD LONGITUDINAL PULSE

HH-53C USAF 67-14993

FLIGHT COND	AVG GW (LBS)	AVG CG (IN)	AVG ALT (FT)	AVG FAT (DEG C)	ROTOR SPEED (RPM)	AFCS COND
LF 113KCAS	41000	328	7000	-18.0	185	OFF

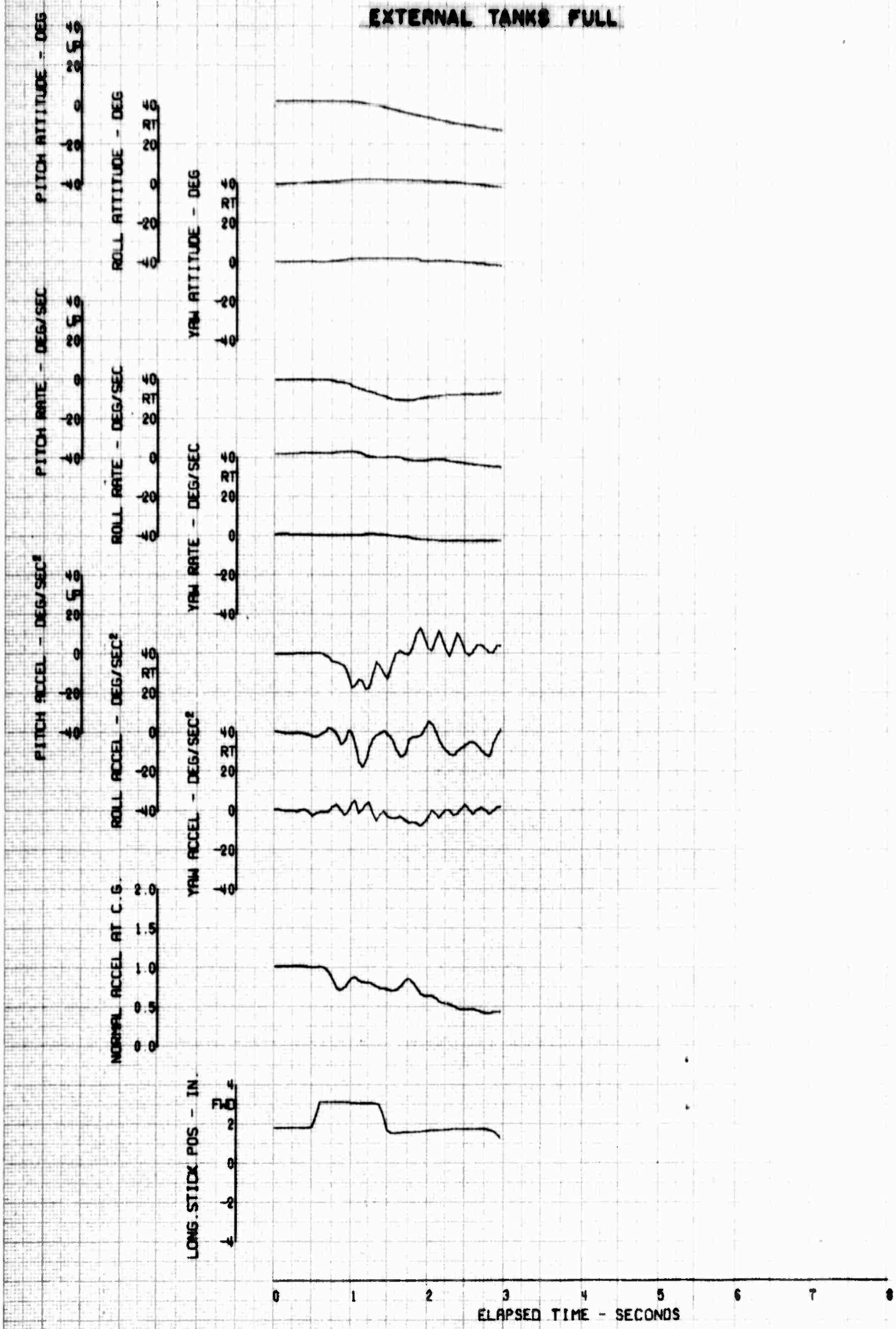

FIGURE 81. REACTION TO A FORWARD LONGITUDINAL PULSE

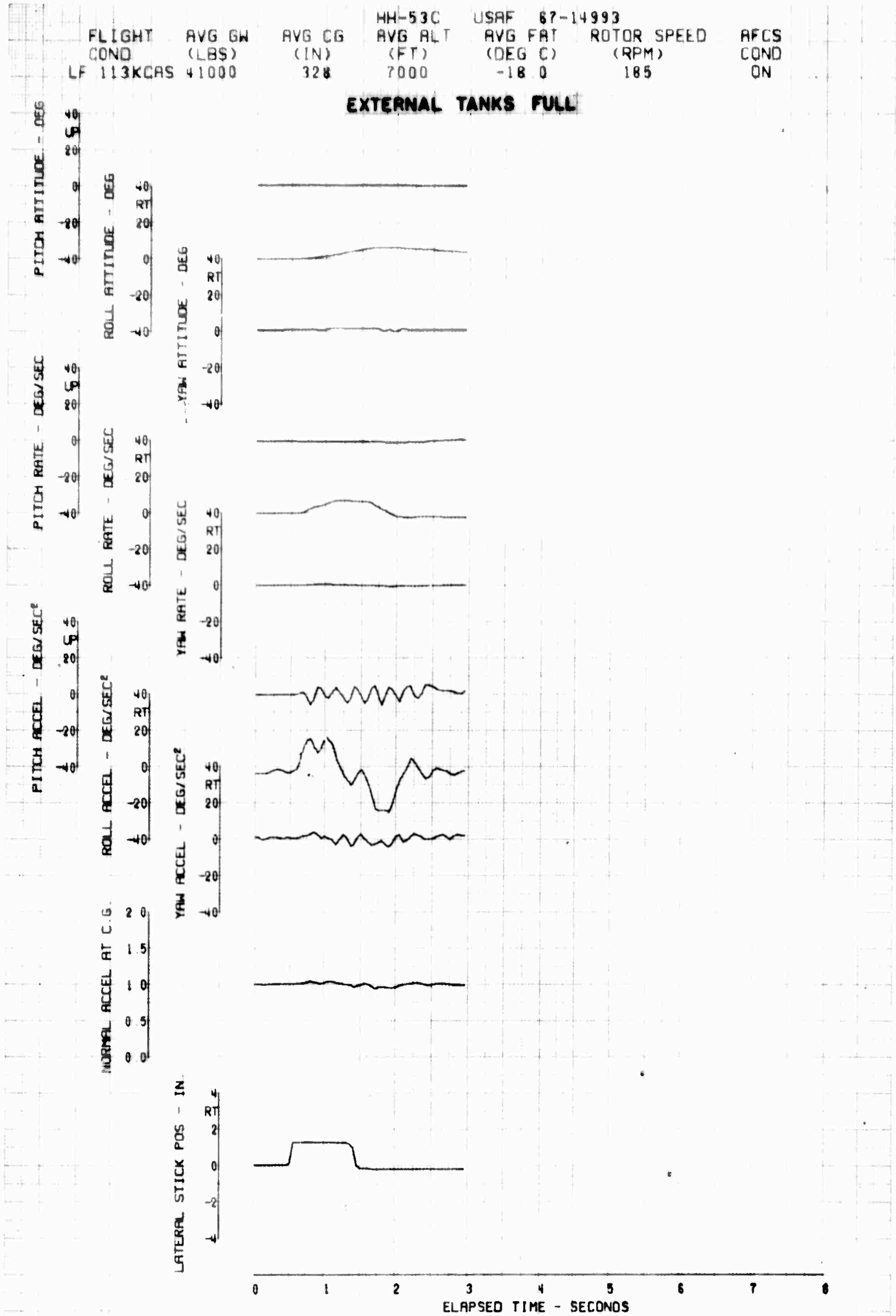

FIGURE 82. REACTION TO A RIGHT LATERAL PULSE

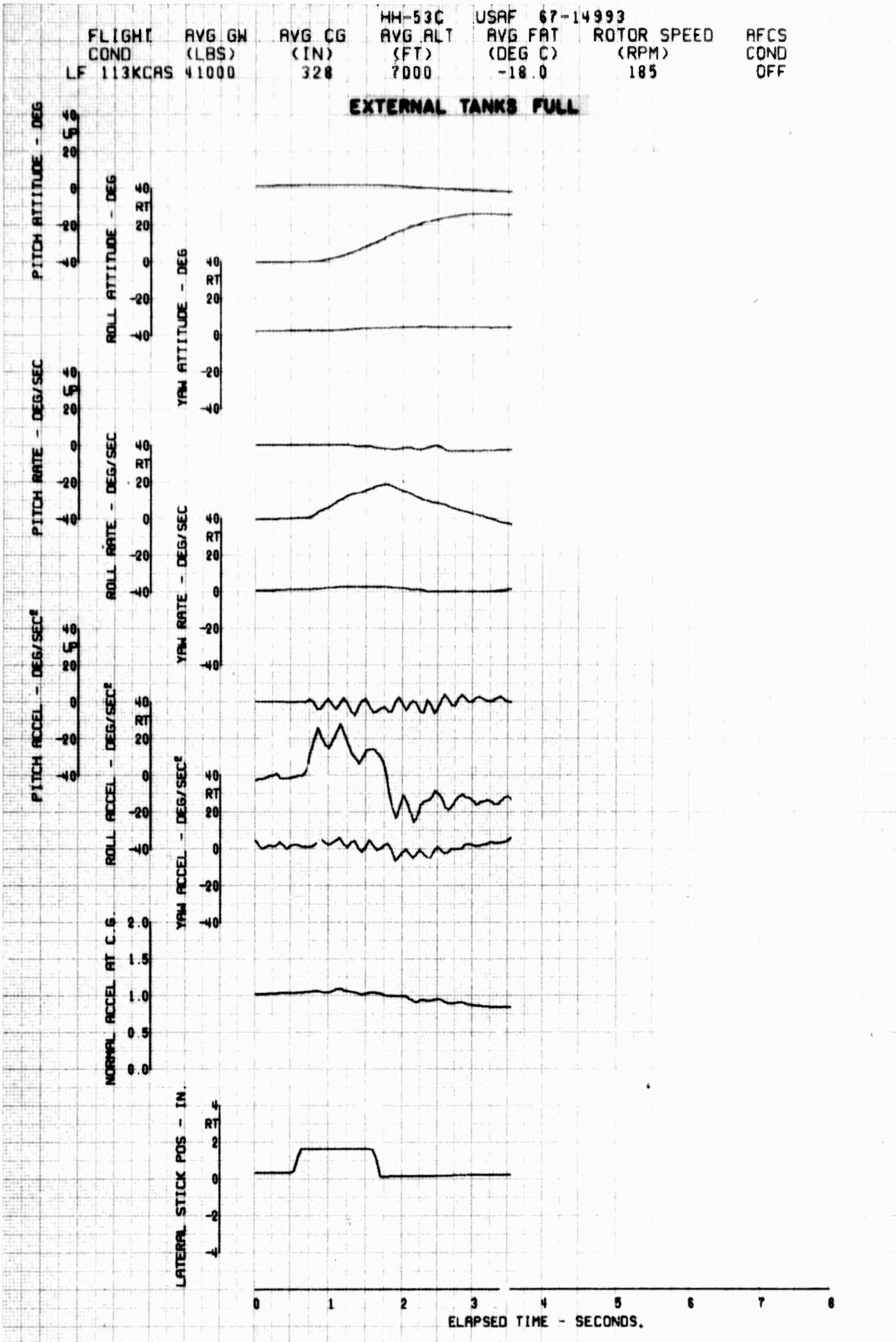

FIGURE 83. REACTION TO A RIGHT LATERAL PULSE

HH-53C USAF 67-14993

FLIGHT COND	AVG GW (LBS)	AVG CG (IN)	AVG ALT (FT)	AVG FAT (DEG C)	ROTOR SPEED (RPM)	AFCS COND
LF 113KCAS	41000	328	7000	-18.0	185	ON

EXTERNAL TANKS FULL

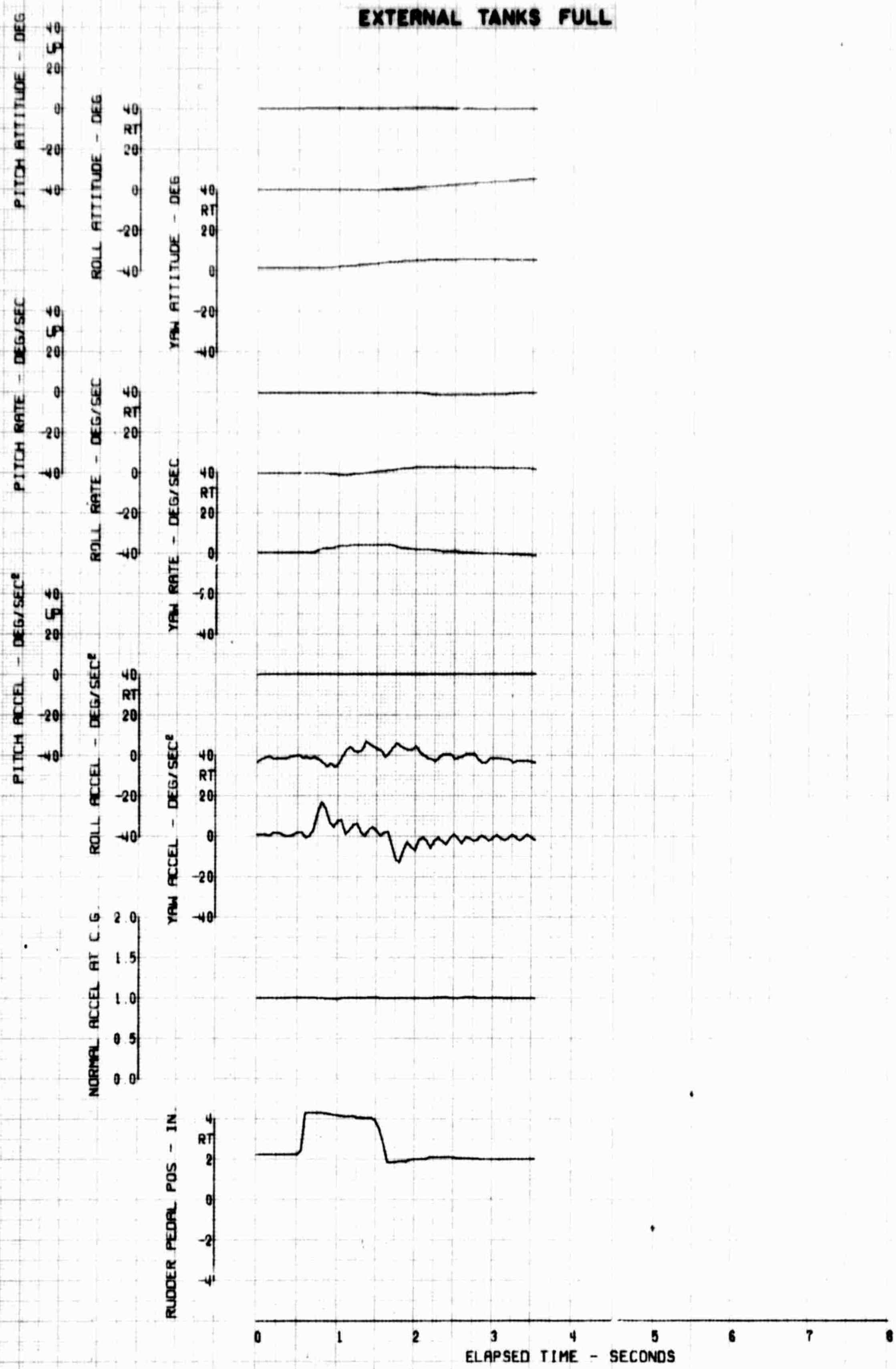

FIGURE 84 REACTION TO A RIGHT DIRECTIONAL PULSE

HH-53C USAF 67-14993

FLIGHT COND	AVG GW (LBS)	AVG CG (IN)	AVG ALT (FT)	AVG FAT (DEG C)	ROTOR SPEED (RPM)	AFCS COND
LF 113KCAS	41000	328	7000	-18 0	185	OFF

EXTERNAL TANKS FULL

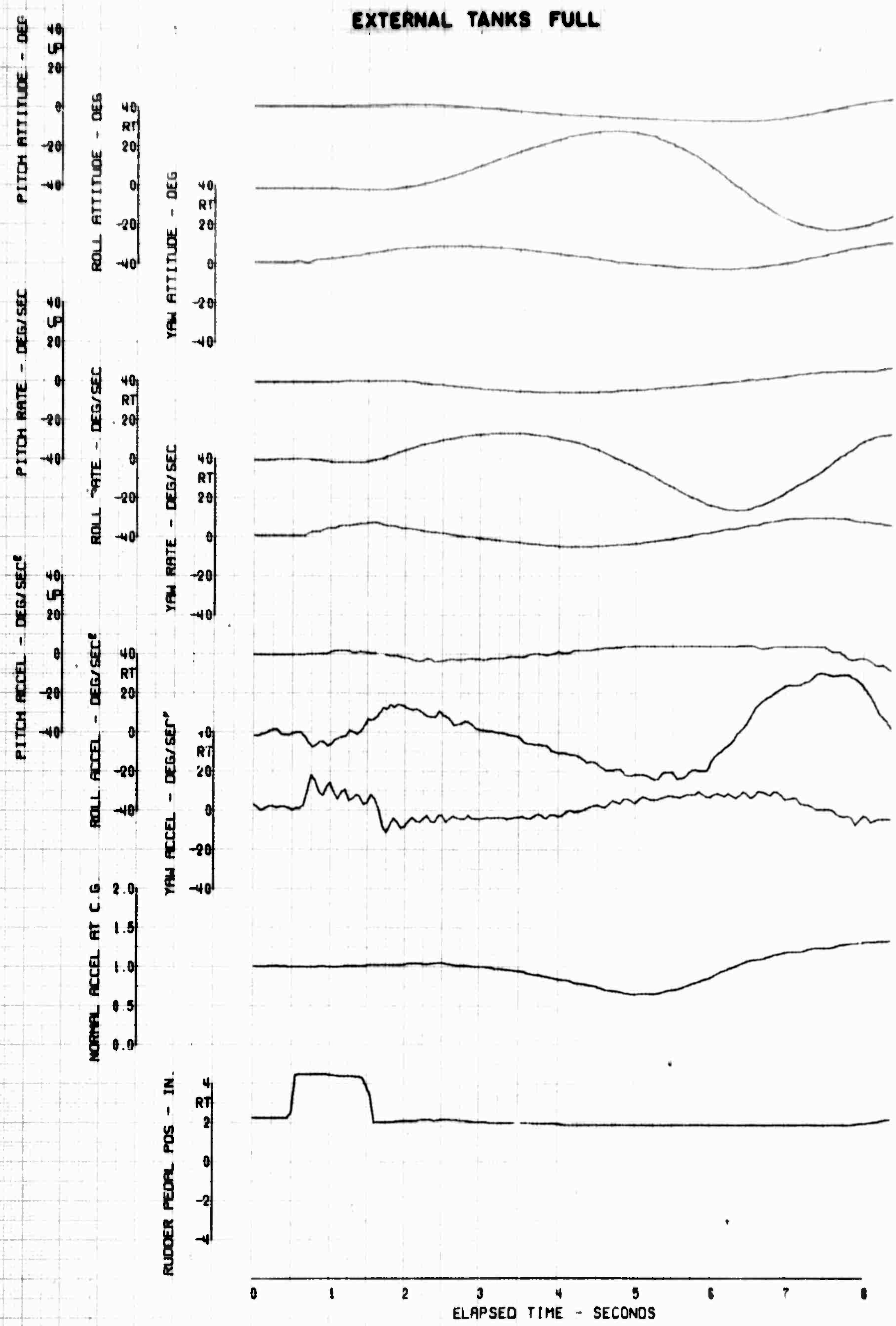

FIGURE 85 REACTION TO A RIGHT DIRECTIONAL PULSE

HH-53C USAF 67-14993

FLIGHT COND	AVG GW (LBS)	AVG CG (IN)	AVG ALT (FT)	AVG FAT (DEG C)	ROTOR SPEED (RPM)	AFCS COND
HOV IGE	31000	352	300	10	185	ON

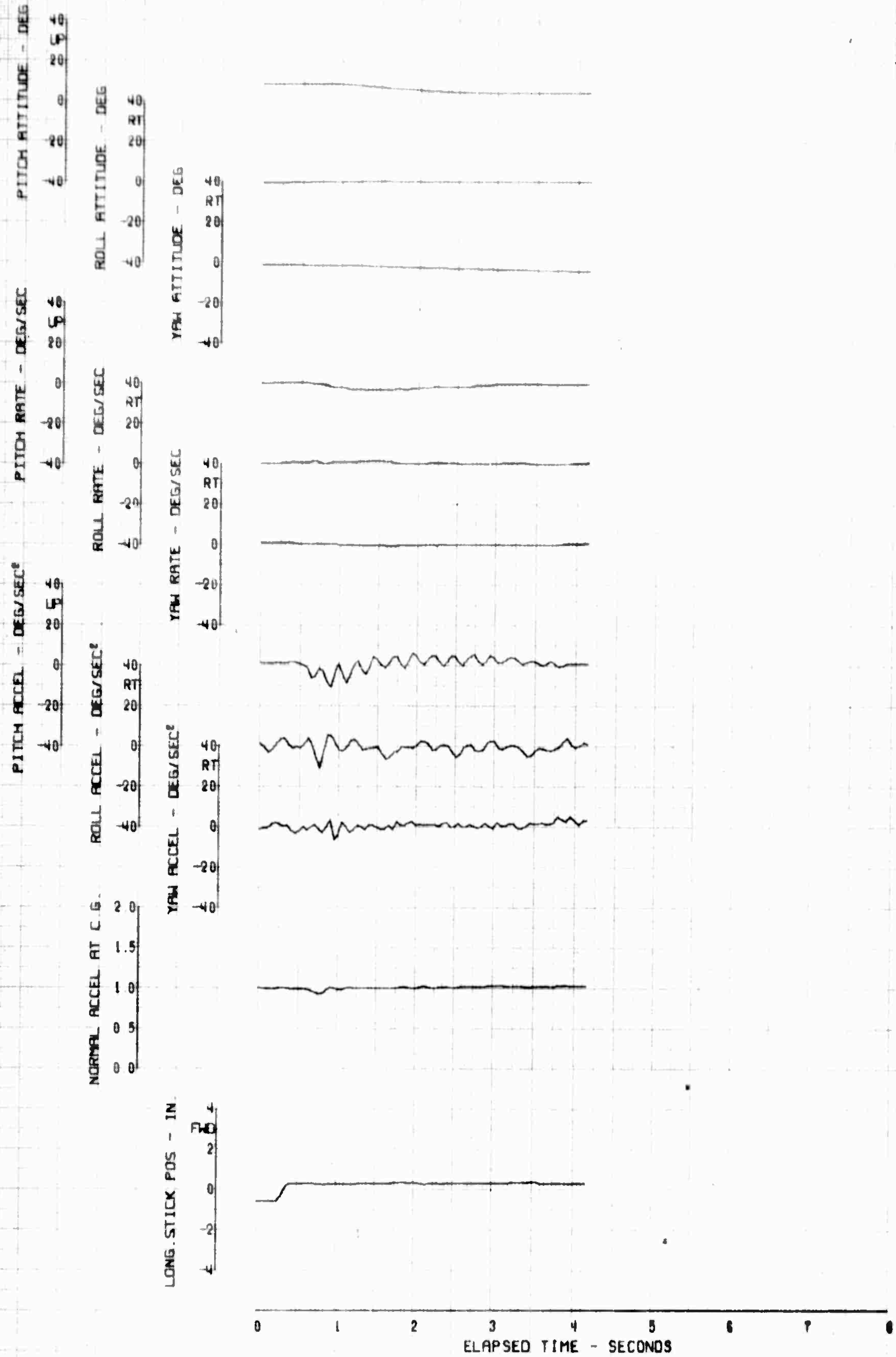

FIGURE 86 REACTION TO A FORWARD LONGITUDINAL STEP

	HH-53C	USAF 67-14993				
FLIGHT COND	AVG GW (LBS)	AVG CG (IN)	AVG ALT (FT)	AVG FAT (DEG C)	ROTOR SPEED (RPM)	AFCS COND
HOV IGE	31000	352	300	10	185	OFF

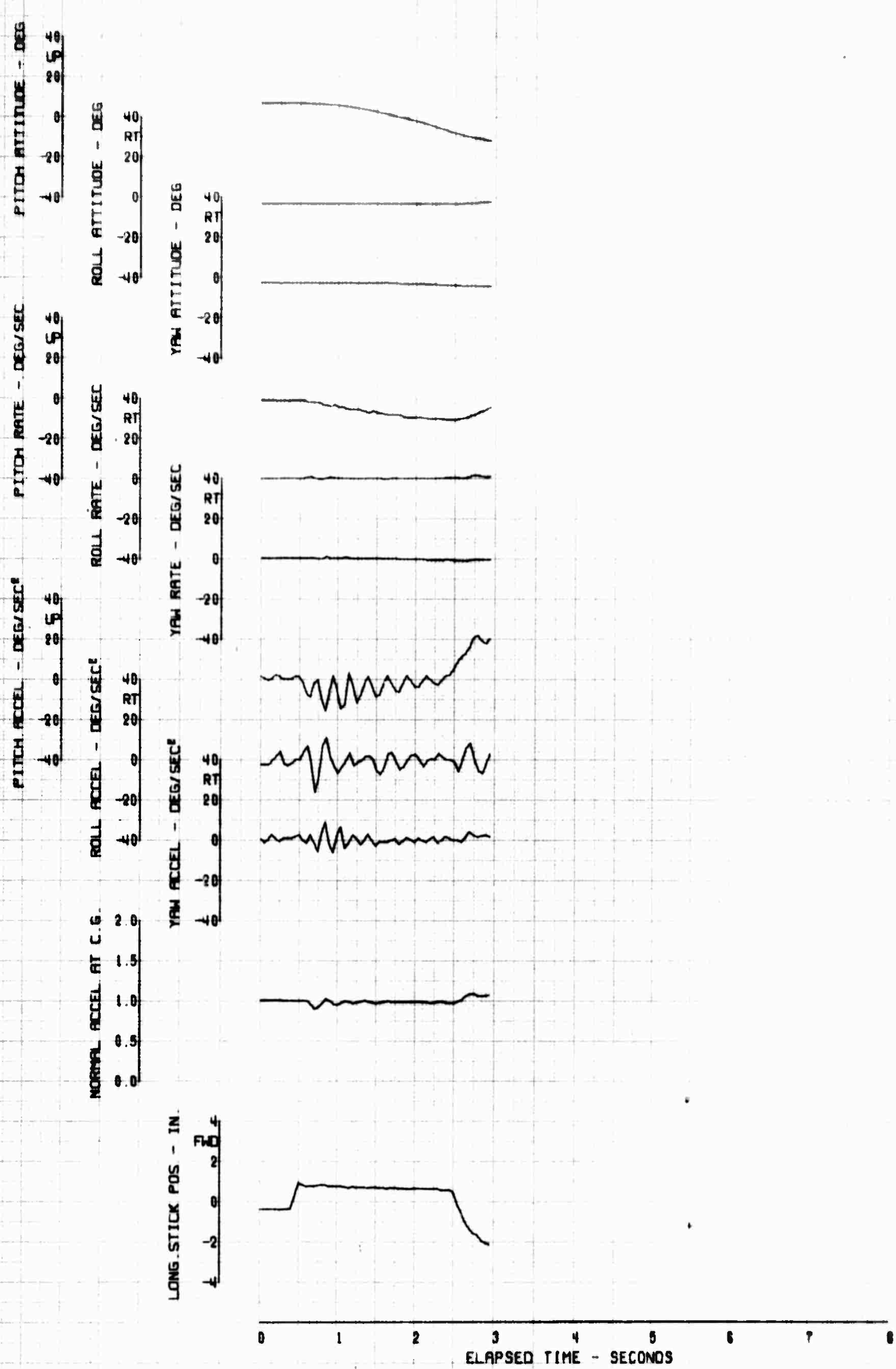

FIGURE 87. REACTION TO A FORWARD LONGITUDINAL STEP

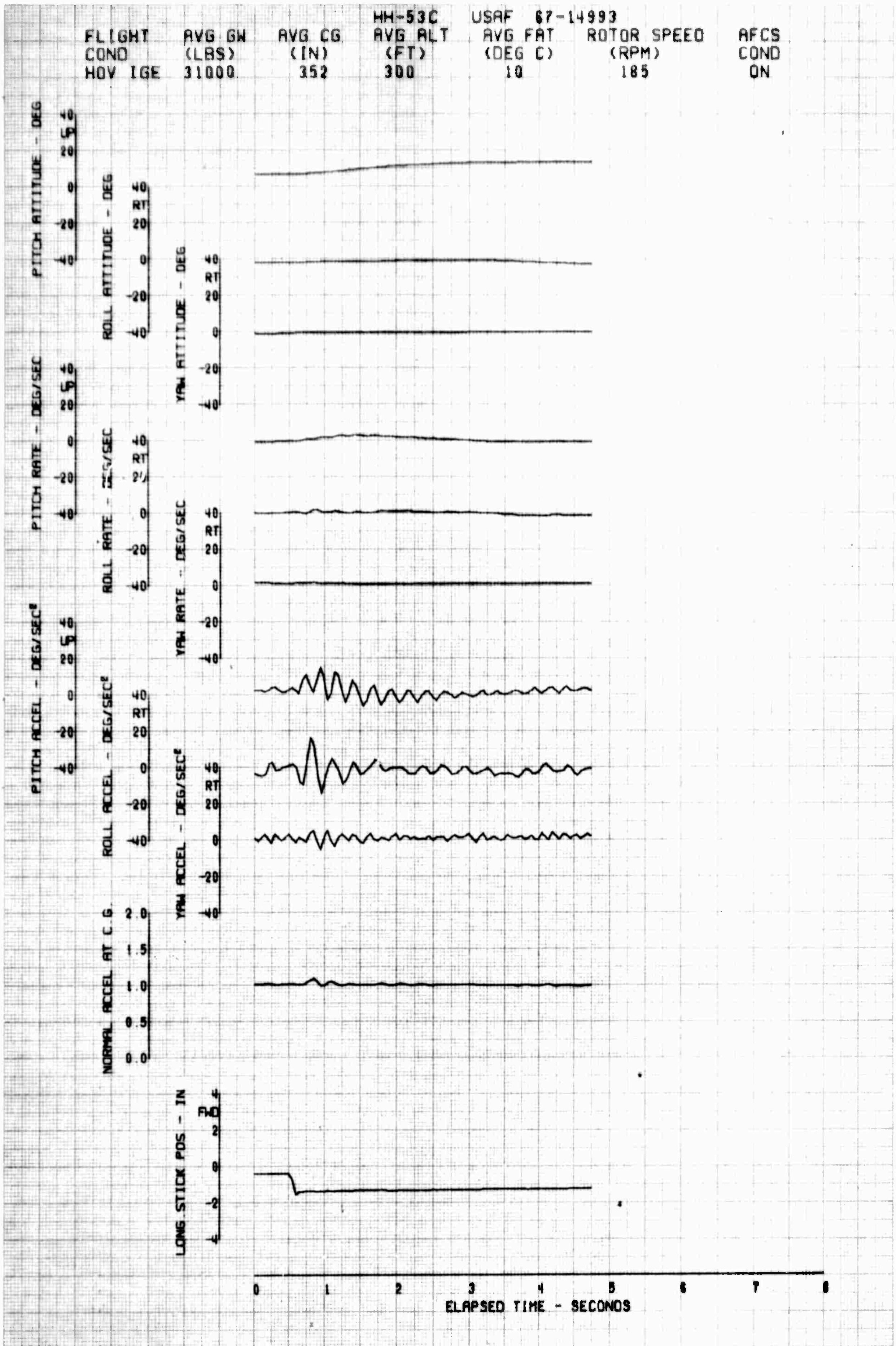

FIGURE 88 REACTION TO AN AFT LONGITUDINAL STEP

HH-53C USAF 67-14993

FLIGHT COND	AVG GW (LBS)	AVG CG (IN)	AVG ALT (FT)	AVG FAT (DEG C)	ROTOR SPEED (RPM)	AFCS COND
HOV IGE	31000	352	300	10	185	OFF

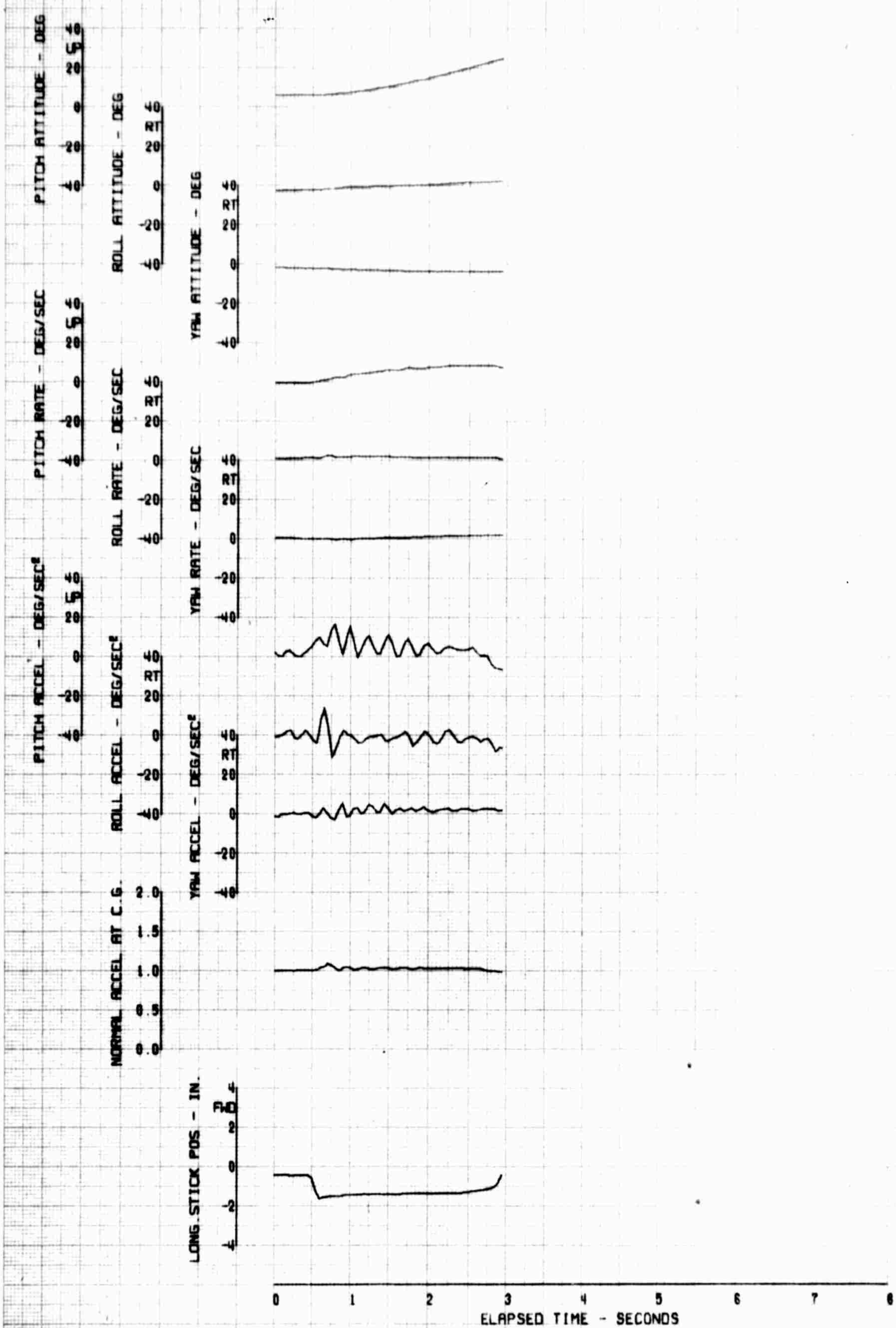

FIGURE 69 REACTION TO AN AFT LONGITUDINAL STEP

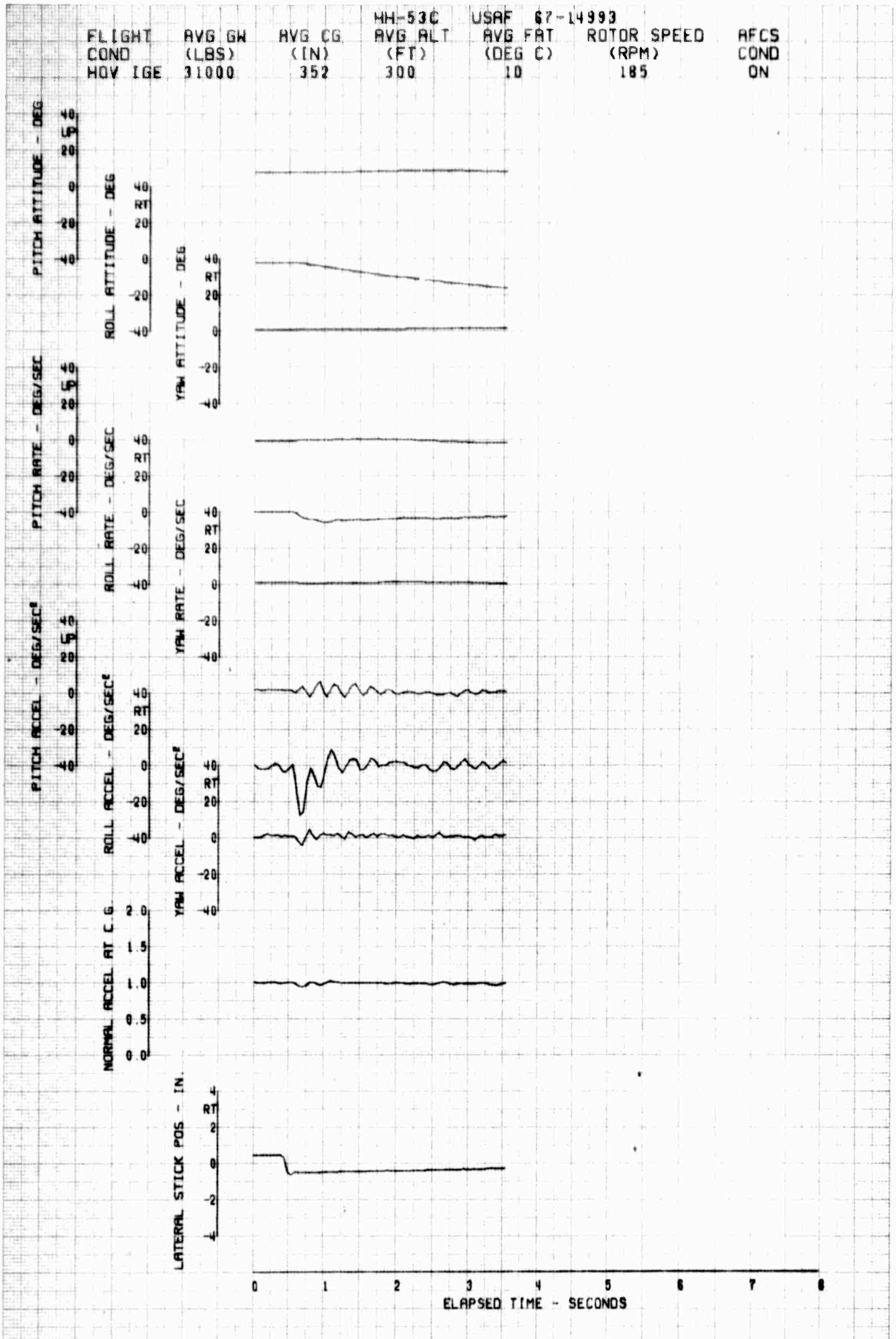

FIGURE 90. REACTION TO A LEFT LATERAL STEP

HH-53C USAF 67-14993

FLIGHT COND	AVG GW (LBS)	AVG CG (IN)	AVG ALT (FT)	AVG FAT (DEG C)	ROTOR SPEED (RPM)	AFCS COND
HOV IGE	31000	352	300	10	185	OFF

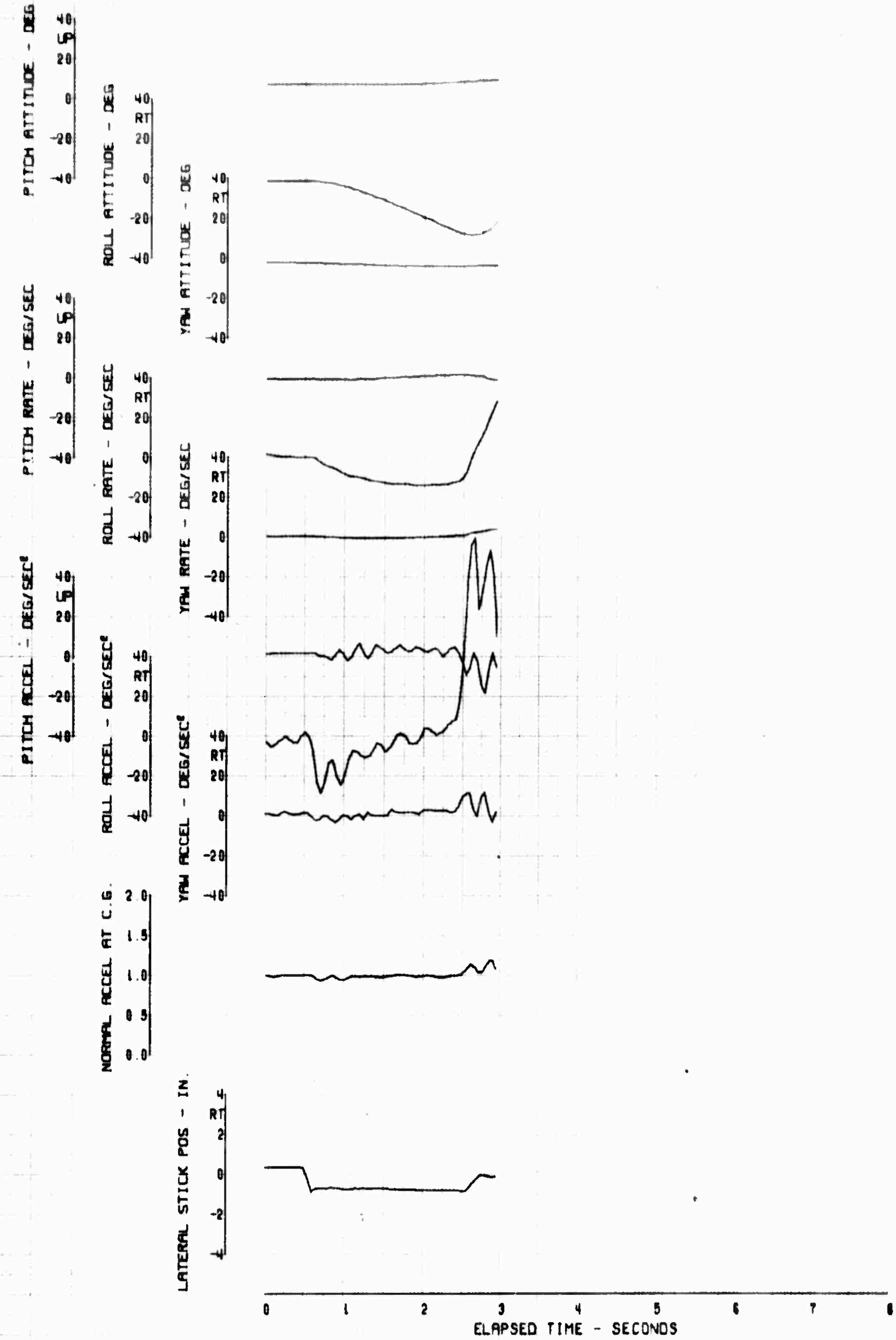

FIGURE 91 REACTION TO A LEFT LATERAL STEP

HH-53C USAF 67-14993

FLIGHT COND.	AVG GW (LBS)	AVG CG (IN)	AVG ALT (FT)	AVG FAT (DEG C)	ROTOR SPEED (RPM)	AFCS COND
HOV IGE	31000	352	300	10	185	ON

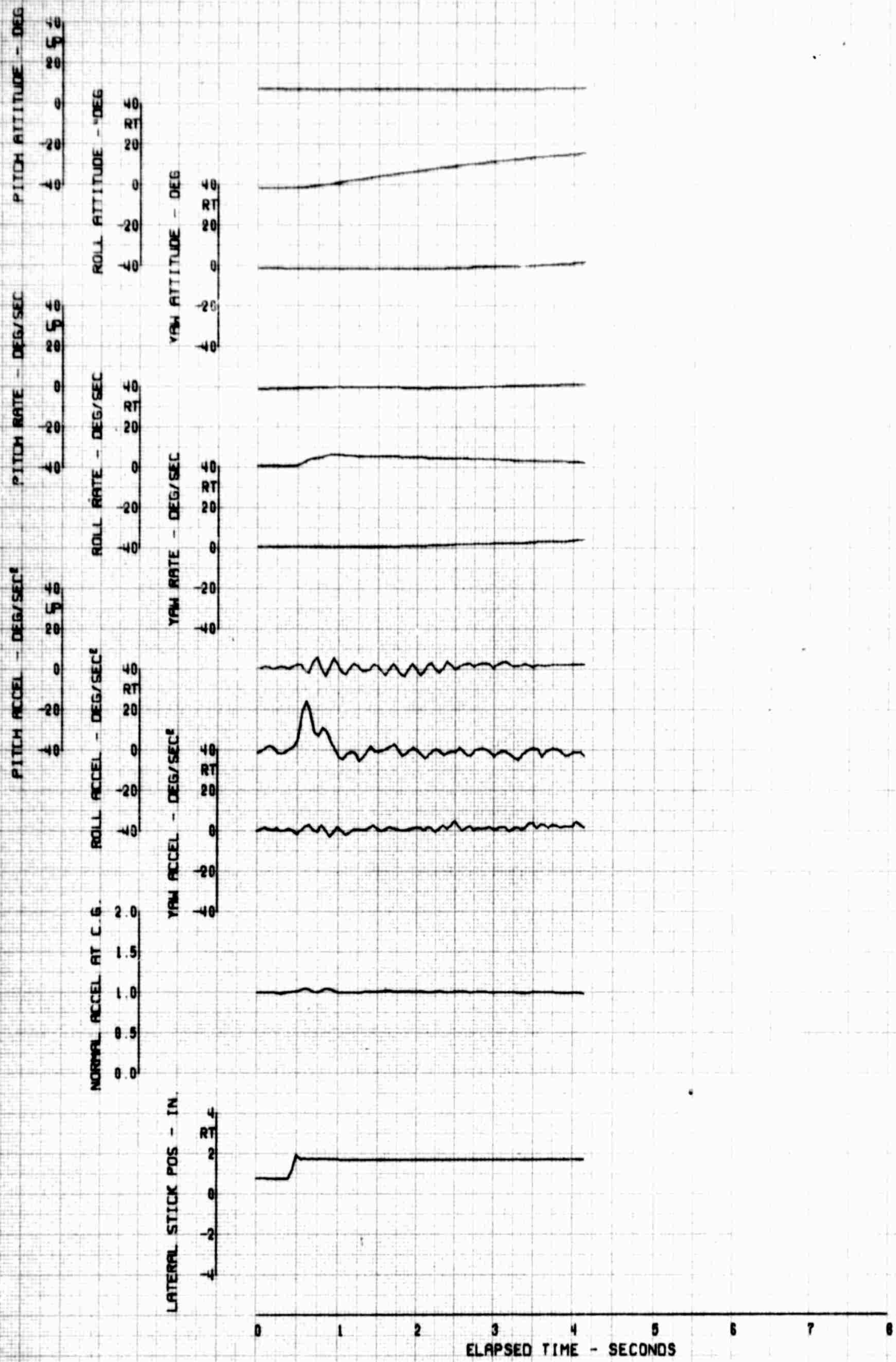

FIGURE 72. REACTION TO A RIGHT LATERAL STEP

HH-53C USAF 67-14993

FLIGHT COND	AVG GW (LBS)	AVG CG (IN)	AVG ALT (FT)	AVG FAT (DEG C)	ROTOR SPEED (RPM)	AFCS COND
HOV IGE	31000	352	300	10	185	OFF

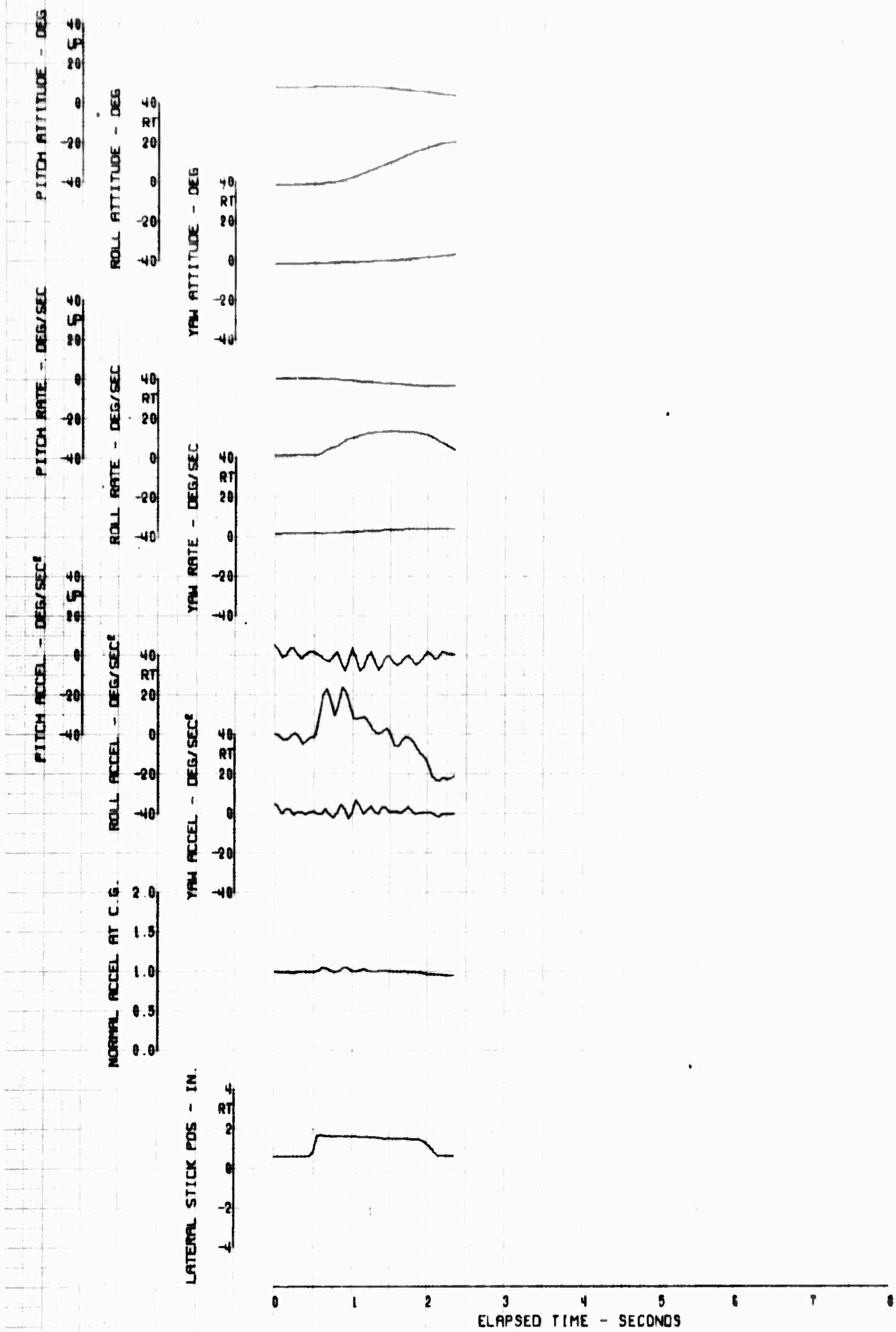

FIGURE 93 REACTION TO A RIGHT LATERAL STEP

HH-53C USAF 67-14993

FLIGHT COND	AVG GW (LBS)	AVG CG (IN)	AVG ALT (FT)	AVG FAT (DEG C)	ROTOR SPEED (RPM)	AFCS COND
HOV IGE	31000	352	300	10	185	ON

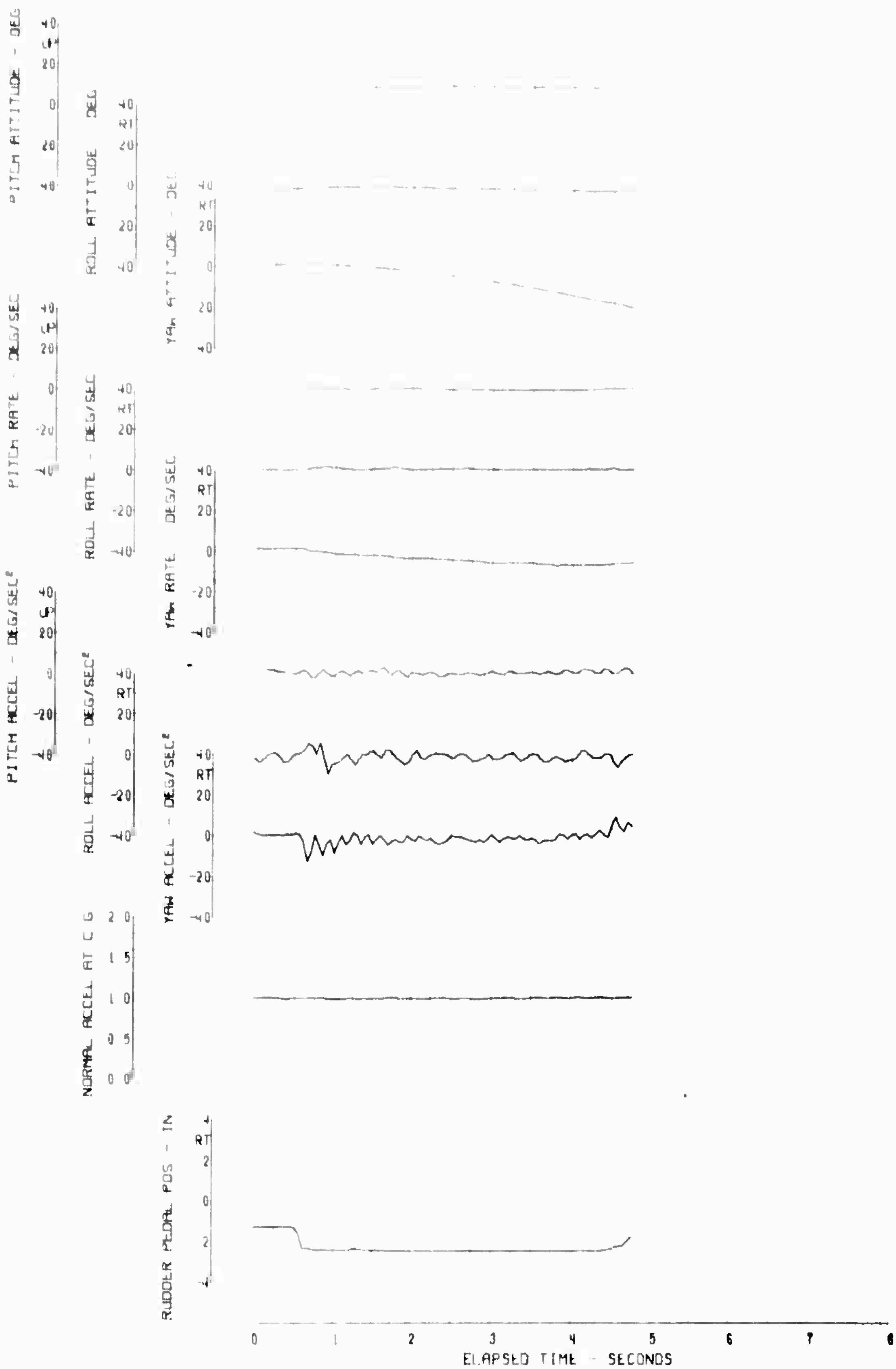

FIGURE 94 REACTION TO A LEFT DIRECTIONAL STEP

HH-53C USAF 67-14993

FLIGHT COND	AVG GW (LBS)	AVG CG (IN)	AVG ALT (FT)	AVG FAT (DEG C)	ROTOR SPEED (RPM)	AFCS COND
HOV IGE	31000	352	300	10	185	OFF

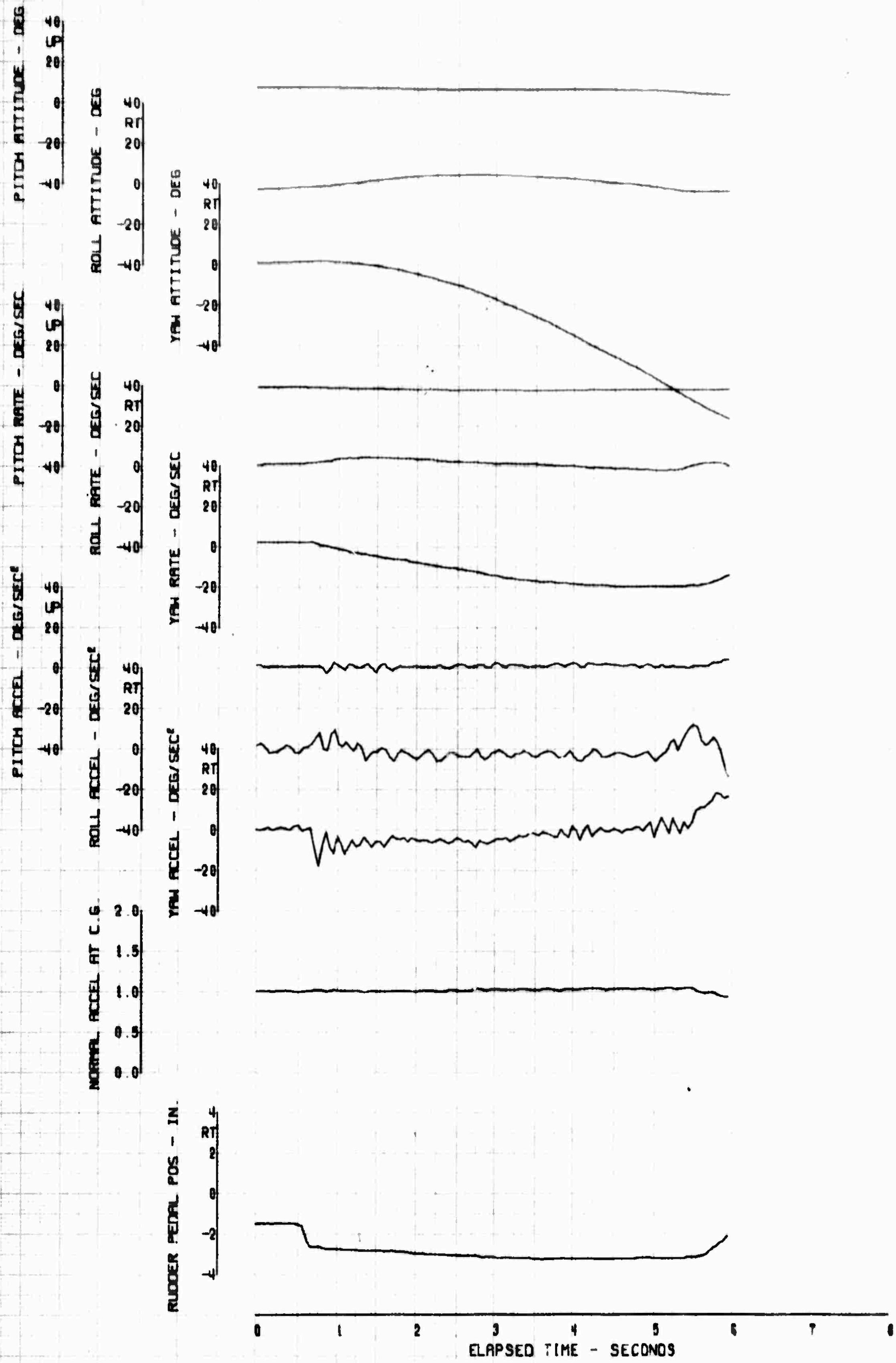

FIGURE 95 REACTION TO A LEFT DIRECTIONAL STEP

HH-53C USAF 67-14993

FLIGHT COND	AVG GW (LBS)	AVG CG (IN)	AVG ALT (FT)	AVG FAT (DEG C)	ROTOR SPEED (RPM)	AFCS COND
HOV IGE	31000	352	300	10	185	ON

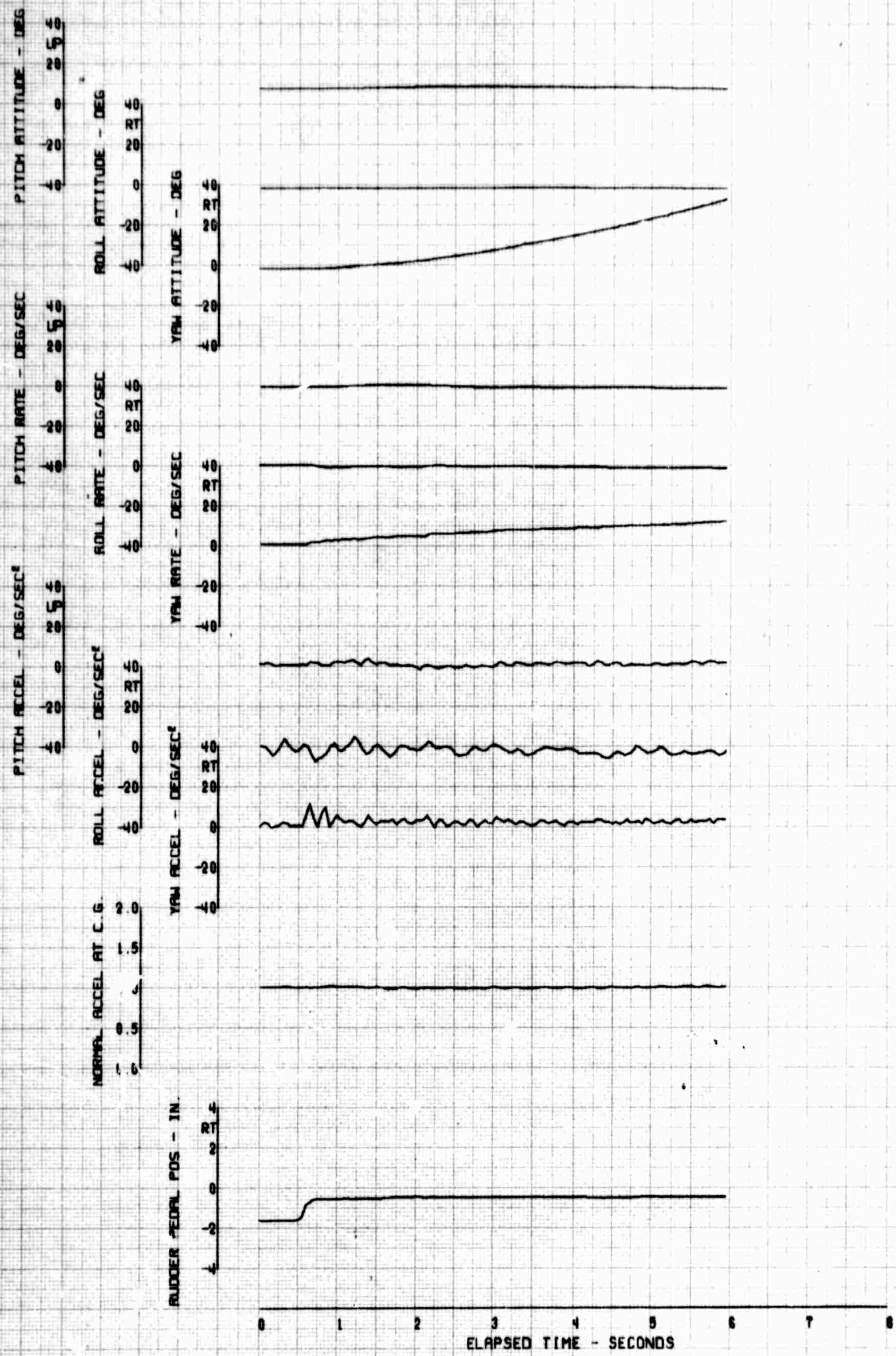

FIGURE 96. REACTION TO A RIGHT DIRECTIONAL STEP

HH-53C USAF 67-14993

FLIGHT COND	AVG GW (LBS)	AVG CG (IN)	AVG ALT (FT)	AVG FAT (DEG C)	ROTOR SPEED (RPM)	AFCS COND
HOV IGE	31000	352	300	10	185	OFF

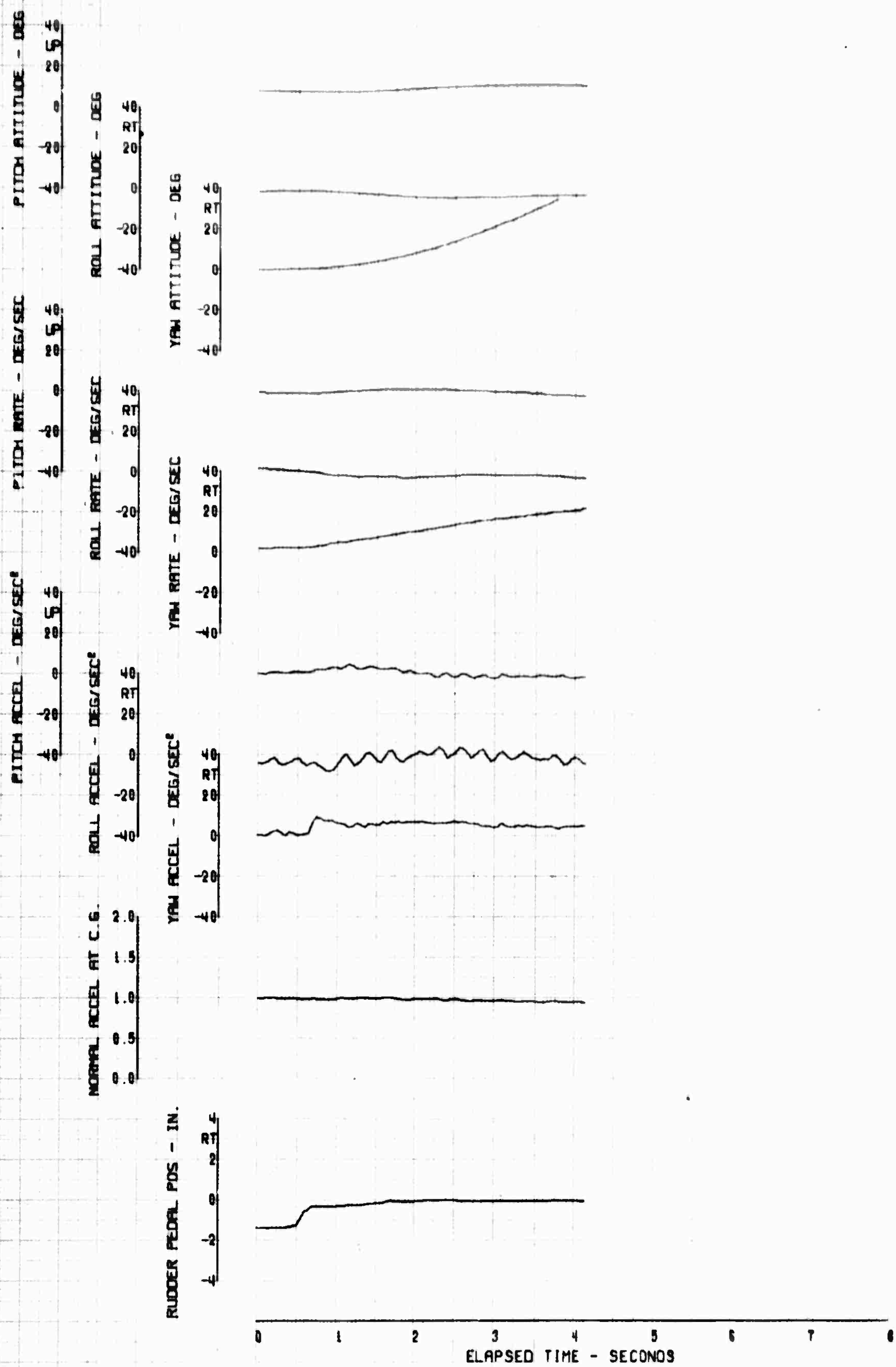

FIGURE 97 REACTION TO A RIGHT DIRECTIONAL STEP

HH-53C USAF 67-14993

FLIGHT COND	AVG GW (LBS)	AVG CG (IN)	AVG ALT (FT)	AVG FAT (DEG C)	ROTOR SPEED (RPM)	AFCS COND
HOV IGE	31000	328	300	10	185	ON

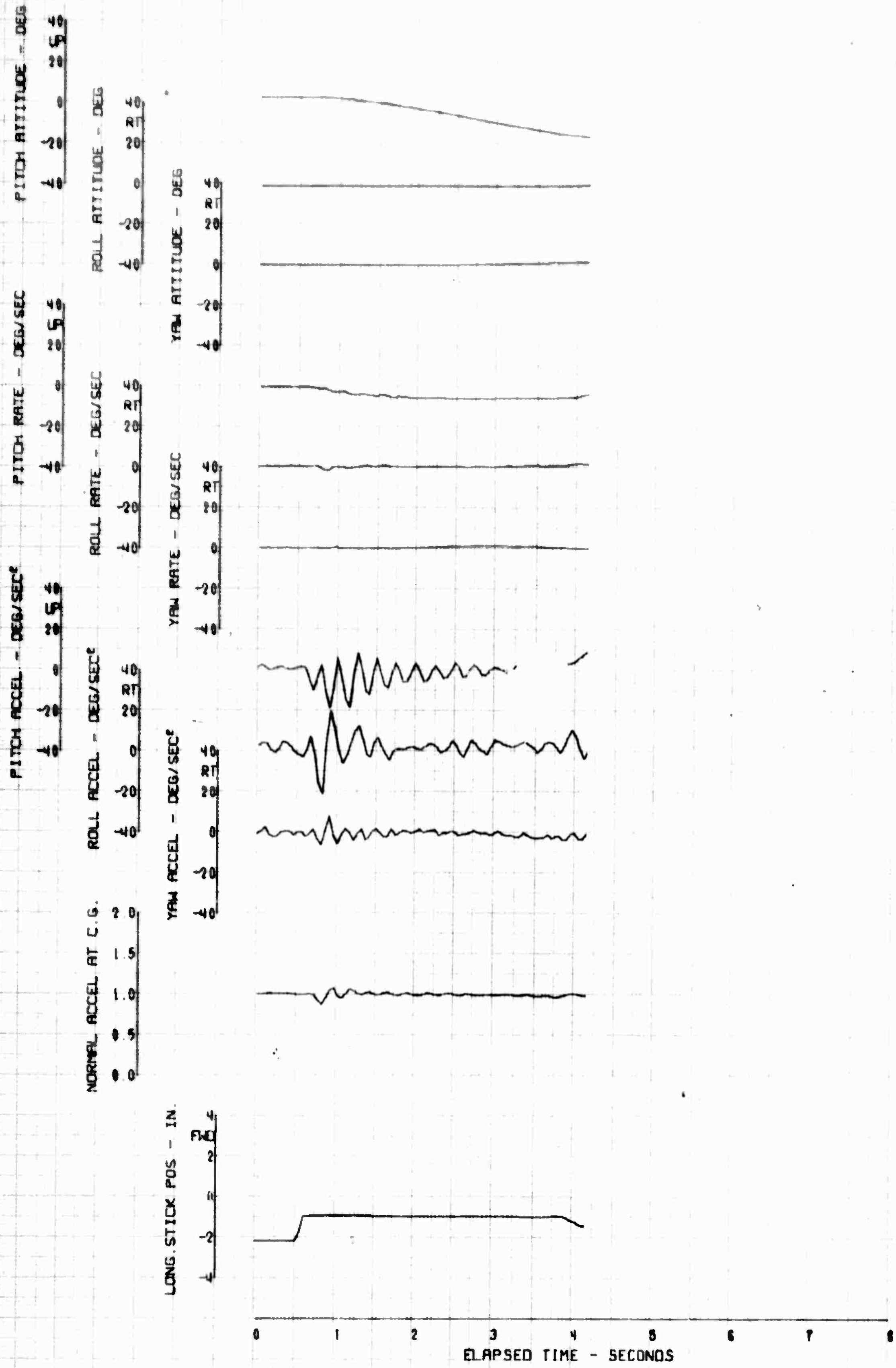

FIGURE 98. REACTION TO A FORWARD LONGITUDINAL STEP

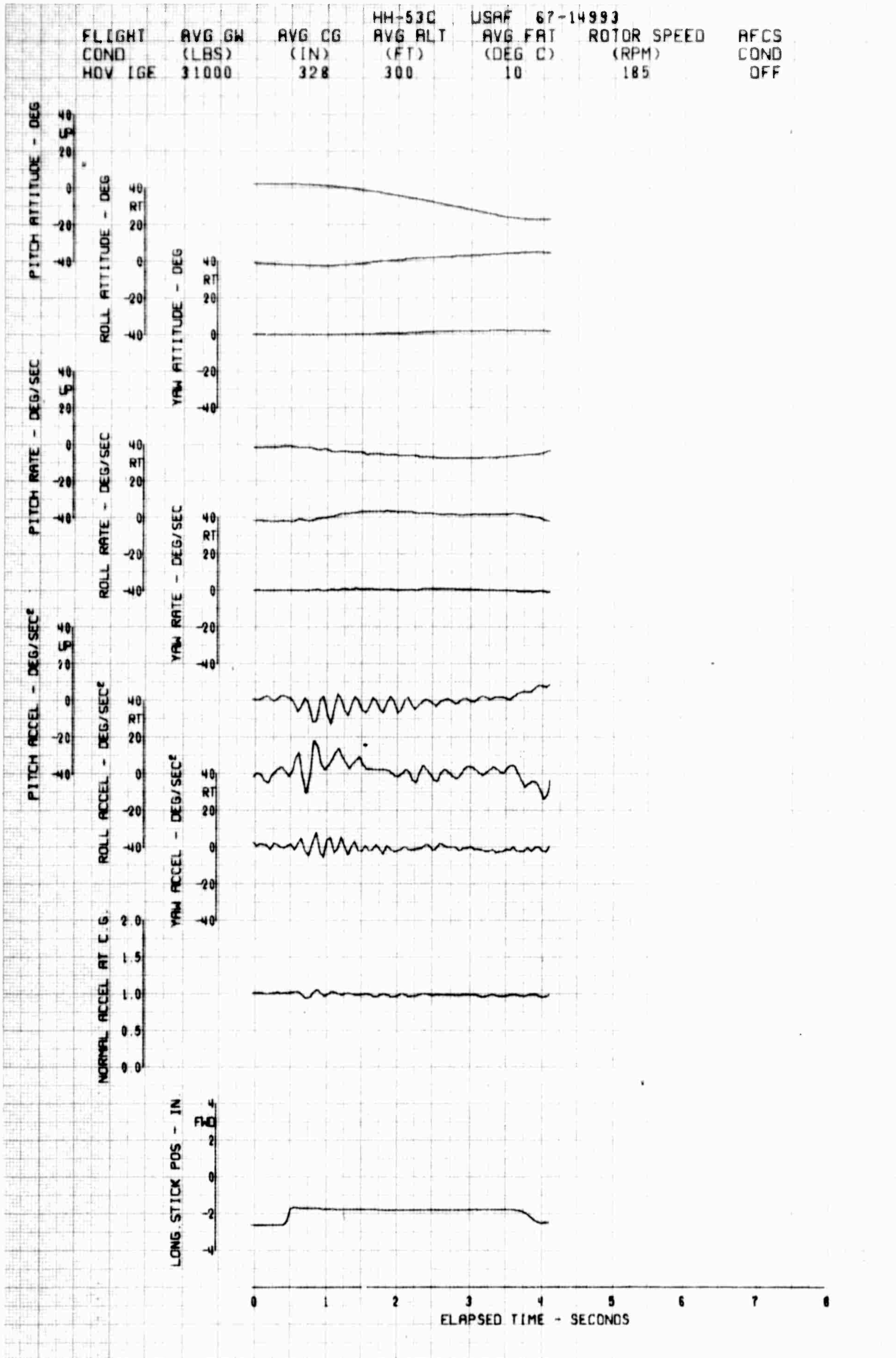

FIGURE 97 REACTION TO A FORWARD LONGITUDINAL STEP

HH-53C USAF 67-14993

FLIGHT COND	AVG GW (LBS)	AVG CG (IN)	AVG ALT (FT)	AVG FAT (DEG C)	ROTOR SPEED (RPM)	AFCS COND
HOV IGE	31000	328	300	10	185	ON

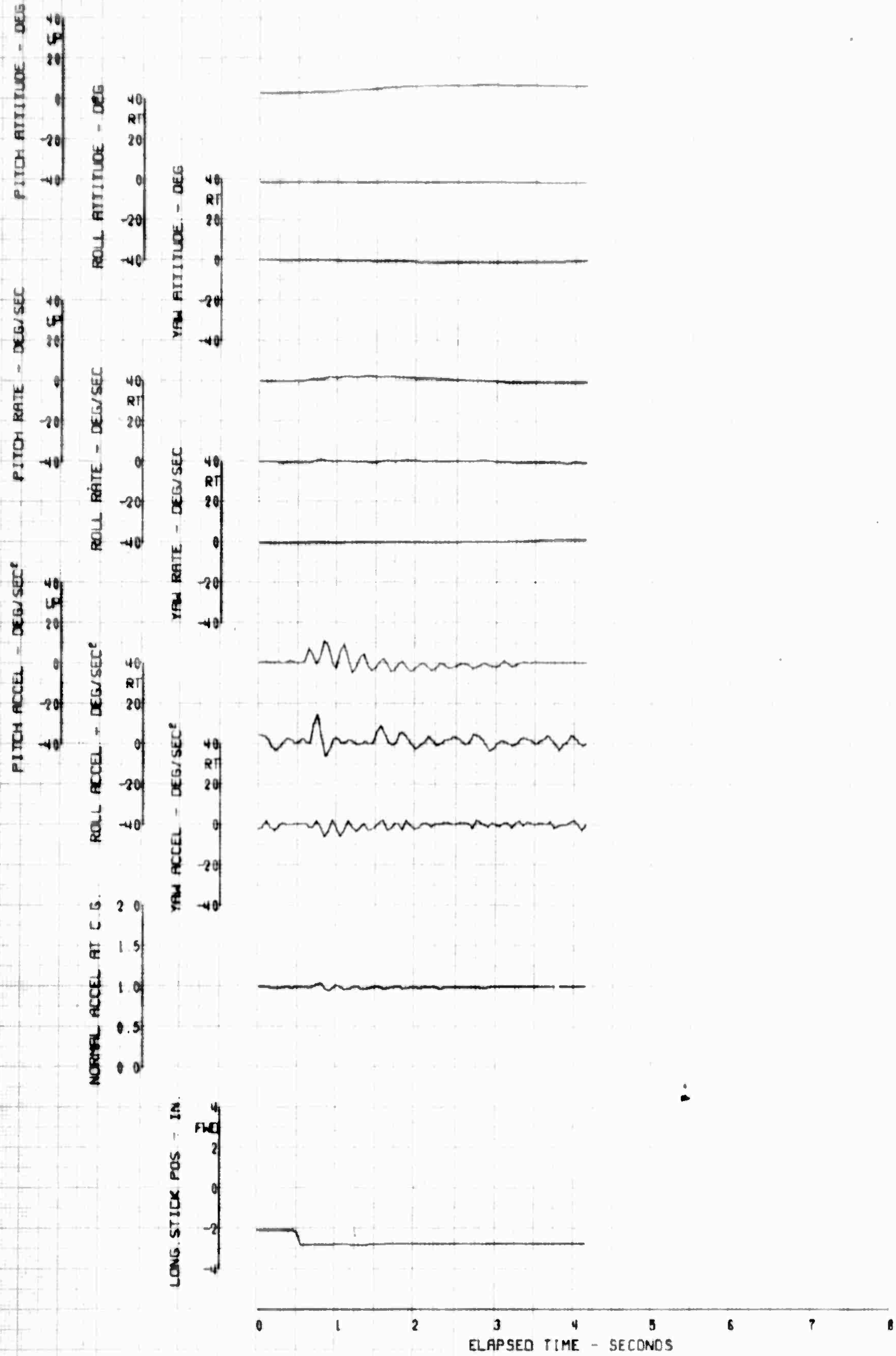

FIGURE 100 REACTION TO AN AFT LONGITUDINAL STEP

HH-53C USAF 67-14993

FLIGHT COND	AVG GW (LBS)	AVG CG (IN)	AVG ALT (FT)	AVG FAT (DEG C)	ROTOR SPEED (RPM)	AFCS COND
HOV IGE	31000	328	300	10	185	OFF

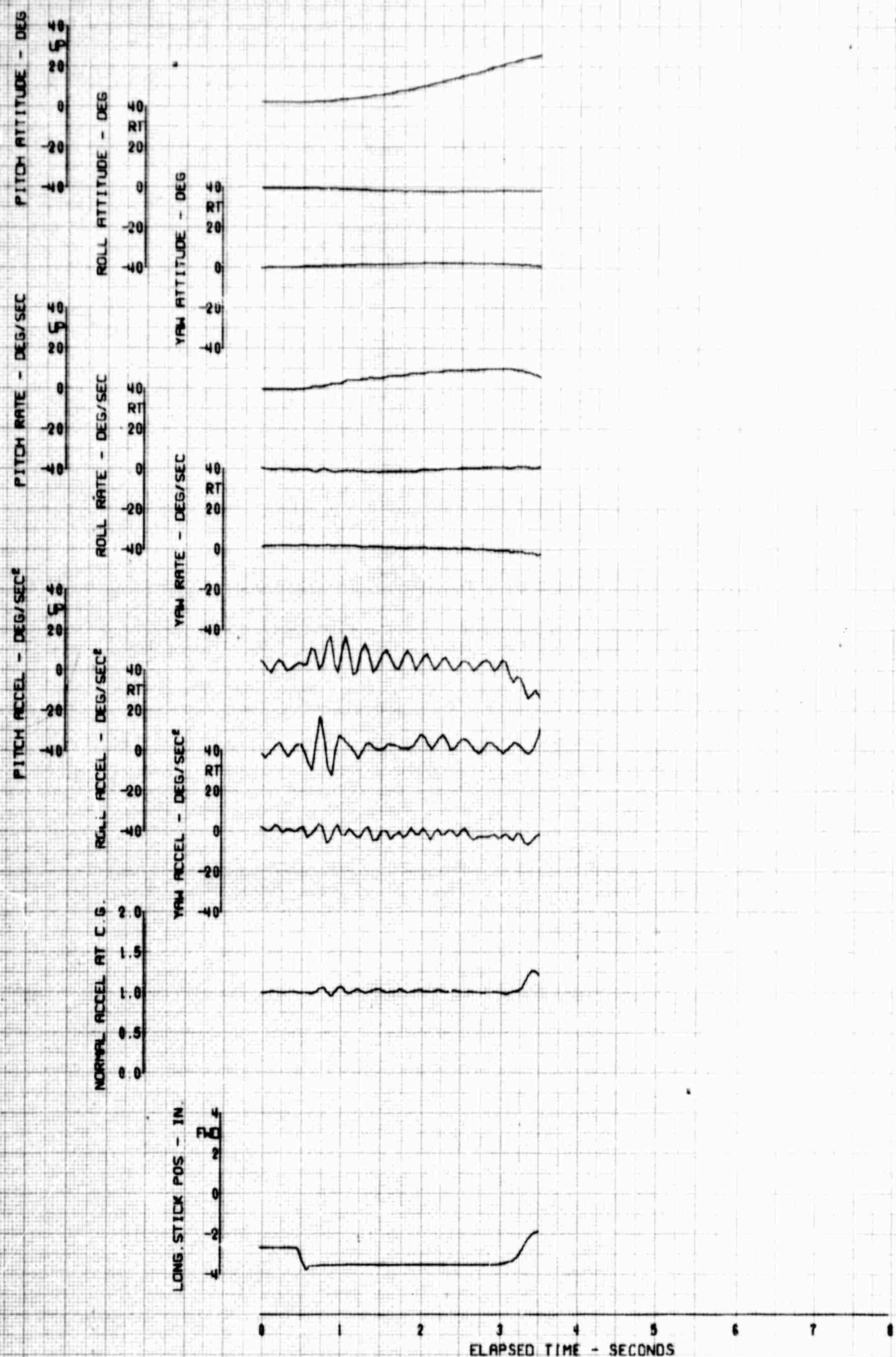

FIGURE 101. REACTION TO AN AFT LONGITUDINAL STEP

HH-53C USAF 67-14993

FLIGHT COND	AVG GW (LBS)	AVG CG (IN)	AVG ALT (FT)	AVG FAT (DEG C)	ROTOR SPEED (RPM)	AFCS COND
HOV IGE	31000	328	300	10	185	ON

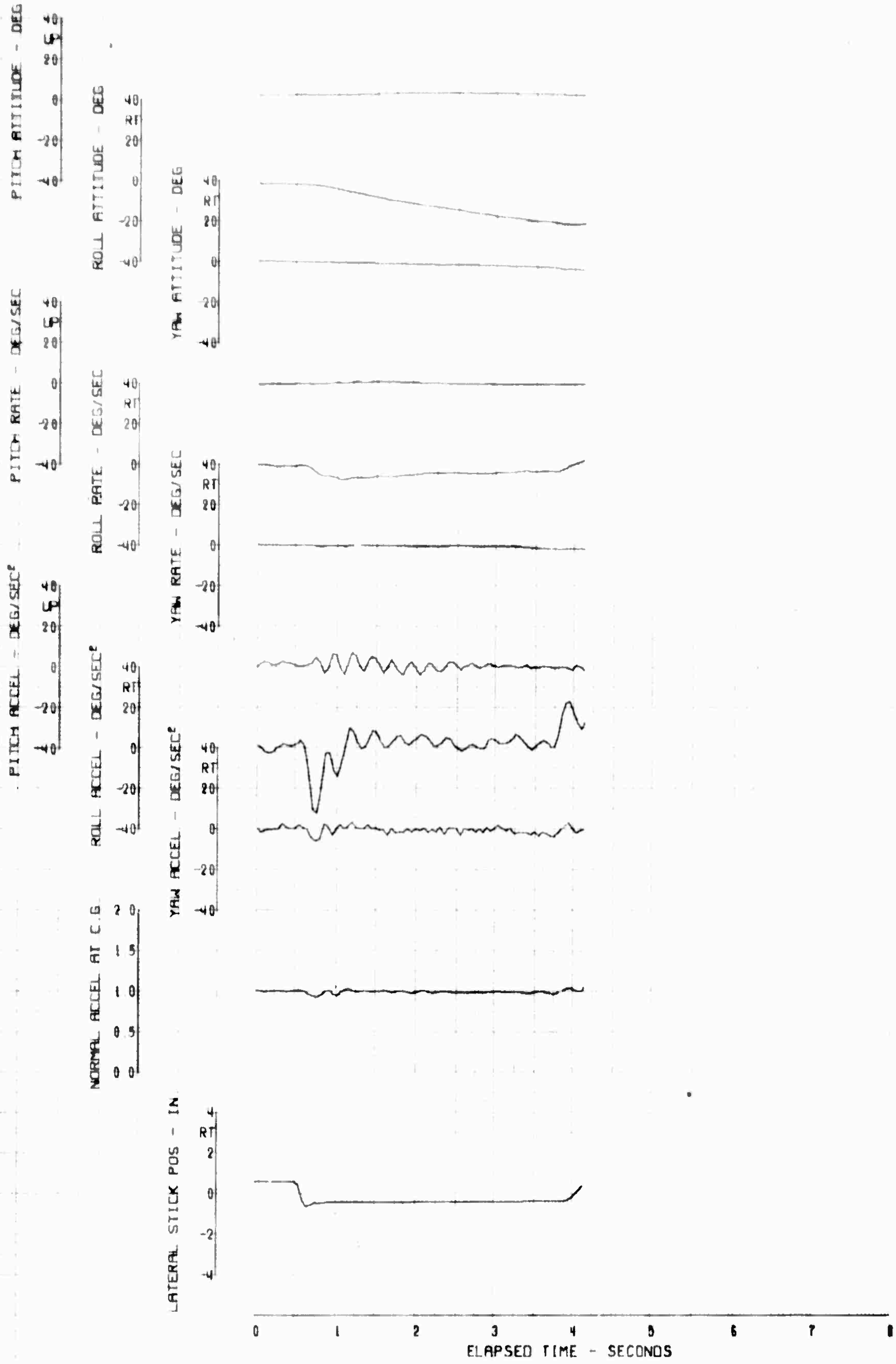

FIGURE 102 REACTION TO A LEFT LATERAL STEP

HH-53C USAF 67-14993

FLIGHT COND	AVG GW (LBS)	AVG CG (IN)	AVG ALT (FT)	AVG FAT (DEG C)	ROTOR SPEED (RPM)	AFCS COND
HOV IGE	31000	328	300	10	185	OFF

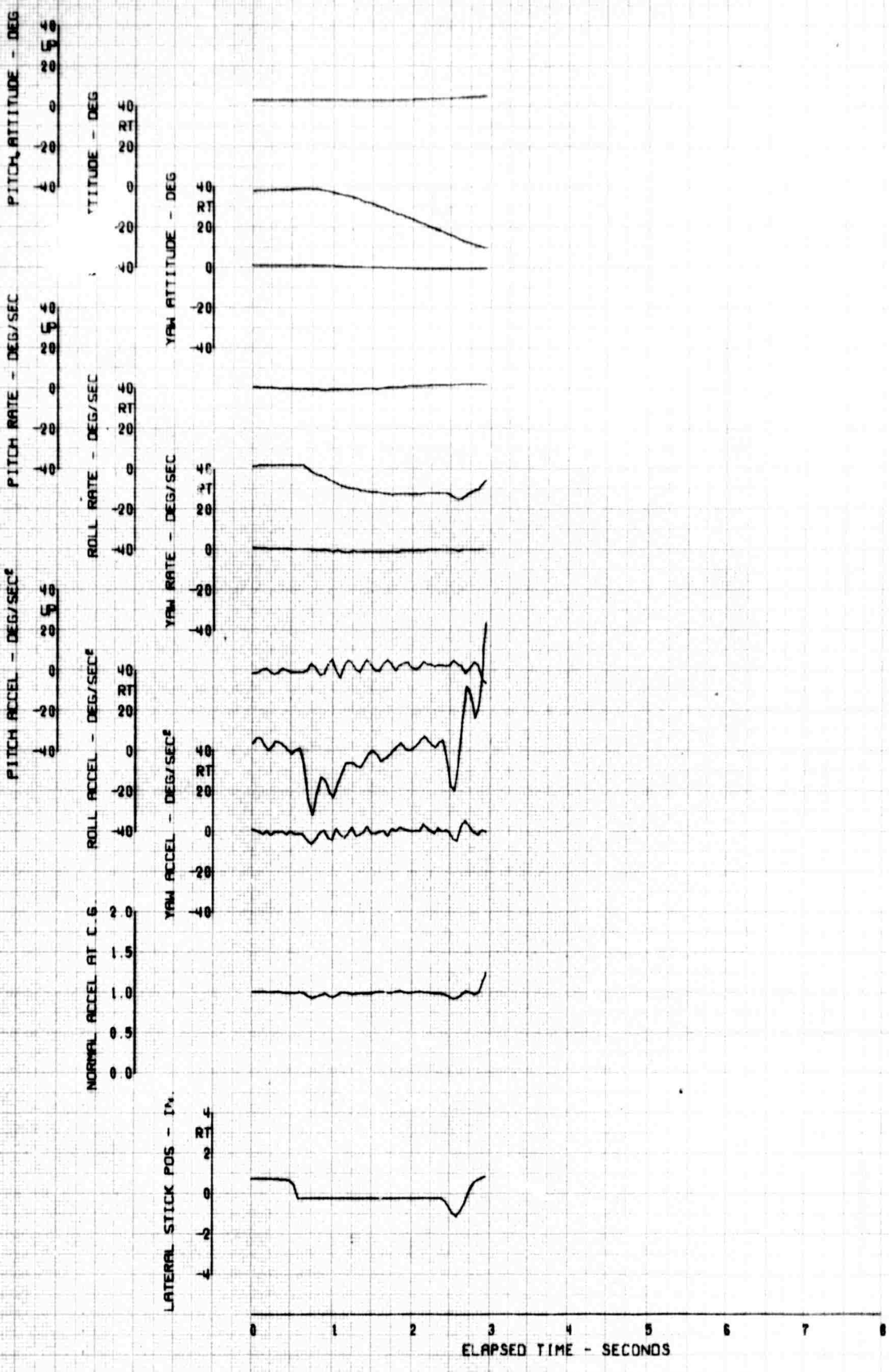

FIGURE 103 REACTION TO A LEFT LATERAL STEP

HH-53C USAF 67-14993

FLIGHT COND	AVG GW (LBS)	AVG CG (IN)	AVG ALT (FT)	AVG FAT (DEG C)	ROTOR SPEED (RPM)	AFCS COND
HOV IGE	31000	328	300	10	185	ON

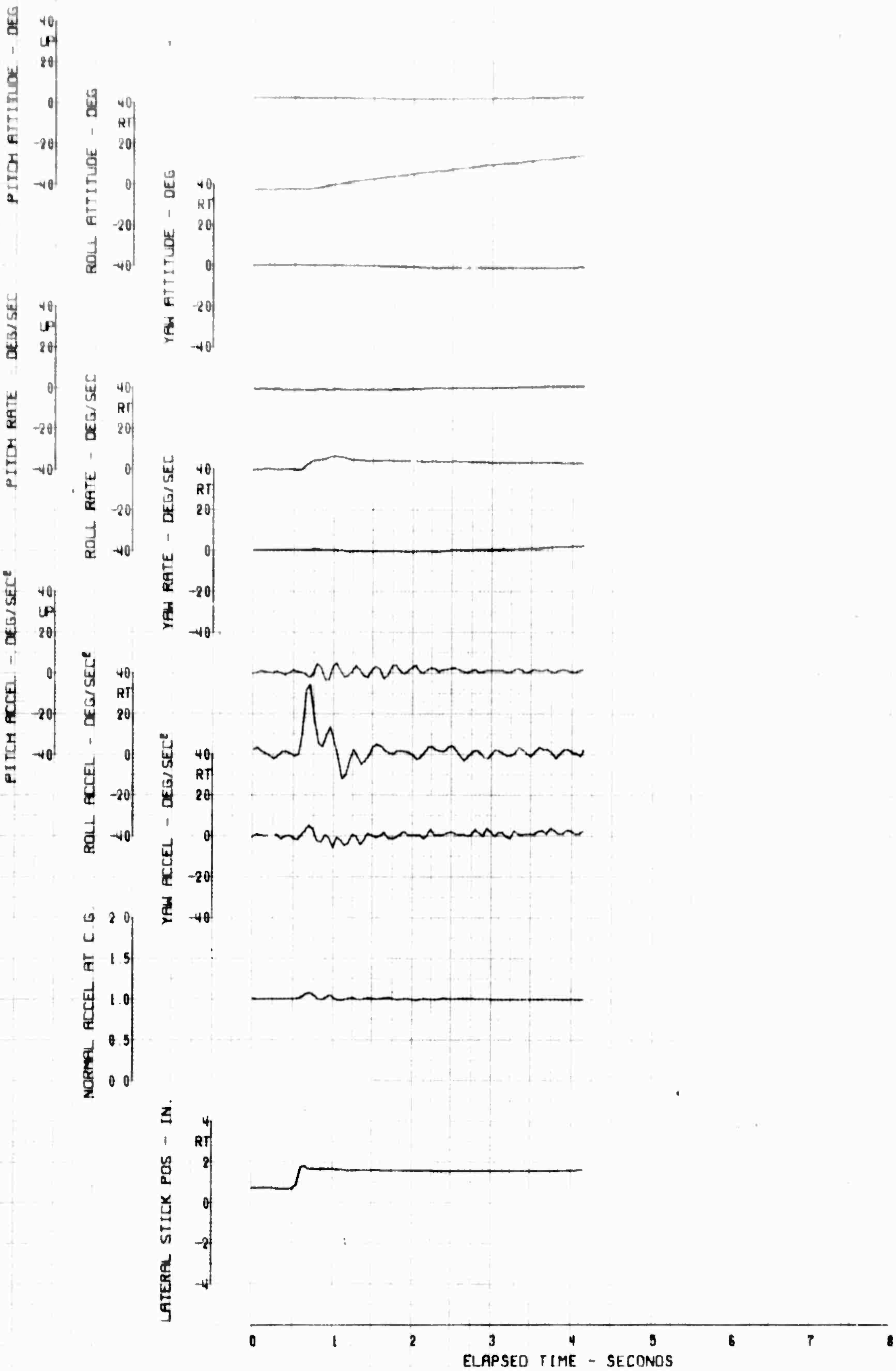

FIGURE 104 REACTION TO A RIGHT LATERAL STEP

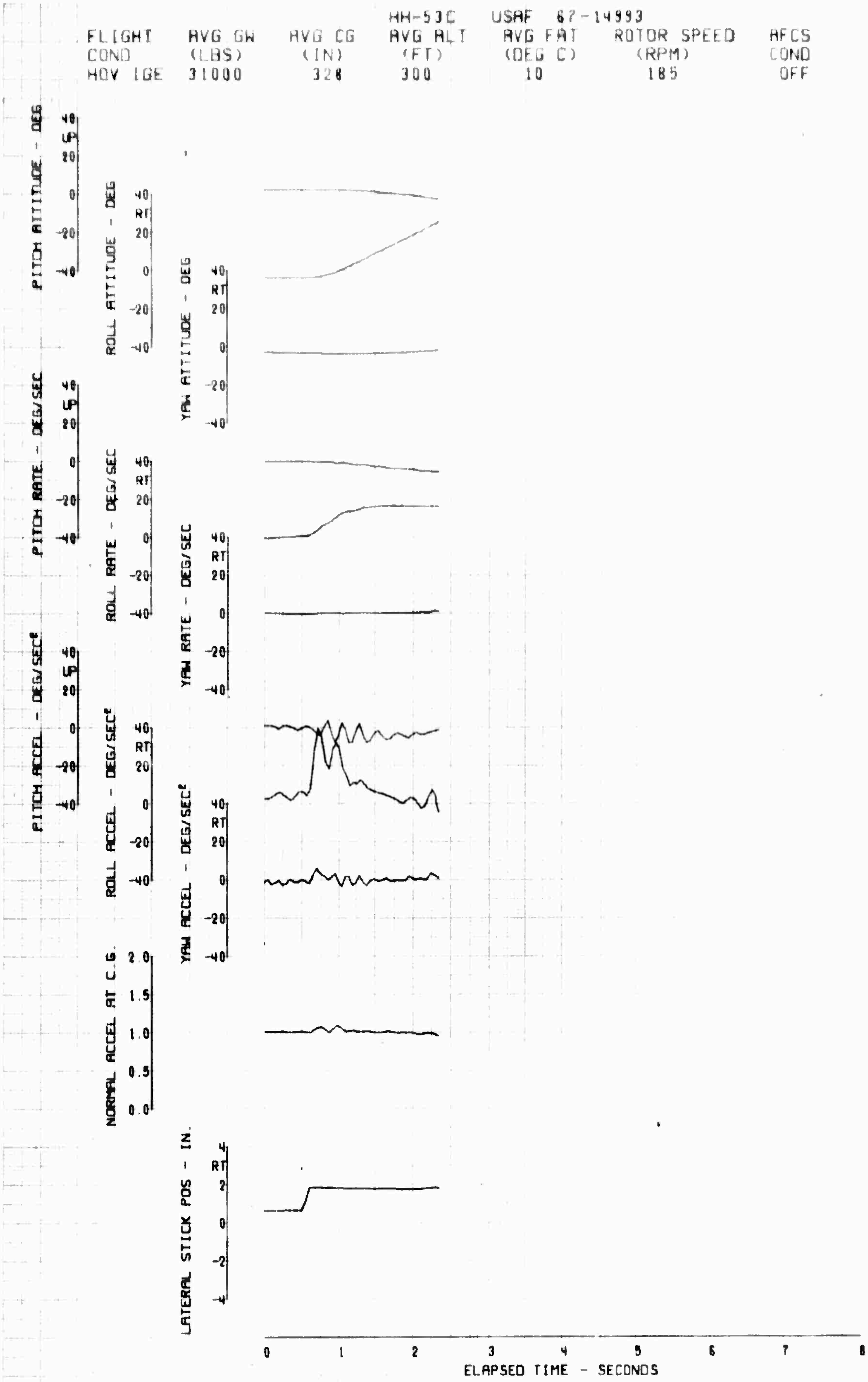

FIGURE 105 REACTION TO A RIGHT LATERAL STEP

HH-53C USAF 67-14993

FLIGHT COND	AVG GW (LBS)	AVG CG (IN)	AVG ALT (FT)	AVG FAT (DEG C)	ROTOR SPEED (RPM)	AFCS COND
HOV IGE	31000	328	300	10	185	ON

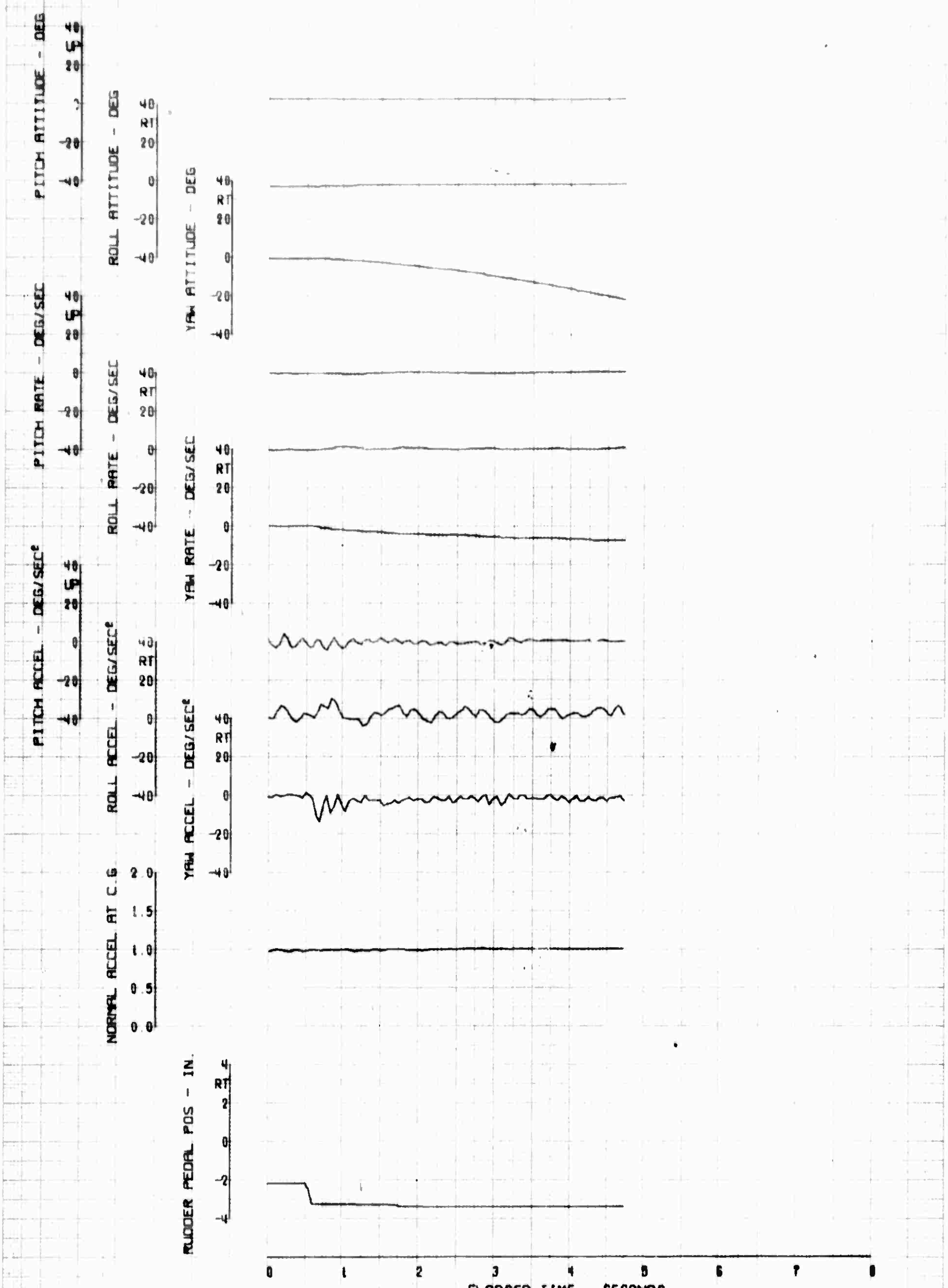

FIGURE 106. REACTION TO A LEFT DIRECTIONAL STEP

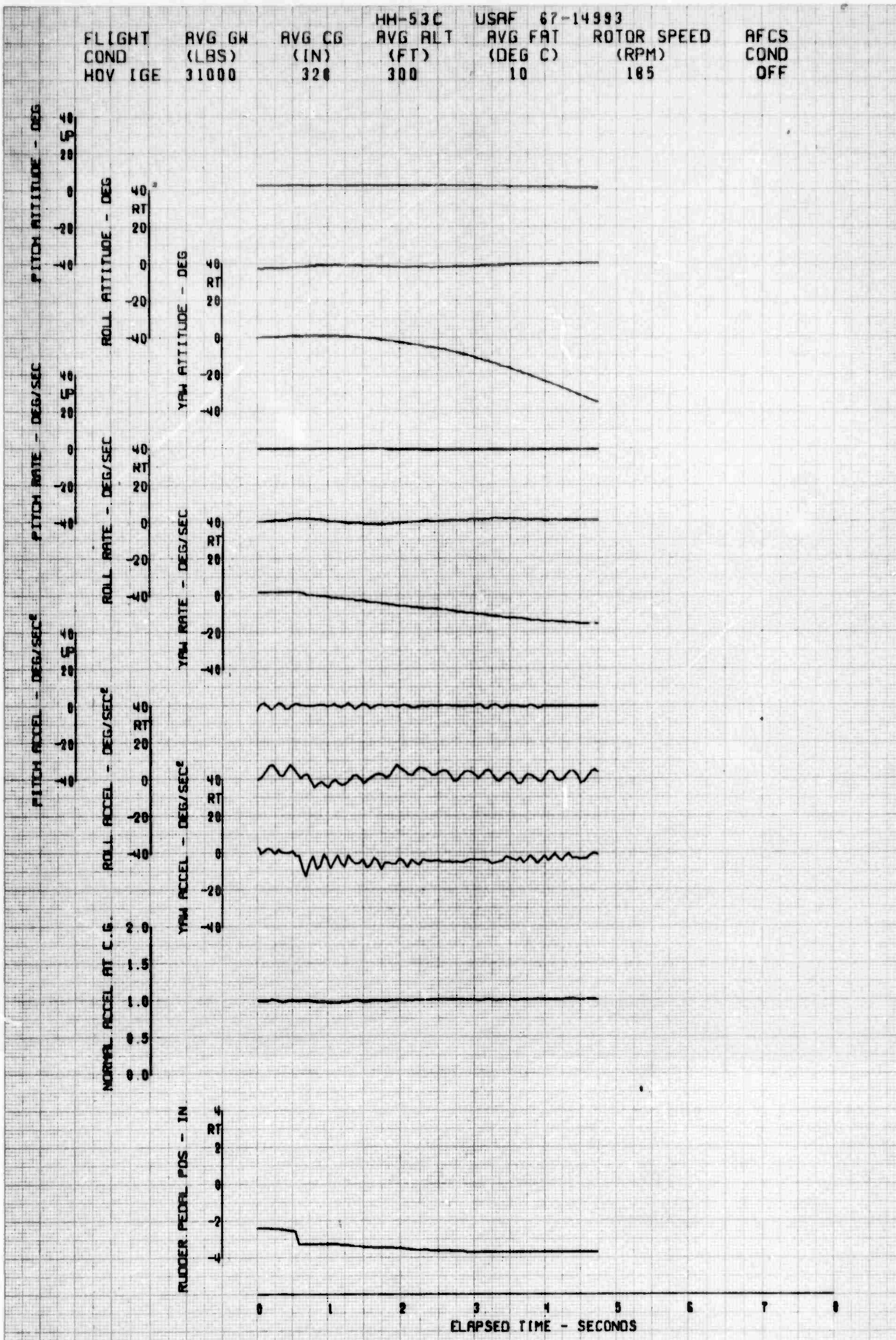

FIGURE 107 REACTION TO A LEFT DIRECTIONAL STEP

HH-53C USAF 67-14993

FLIGHT COND	AVG GW (LBS)	AVG CG (IN)	AVG ALT (FT)	AVG FAT (DEG C)	ROTOR SPEED (RPM)	AFCS COND
HOV IGE	31000	326	300	10	185	ON

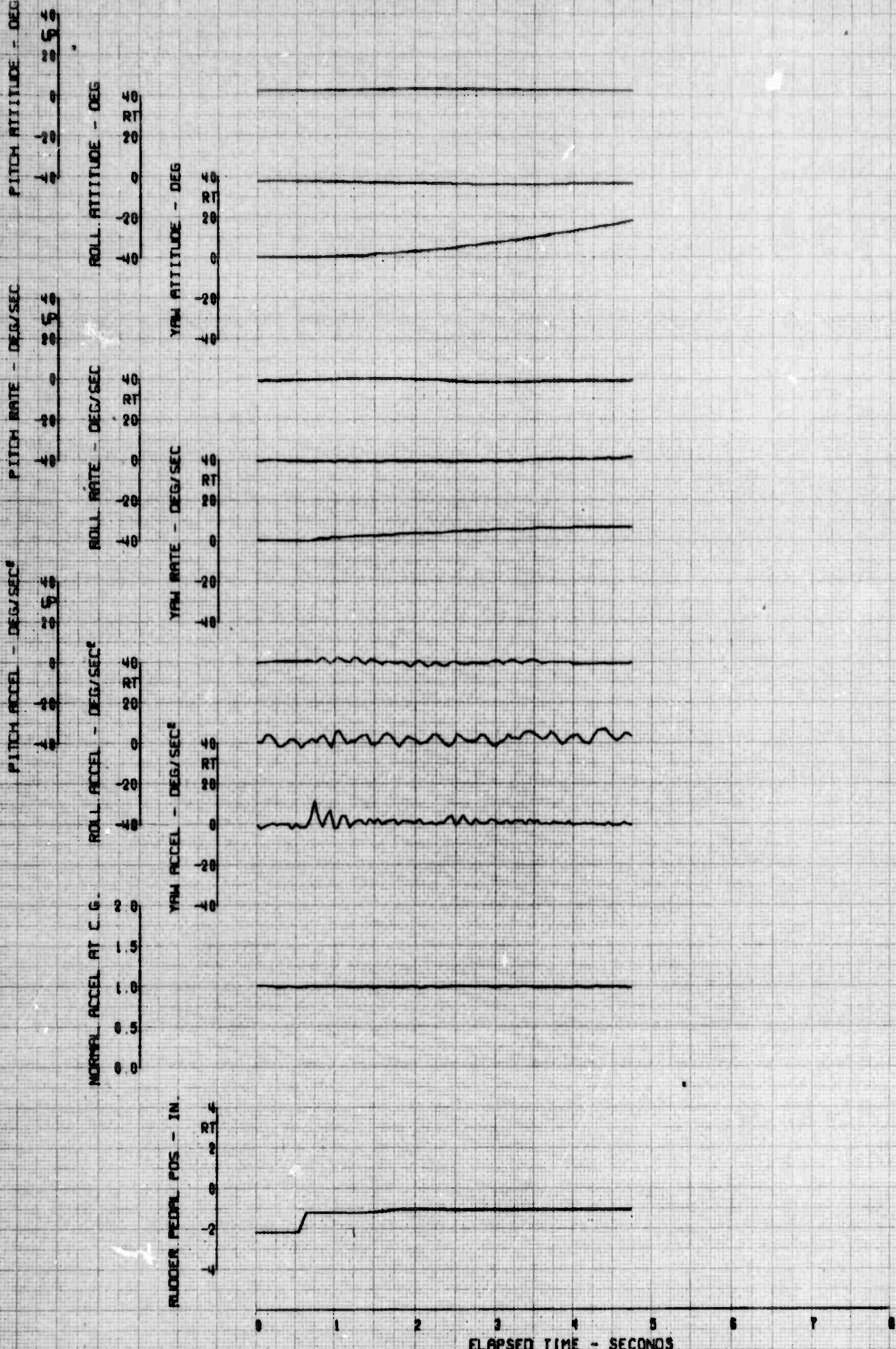

FIGURE 108. REACTION TO A RIGHT DIRECTIONAL STEP

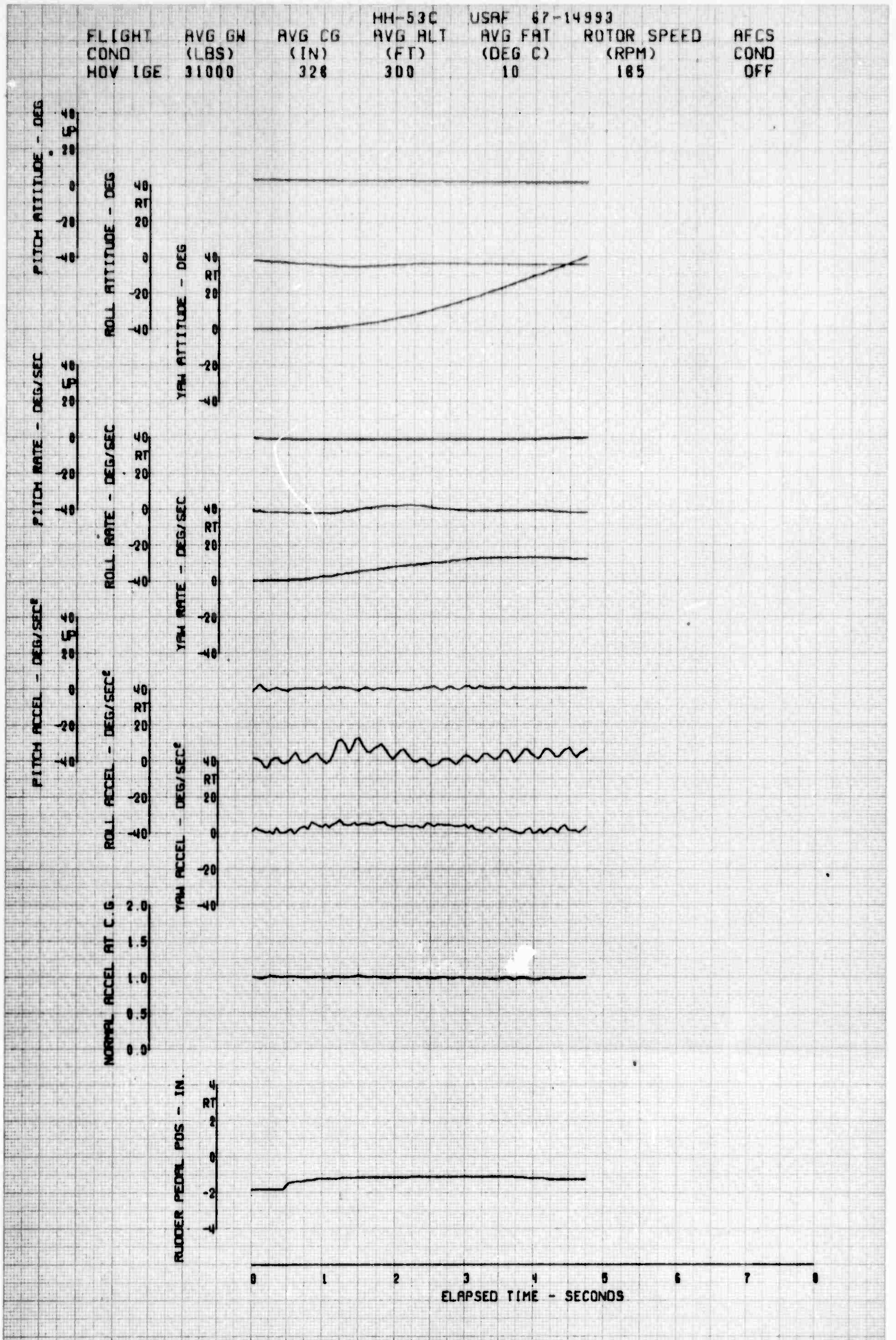

FIGURE 109 REACTION TO A RIGHT DIRECTIONAL STEP

HH-53C USAF S/N 67-14993

Sym	Flight Condition	Avg GW (lb)	cg (in.)	Avg Press. Alt (ft)	Avg FAT (°C)	Rotor Speed (rpm)	AFCS	Trim A/S (kt)
○	Hover	31,000	328	300	10	185	ON	0
□	Hover	31,000	328	300	10	185	OFF	0

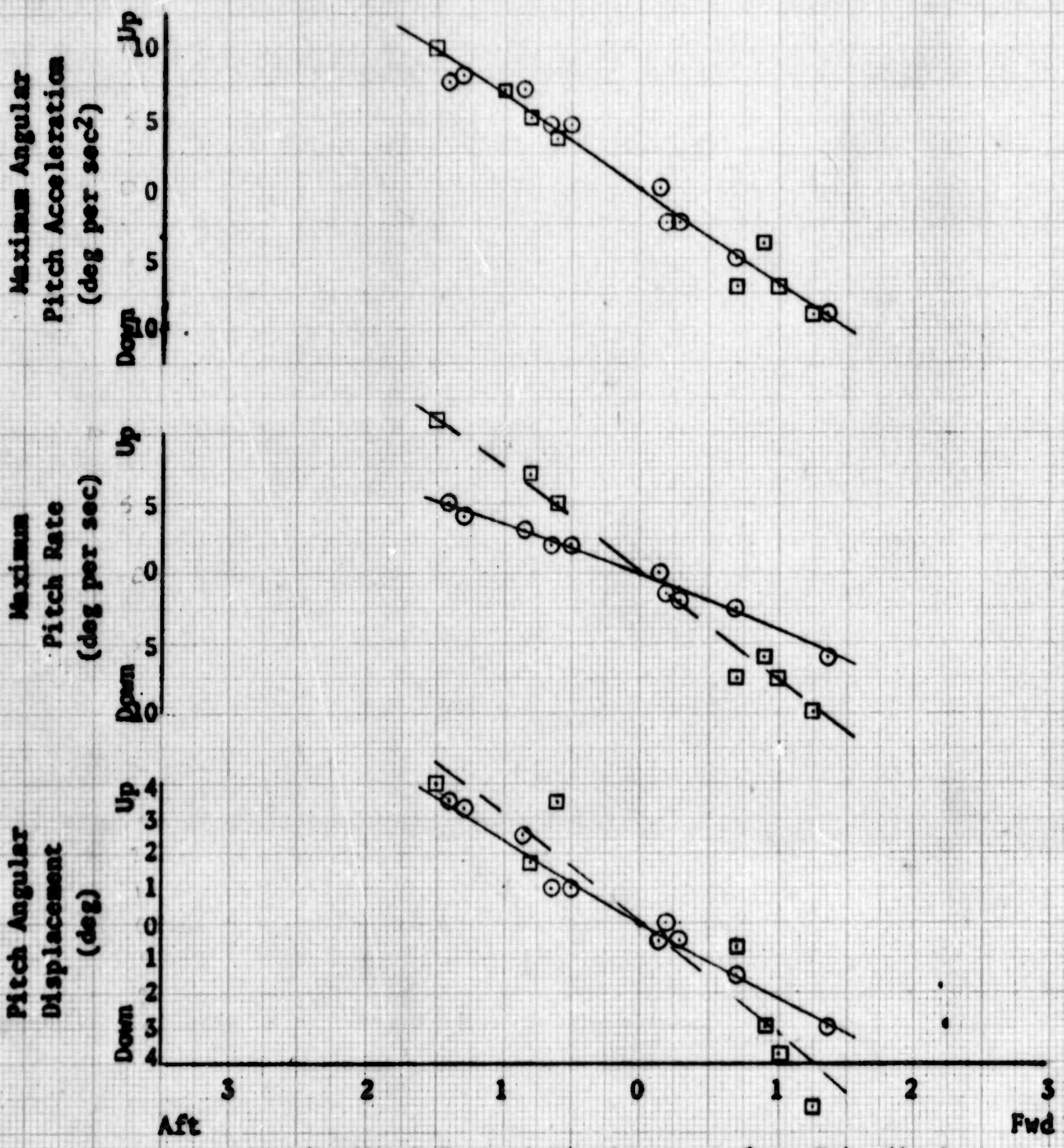

Figure 110. Longitudinal Controllability

HH-53C USAF S/N 67-14993

Sym	Flight Condition	Avg GW (lb)	cg (in.)	Avg Press. Alt (ft)	Avg FAT (°C)	Rotor Speed (rpm)	AFCS	Trim A/S (kt)
○	Hover	31,000	328	300	10	185	ON	0
□	Hover	31,000	328	300	10	185	OFF	0

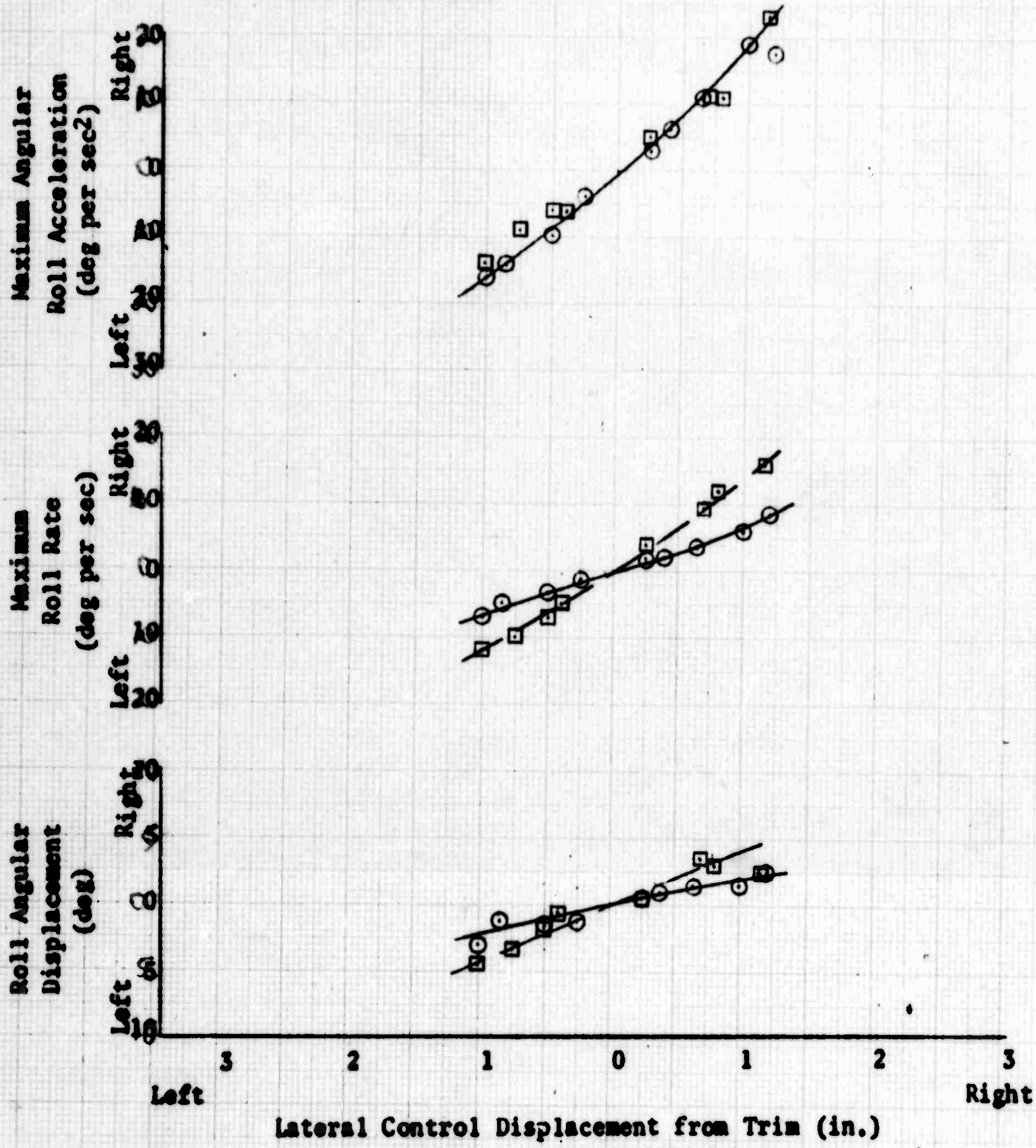

Figure 111. Lateral Controllability

HH-53C USAF S/N 67-14993

Sym	Flight Condition	Avg GW (lb)	cg (in.)	Avg Press. Alt (ft)	Avg FAT (°C)	Rotor Speed (rpm)	AFCS	Trim A/S (kt)
○	Hover	31,000	328	300	10	185	ON	0
□	Hover	31,000	328	300	10	185	OFF	0

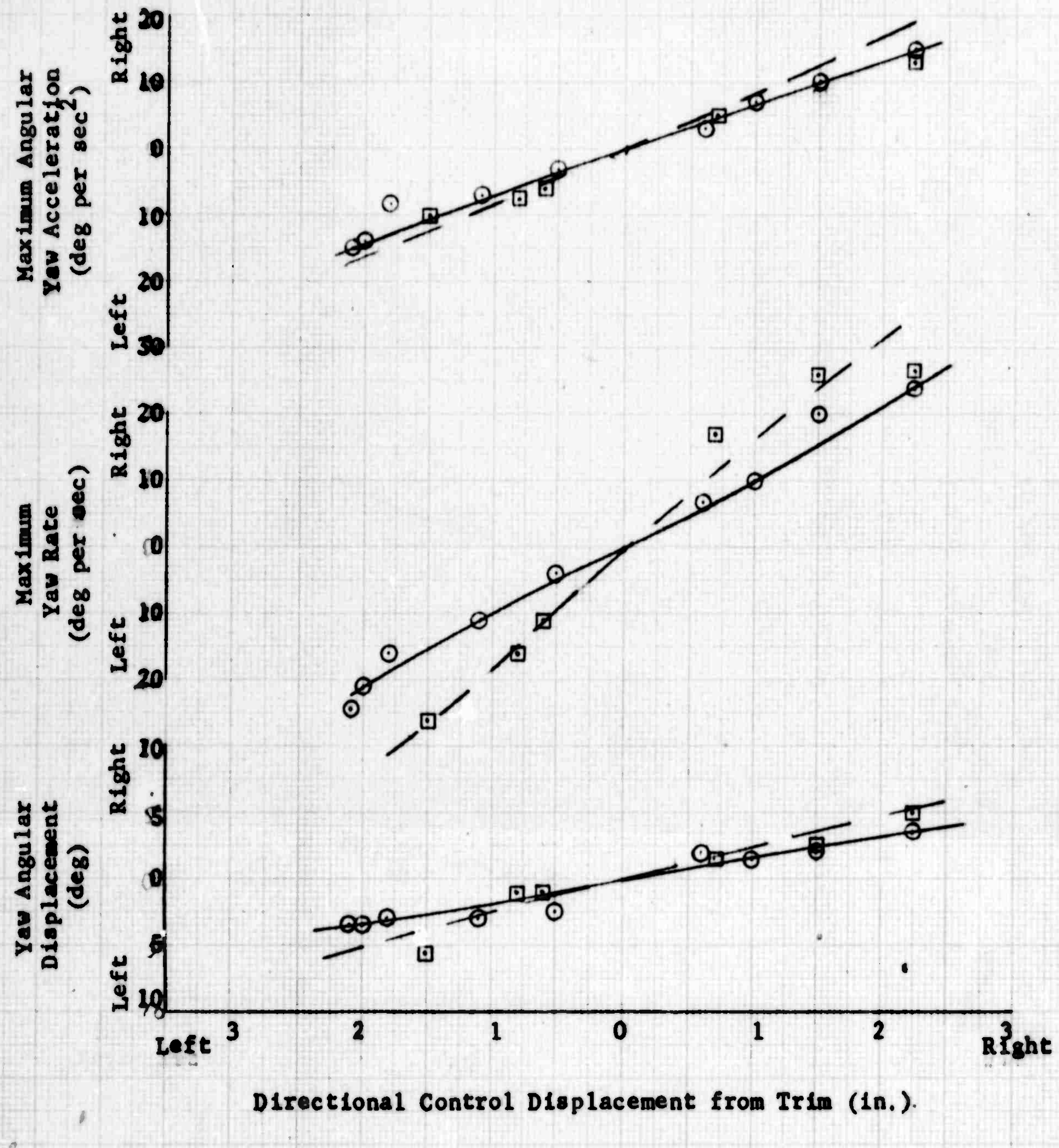

Figure 118. Directional Controllability

HH-53C USAF S/N 67-14993

Sym	Flight Condition	Avg GW (lb)	cg (in.)	Avg Press. Alt (ft)	Avg FAT (°C)	Rotor Speed (rpm)	AFCS	Trim A/S (kt)
○	Hover	31,000	352	300	10	185	ON	0
□	Hover	31,000	352	300	10	185	OFF	0

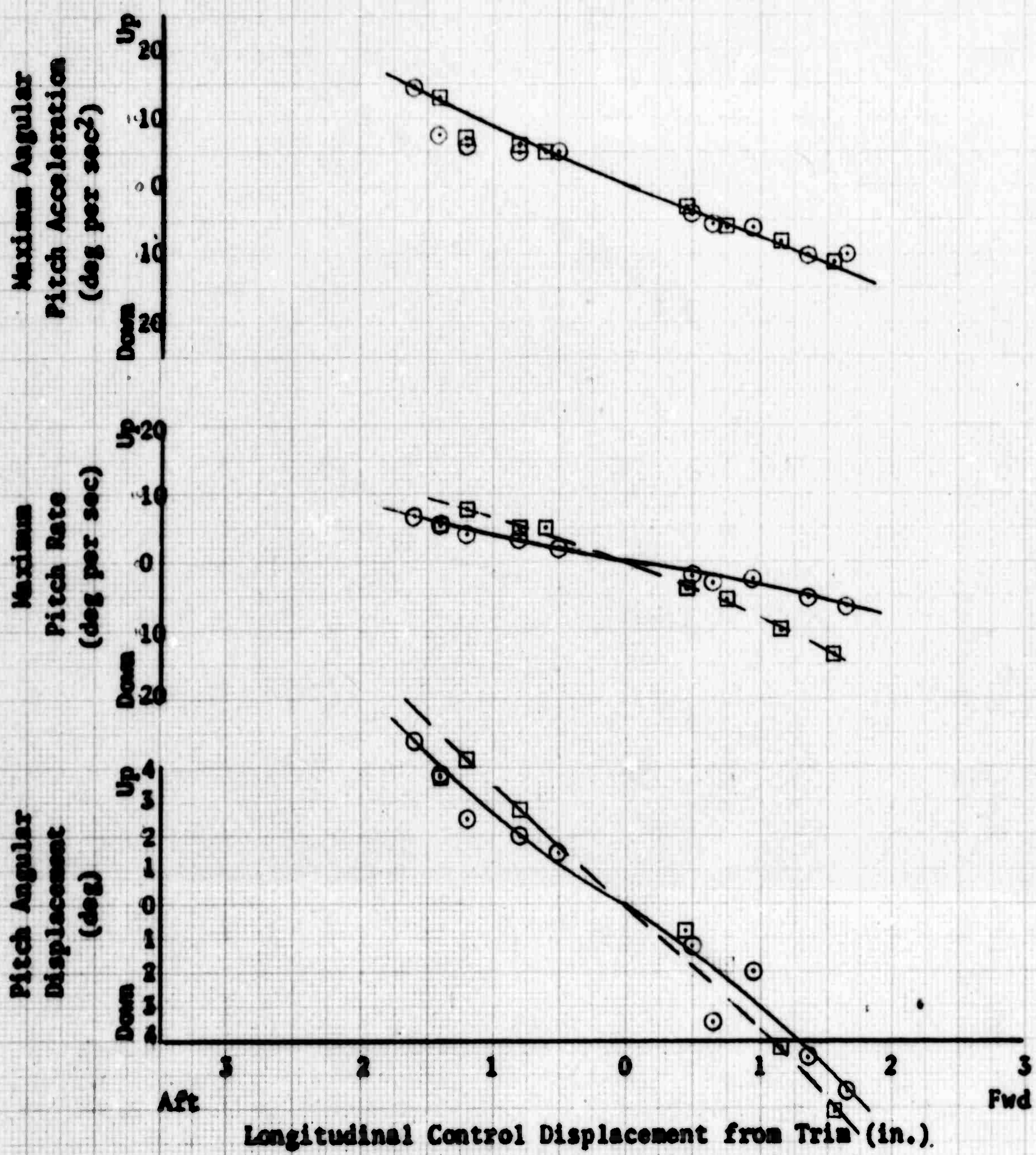

Figure 118. Longitudinal Controllability

HH-53C USAF S/N 67-14993

Sym	Flight Condition	Avg GW (lb)	cg (in.)	Avg Press. Alt (ft)	Avg FAT (°C)	Rotor Speed (rpm)	AFCS	Trim A/S (kt)
○	Hover	31,000	352	300	10	185	ON	0
□	Hover	31,000	352	300	10	185	OFF	0

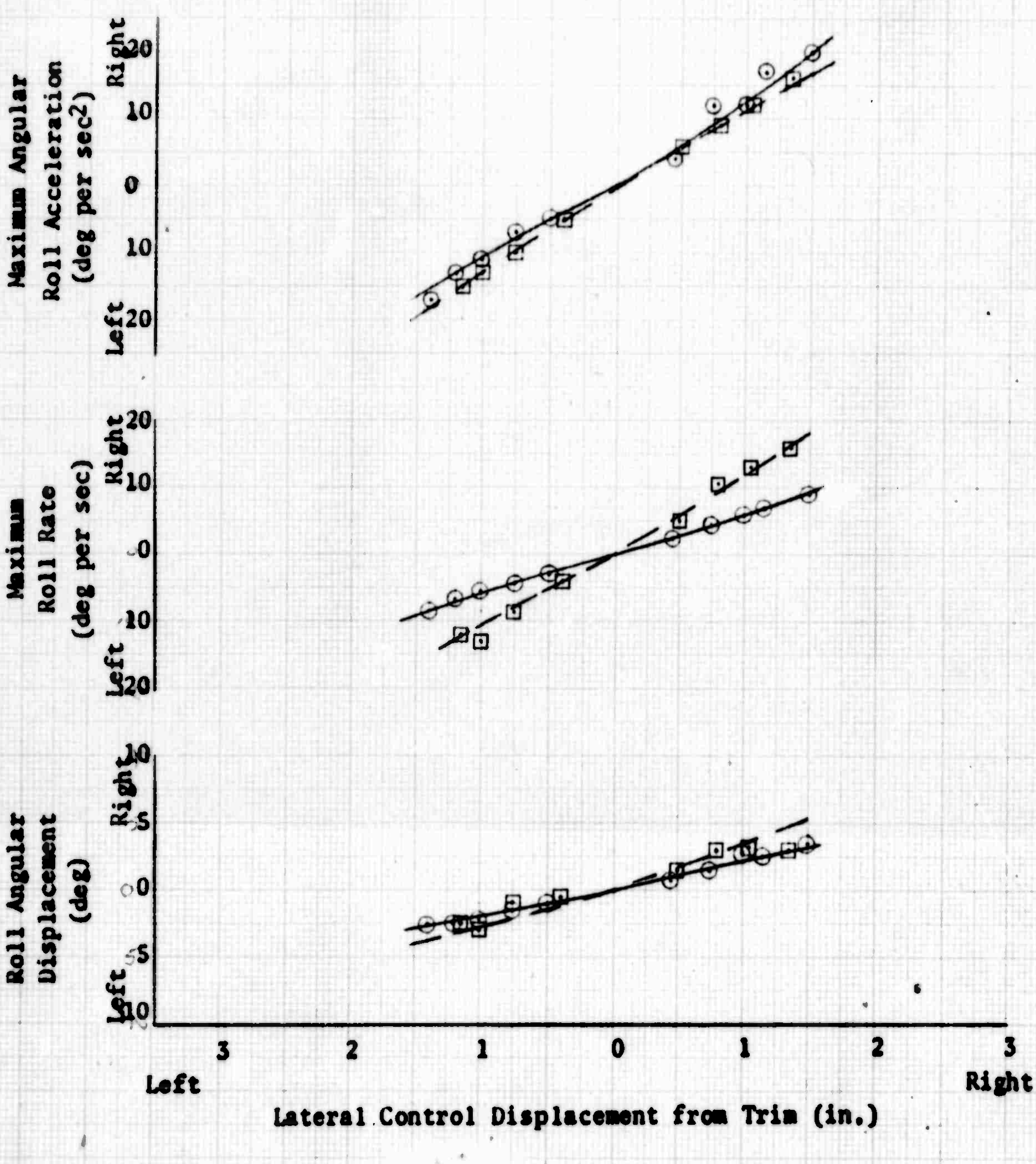

Figure 114. Lateral Controllability

HH-53C USAF S/N 67-14993

Sym	Flight Condition	Avg GW (lb)	cg (in.)	Avg Press. Alt (ft)	Avg FAT (°C)	Rotor Speed (rpm)	AFCS	Trim A/S (kt)
○	Hover	31,000	352	300	10	185	ON	0
□	Hover	31,000	352	300	10	185	OFF	0

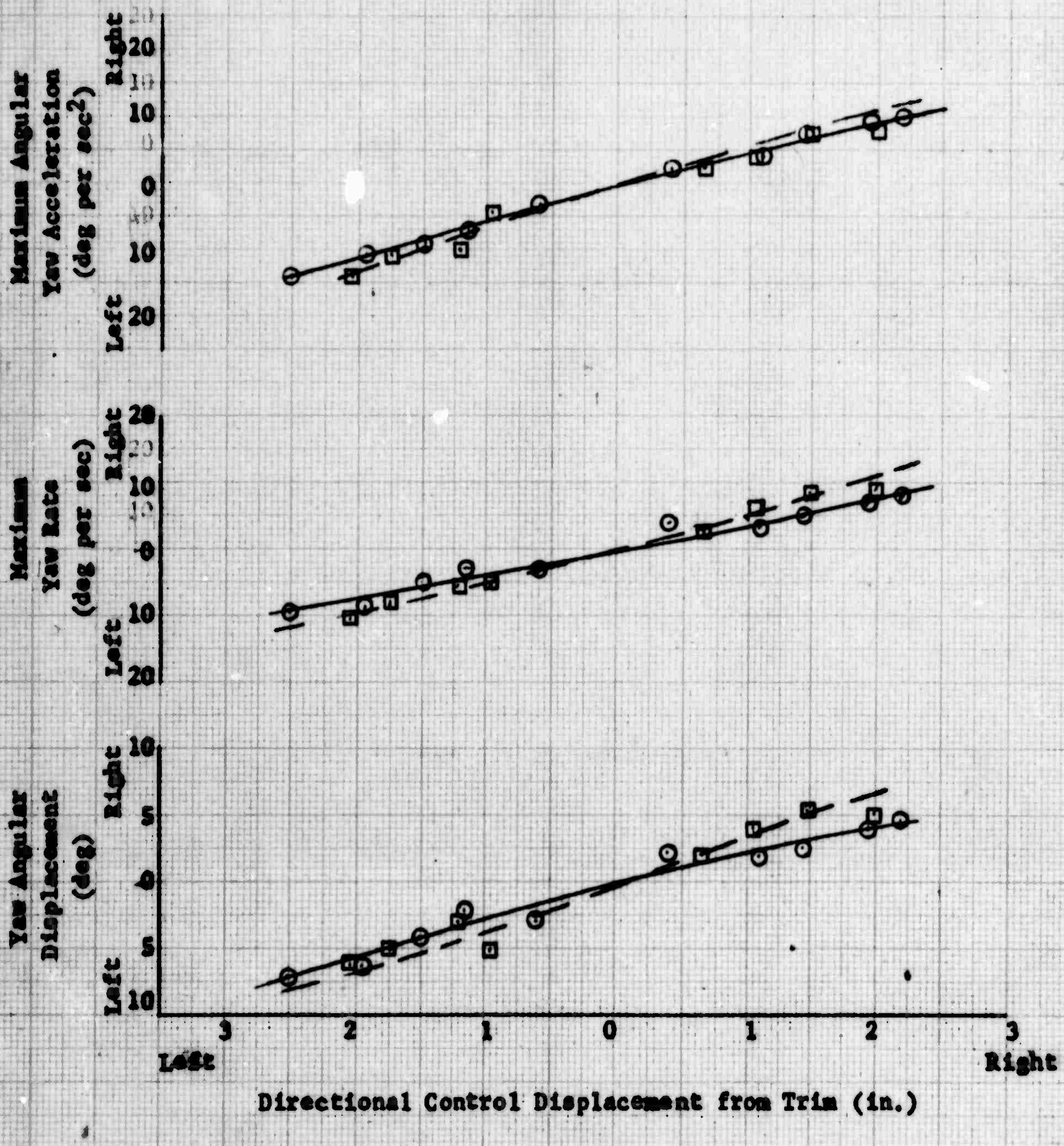

Figure [illegible] Directional Controllability

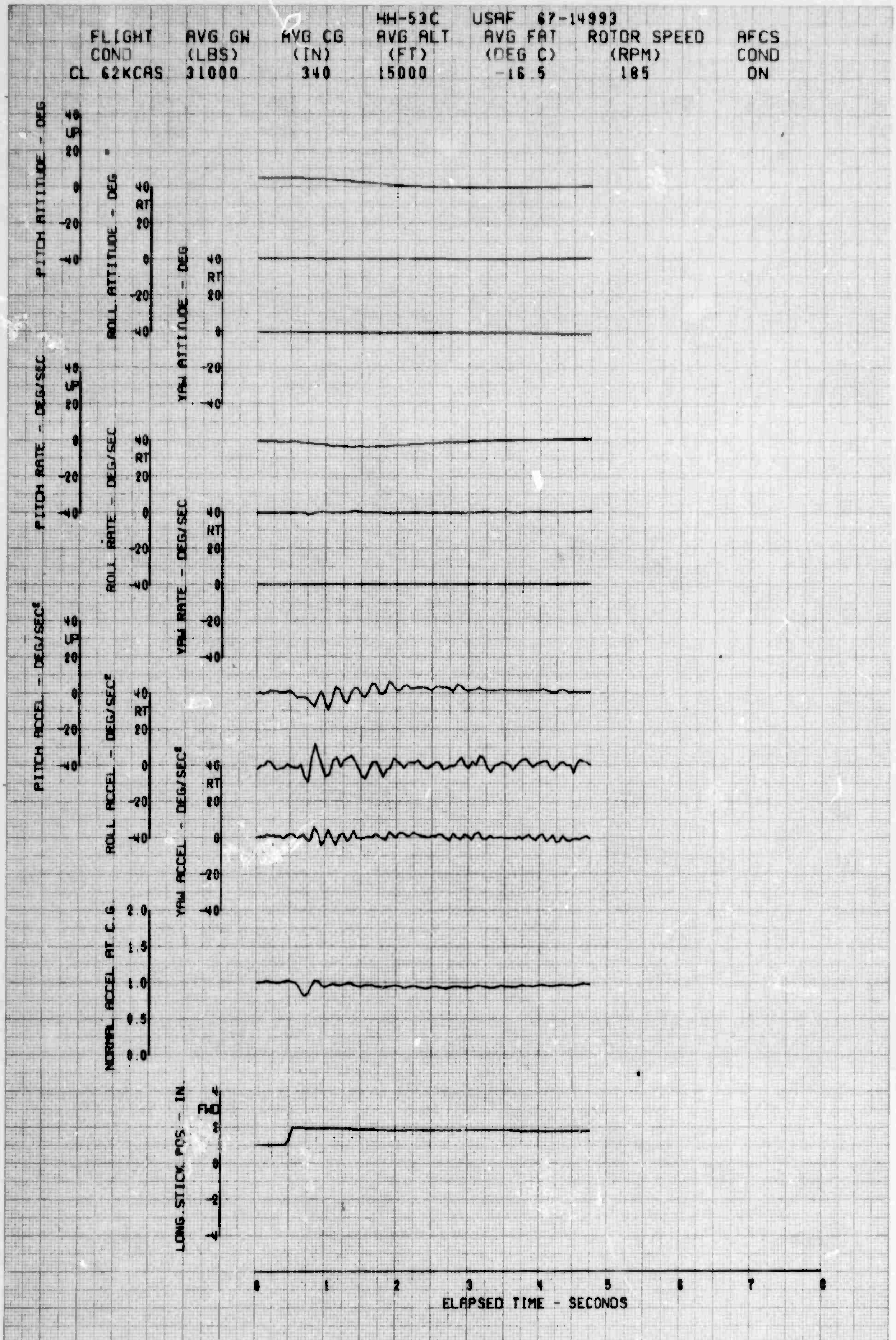

FIGURE 116. REACTION TO A FORWARD LONGITUDINAL STEP

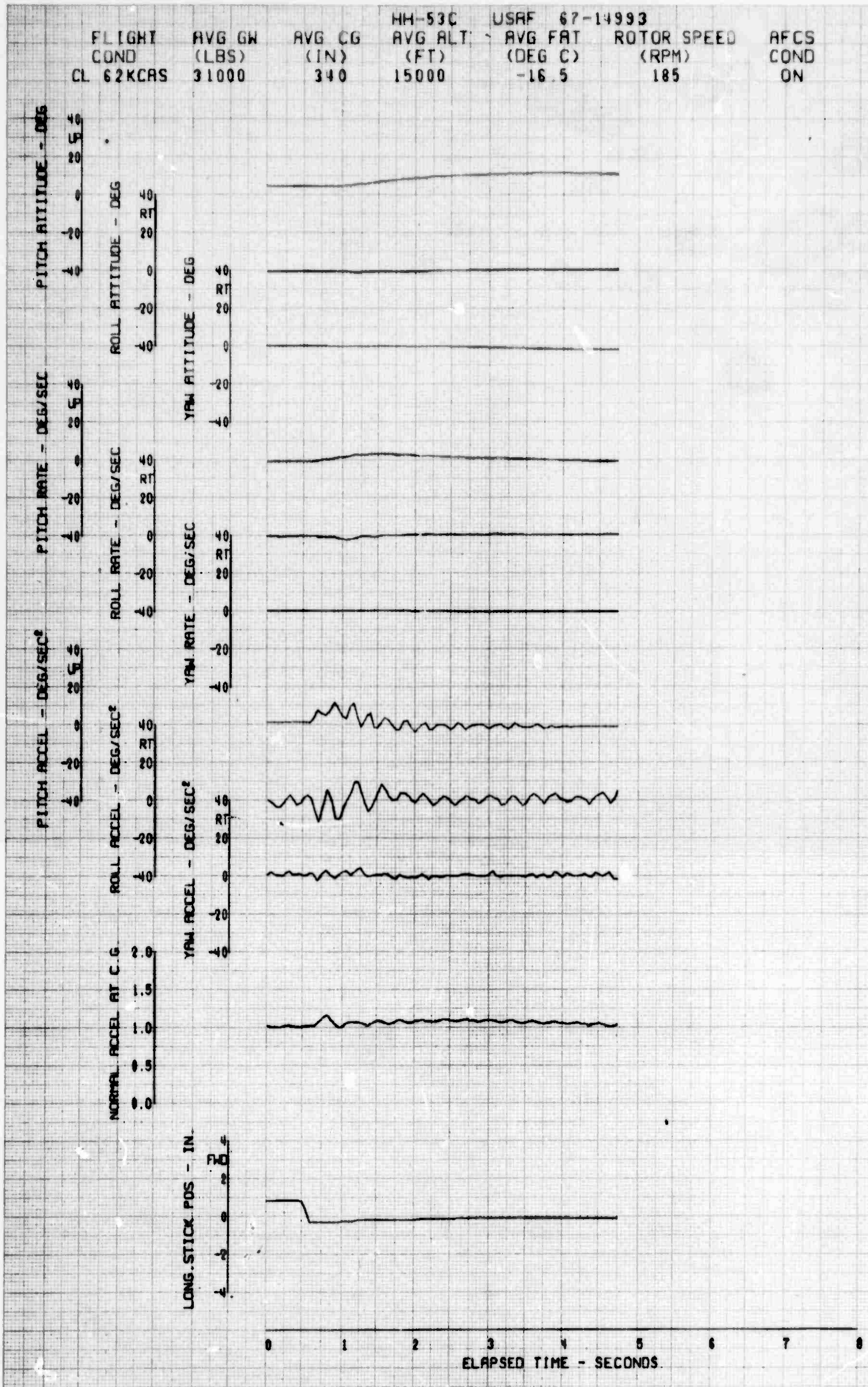

FIGURE 117. REACTION TO AN AFT LONGITUDINAL STEP

HH-53C USAF 67-14993

FLIGHT COND	AVG GW (LBS)	AVG CG (IN)	AVG ALT (FT)	AVG FAT (DEG C)	ROTOR SPEED (RPM)	AFCS COND
CL 62KCAS	31000	340	15000	-16.5	185	ON

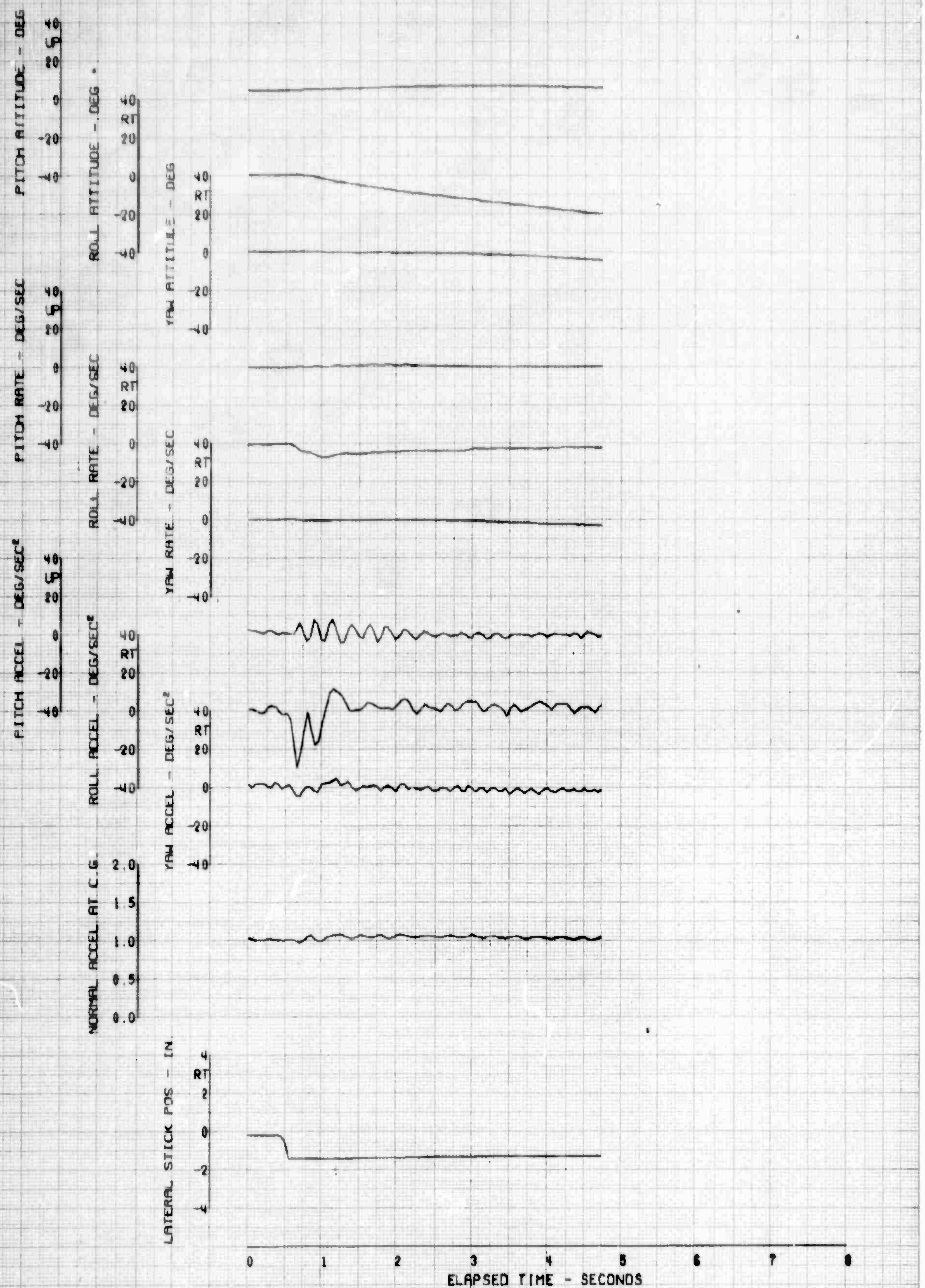

FIGURE 118. REACTION TO LEFT LATERAL STEP

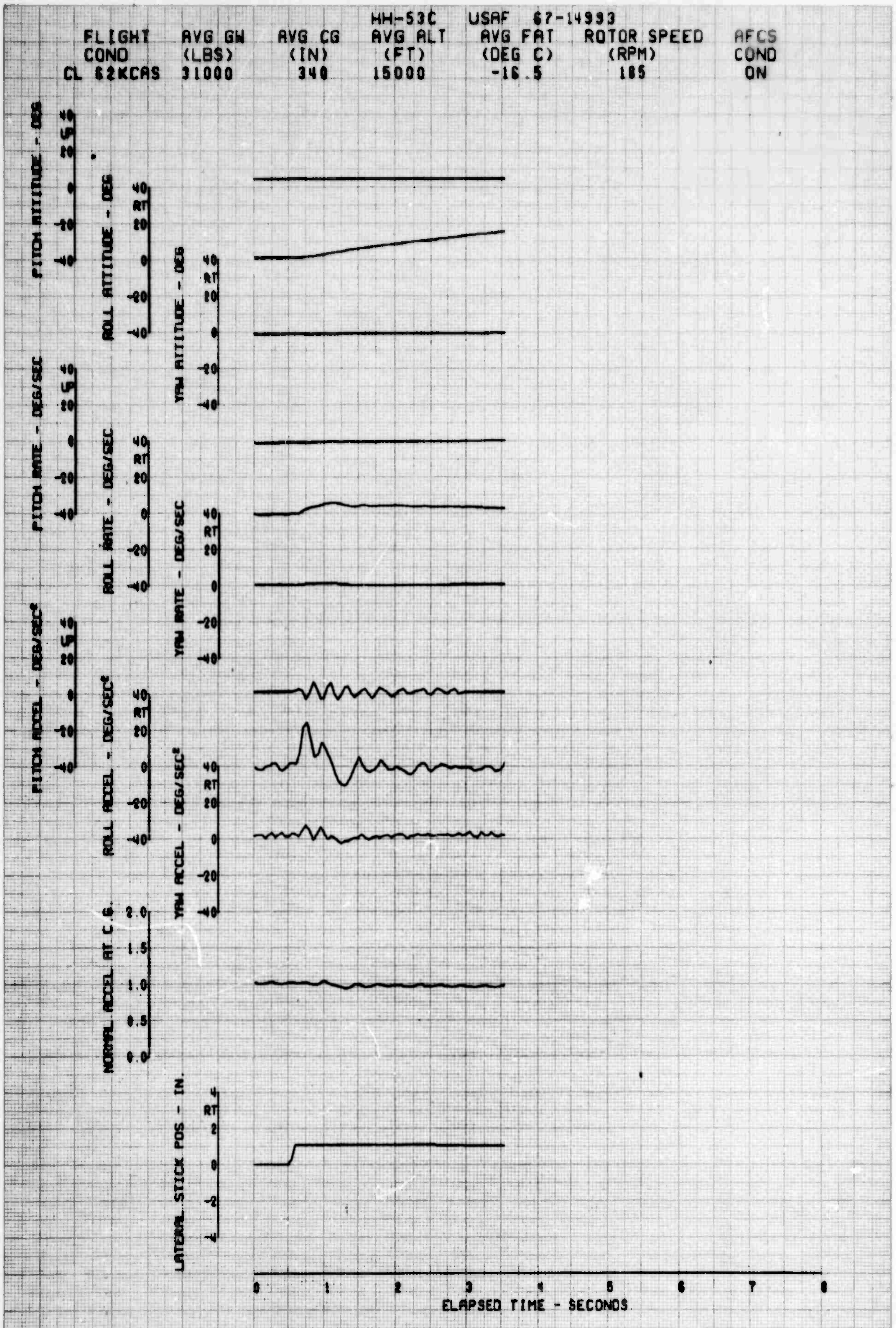

FIGURE 117 REACTION TO A RIGHT LATERAL STEP

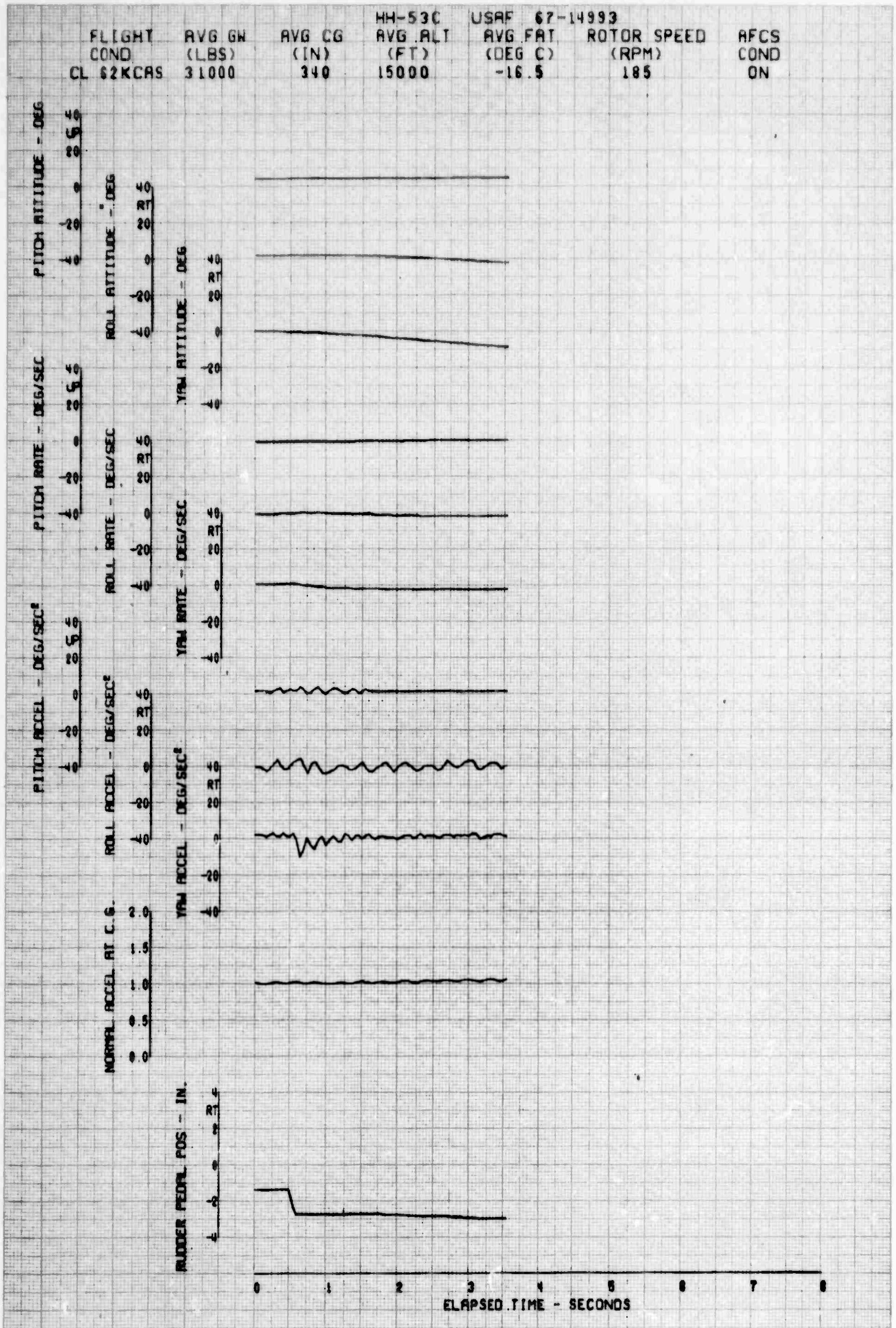

FIGURE 120. REACTION TO LEFT DIRECTIONAL STEP

HH-53C USAF 67-14993

FLIGHT COND	AVG GW (LBS)	AVG CG (IN)	AVG ALT (FT)	AVG FAT (DEG C)	ROTOR SPEED (RPM)	AFCS COND
CL 62KCAS	31000	340	15000	-16.5	185	ON

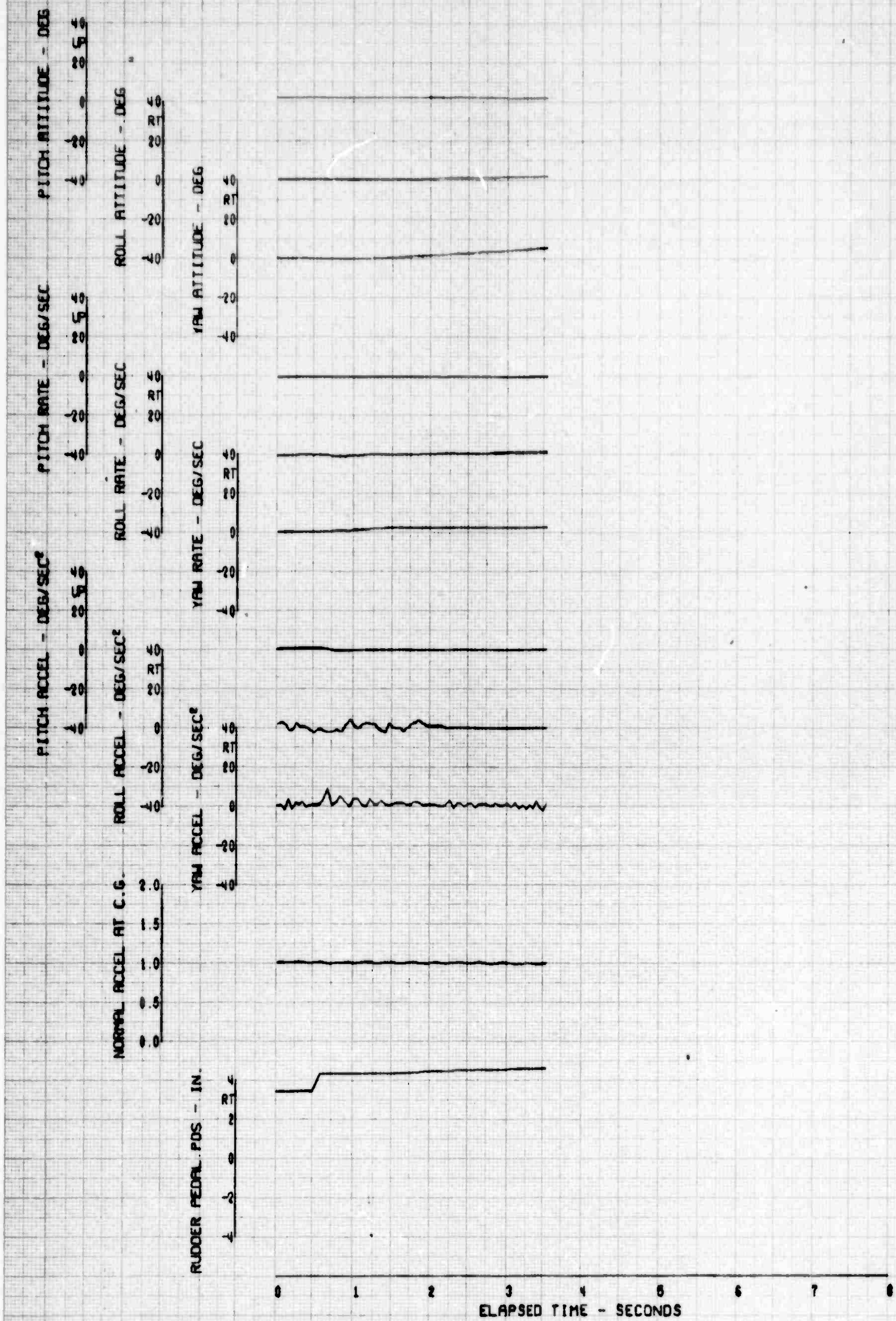

FIGURE 121. REACTION TO RIGHT DIRECTIONAL STEP

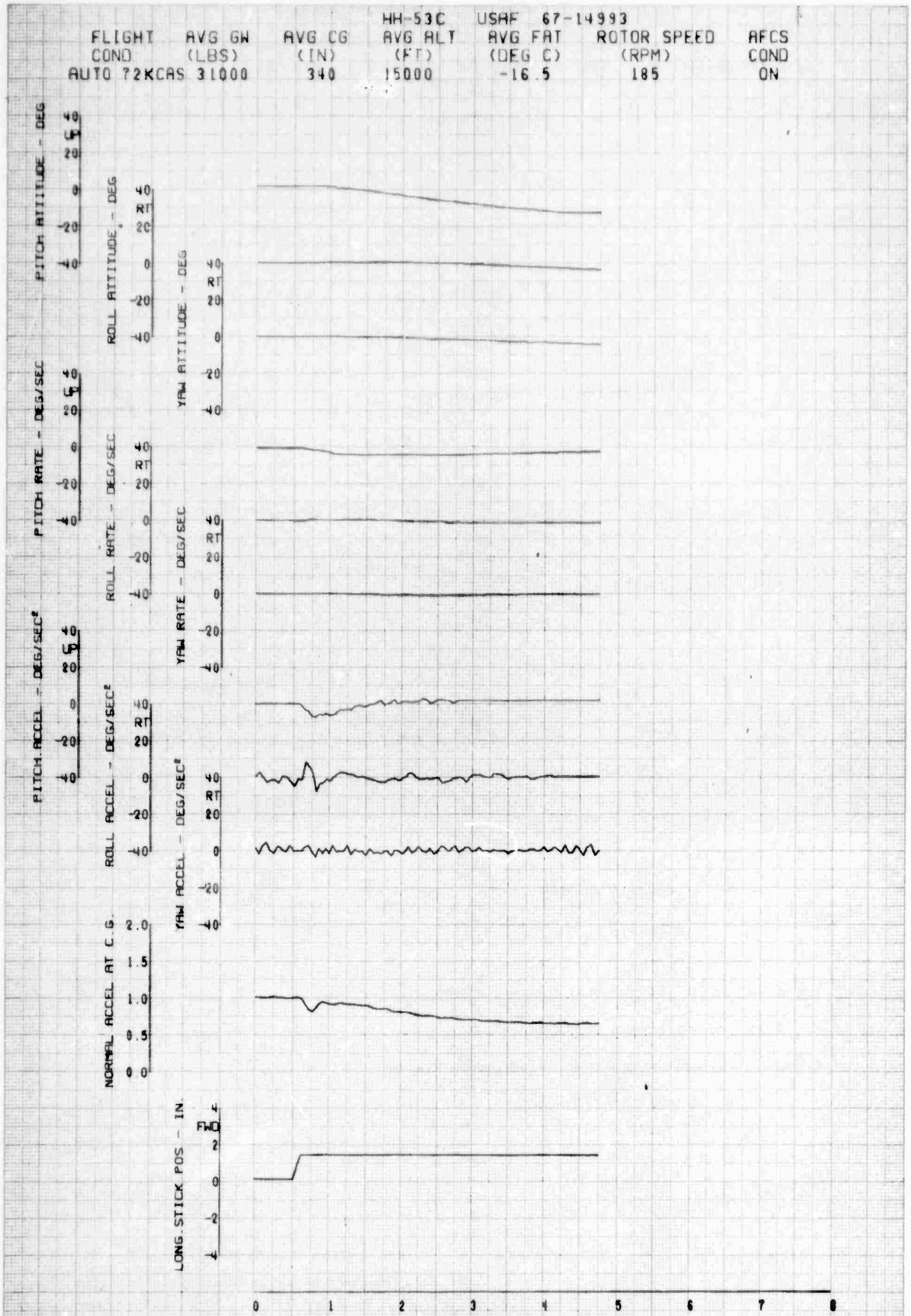

FIGURE 122. REACTION TO A FORWARD LONGITUDINAL STEP

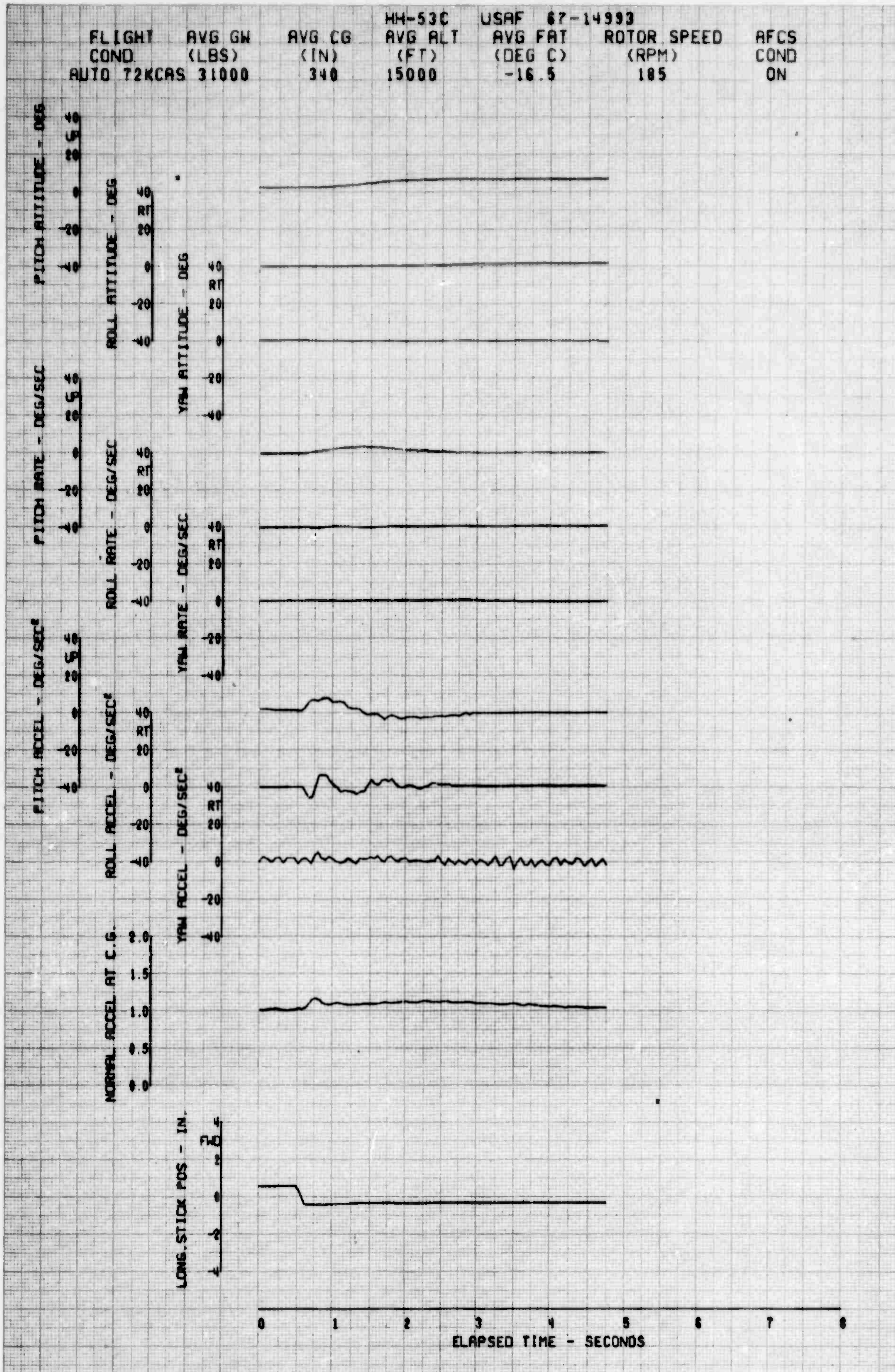

FIGURE 129. REACTION TO AN AFT LONGITUDINAL STEP

HH-53C USAF 67-14993

FLIGHT COND	AVG GW (LBS)	AVG CG (IN)	AVG ALT (FT)	AVG FAT (DEG C)	ROTOR SPEED (RPM)	AFCS COND
AUTO 72KCAS	31000	340	15000	-16.5	185	ON

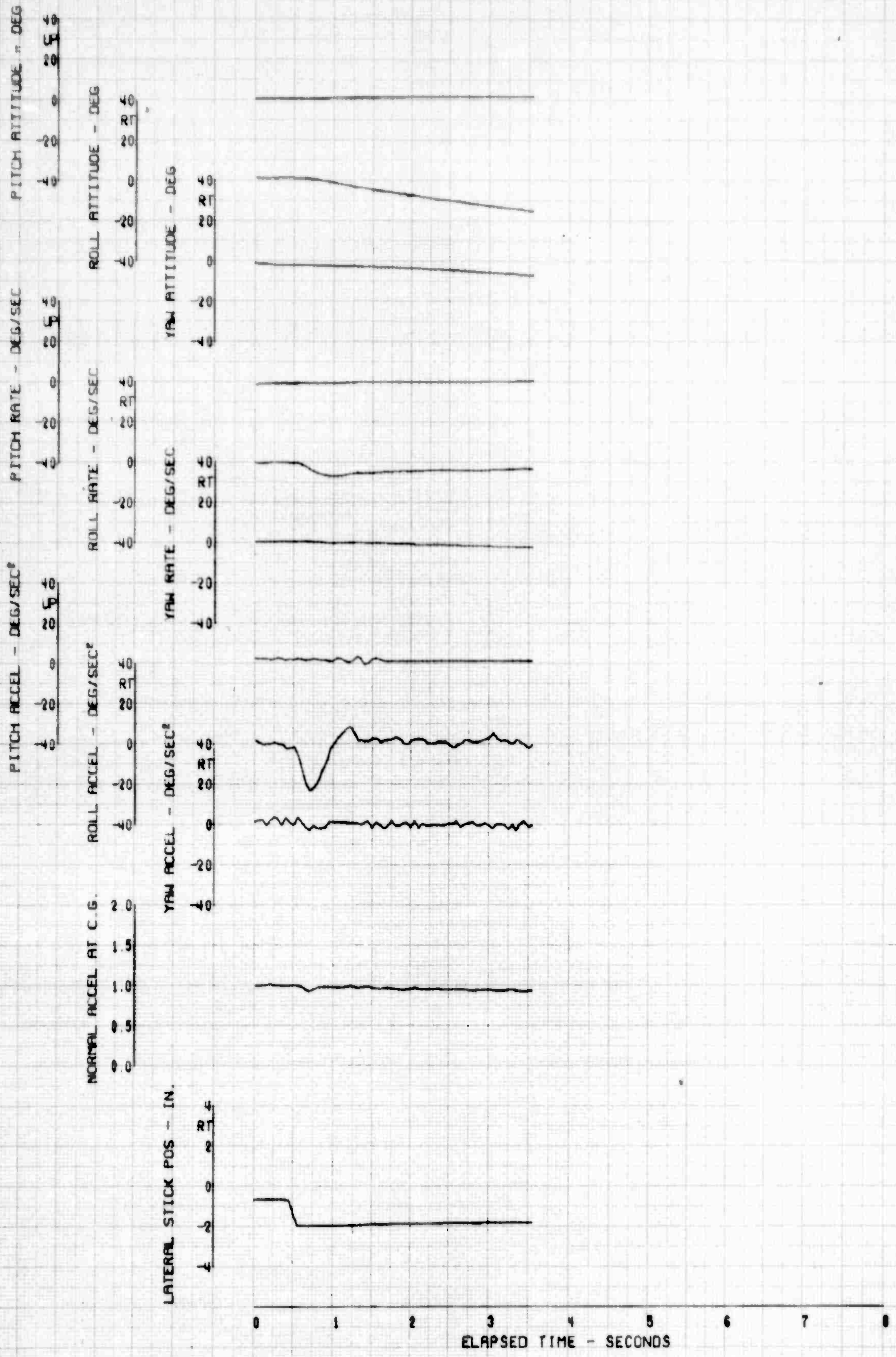

FIGURE 124 REACTION TO LEFT LATERAL STEP

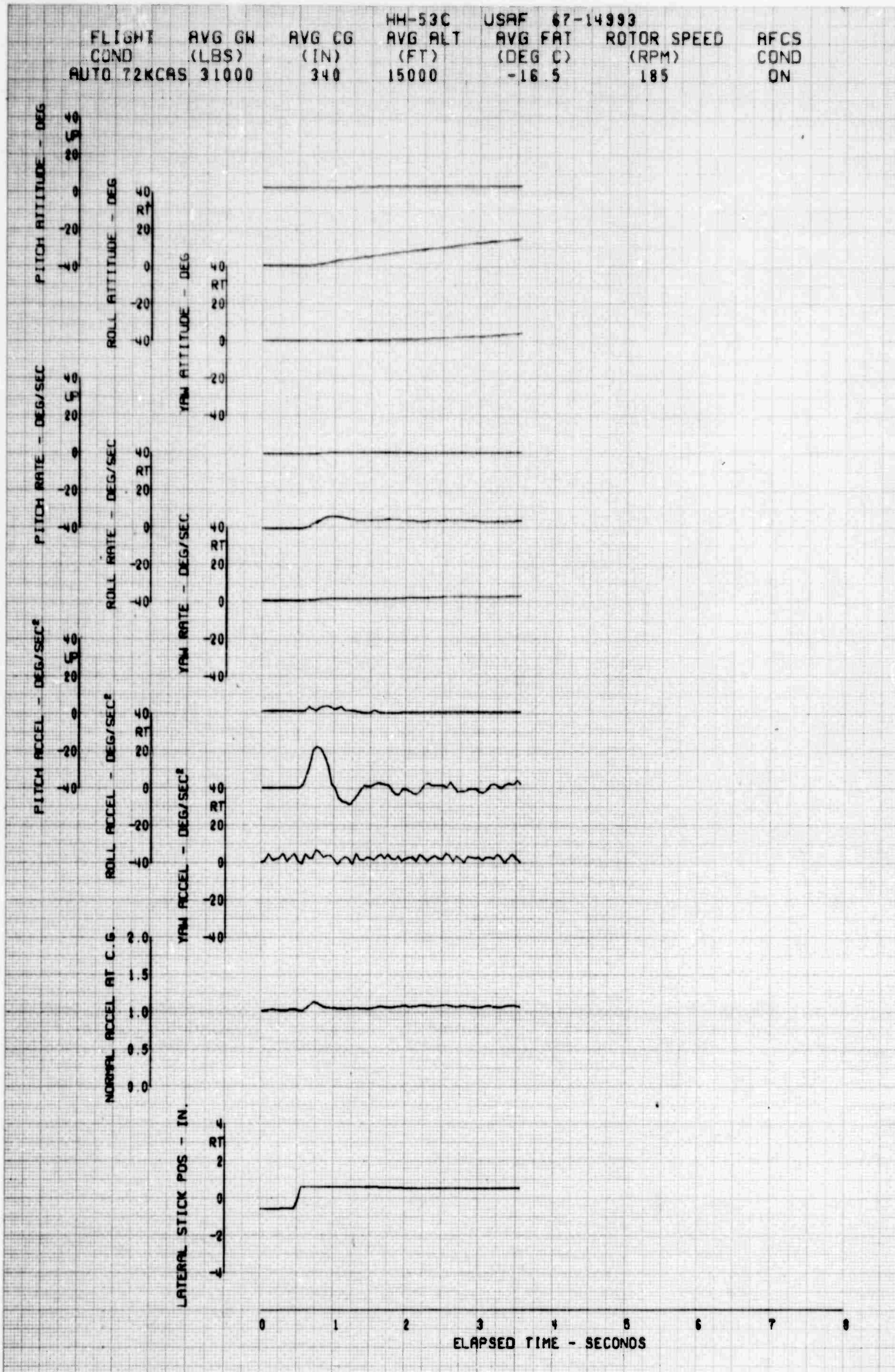

FIGURE 125. REACTION TO A RIGHT LATERAL STEP

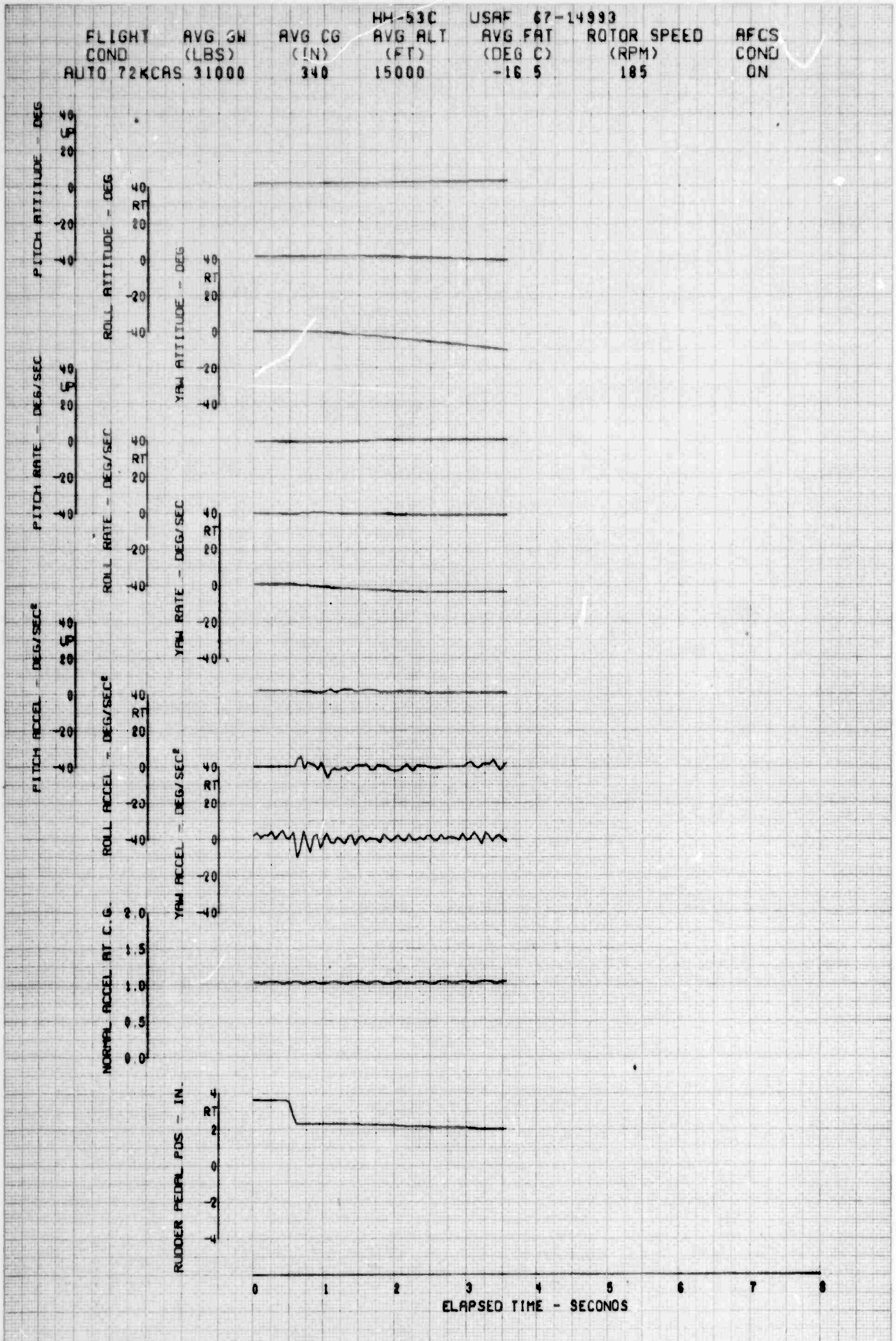

FIGURE 126. REACTION TO LEFT DIRECTIONAL STEP

HH-53C USAF 67-14993

FLIGHT COND	AVG GW (LBS)	AVG CG (IN)	AVG ALT (FT)	AVG FAT (DEG C)	ROTOR SPEED (RPM)	AFCS COND
AUTO 72KCAS	31000	340	15000	-16.5	185	ON

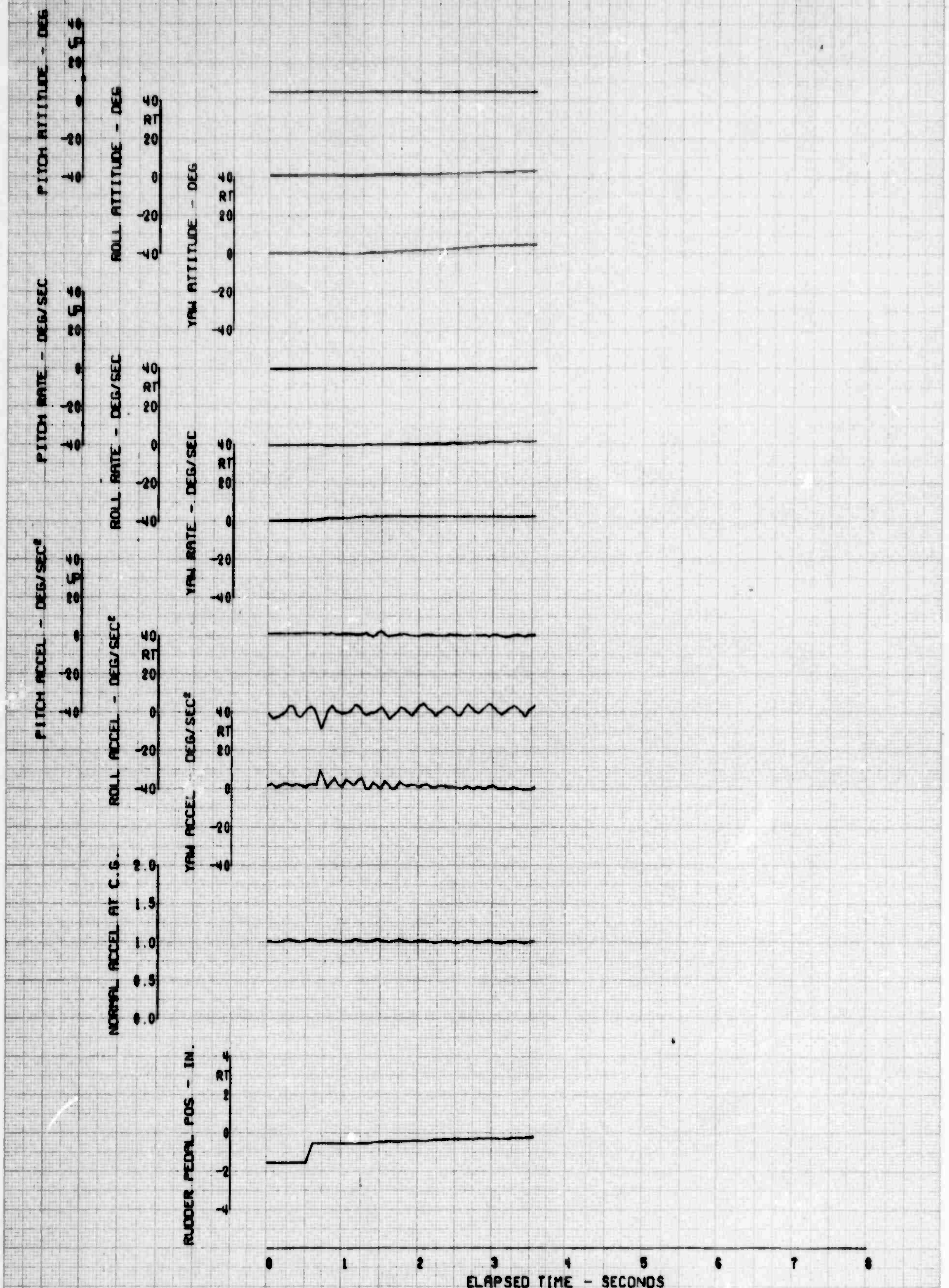

FIGURE 127 REACTION TO RIGHT DIRECTIONAL STEP

HH-53C USAF S/N 67-14993

Sym	Flight Condition	Avg GW (lb)	cg (in.)	Avg Press. Alt (ft)	Avg FAT (°C)	Rotor Speed (rpm)	AFCS	Trim A/S (kt)
○	Climb	31,000	340	15,000	-16.5	185	ON	62
□	Auto Rotation	31,000	340	15,000	-16.5	185	ON	72

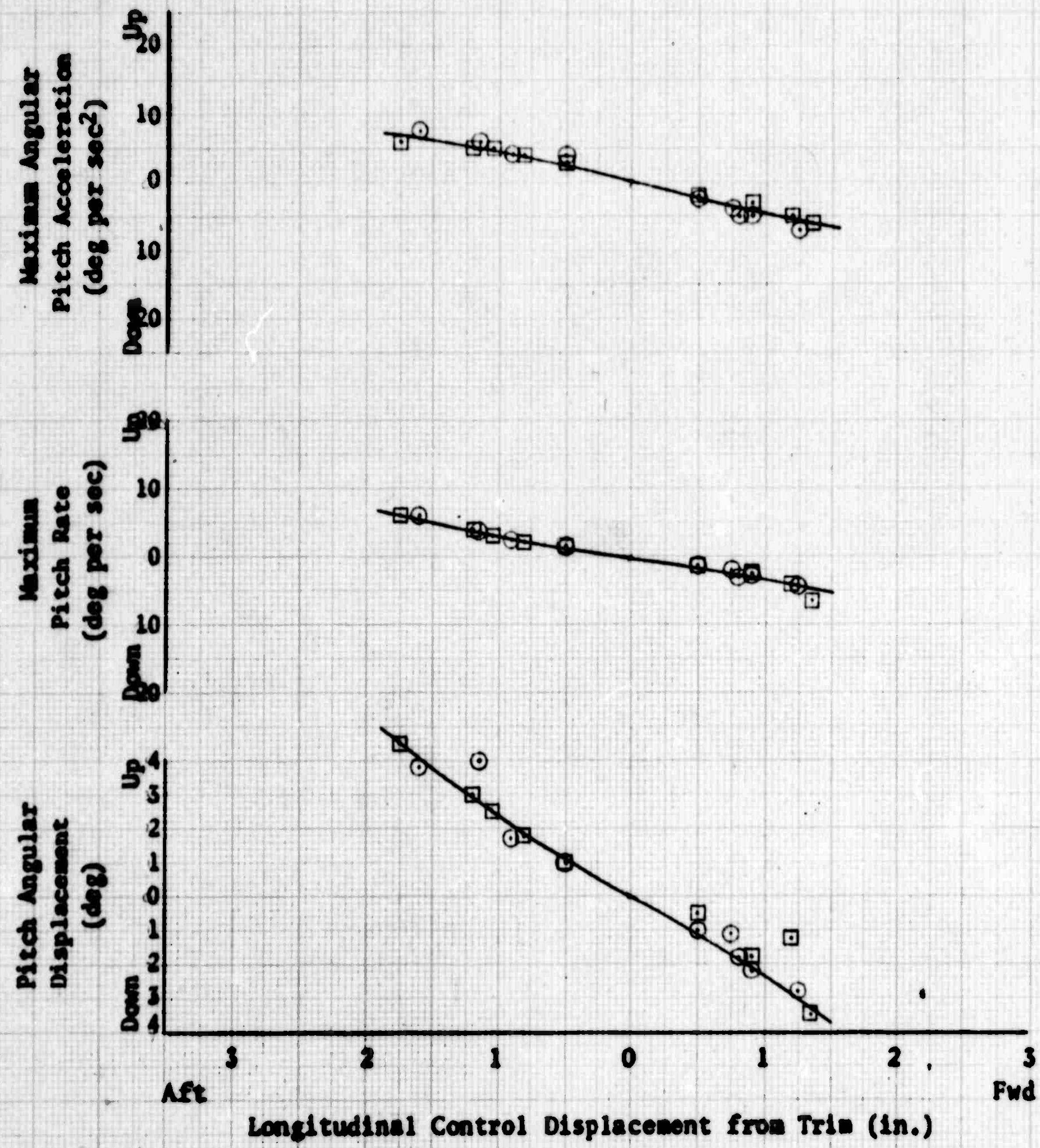

Figure 128 Longitudinal Controllability

HH-53C USAF S/N 67-14993

Sym	Flight Condition	Avg GW (lb)	cg (in.)	Avg Press. Alt (ft)	Avg FAT (°C)	Rotor Speed (rpm)	AFCS	Trim A/S (kt)
○	Climb	31,000	340	15,000	-16.5	185	ON	62
□	Auto Rotation	31,000	340	15,000	-16.5	185	ON	72

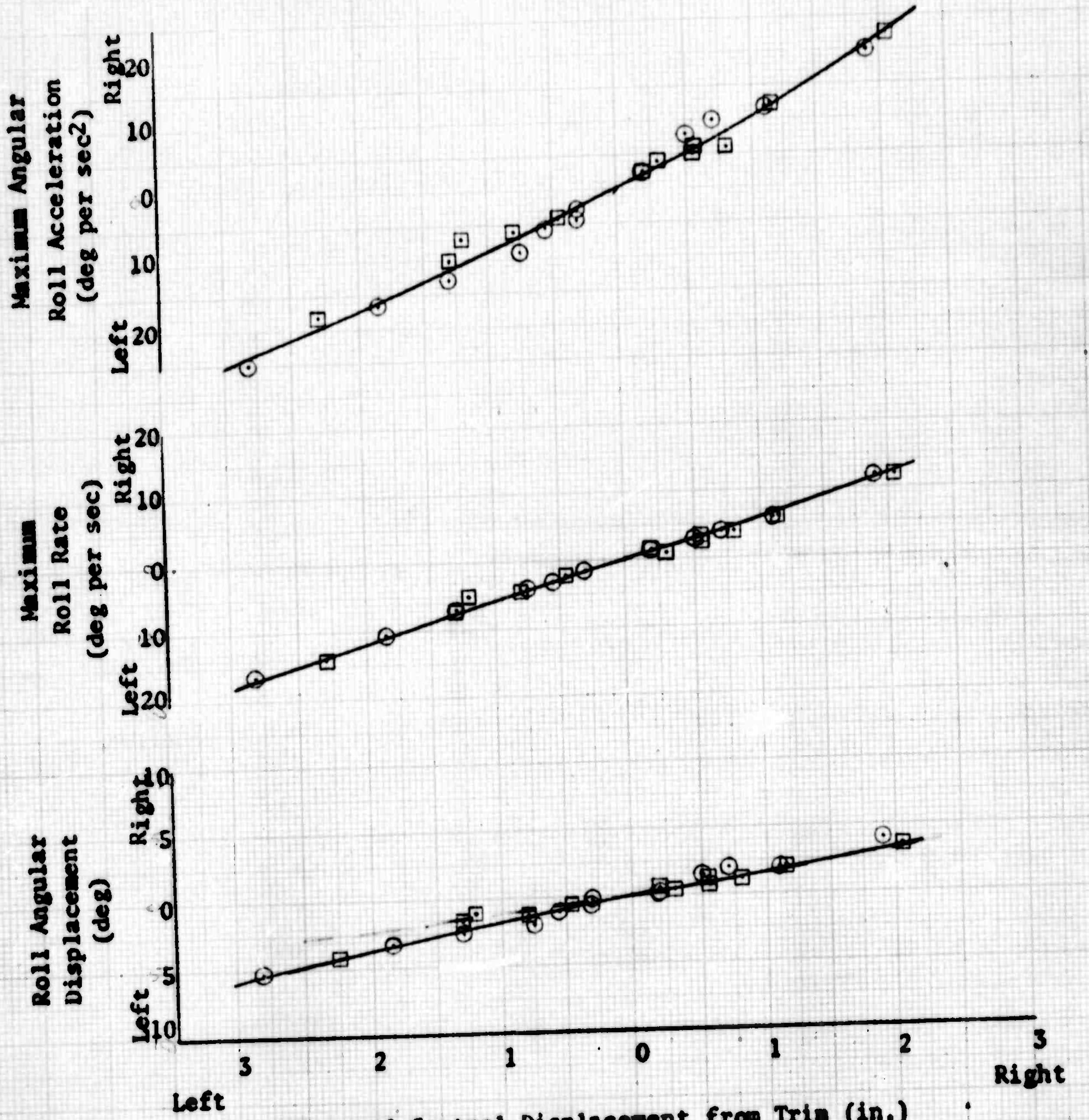

Figure 129. Lateral Controllability

HH-53C USAF S/N 67-14993

Sym	Flight Condition	Avg GW (lb)	cg (in.)	Avg Press. Alt (ft)	Avg FAT (°C)	Rotor Speed (rpm)	AFCS	Trim A/S (kt)
○	Climb	31,000	340	15,000	-16.5	185	ON	62
□	Auto Rotation	31,000	340	15,000	-16.5	185	ON	72

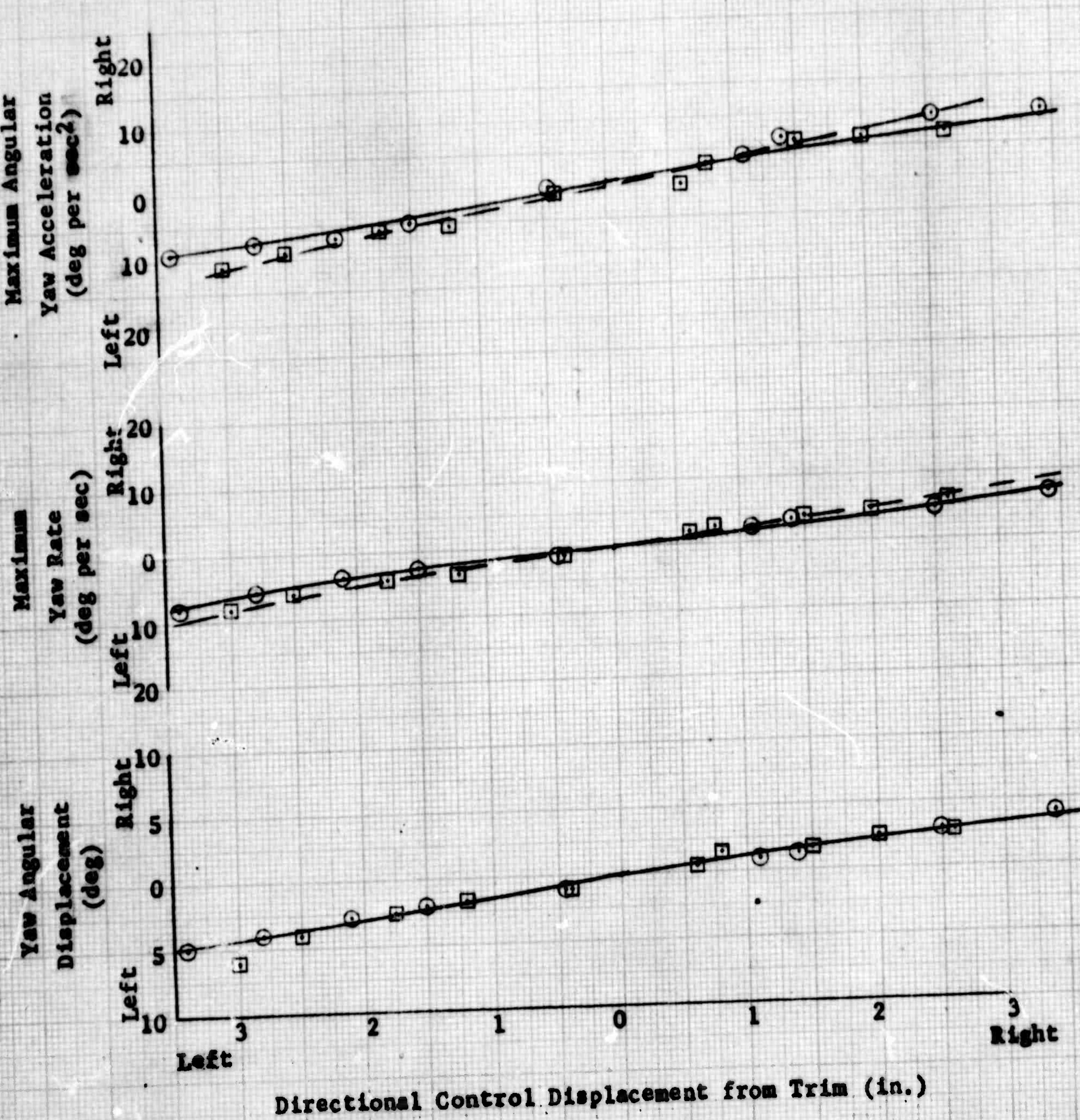

Figure 130. Directional Controllability

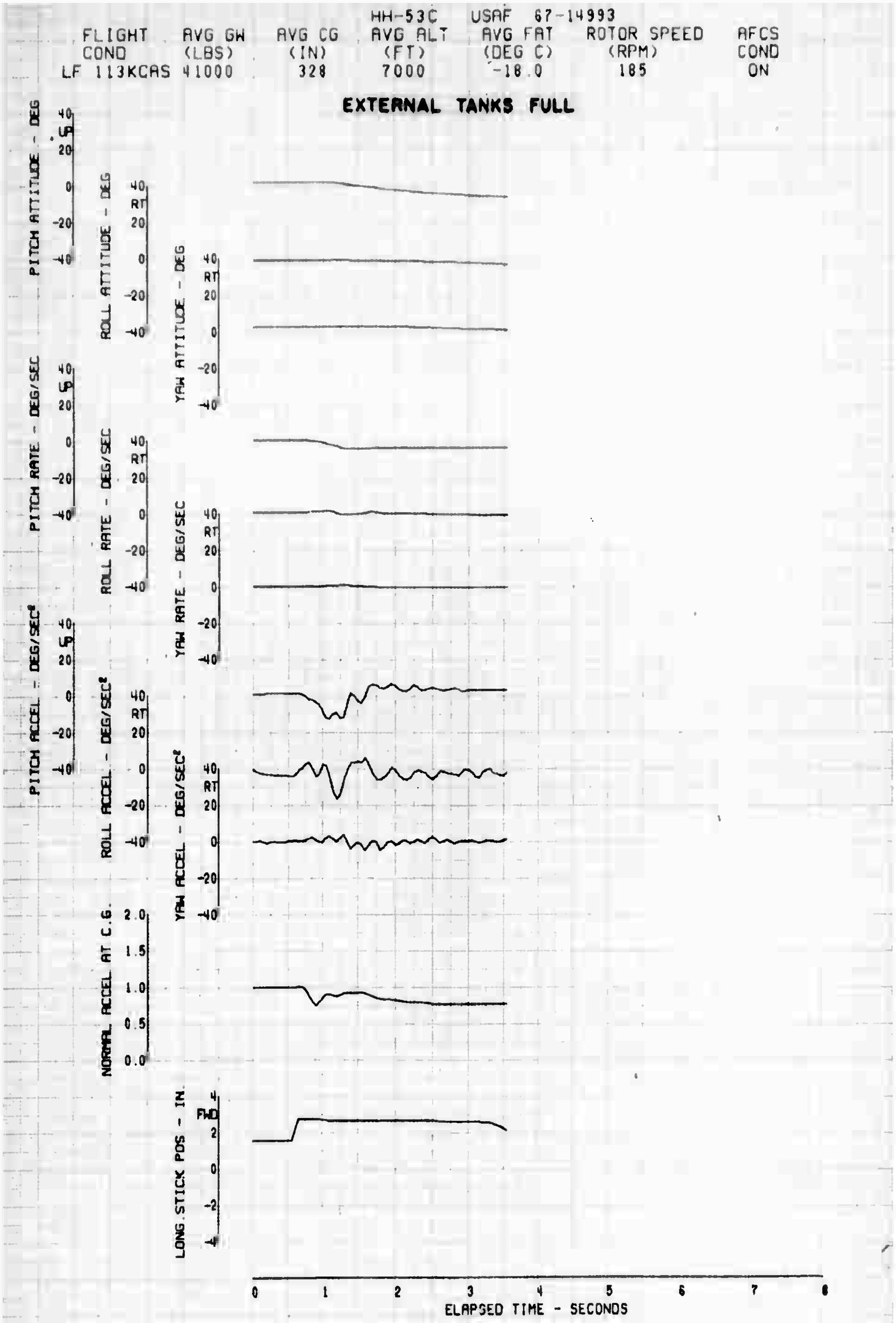

FIGURE 131. REACTION TO A FORWARD LONGITUDINAL STEP

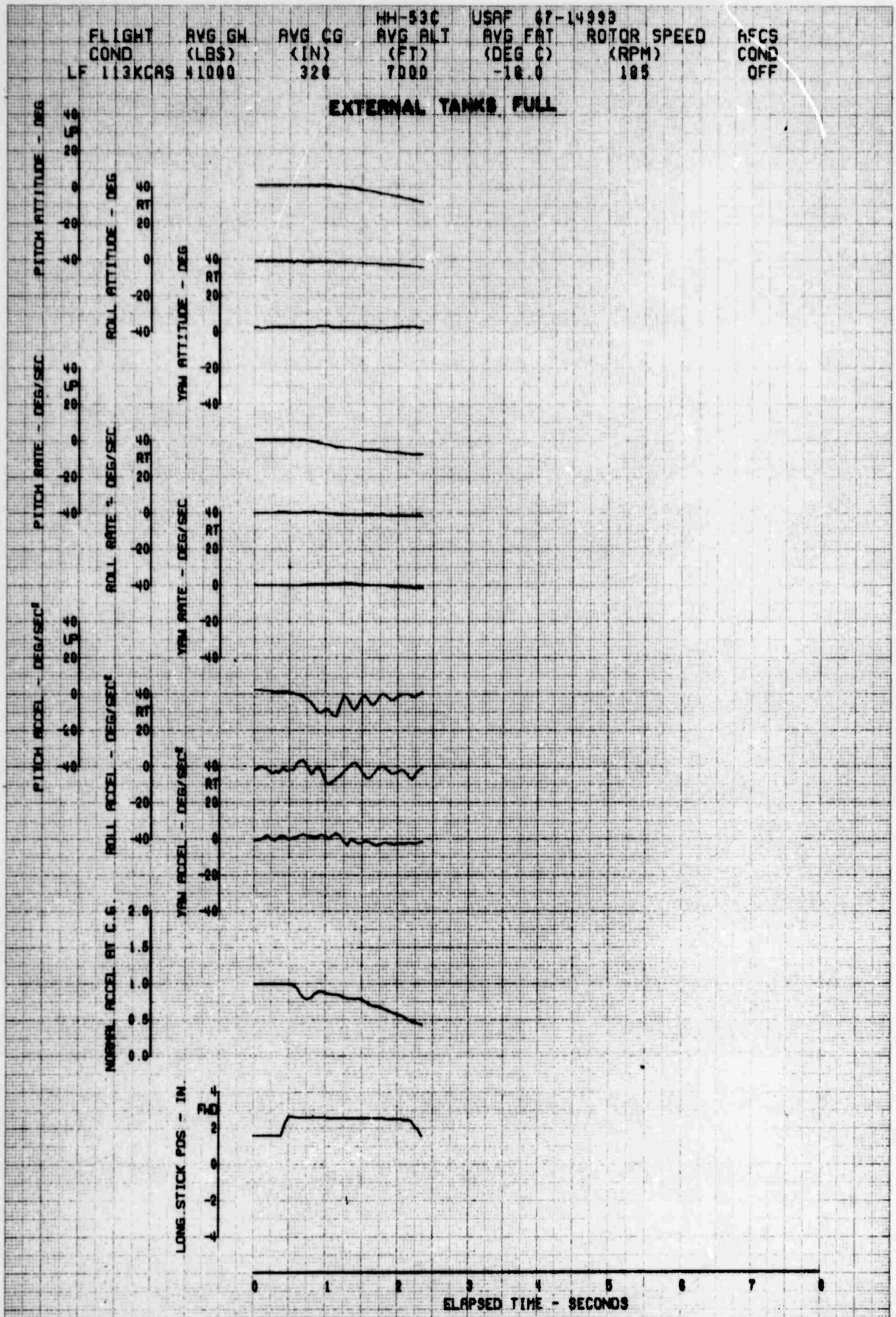

FIGURE 132. REACTION TO A FORWARD LONGITUDINAL STEP

			HH-53C	USAF 67-14993		
FLIGHT COND	AVG GW (LBS)	AVG CG (IN)	AVG ALT (FT)	AVG FAT (DEG C)	ROTOR SPEED (RPM)	AFCS COND
LF 113KCAS	41000	328	7000	-18.0	185	ON

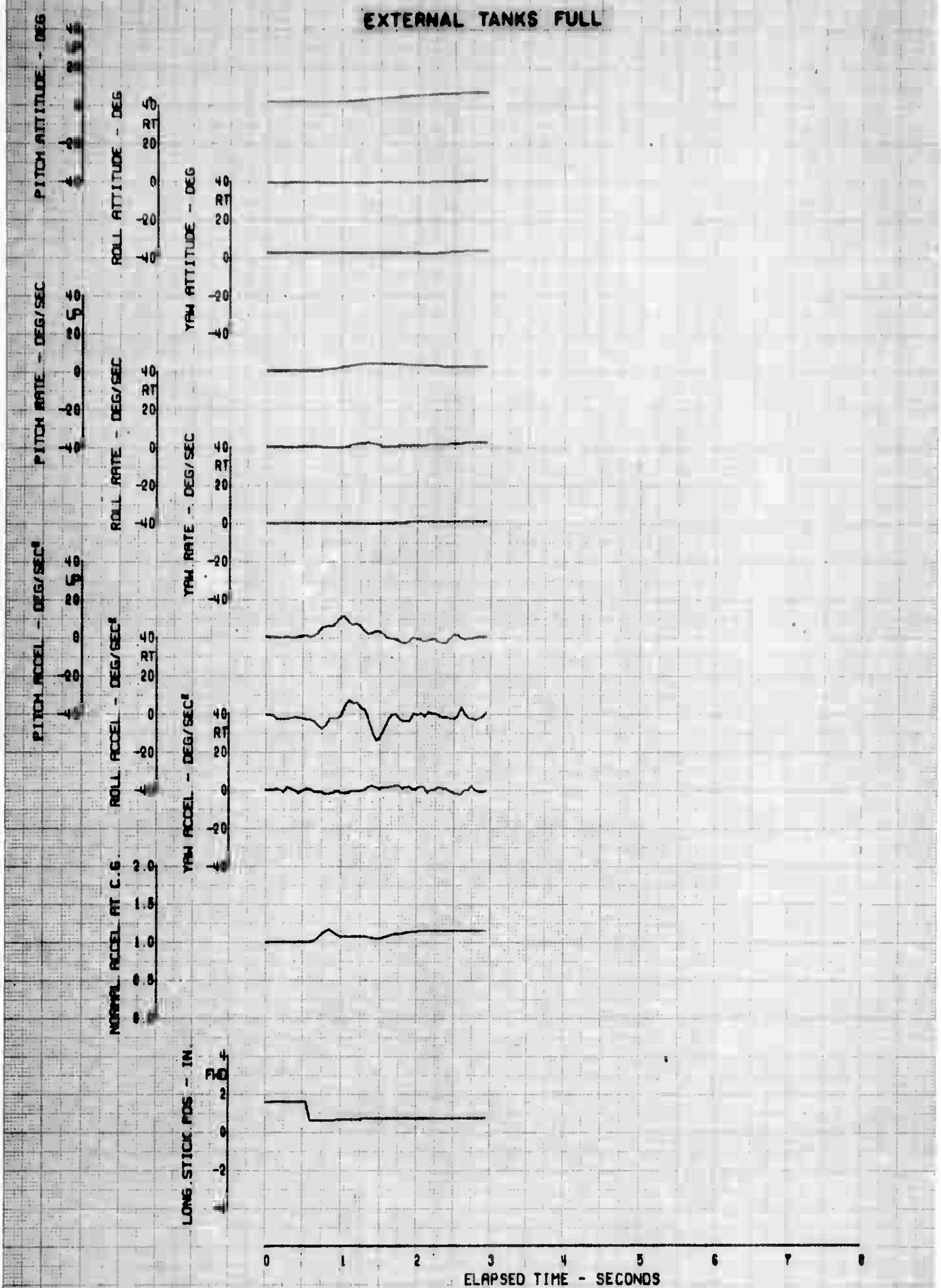

FIGURE 133. REACTION TO AN AFT LONGITUDINAL STEP

HH-53C USAF 67-14993

FLIGHT COND	AVG GW (LBS)	AVG CG (IN)	AVG ALT (FT)	AVG FAT (DEG C)	ROTOR SPEED (RPM)	AFCS COND
LF 113KCAS	41000	328	7000	-18.0	185	OFF

EXTERNAL TANKS FULL

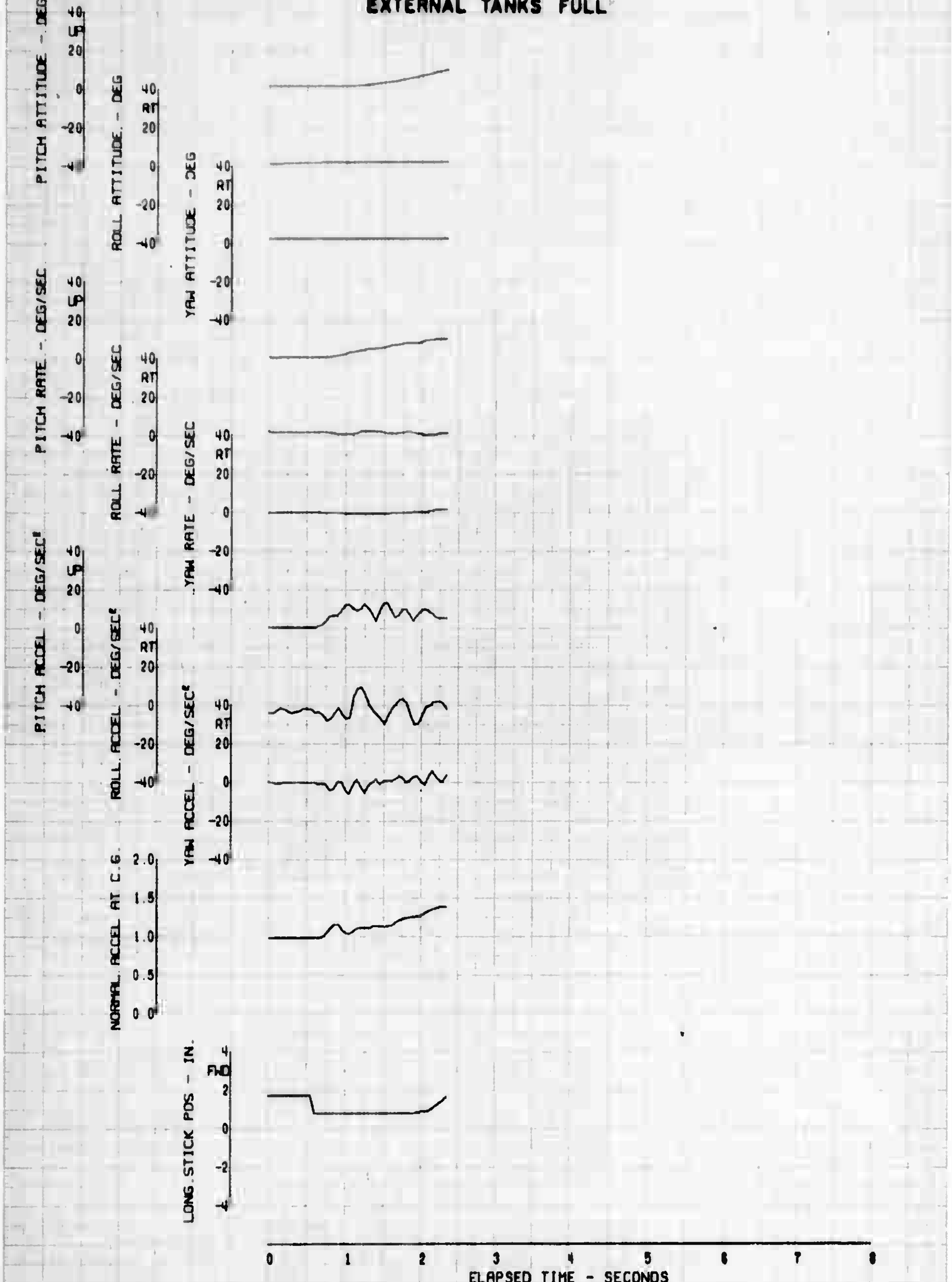

FIGURE 134. REACTION TO AN AFT LONGITUDINAL STEP

HH-53C USAF 67-14993

FLIGHT COND	AVG GW (LBS)	AVG CG (IN)	AVG ALT (FT)	AVG FAT (DEG C)	ROTOR SPEED (RPM)	AFCS COND
LF 113KCAS	41000	328	7000	-18.0	185	ON

EXTERNAL TANKS FULL

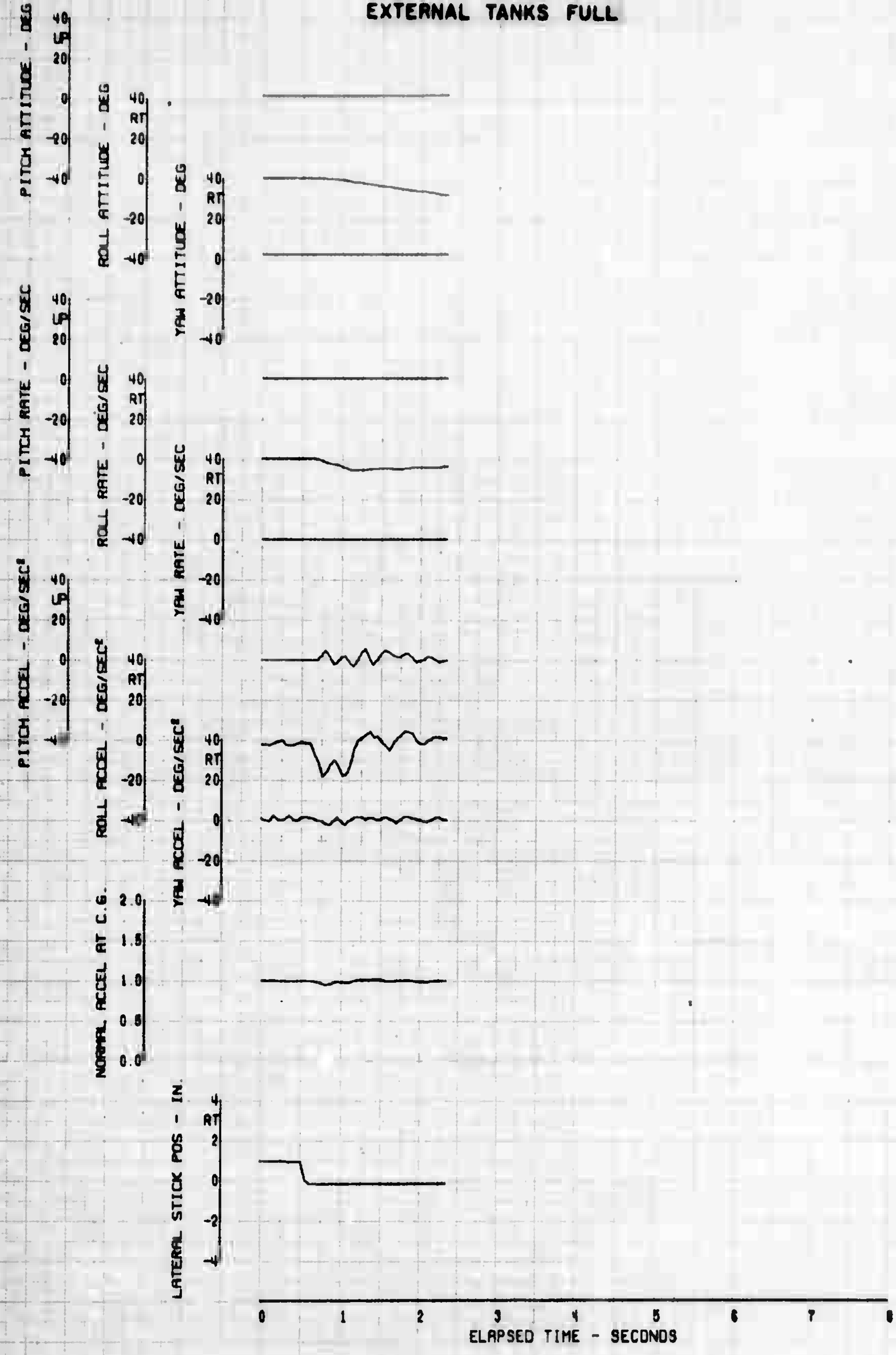

FIGURE 135 REACTION TO A LEFT LATERAL STEP

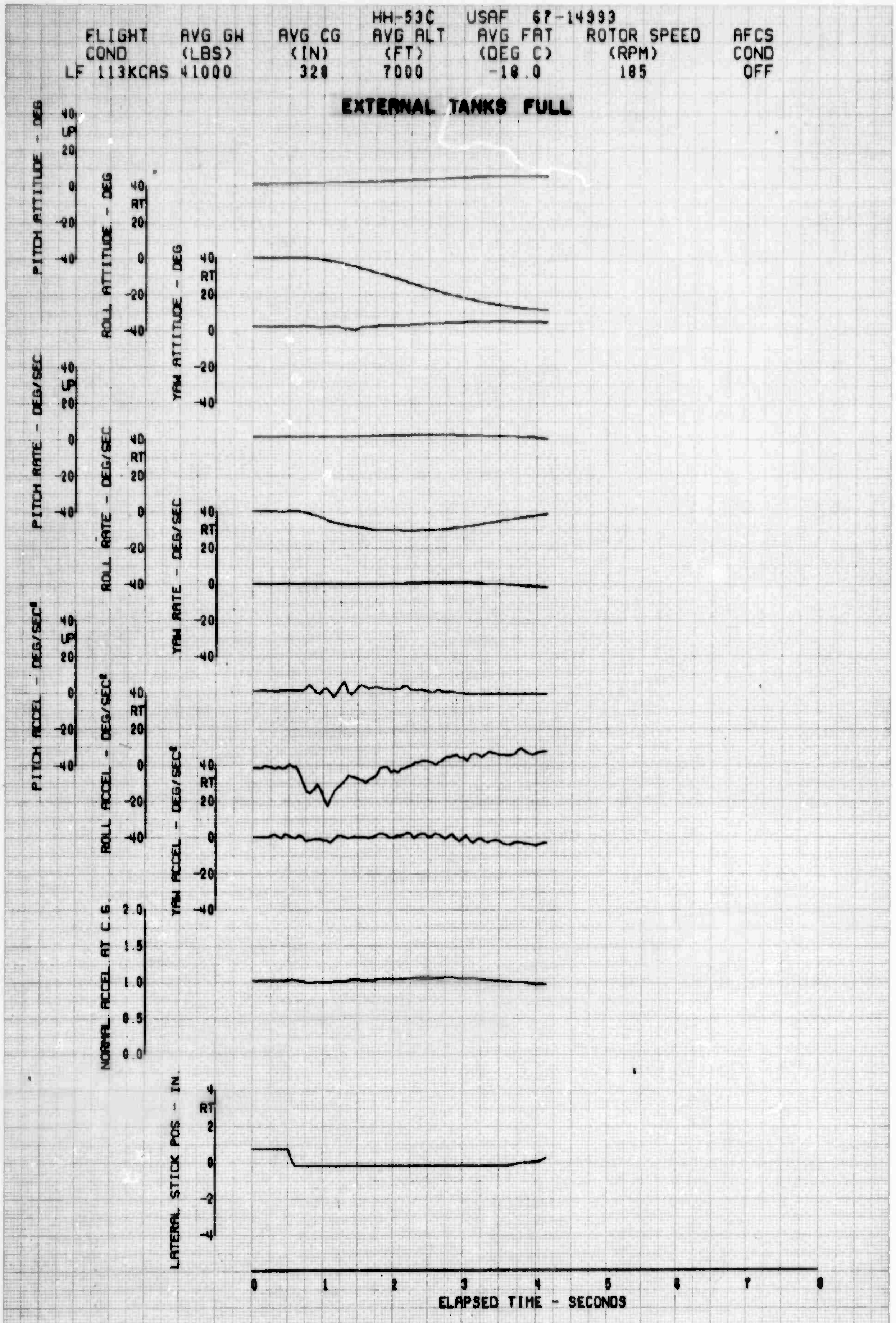

FIGURE 136. REACTION TO A LEFT LATERAL STEP

HH-53C USAF 67-14993

FLIGHT COND	AVG GW (LBS)	AVG CG (IN)	AVG ALT (FT)	AVG FAT (DEG C)	ROTOR SPEED (RPM)	AFCS COND
LF 113KCAS	41000	328	7000	-18.0	185	ON

EXTERNAL TANKS FULL

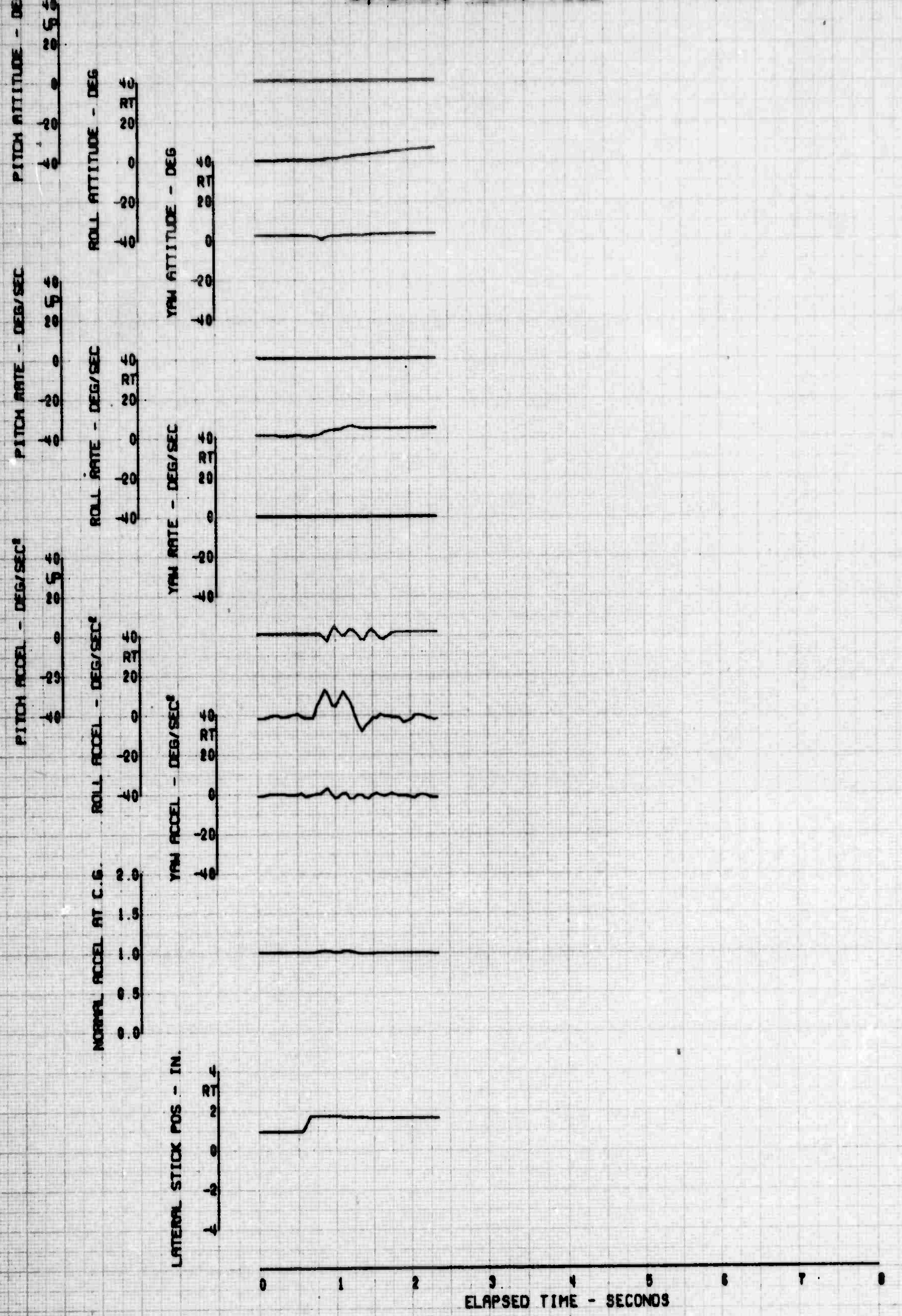

FIGURE 137 REACTION TO A RIGHT LATERAL STEP

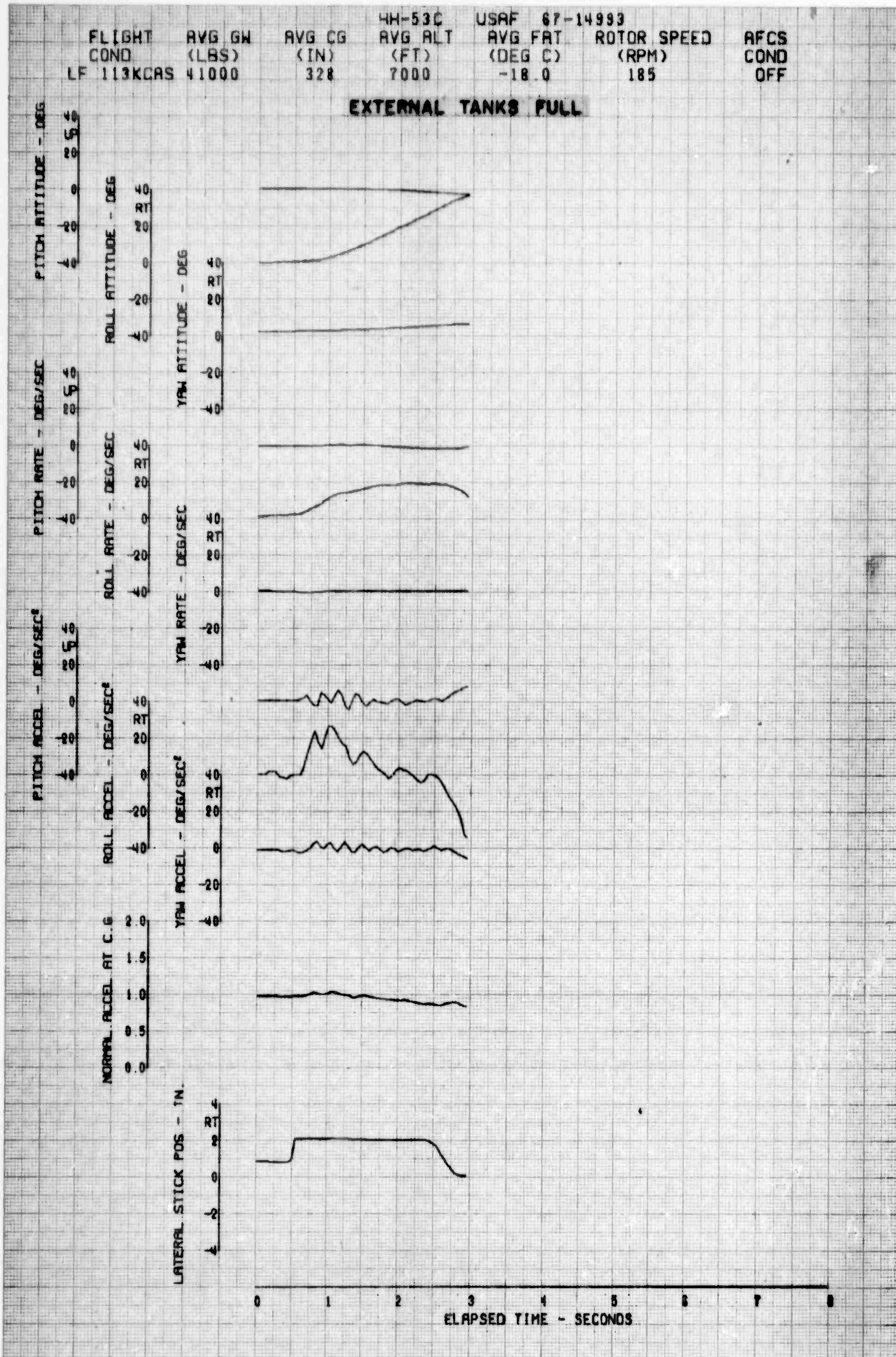

FIGURE 130 REACTION TO A RIGHT LATERAL STEP

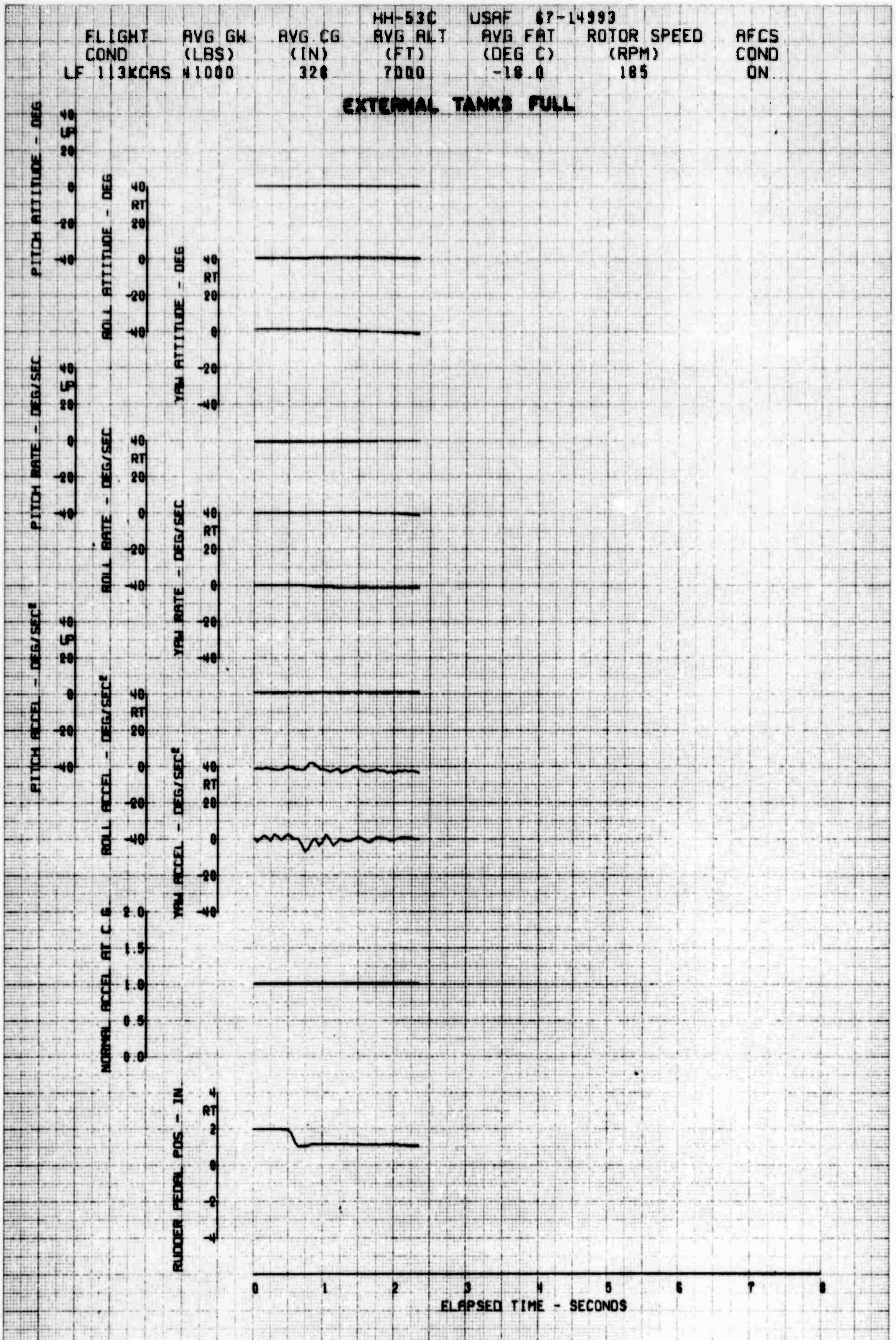

FIGURE 139 REACTION TO A LEFT DIRECTIONAL STEP

HH-53C USAF 67-14993

FLIGHT COND	AVG GW (LBS)	AVG CG (IN)	AVG ALT (FT)	AVG FAT (DEG C)	ROTOR SPEED (RPM)	AFCS COND
LF 113KCAS	41000	328	7000	-18.0	185	ON

EXTERNAL TANKS FULL

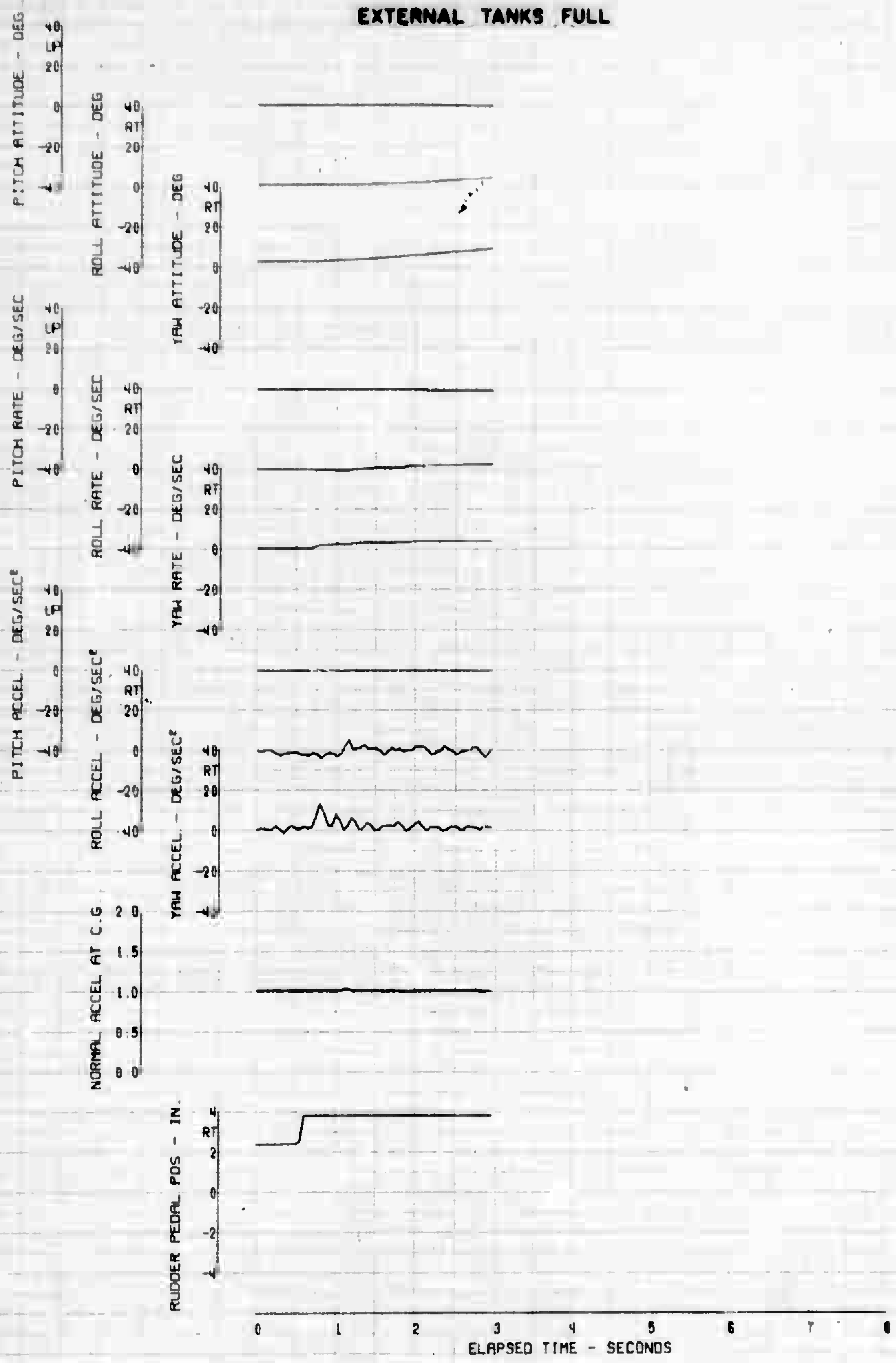

FIGURE 140. REACTION TO A RIGHT DIRECTIONAL STEP

HH-53C USAF 67-14993

FLIGHT COND	AVG GW (LBS)	AVG CG (IN)	AVG ALT (FT)	AVG FAT (DEG C)	ROTOR SPEED (RPM)	AFCS COND
LF 113KCAS	41000	328	7000	-18.0	185	OFF

EXTERNAL TANKS FULL

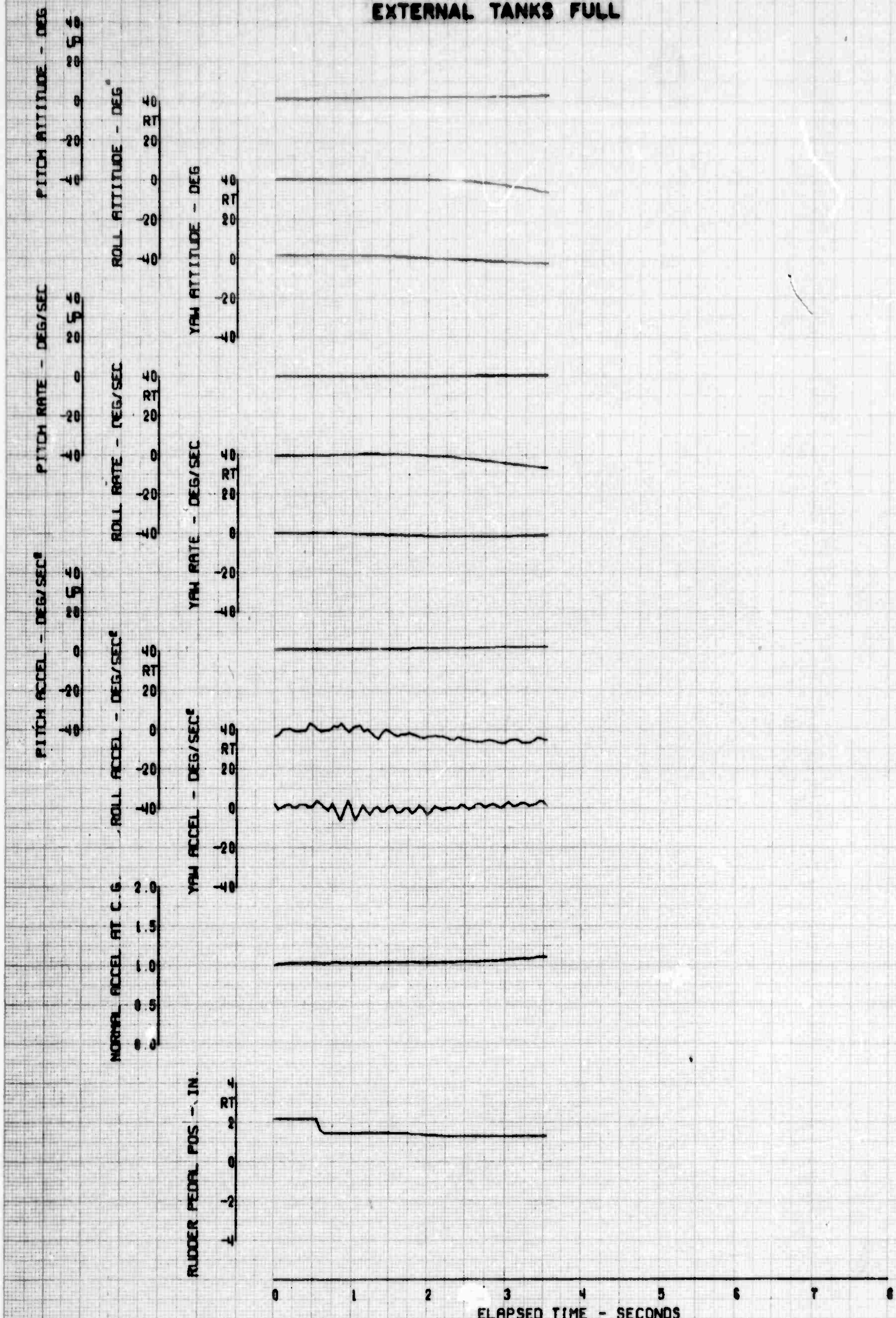

FIGURE 141 REACTION TO A LEFT DIRECTIONAL STEP

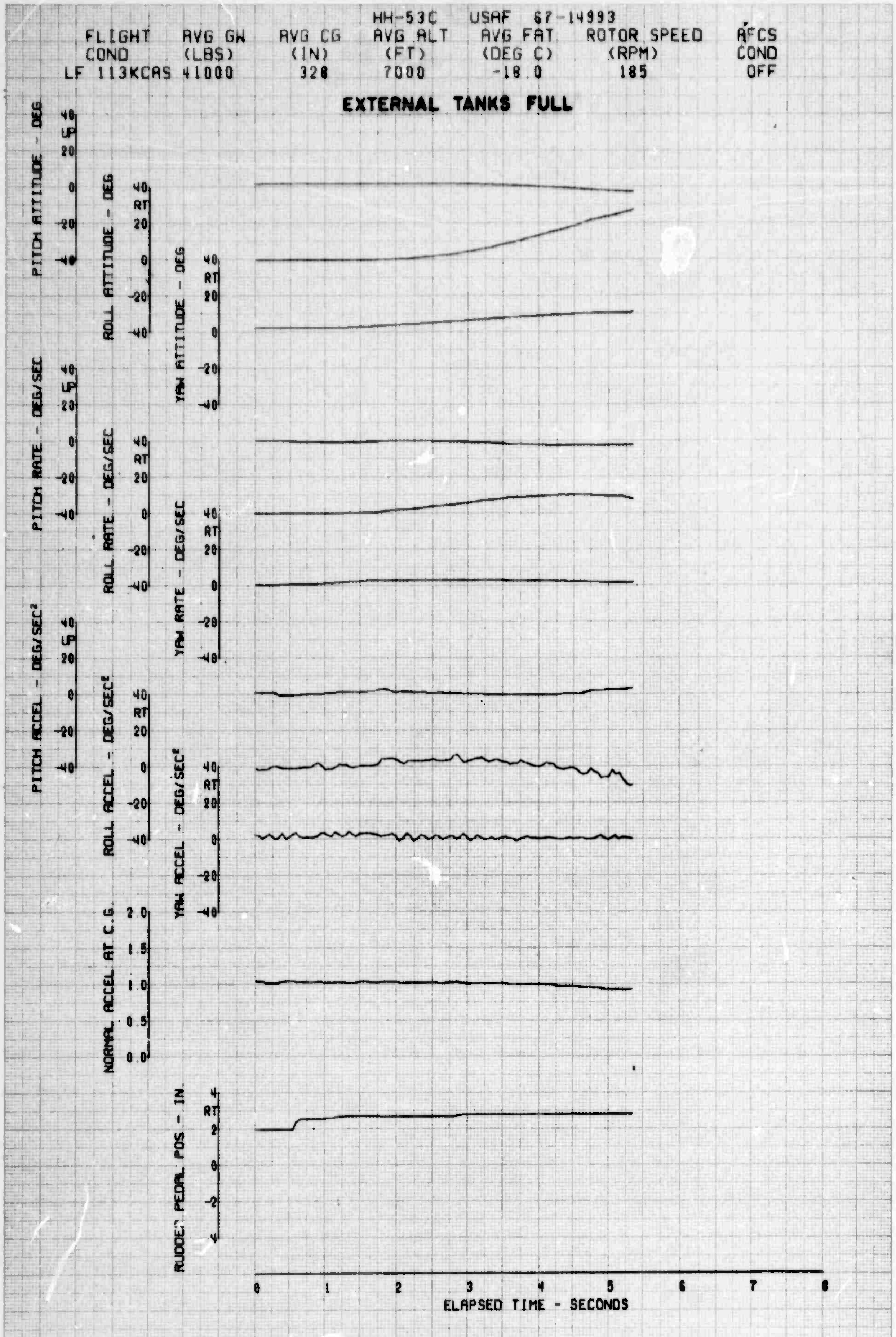

FIGURE 142. REACTION TO A RIGHT DIRECTIONAL STEP

HH-53C USAF S/N 67-14993

Sym	Flight Condition	Avg GW (lb)	cg (in.)	Avg Press. Alt (ft)	Avg FAT (°C)	Rotor Speed (rpm)	AFCS	Trim A/S (kt)
○	Level Flight	41,000	328	7,000	-18	185	ON	113
□	Level Flight	41,000	328	7,000	-18	185	OFF	113

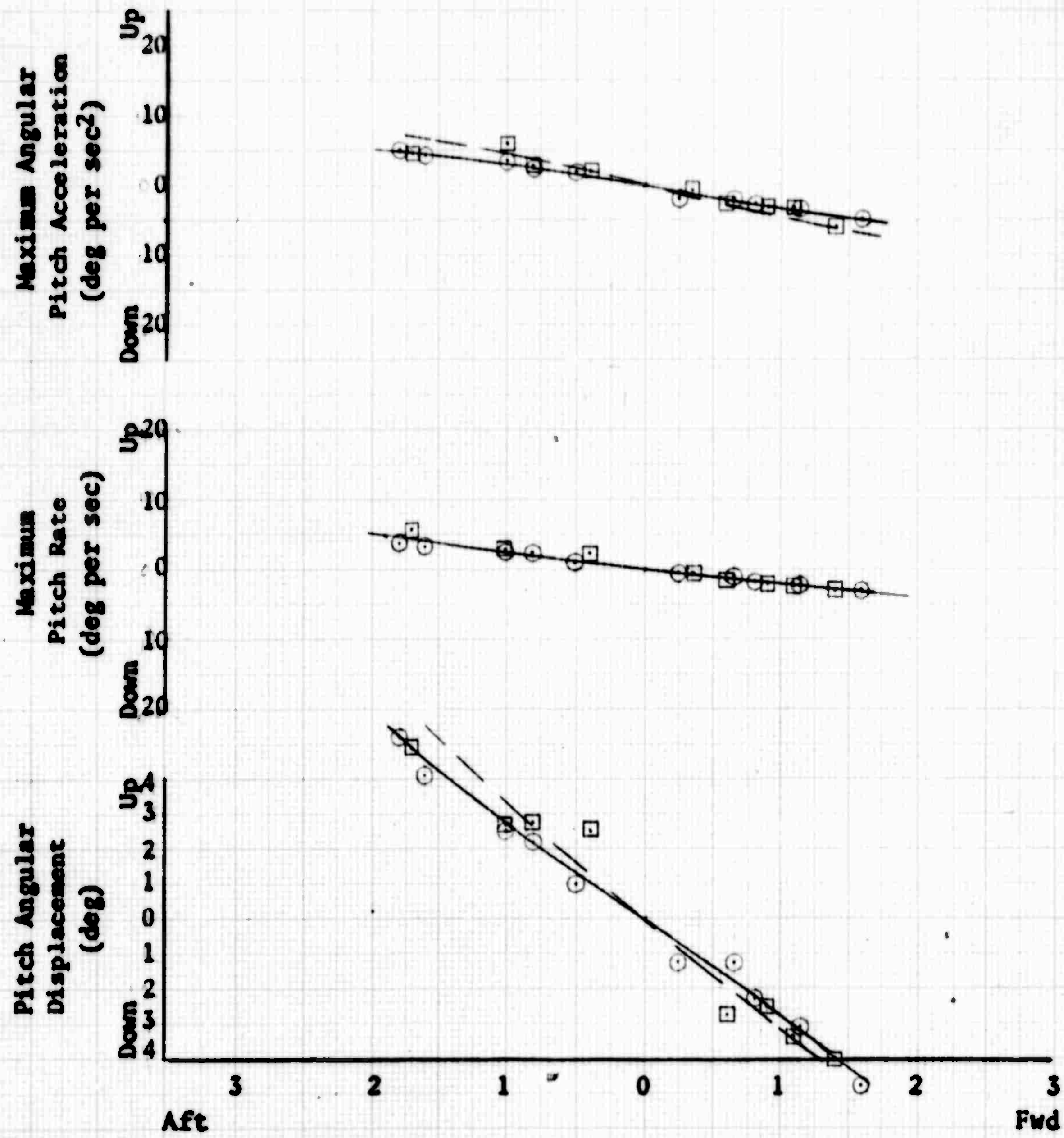

Figure 143. Longitudinal Controllability

HH-53C USAF S/N 67-14993

Sym	Flight Condition	Avg GW (lb)	cg (in.)	Avg Press. Alt (ft)	Avg FAT (°C)	Rotor Speed (rpm)	AFCS	Trim A/S (kt)
○	Level Flight	41,000	328	7,000	-18	185	ON	113
□	Level Flight	41,000	328	7,000	-18	185	OFF	113

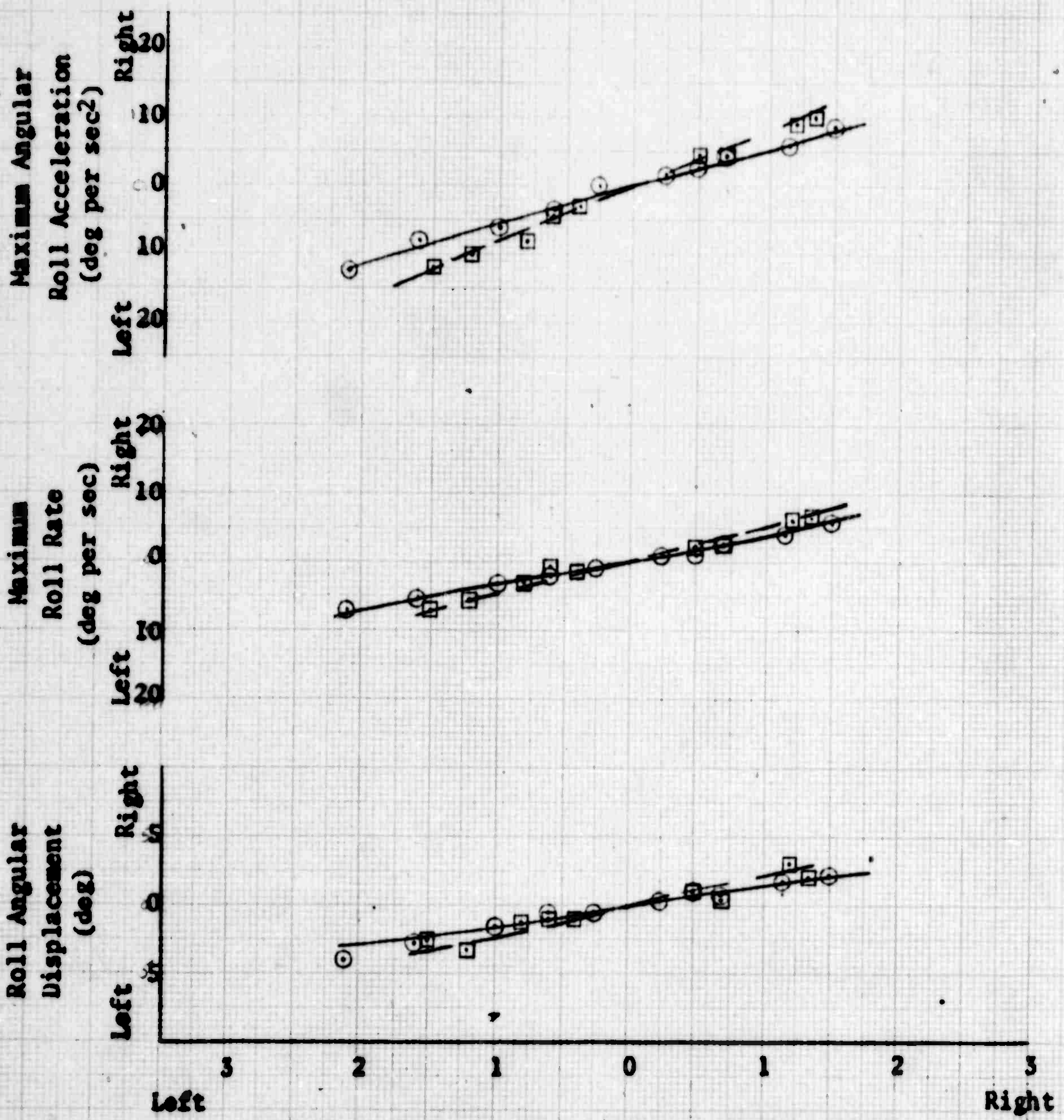

Figure 144. Lateral Controllability

HH-53C USAF S/N 67-14993

Sym	Flight Condition	Avg GW (lb)	cg (in.)	Avg Press. Alt (ft)	Avg FAT (°C)	Rotor Speed (rpm)	AFCS	Trim A/S (kt)
○	Level Flight	41,000	328	7,000	-18	185	ON	113
□	Level Flight	41,000	328	7,000	-18	185	OFF	113

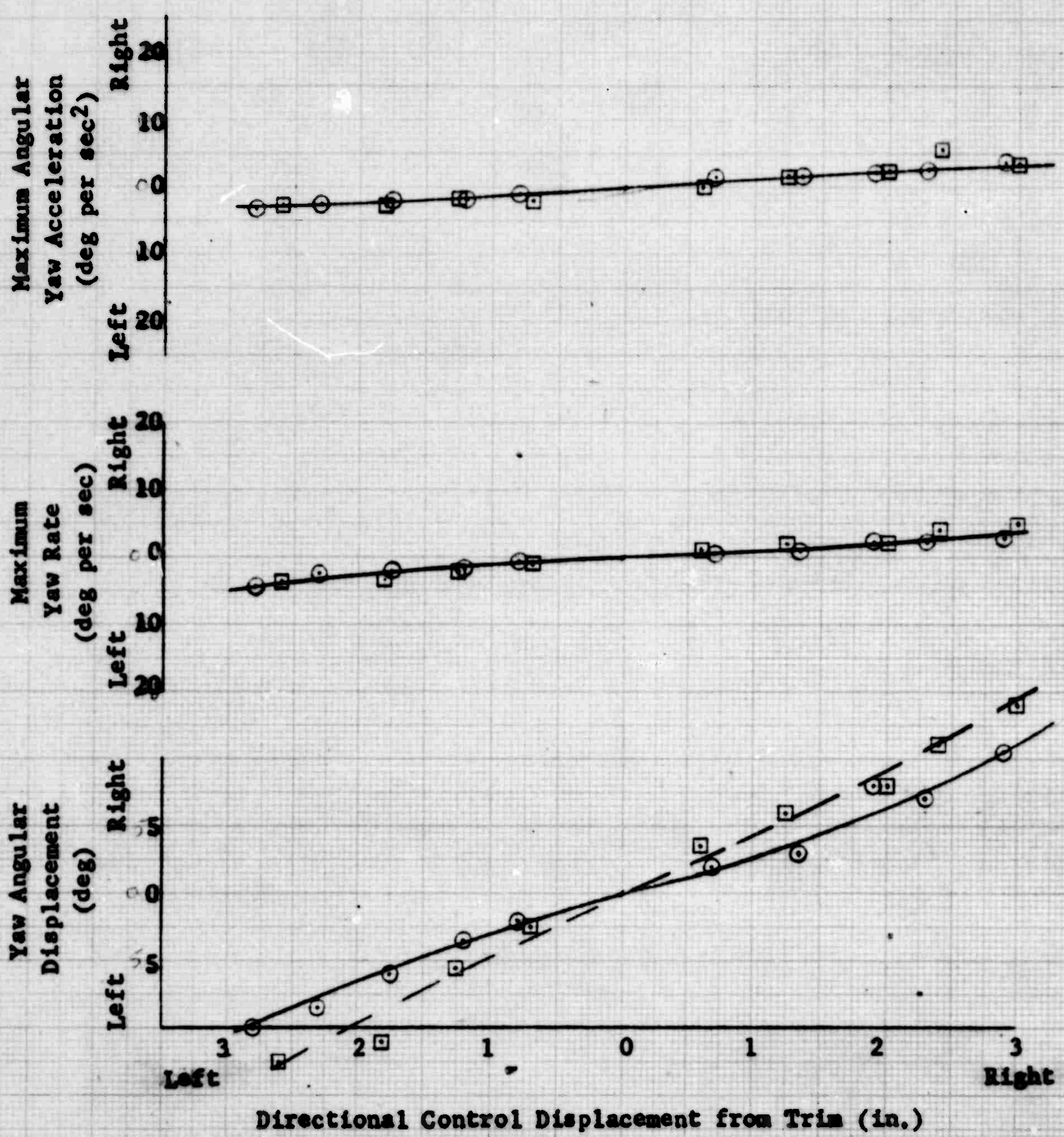

Figure 145. Directional Controllability

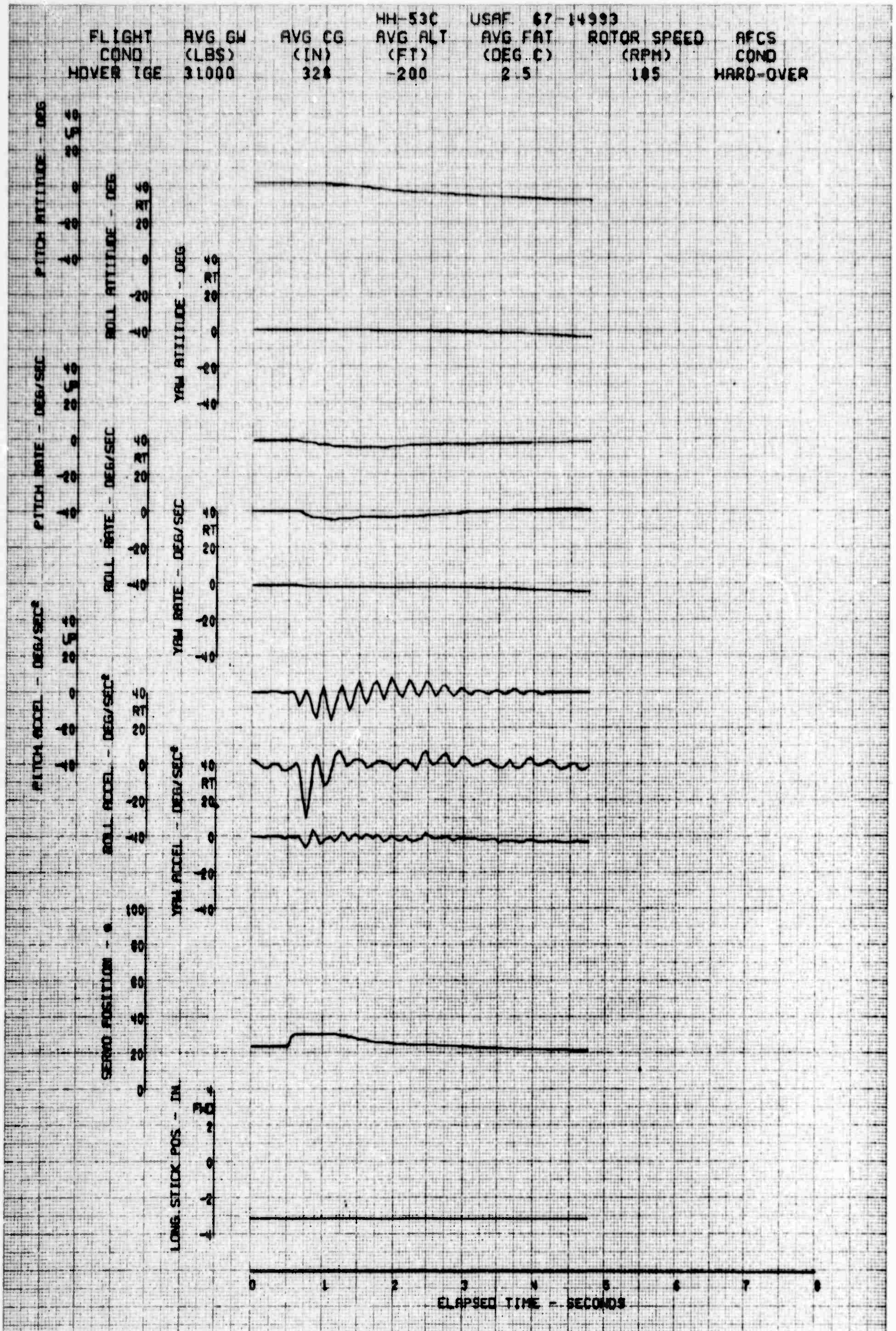

FIGURE 146. REACTION TO A FORWARD LONGITUDINAL HARD-OVER

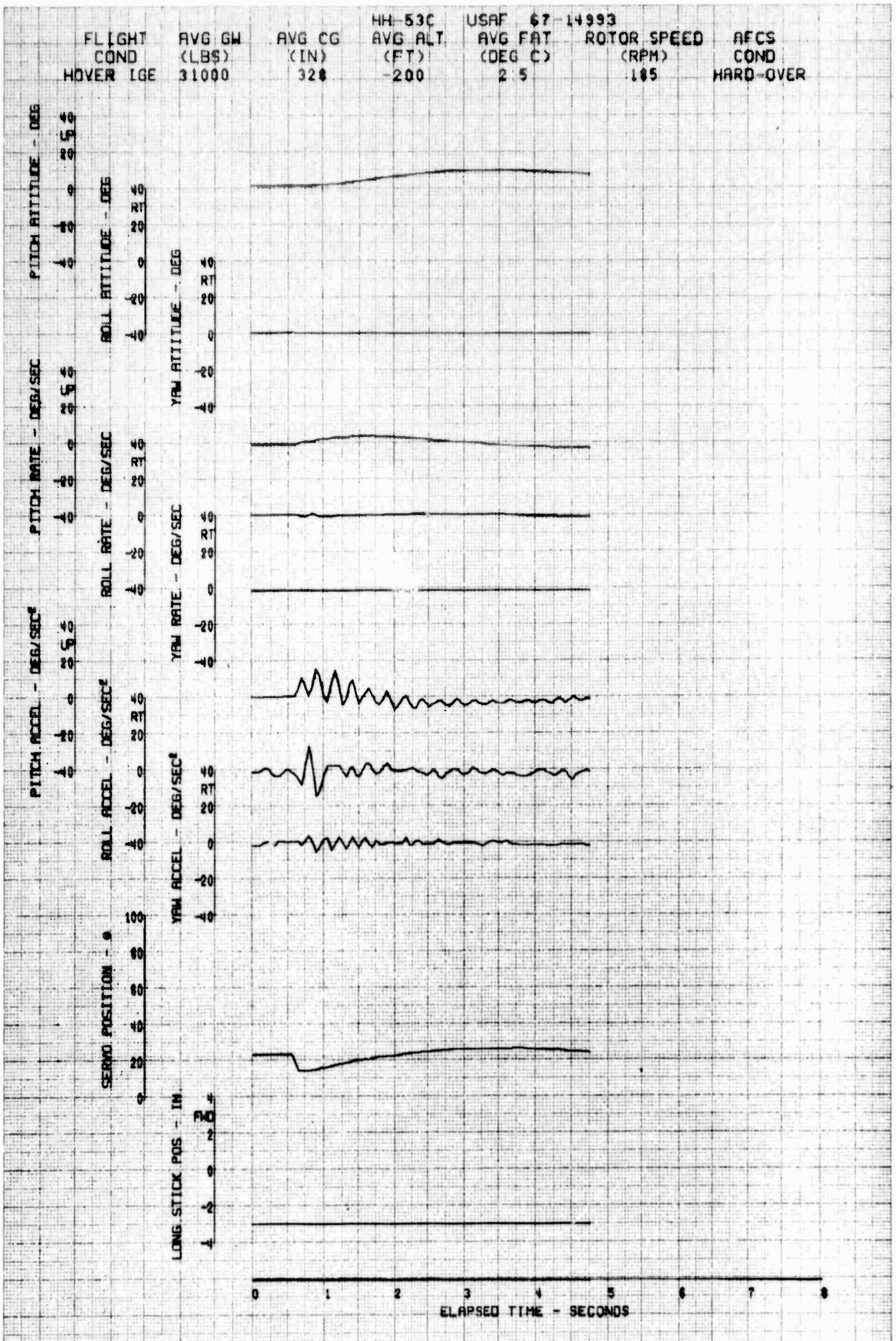

FIGURE 147 REACTION TO AN AFT LONGITUDINAL HARD-OVER

HH-53C USAF 67-14993

FLIGHT COND	AVG GW (LBS)	AVG CG (IN)	AVG ALT (FT)	AVG FAT (DEG C)	ROTOR SPEED (RPM)	AFCS COND
HOVER IGE	31000	328	-200	2.5	185	HARD-OVER

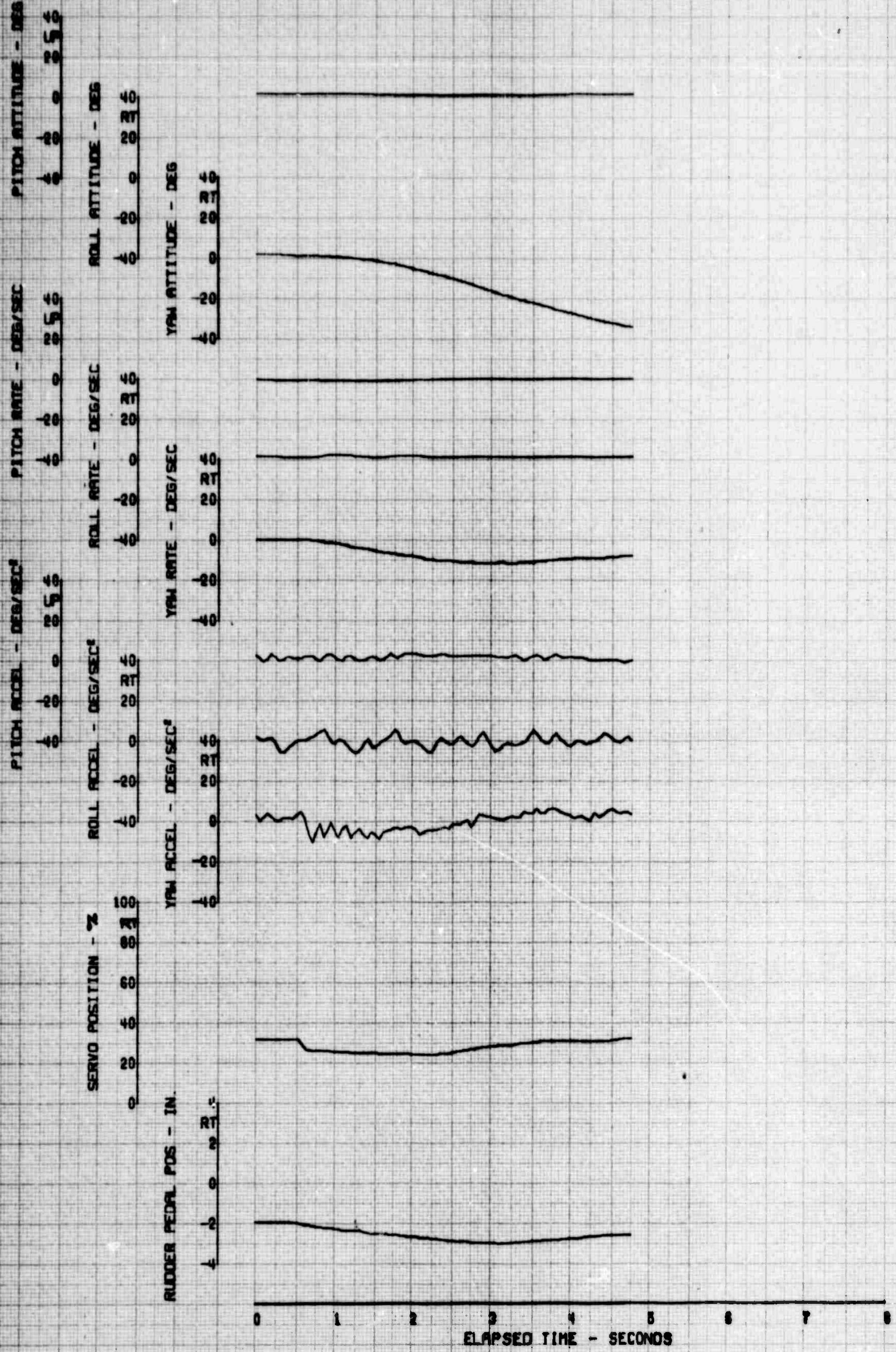

FIGURE 146. REACTION TO A LEFT DIRECTIONAL HARD-OVER

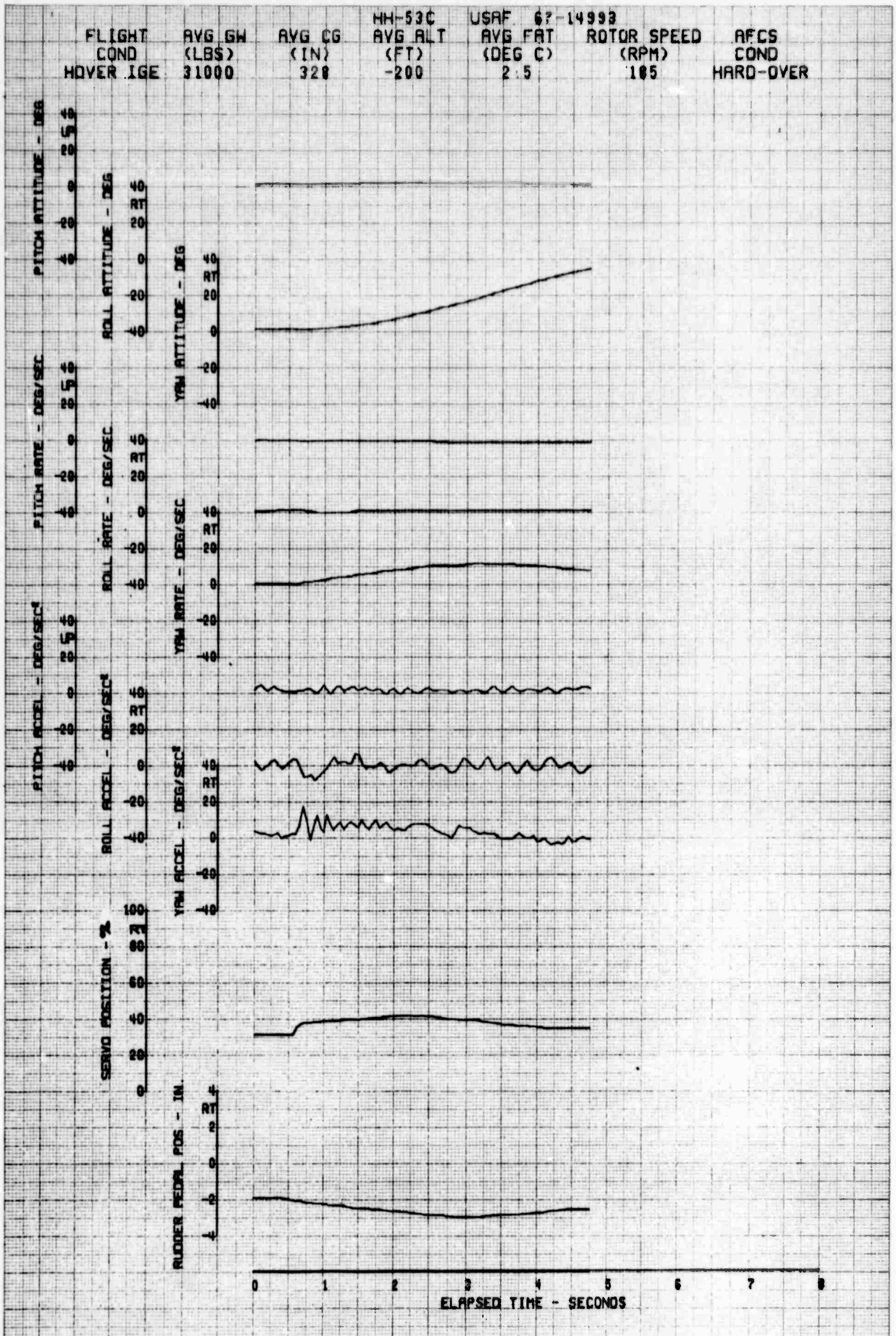

FIGURE 147. REACTION TO A RIGHT DIRECTIONAL HARD-OVER

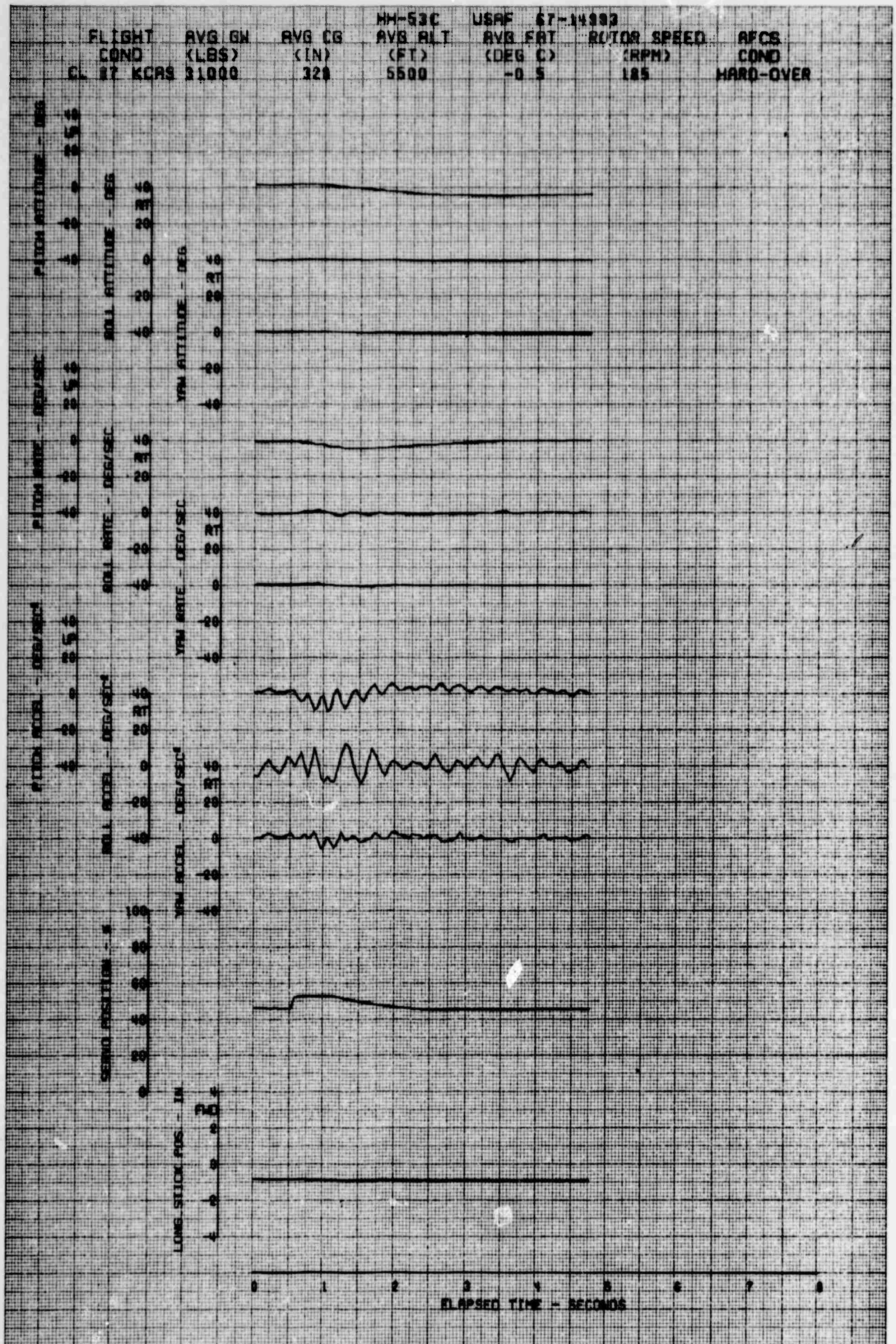

FIGURE 150. REACTION TO A FORWARD LONGITUDINAL HARD-OVER

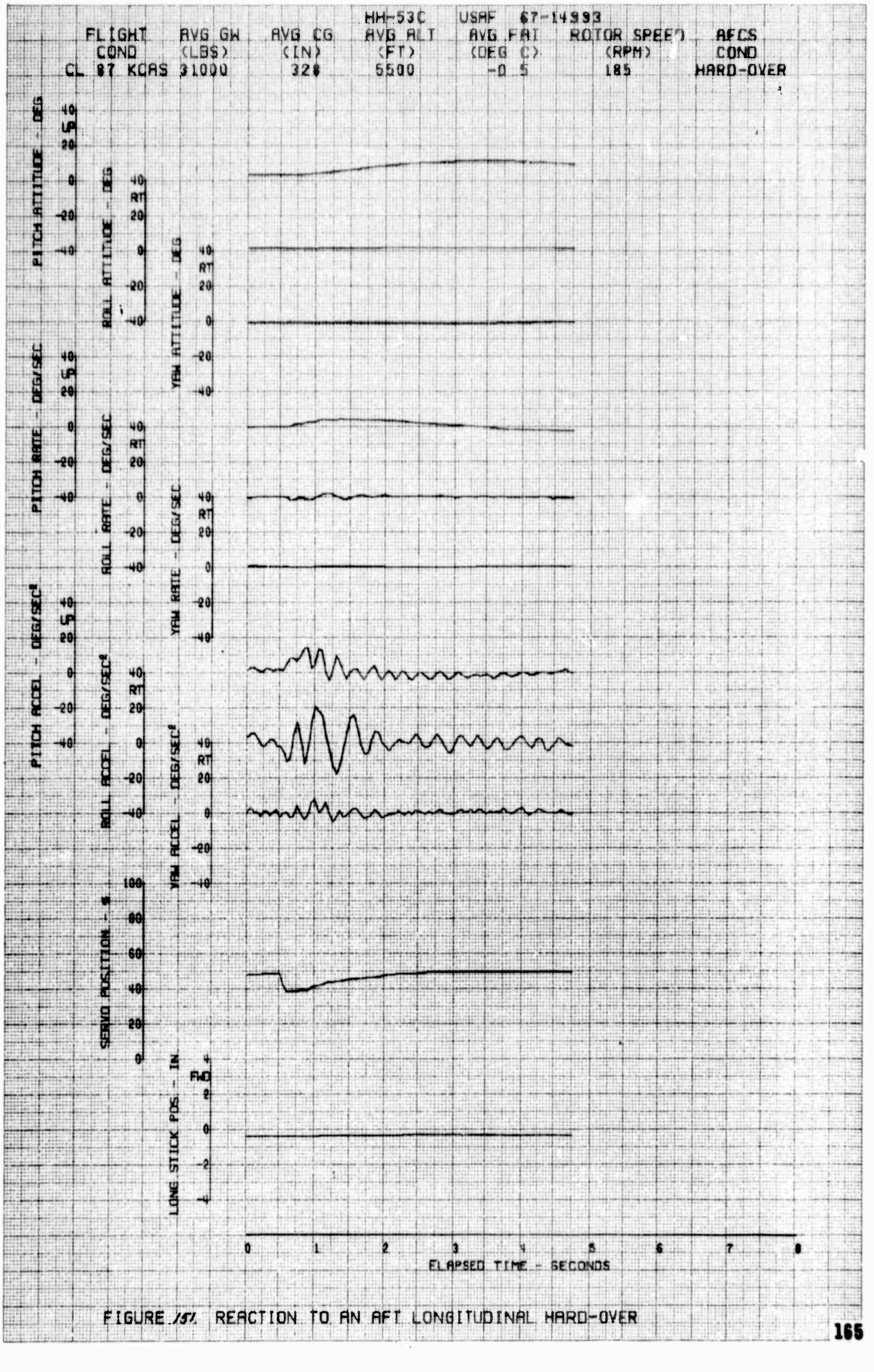

FIGURE 151 REACTION TO AN AFT LONGITUDINAL HARD-OVER

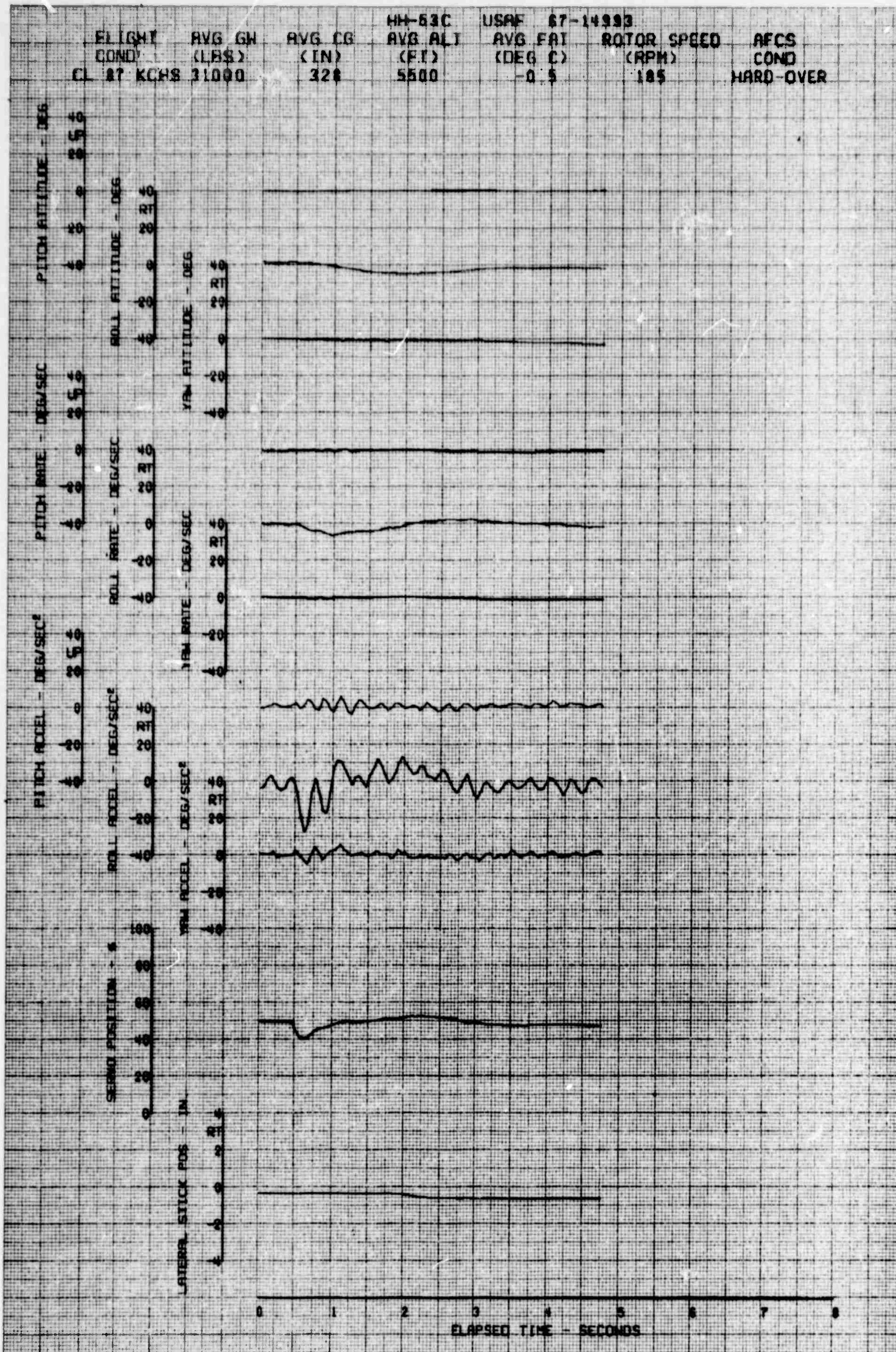

FIGURE 158 REACTION TO A LEFT LATERAL HARD-OVER

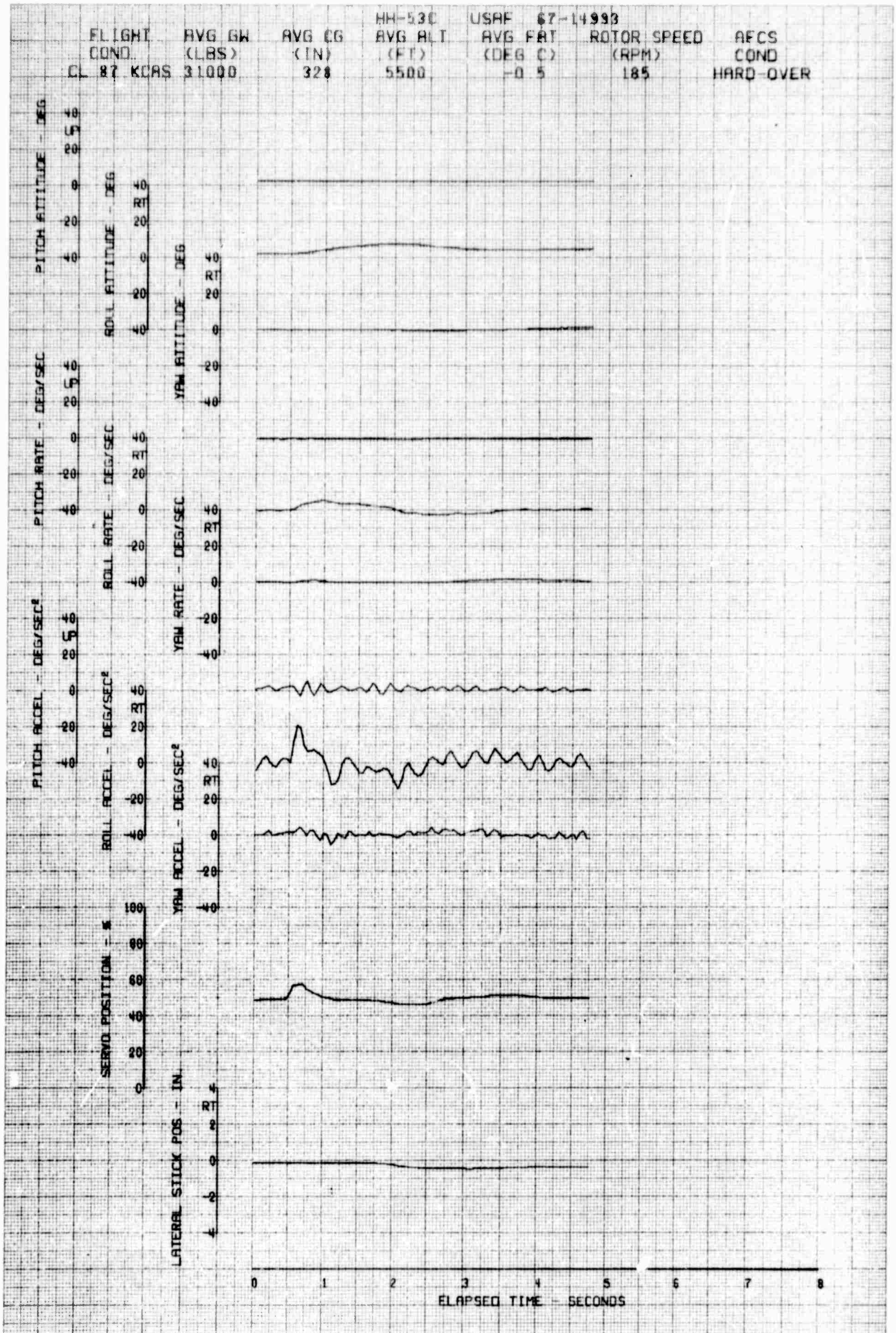

FIGURE 153. REACTION TO A RIGHT LATERAL HARD-OVER

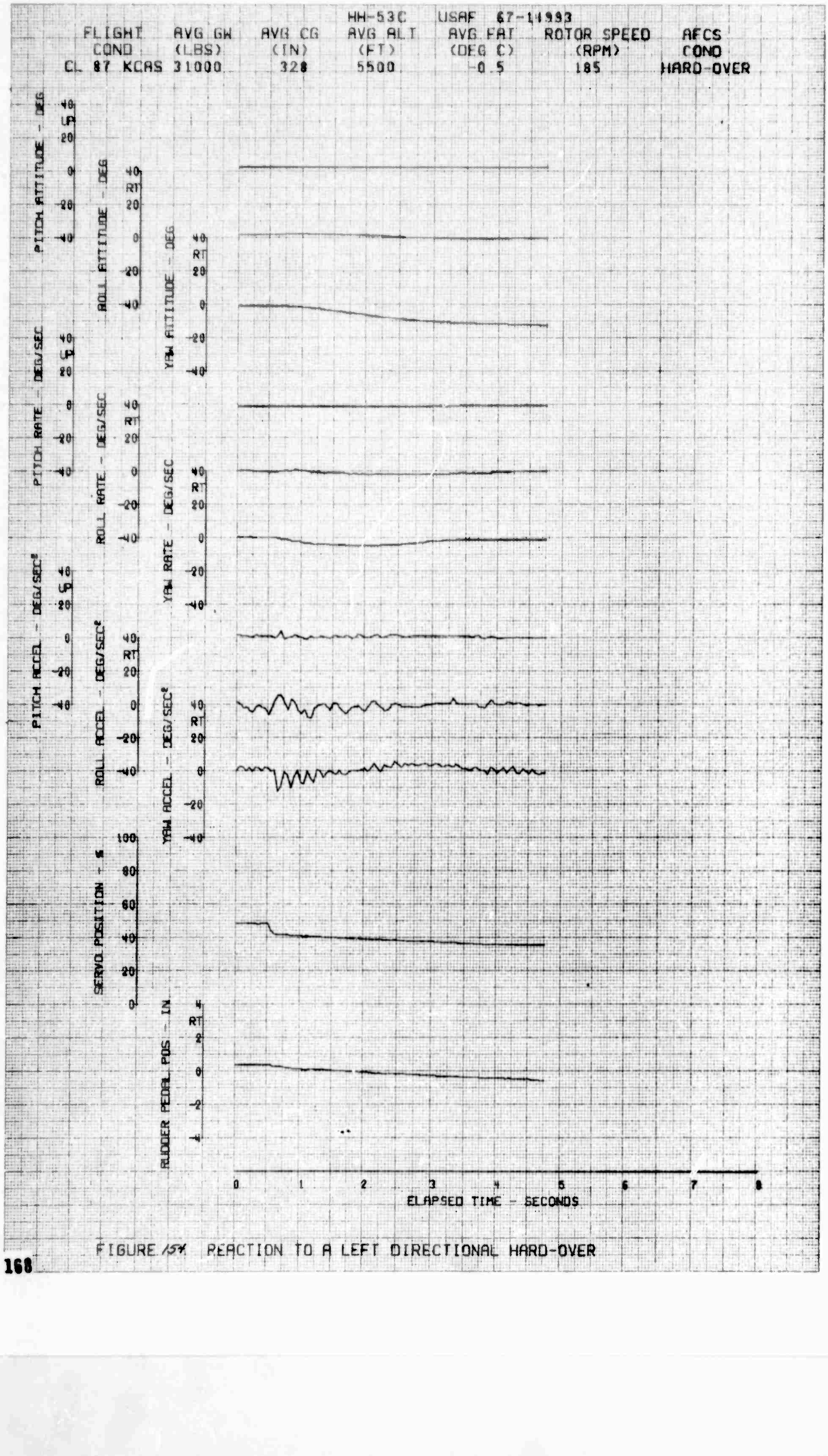

FIGURE 15% REACTION TO A LEFT DIRECTIONAL HARD-OVER

HH-53C USAF 67-14993

FLIGHT COND	AVG GW (LBS)	AVG CG (IN)	AVG ALT (FT)	AVG FAT (DEG C)	ROTOR SPEED (RPM)	AFCS COND
CL 87 KCAS	31000	328	5500	-0.5	185	HARD-OVER

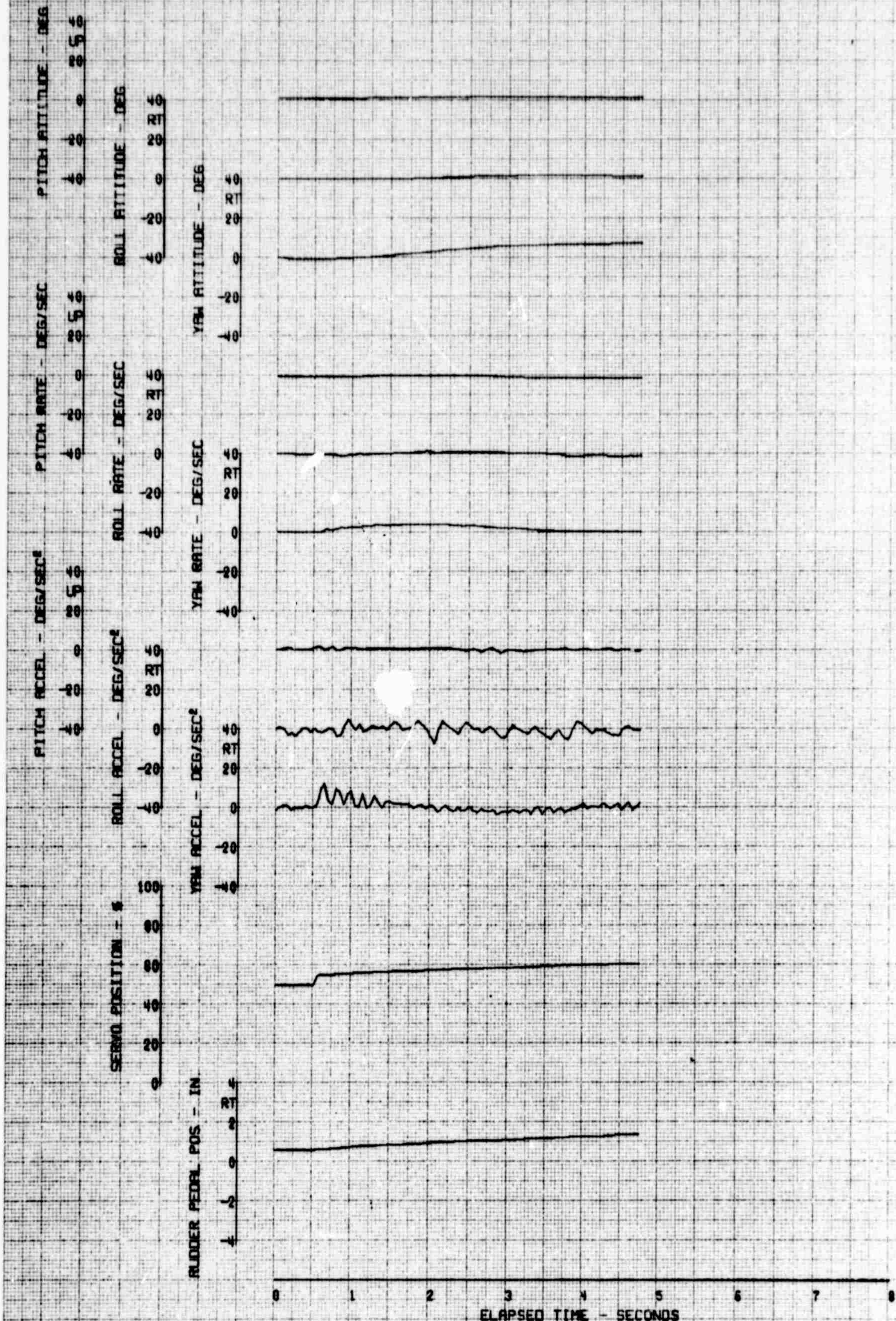

FIGURE 155. REACTION TO A RIGHT DIRECTIONAL HARD-OVER

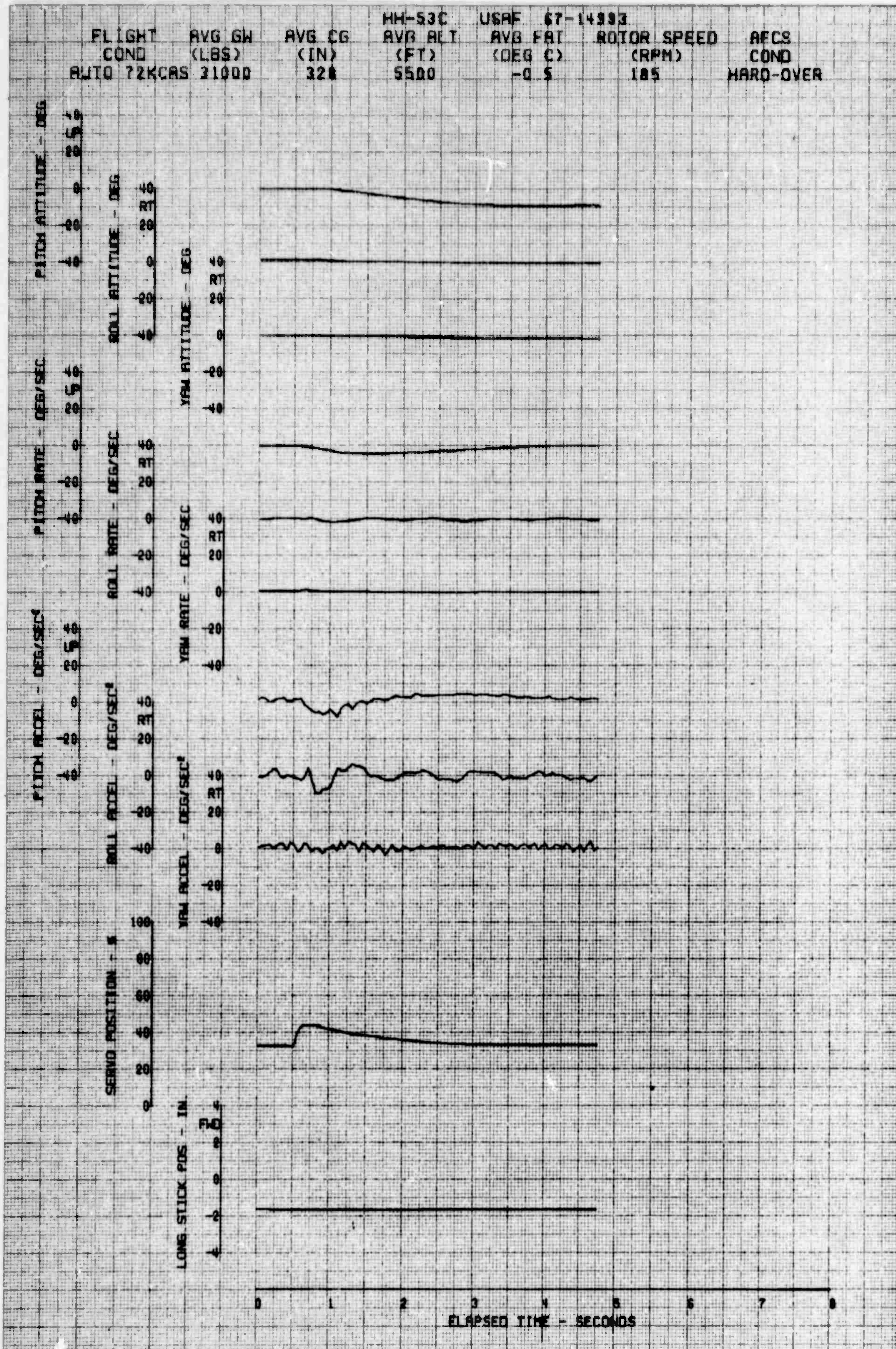

FIGURE 156. REACTION TO A FORWARD LONGITUDINAL HARD-OVER

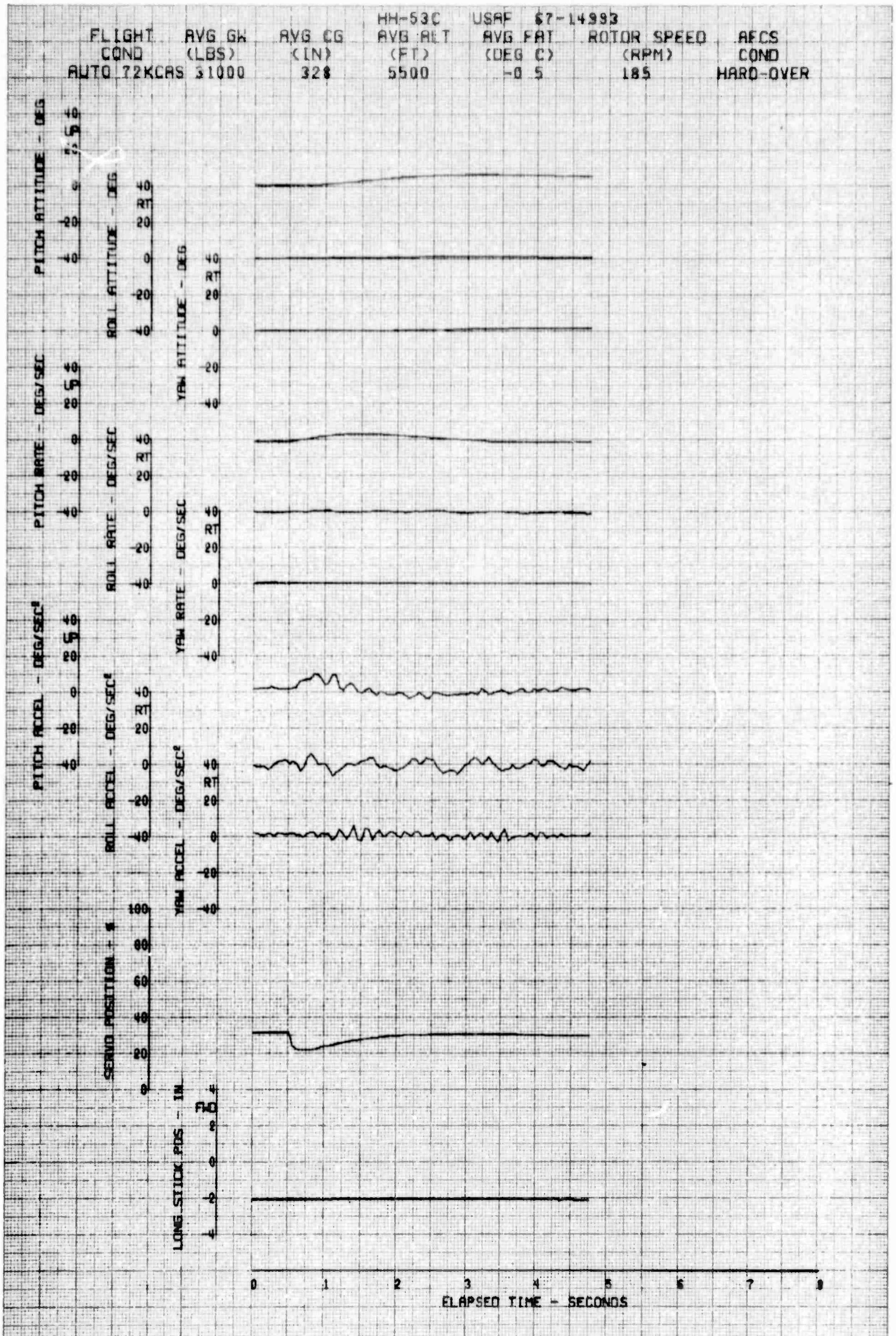

FIGURE 157 REACTION TO AN AFT LONGITUDINAL HARD-OVER

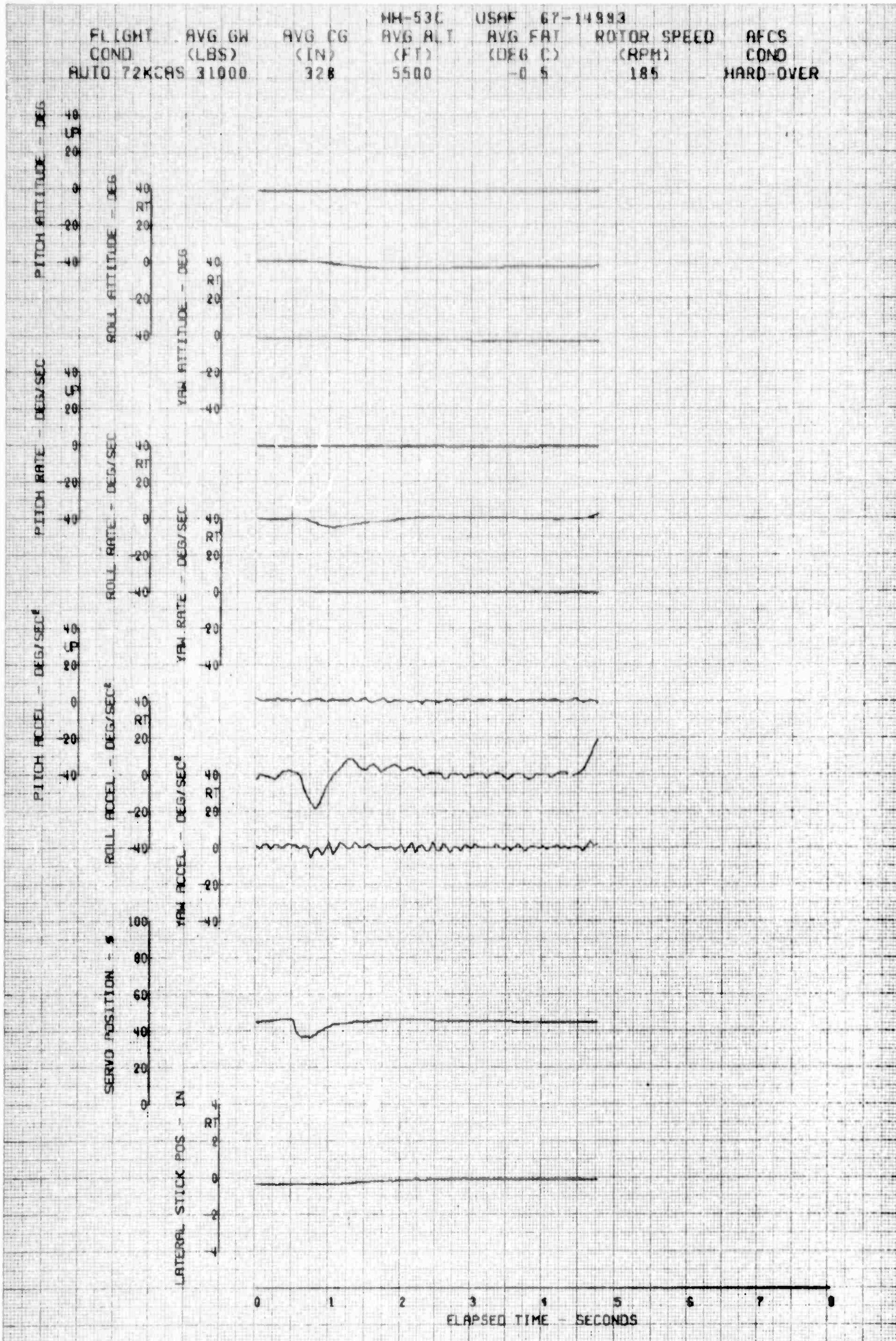

FIGURE 138. REACTION TO A LEFT LATERAL HARD-OVER

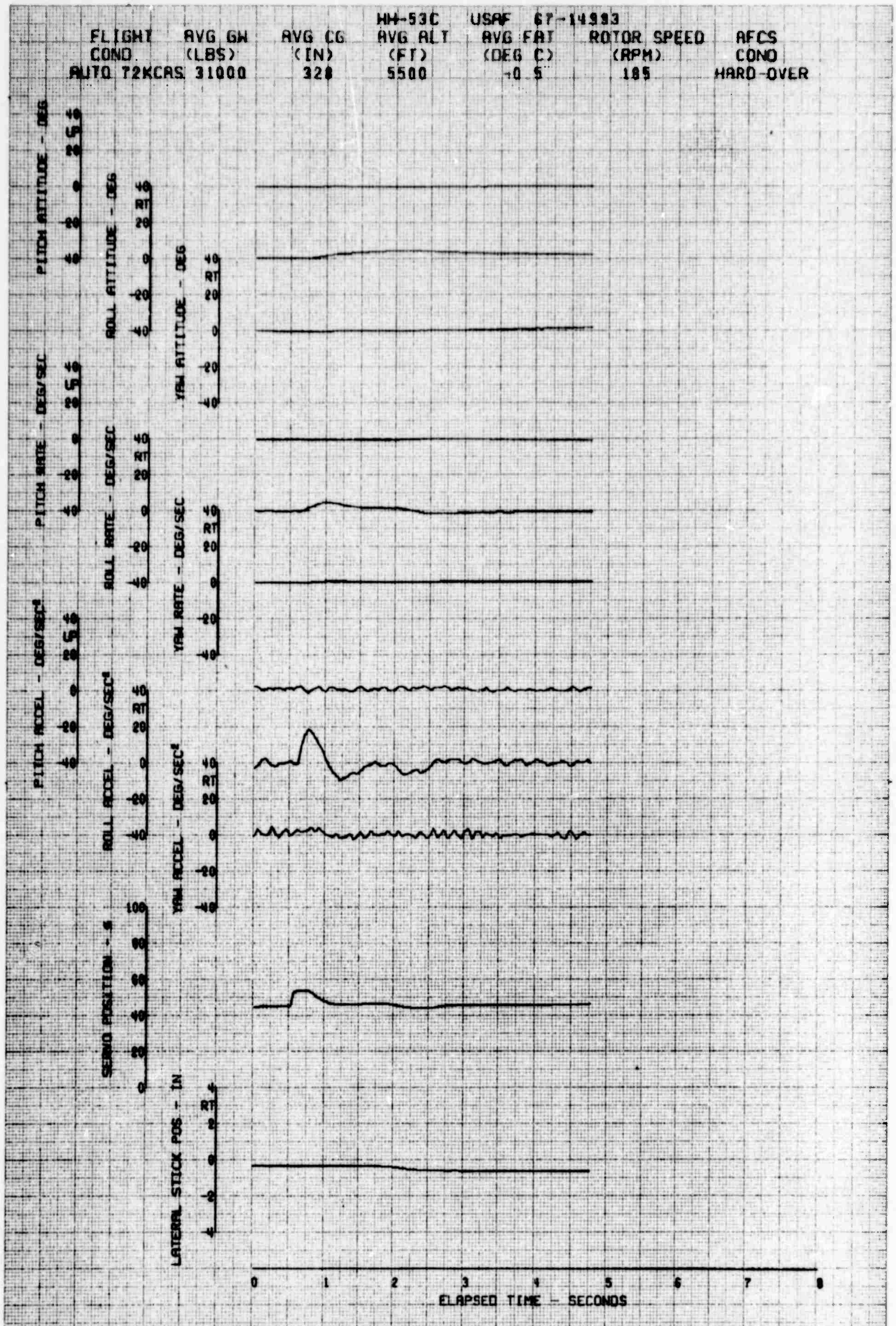

FIGURE 157. REACTION TO A RIGHT LATERAL HARD-OVER

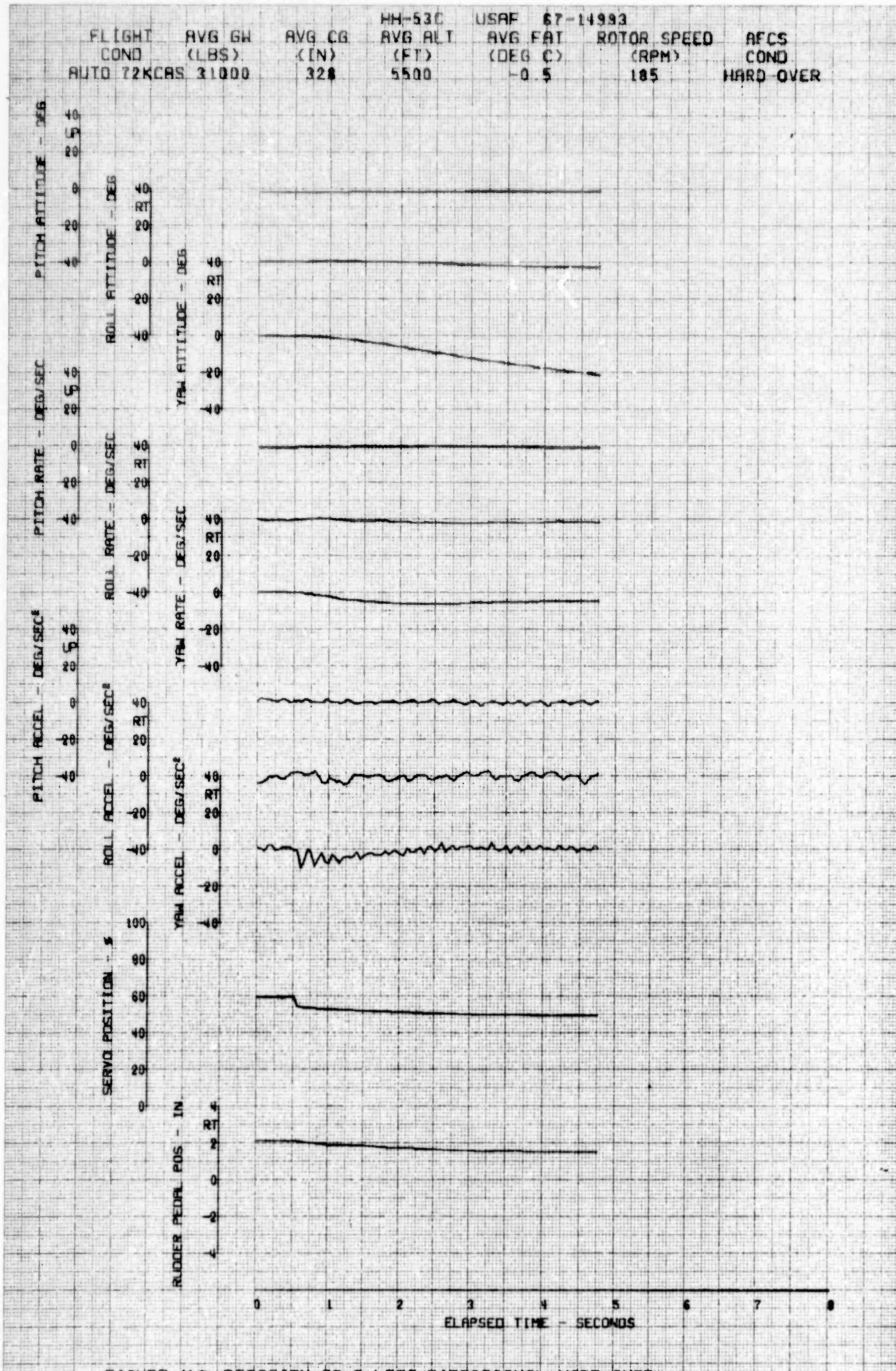

FIGURE 160 REACTION TO A LEFT DIRECTIONAL HARD-OVER

HH-53C USAF 67-14993

FLIGHT COND	AVG GW (LBS)	AVG CG (IN)	AVG ALT (FT)	AVG FAT (DEG C)	ROTOR SPEED (RPM)	AFCS COND
AUTO 72KCAS	31000	328	5500	-0.5	185	HARD-OVER

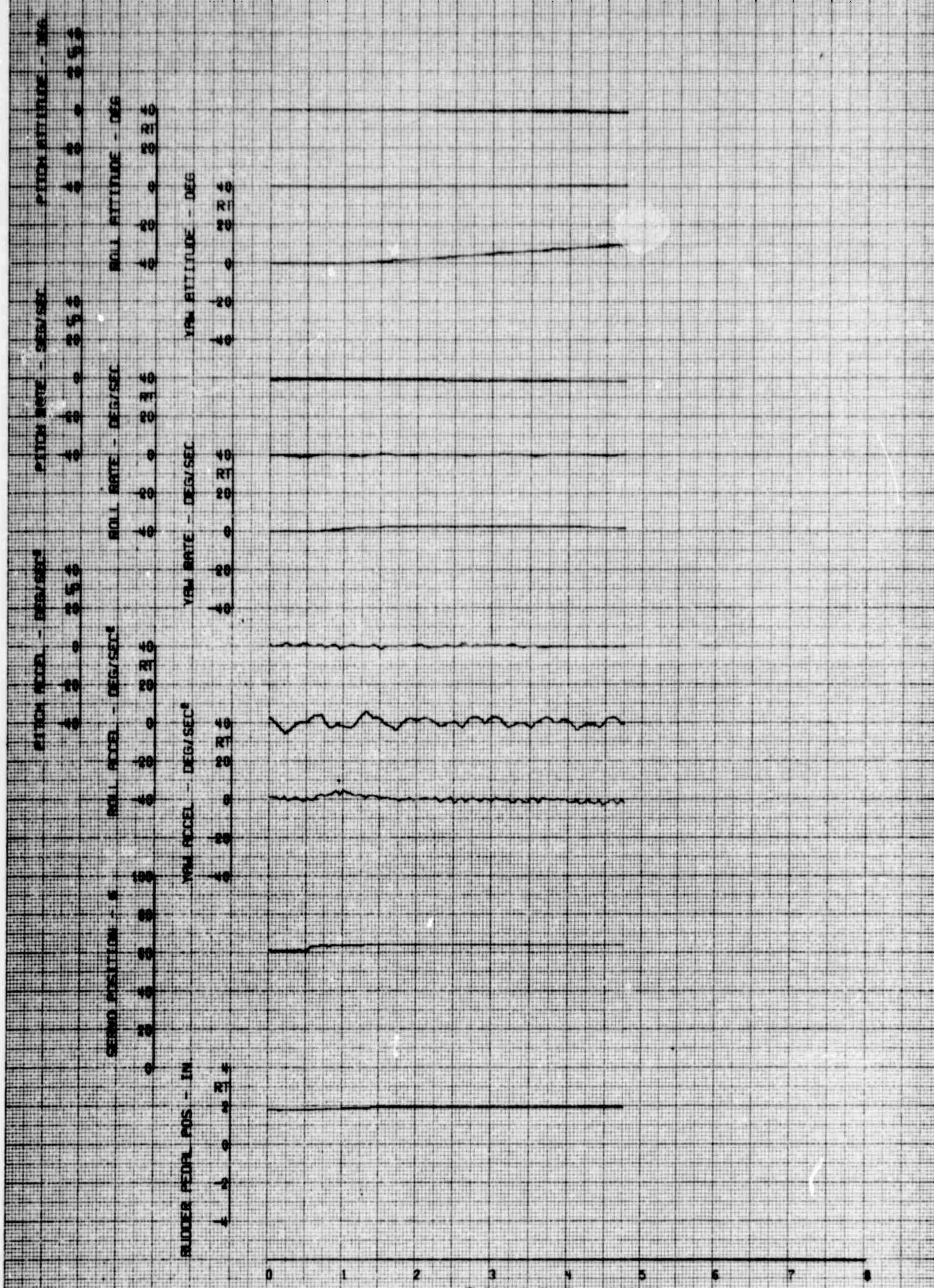

FIGURE 161 REACTION TO A RIGHT DIRECTIONAL HARD-OVER

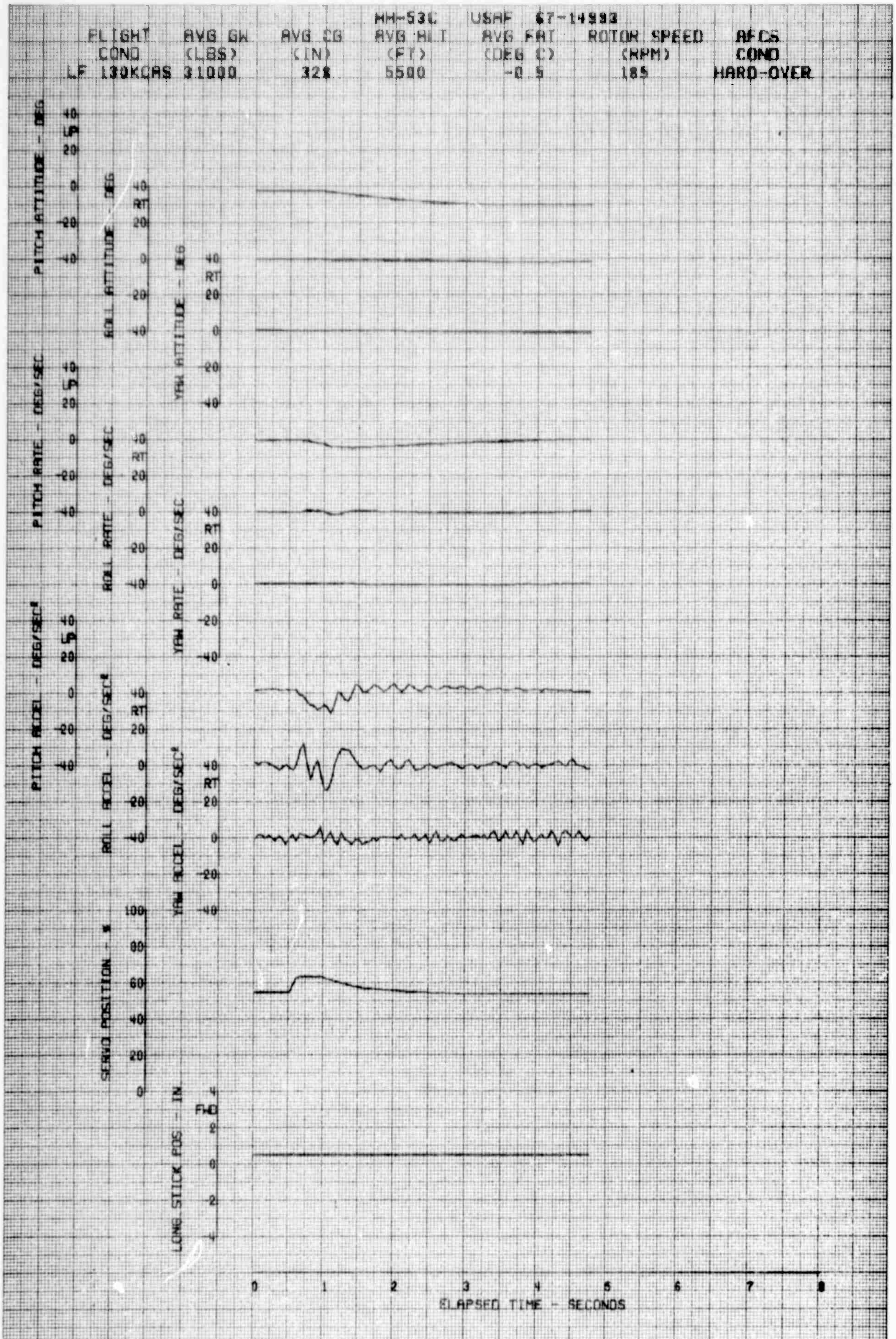

FIGURE 162 REACTION TO A FORWARD LONGITUDINAL HARD-OVER

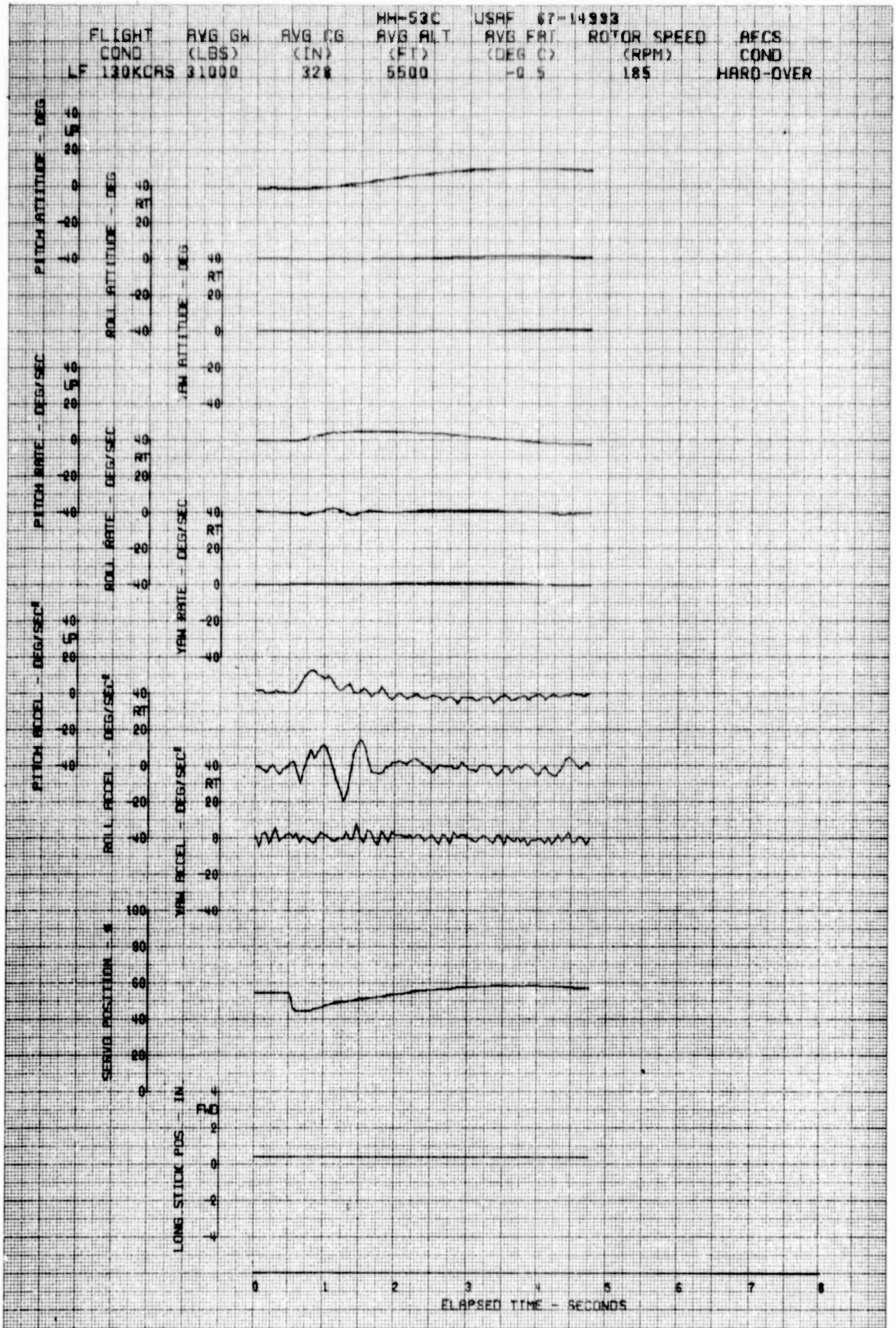

FIGURE 168. REACTION TO AN AFT LONGITUDINAL HARD-OVER

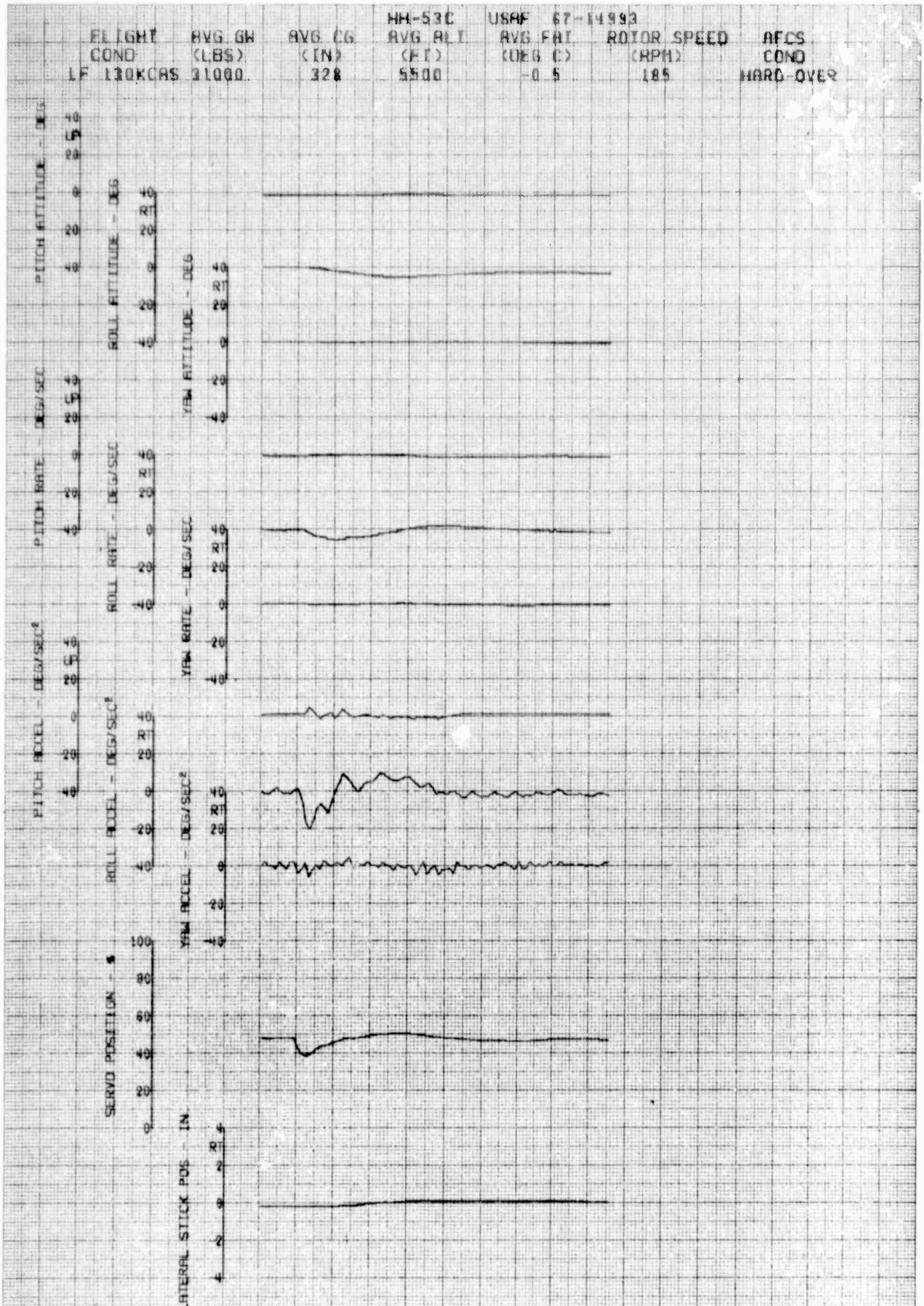

FIGURE 164. REACTION TO A LEFT LATERAL HARD-OVER

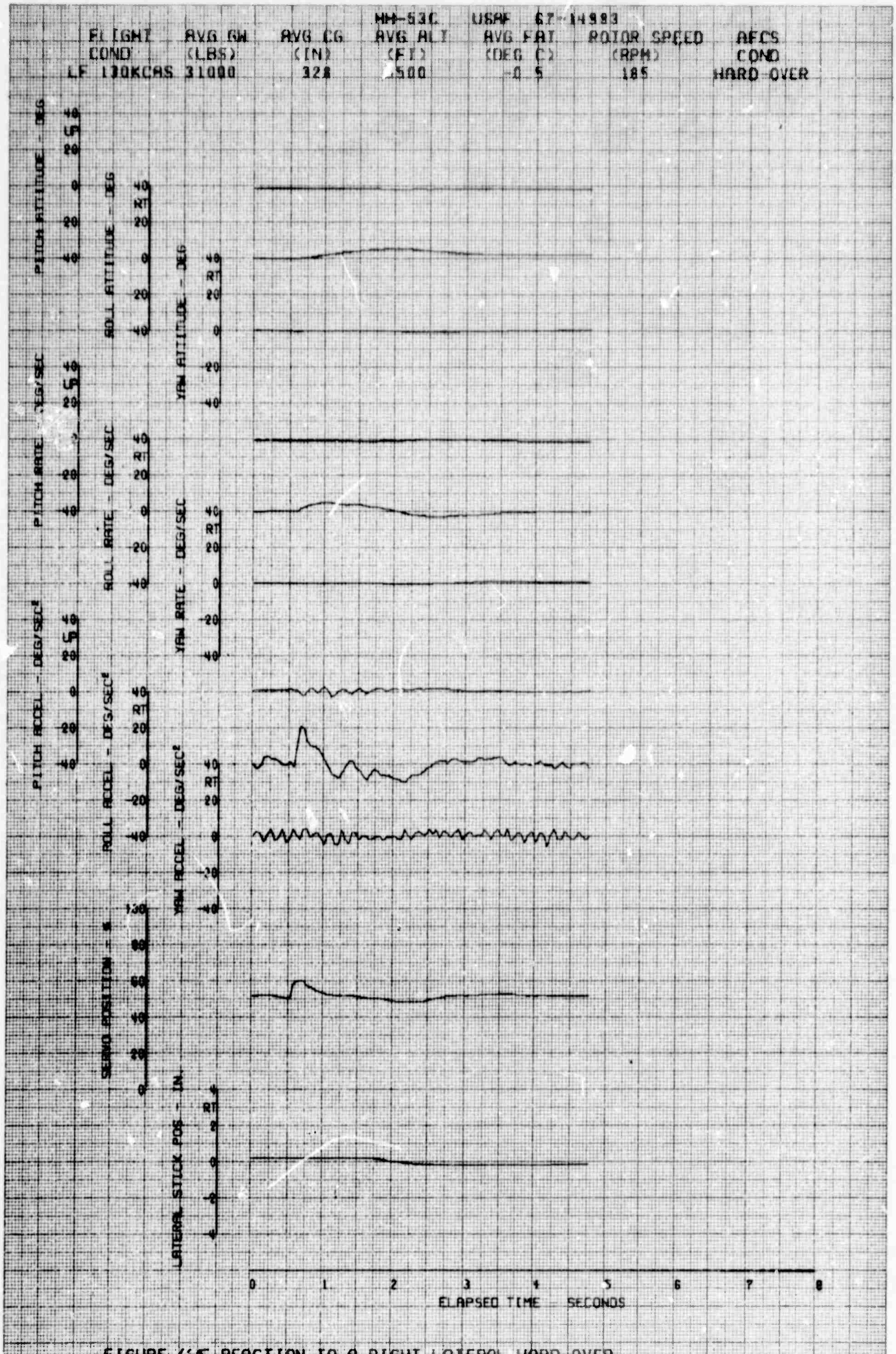

FIGURE 165 REACTION TO A RIGHT LATERAL HARD-OVER

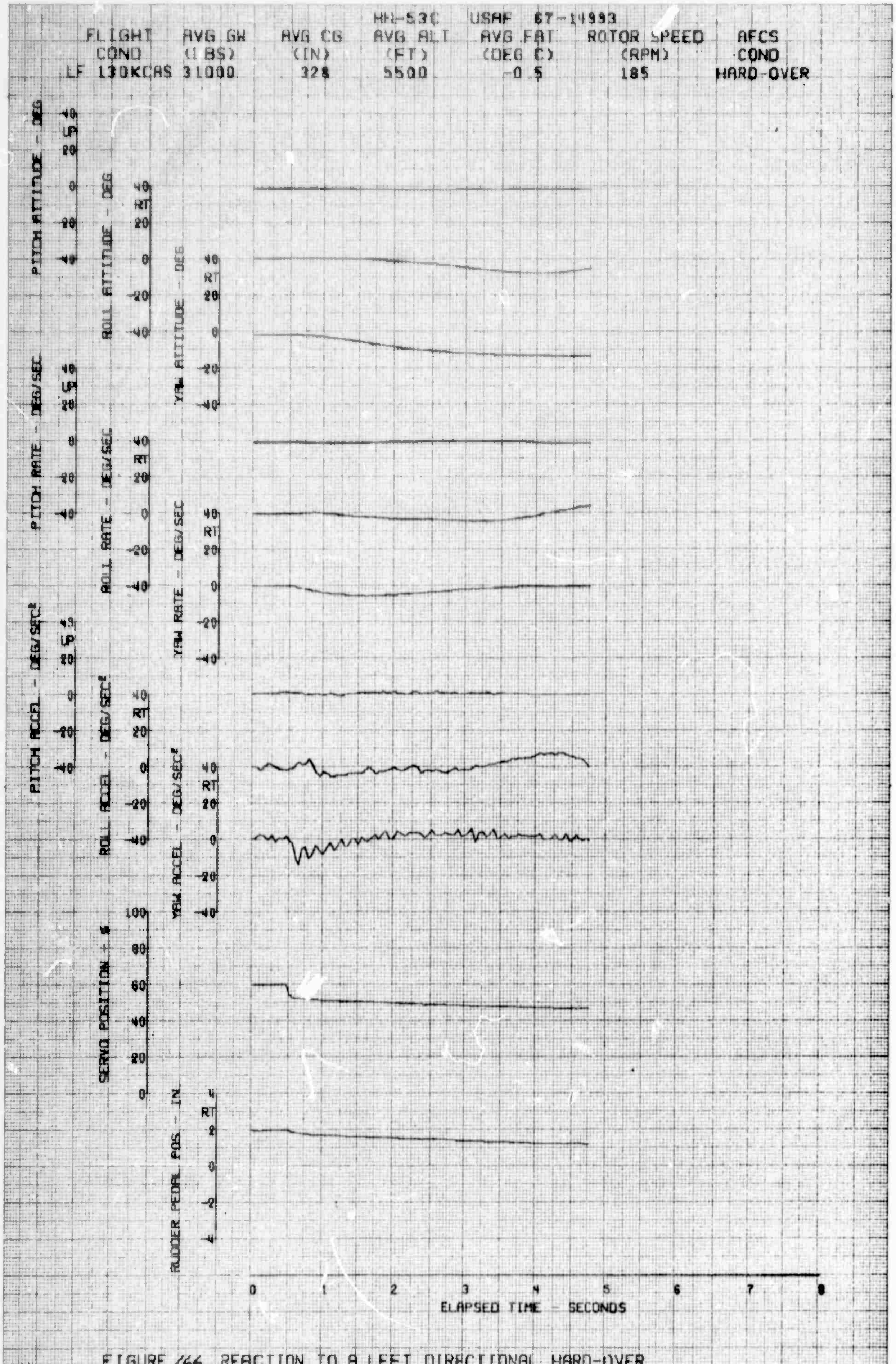

FIGURE 166. REACTION TO A LEFT DIRECTIONAL HARD-OVER

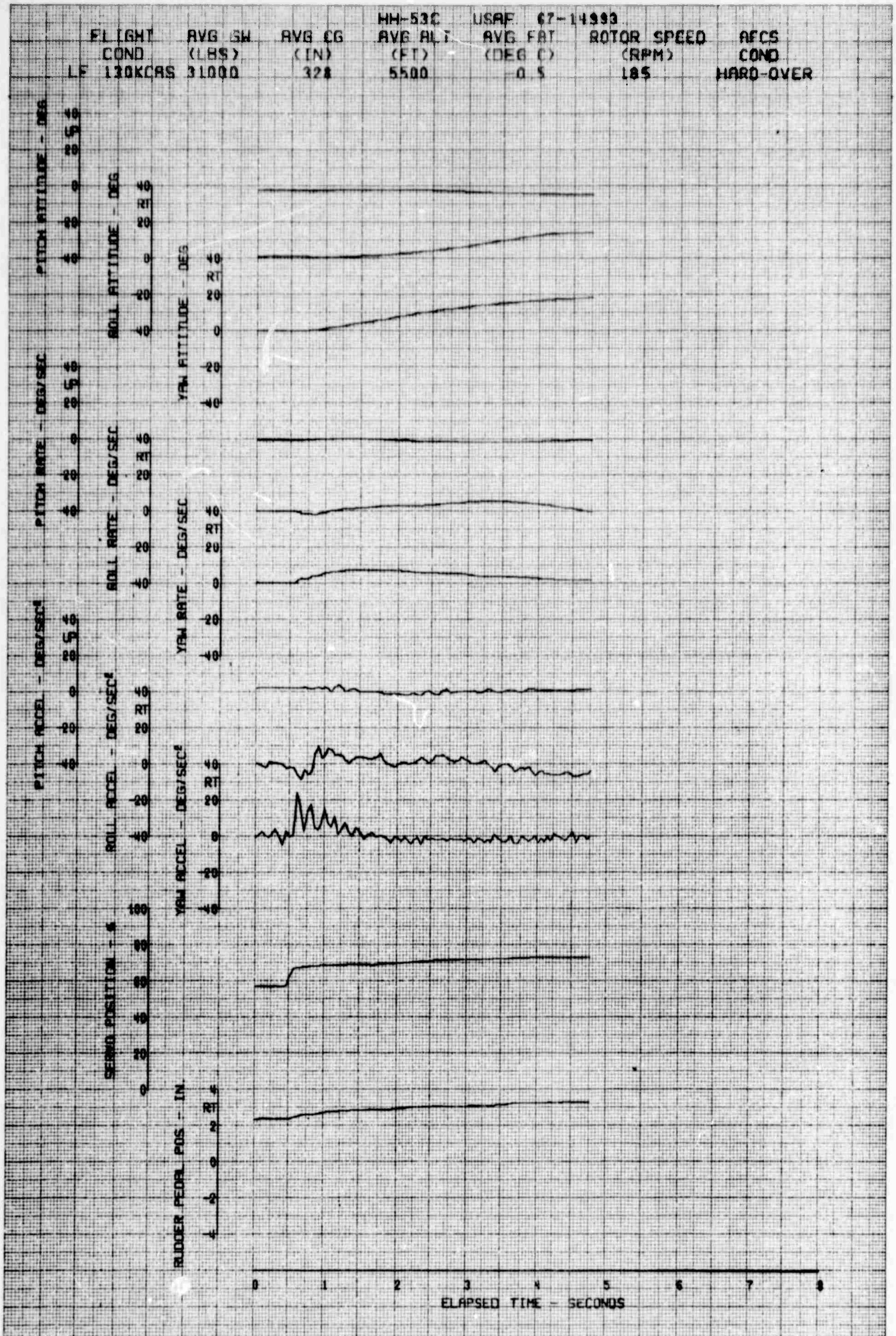

FIGURE 167 REACTION TO A RIGHT DIRECTIONAL HARD-OVER

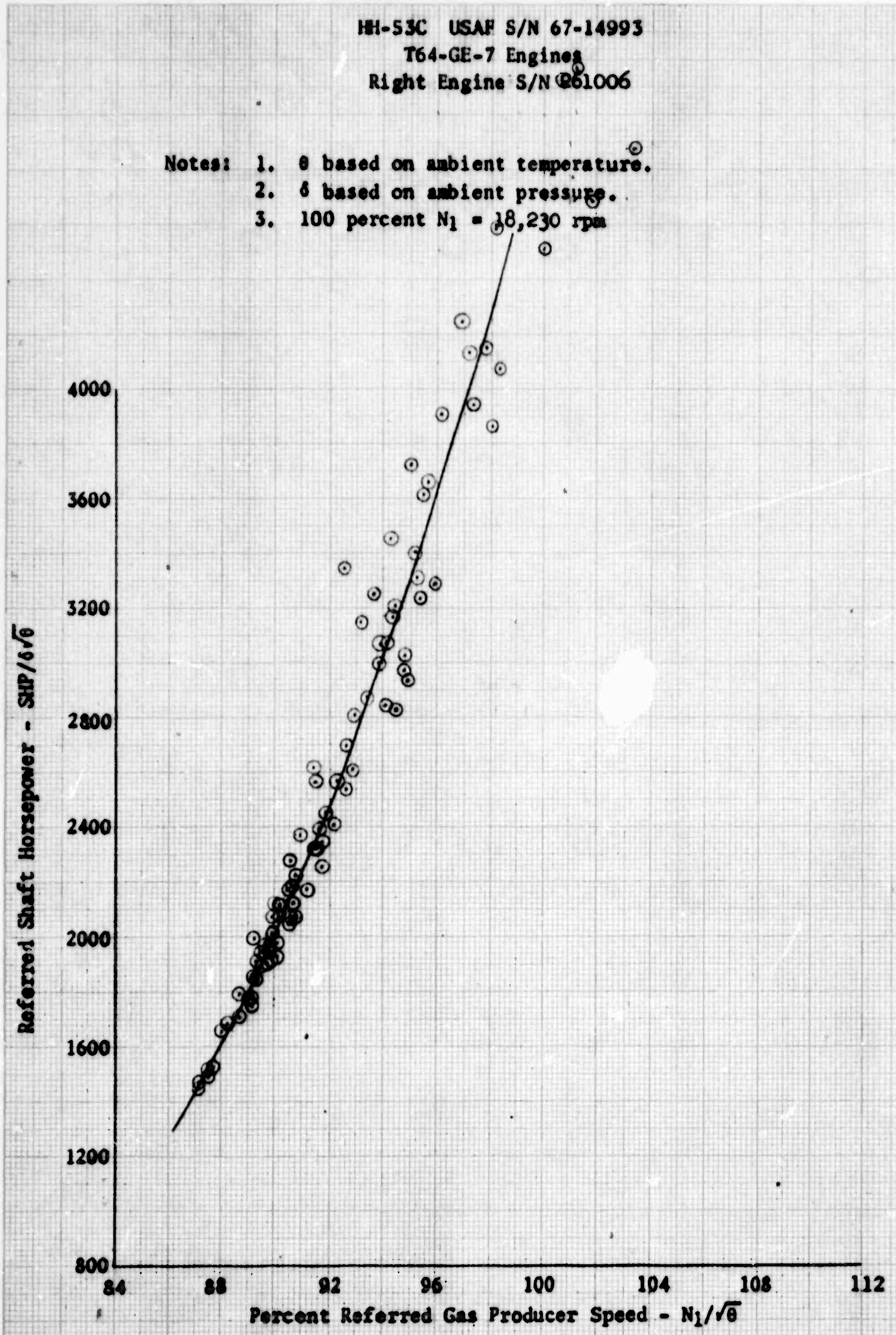

Figure 16a. Engine Characteristics

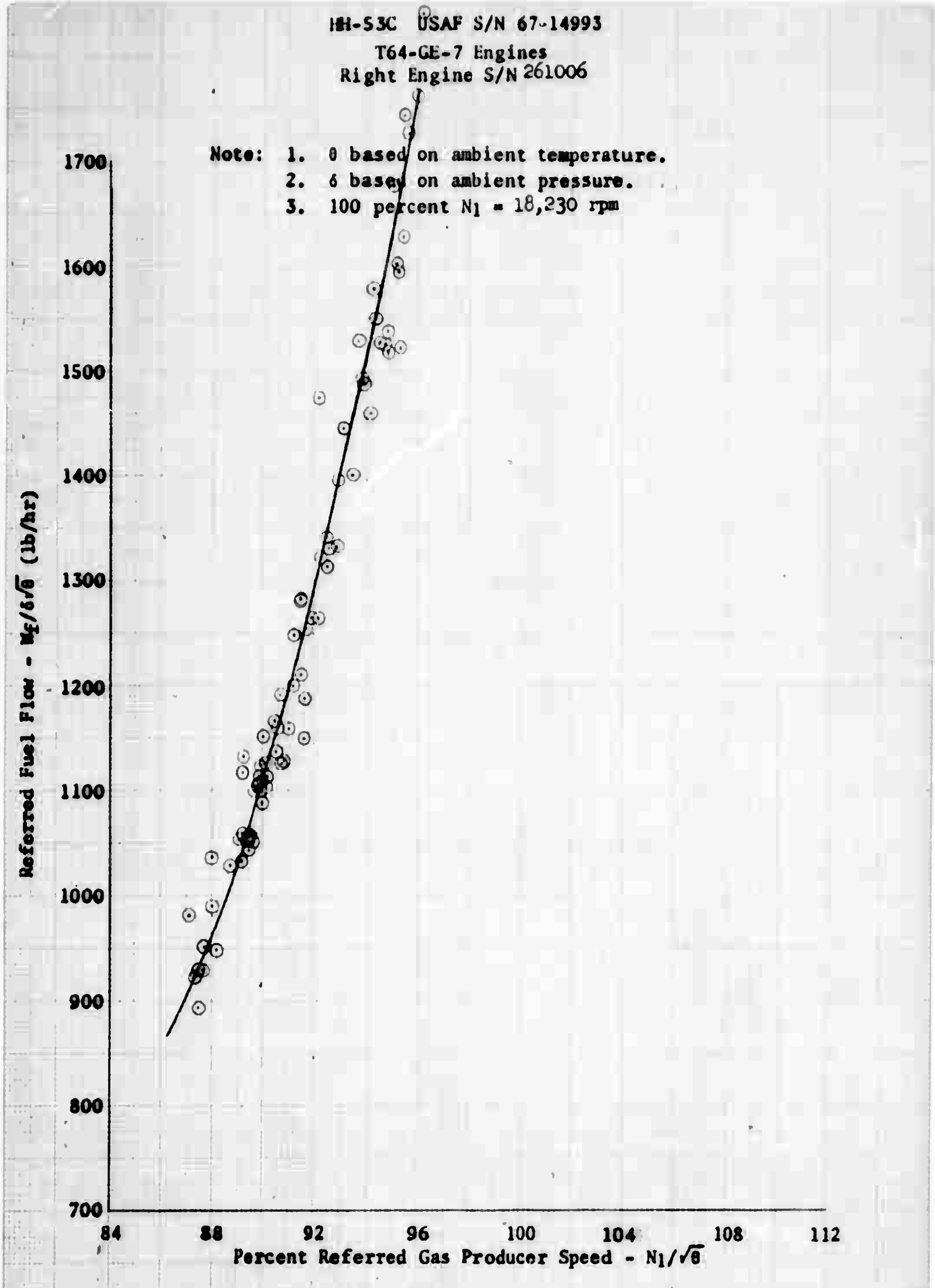

Figure 169. Engine Characteristics

HH-53C USAF S/N 67-14993
T64-GE-7 Engines
Right Engine S/N 261006

Notes: 1. based on ambient temperature
2. 100 percent N_1 - 18,230 rpm

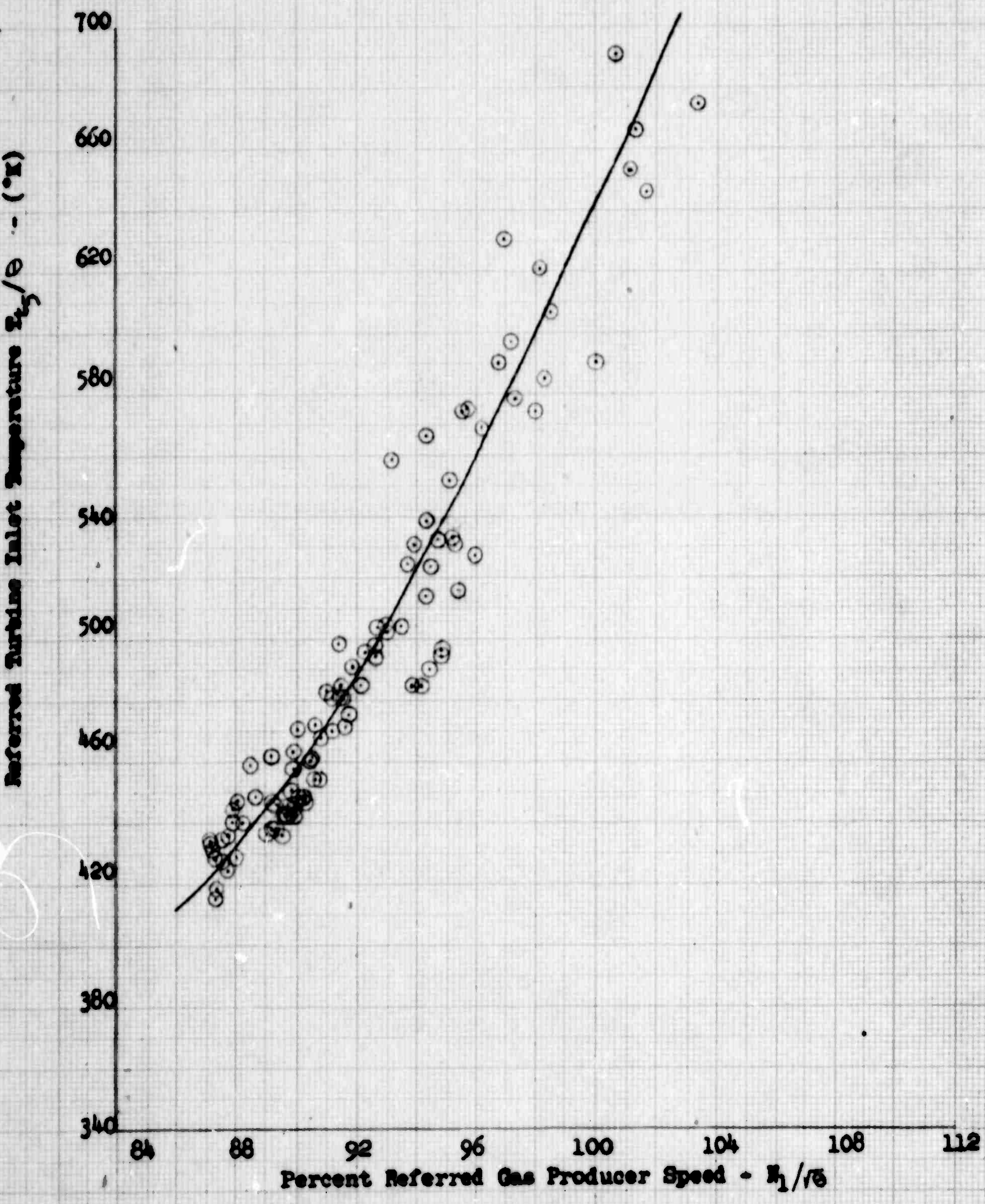

Figure 170. Engine Characteristics

HH-53C USAF S/N 67-14993

T64-GE-7 Engines

Right Engine S/N 261006

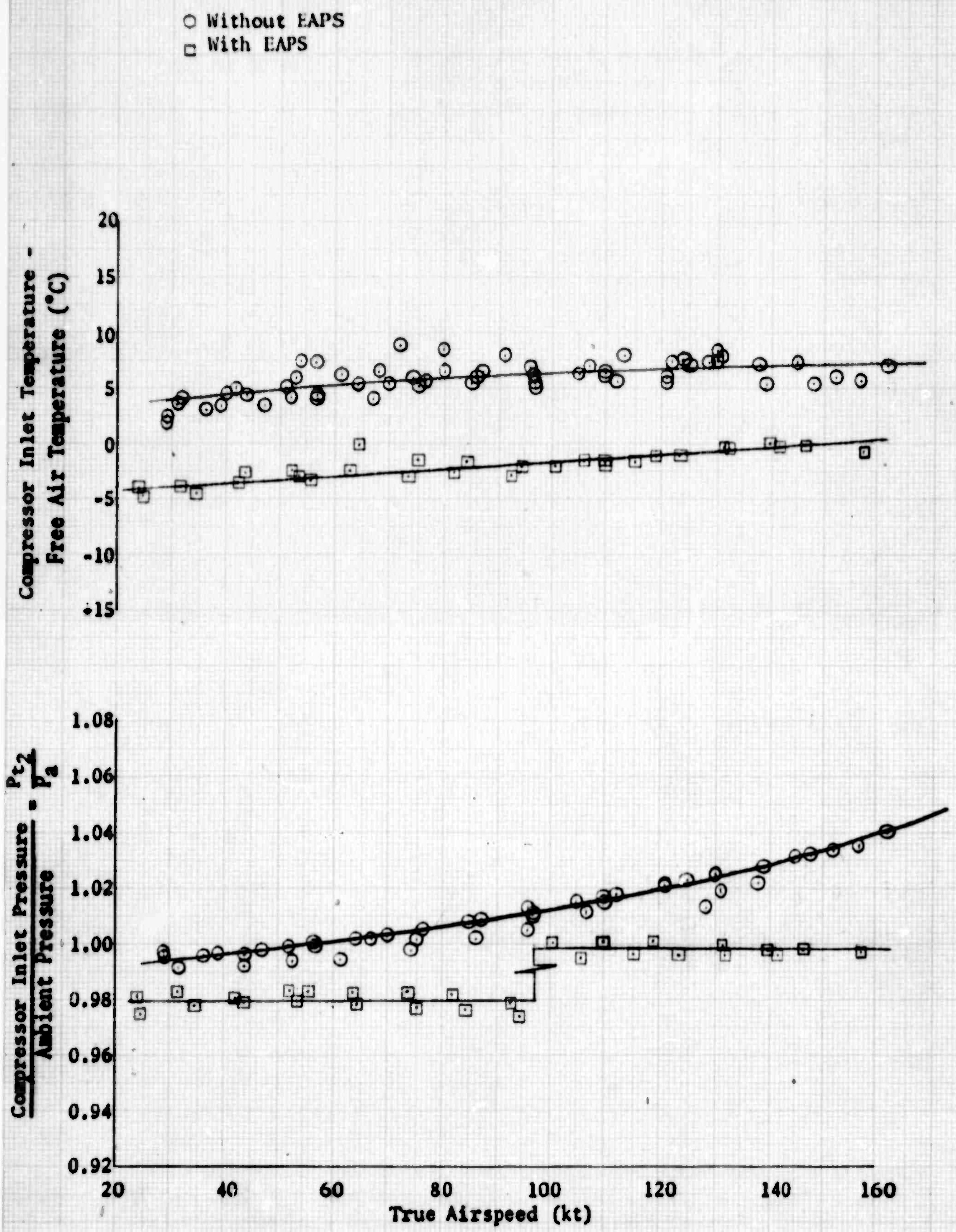

Figure 171. Engine Characteristics

HH-53C USAF S/N 67-14993
T64-GE-7 Engines
Left Engine S/N 261005

Notes: 1. θ based on ambient temperature.
2. δ based on ambient pressure
3. 100 percent N_1 = 18,230 rpm

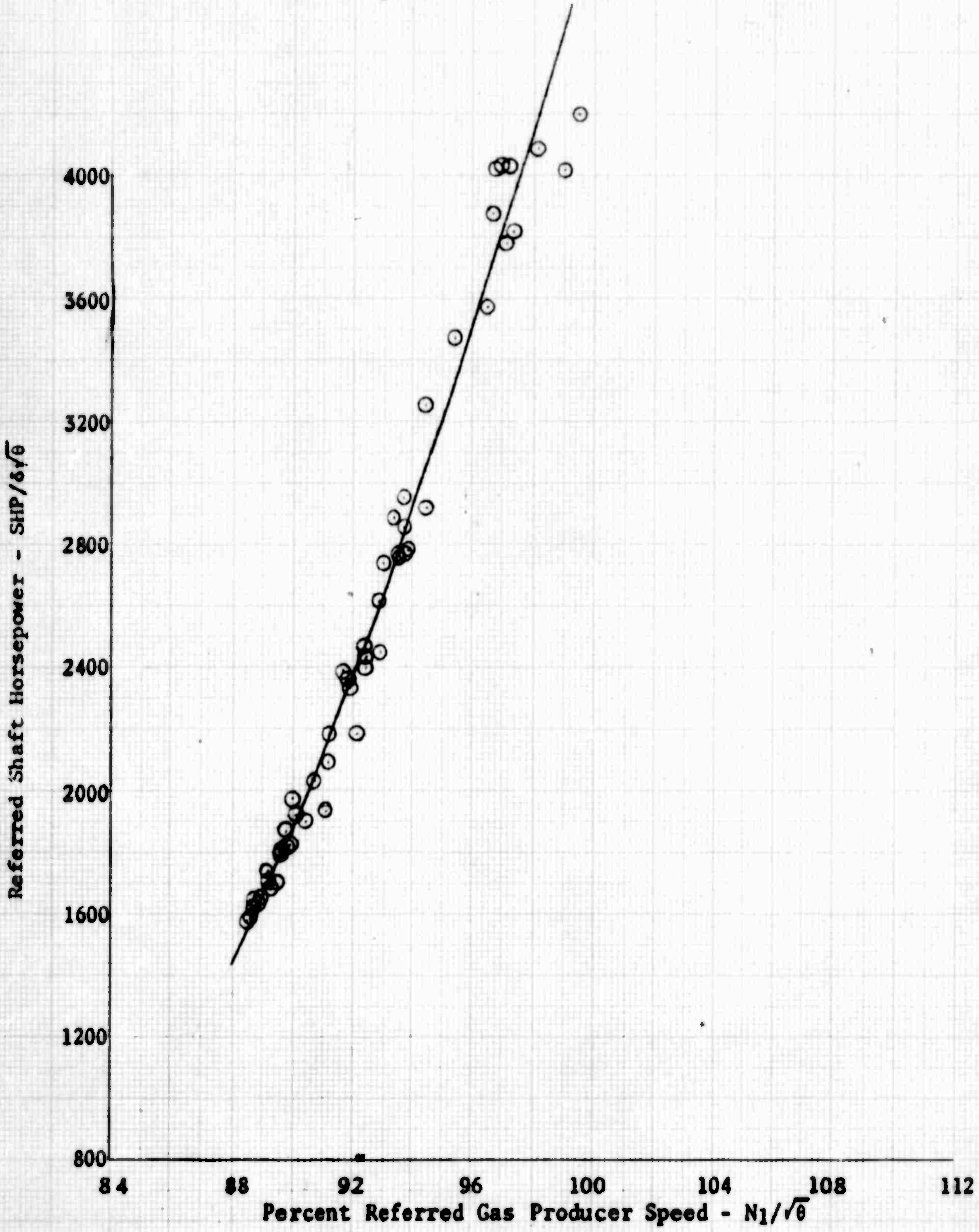

Figure 172. Engine Characteristics

HH-53C USAF S/N 67-14993

T64-GE-7 Engines

Left Engine S/N 261005

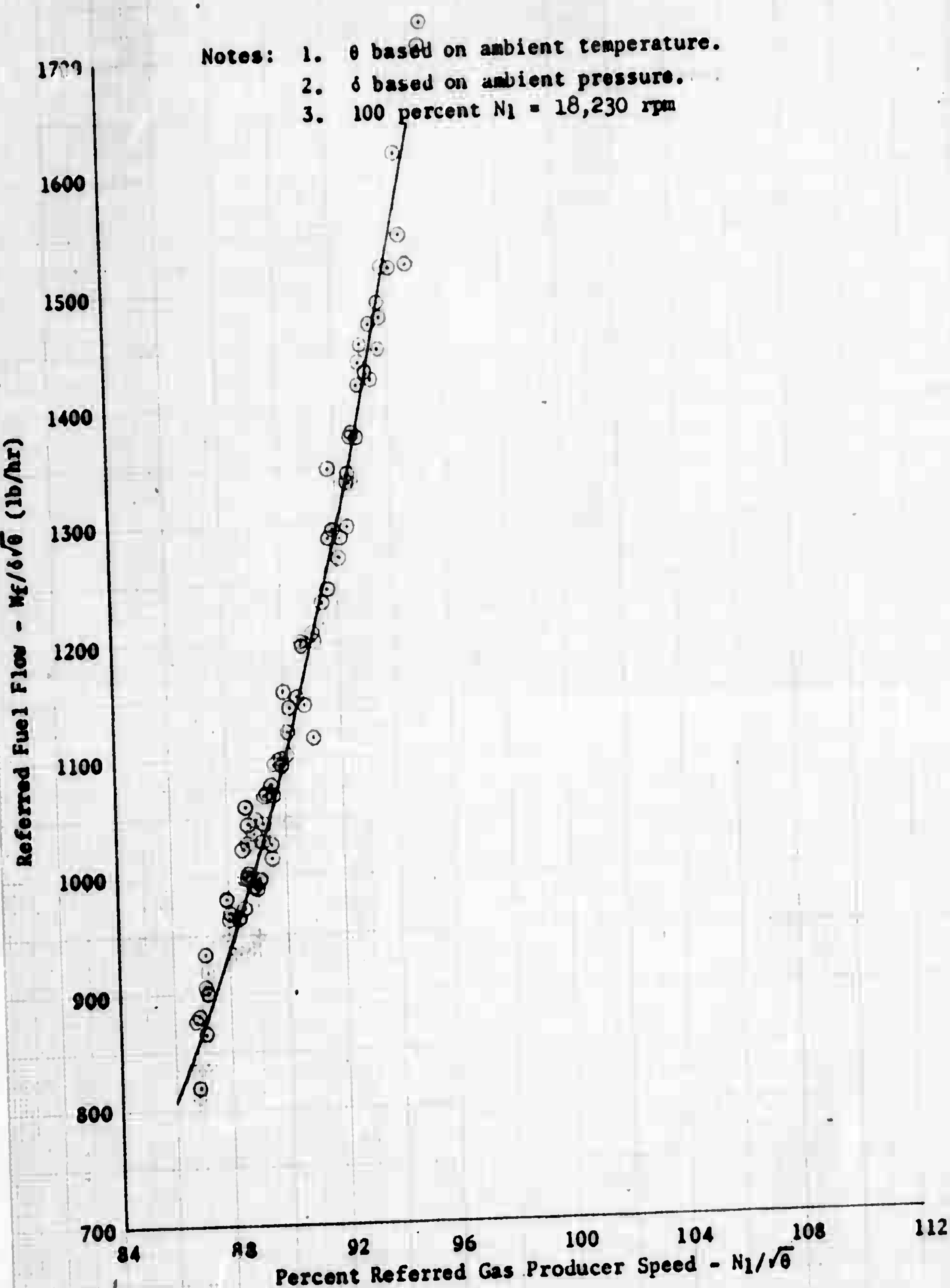

Figure/X9. Engine Characteristics

HH-53C USAF S/N 67-14993
T64-GE-7 Engines
Left Engine S/N 261005

Notes: 1. θ based on ambient temperature
2. 100 percent N_1 = 18,230 rpm

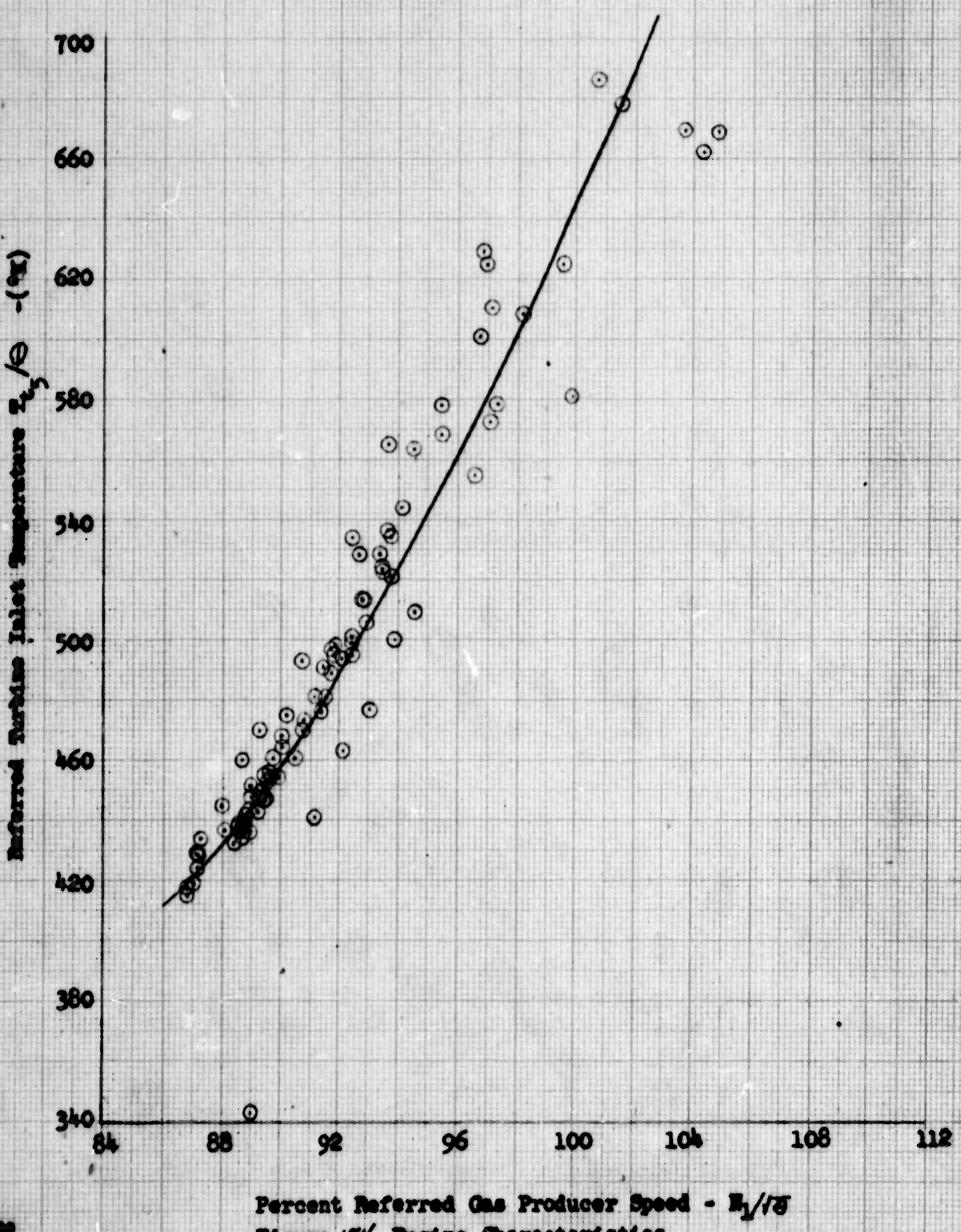

Figure 174 Engine Characteristics

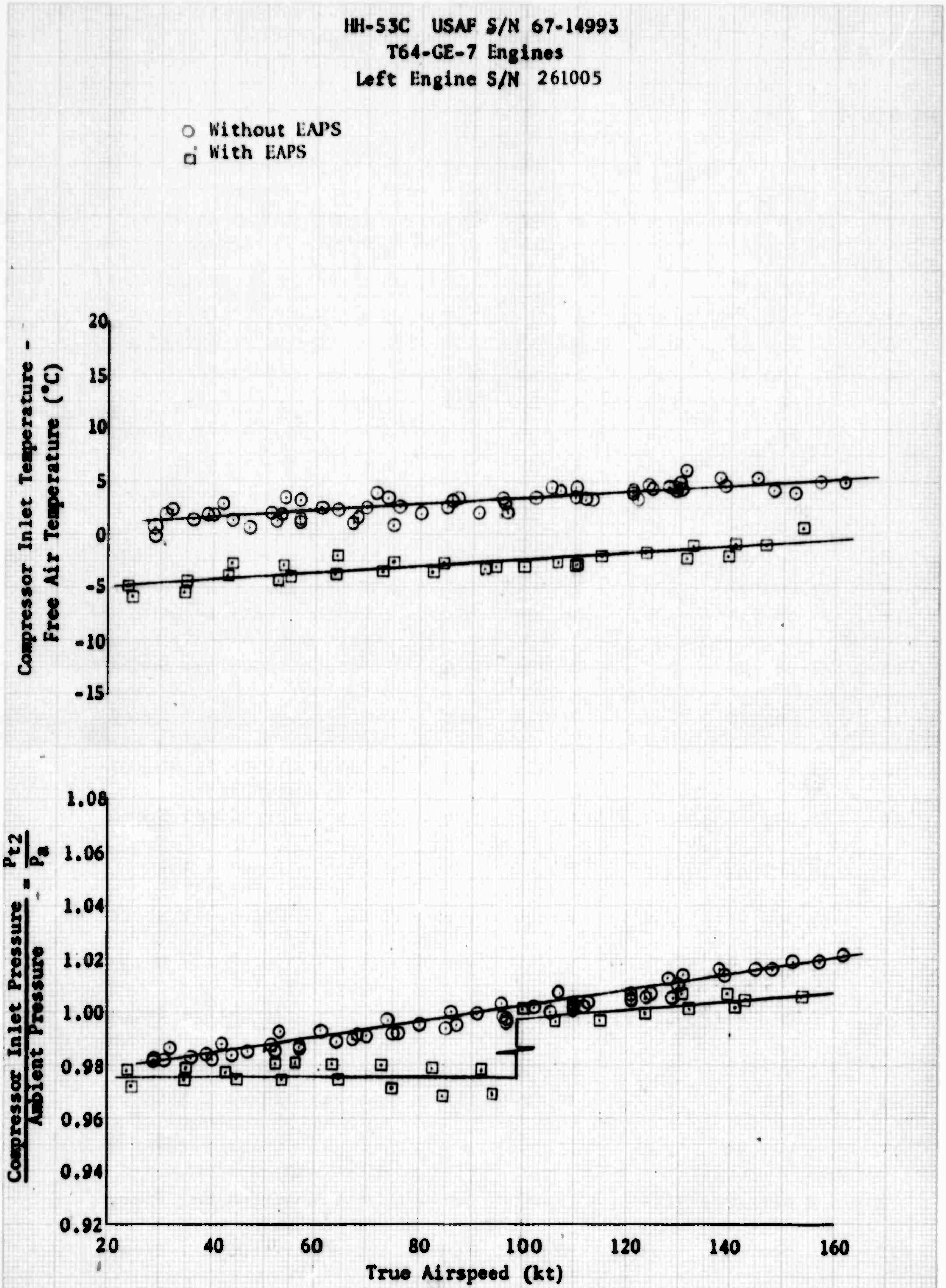

Figure 175. Engine Characteristics

FLIGHT LOG

Flight No.	Date	Flight Time	ESGW	cg	Test
1	26 Aug 69	1.3	38,322	Mid	Level Flight Performance
2	27 Aug 69	1.3	38,422	Mid	Level Flight Performance
3	28 Aug 69	1.0	29,948	Mid	Level Flight Performance
4	29 Aug 69	1.0	38,522	Mid	Level Flight Performance
5	10 Sep 69	1.2	30,718	Mid	Level Flight Performance
6	10 Sep 69	1.5	30,664	Mid	Level Flight Performance
7	11 Sep 69	1.9	30,739	Mid	Airspeed Calibration
8	11 Sep 69	1.2	30,589	Mid	Level Flight Performance
9	11 Sep 69	1.0	35,364	Mid	Level Flight Performance
10	12 Sep 69	0.8	30,618	Mid	Level Flight Performance
11	12 Sep 69	1.0	36,008	Mid	Level Flight Performance
12	16 Sep 69	0.3	30,618	Mid	Tethered Hovering
13	19 Sep 69	1.3	33,168	Mid	Level Flight Performance
14	20 Sep 69	2.1	36,400	Mid	Sawtooth Climbs & Autorotational Descents
15	22 Sep 69	0.7	32,038	Aft	Static Longitudinal Speed Stability
16	23 Sep 69	1.2	32,038	Aft	Static Longitudinal Speed Stability
17	23 Sep 69	1.3	32,038	Aft	Sawtooth Climbs & Autorotational Descents
18	23 Sep 69	1.3	32,128	Aft	Static Longitudinal Speed Stability
19	24 Sep 69	2.0	36,400	Mid	Sawtooth Climbs & Autorotational Descents
20	30 Sep 69	1.1	38.158	Aft	Static Longitudinal Speed Stability
21	30 Sep 69	0.8	38,158	Aft	Static Longitudinal Speed Stability
22	30 Sep 69	0.7	38,158	Aft	Static Longitudinal Speed Stability
23	1 Oct 69	0.2	30,732	Mid	Tethered Hovering
24	1 Oct 69	1.8	36,400	Mid	Sawtooth Climbs & Autorotational Descents
25	4 Oct 69	1.5	36,000	Mid	Sawtooth Climbs & Autorotational Descents
26	4 Oct 69	0.9	42,000	Aft	Static Longitudinal Speed Stability
27	6 Oct 69	1.4	32,000	Fwd	Static Longitudinal Speed Stability

Flight No.	Date	Flight Time	ESGW	cg	Test
28	7 Oct 69	0.2	30,730	Mid	Tethered Hovering
29	9 Oct 69	1.0	30,730	Mid	Tethered Hovering
30	10 Oct 69	1.1	38,000	Fwd	Static Longitudinal Speed Stability
31	13 Oct 69	0.7	42,000	Aft	Static Longitudinal Speed Stability
32	15 Oct 69	1.5	32,000	Aft	Static Longitudinal Speed Stability
33	15 Oct 69	1.2	38,000	Aft	Static Longitudinal Speed Stability
34	15 Oct 69	0.8	42,000	Aft	Static Longitudinal Speed Stability
35	16 Oct 69	1.1	42,000	Fwd	Static Longitudinal Speed Stability
36	16 Oct 69	0.8	42,000	Fwd	Static Longitudinal Speed Stability
37	18 Oct 69	1.0	42,000	Aft	Static Longitudinal Speed Stability
38	20 Oct 69	1.0	32,323	Mid	Tethered Hovering
39	20 Oct 69	1.2	42,000	Aft	Static Longitudinal Speed Stability
40	21 Oct 69	0.9	32,000	Aft	Static Directional Stability
41	23 Oct 69	0.7	31,000	Aft	Static Directional Stability
42	24 Oct 69	0.3	30,187	Mid	Tethered Hovering
43	25 Oct 69	1.3	42,000	Aft	Static Directional Stability
44	28 Oct 69	1.3	42,000	Aft	Static Directional Stability
45	29 Oct 69	1.0	42,000	Aft	Static Directional Stability
46	29 Oct 69	0.9	42,000	Aft	Static Directional Stability
47	30 Oct 69	1.0	38,000	Aft	Static Directional Stability
48	30 Oct 69	1.2	32,000	Aft	Static Directional Stability
49	31 Oct 69	1.3	32,000	Aft	Static Directional Stability
50	12 Nov 69	1.2	32,000	Aft	Dynamic Stability and Controllability
51	12 Nov 69	1.2	32,000	Fwd	Dynamic Stability and Controllability, Hover
52	13 Nov 69	1.3	32,000	Aft	Dynamic Stability and Controllability
53	13 Nov 69	1.3	32,000	Aft	Dynamic Stability and Controllability
54	17 Nov 69	1.2	32,000	Aft	Dynamic Stability and Controllability
55	17 Nov 69	1.3	32,000	Aft	Dynamic Stability and Controllability

Flight No.	Date	Flight Time	ESGW	cg	Test
56	17 Nov 69	0.7	32,000	Aft	Dynamic Stability and Controllability, Climb
57	20 Nov 69	1.2	32,000	Mid	Dynamic Stability and Controllability, Climb
58	20 Nov 69	0.9	32,000	Fwd	Hardovers, AFCS
59	21 Nov 69	0.6	32,000	Fwd	Hardovers, AFCS, Hover
60	22 Nov 69	0.3	30,569	Mid	Tethered Hover
61	24 Nov 69	1.1	30,569	Mid	Tethered Hover and Free Hover
62	2 Dec 69	1.3	42,000	Aft	Dynamic Stability and Controllability, Tanks Full
63	4 Dec 69	1.3	42,000	Aft	Dynamic Stability and Controllability, Tanks Full
64	9 Dec 69	1.1	42,000	Aft	Dynamic Stability and Controllability, Tanks Full
65	10 Dec 69	0.4	42,000	Aft	Dynamic Stability and Controllability, Hover, Tanks Full
66	12 Dec 69	0.8	42,000	Aft	Dynamic Stability and Controllability, Hover, Tanks Full
67	12 Dec 69	1.1	42,000	Fwd	Dynamic Stability and Controllability, Hover, Tanks Full
68	16 Dec 69	1.2	42,000	Fwd	Dynamic Stability and Controllability, Tanks Full
69	16 Dec 69	1.2	42,000	Fwd	Dynamic Stability and Controllability, Tanks Full
70	18 Dec 69	1.3	42,000	Fwd	Dynamic Stability and Controllability, Tanks Full
71	18 Dec 69	0.9	42,000	Aft	Dynamic Stability and Controllability, Tanks Full, Climb
72	6 Jan 70	0.9	36,500	Mid	Level Flight Performance
73	6 Jan 70	1.0	36,500	Mid	Level Flight Performance, Gear Down
74	13 Jan 70	1.2	39,500	Mid	Level Flight Performance
75	15 Jan 70	1.1	38,200	Mid	Level Flight Performance
76	20 Jan 70	0.9	42,000	Fwd	Sideward and Rearward
77	20 Jan 70	0.9	42,000	Aft	Dynamic Stability and Controllability, Hover
78	23 Jan 70	0.9	30,925	Mid	Level Flight Performance
79	27 Jan 70	1.3	36,000	Mid	Level Flight Performance
80	6 Feb 70	0.5	42,000	Aft	Dynamic Stability and Controllability

Flight No.	Date	Flight Time	ESGW	cg	Test
81	9 Feb 70	0.7	42,000	Fwd	Sideward (Repeat Flight 76)
82	12 Feb 70	1.1	37,700	Mid	Level Flight Performance
83	12 Feb 70	1.5	30,100	Mid	Level Flight Performance, OGE Hover
84	16 Feb 70	1.0	36,000	Mid	Level Flight Performance
85	16 Feb 70	1.0	36,000	Mid	Level Flight Performance
86	17 Feb 70	1.2	30,200	Mid	Level Flight Performance, EAPS Installed
87	18 Feb 70	0.7	30,200	Mid	Level Flight Performance, EAPS Installed
88	27 Feb 70	0.5	30,500	Mid	Hover Performance, OGE

Fwd cg = 328 in.

Mid cg = 340 in.

Aft cg = 352 in.

REFERENCES

1. Barbini, Wayne J., Balfe, Paul G., Major USAF, Lovrien, Clark E. Jr., Major USAF, FTC-TR-70-8, Category II Performance and Flying Qualities Tests of the HH-53C Helicopter, Air Force Flight Test Center, April 1970.

2. T.O. 1H-53(H) B-1, Flight Manual USAF Series HH-53B, HH-53C Helicopter, 19 August 1968, changed 29 October 1968.

3. Military Specification, Helicopter Flying and Ground Handling Qualities; General Requirements for, MIL-H-8501A, 3 April 1962.

UNCLASSIFIED

Security Classification

DOCUMENT CONTROL DATA - R & D

(Security classification of title, body of abstract and indexing annotation must be entered when the overall report is classified)

1. ORIGINATING ACTIVITY (Corporate author) Air Force Flight Test Center Edwards AFB, California	2a. REPORT SECURITY CLASSIFICATION UNCLASSIFIED 2b. GROUP N/A

3. REPORT TITLE

Category II Performance and Flying Qualities Tests of the HH-53C Helicopter

4. DESCRIPTIVE NOTES (Type of report and inclusive dates)

Final

5. AUTHOR(S) (First name, middle initial, last name)

Wayne J. Barbini
Paul J. Balfe, Major, USAF
Clark E. Lovrien, Jr., Major, USAF

6. REPORT DATE	7a. TOTAL NO. OF PAGES	7b. NO. OF REFS
May 1970	193	3

8a. CONTRACT OR GRANT NO	9a. ORIGINATOR'S REPORT NUMBER(S)
b. PROJECT NO Project Directive 69-2	FTC-SD-70-8
c. Program Structure 482A	9b. OTHER REPORT NO(S) (Any other numbers that may be assigned this report)
d.	N/A

10. DISTRIBUTION STATEMENT

This document may be further distributed by any holder only with the specific prior approval of ASD (ASZTH), Wright-Patterson AFB, Ohio 45433.

11. SUPPLEMENTARY NOTES	12. SPONSORING MILITARY ACTIVITY
None	6512th Test Group Edwards AFB, California

13. ABSTRACT

This substantiating document contains the test techniques, data analysis methods, and test data for the Category II Performance and Flying Qualities Tests of the HH-53C Helicopter. The results, conclusions, and recommendations were presented in FTC-TR-70-8, Category II Performance and Flying Qualities Tests of the HH-53C Helicopter, April 1970.

DD FORM 1 NOV 65 1473

UNCLASSIFIED

Security Classification

14. KEY WORDS	LINK A		LINK B		LINK C	
	ROLE	WT	ROLE	WT	ROLE	WT
HH-53C helicopter performance and flying qualities tests						